Propriétés de spin des états évanescents et effet tunnel dans les semi-conducteurs

Thi Lam Hoai Nguyen

ÉCOLE POLYTECHNIQUE

THÈSE

Présentée pour obtenir

Le GRADE de DOCTEUR de l'ÉCOLE POLYTECHNIQUE

Discipline : PHYSIQUE

par

Nguyễn Thị Lâm Hoài

PROPRIÉTÉS DE SPIN DES ÉTATS ÉVANESCENTS ET EFFET TUNNEL DANS LES SEMI-CONDUCTEURS

SPIN PROPERTIES OF EVANESCENT STATES AND TUNNELING IN SEMICONDUCTORS

Soutenue le 21 janvier 2010 devant la commission d'examen:

Xavier MARIE	Président
Robson FERREIRA	Rapporteur
Henri JAFFRES	Rapporteur
Joël CIBERT	Examinateur
Henri-Jean DROUHIN	Directeur de thèse
Guy FISHMAN	Co-Directeur de thèse

Thèse préparée au Laboratoire LSI de l'École Polytechnique
et au Laboratoire IEF de l'Université Paris 11

A Nam-Duong, mon petit soleil, qui est né et a grandi avec ce travail

Remerciements

J'aimerais tout d'abord exprimer mon infinie reconnaissance à mes deux directeurs de thèse – MM. Henri-Jean Drouhin et Guy Fishman – qui se sont toujours occupés de moi dès le premier jour de mon arrivée en France et sans lesquels cette thèse n'aurait pu se réaliser. Je vous remercie beaucoup, Henri-Jean et Guy, pour m'avoir introduite à la vie scientifique. Merci pour vos explications sur les « subtilités », sur les « sous-entendus » de la physique qui ont, sans aucun doute, clarifié mes pensées parfois naïves et embrouillées. Merci pour votre présence attentive et soutenue pour répondre à toutes mes questions, qu'elles aient été petites ou grandes, difficiles ou évidentes, bonnes ou erronées. Merci pour les idées directrices de la thèse, les discussions instructives entre nous, la vision sur la signification des résultats obtenus : ce sont des ressources précieuses de la thèse. Merci de n'avoir jamais perdu confiance en moi, de m'avoir prodigué des encouragements pour chaque petite « victoire » et de m'avoir encouragée aux moments les plus difficiles où on s'est aperçu des erreurs et retrouvé au point de départ. Mes mots ne peuvent exprimer toute ma gratitude, mes remerciements. Je suis très heureuse d'avoir eu la chance de vous connaître et de travailler avec vous.

Je tiens aussi à remercier MM. Robson Ferreira et Henri Jaffres qui ont accepté d'évaluer mon travail. Je remercie également M. Joël Cibert d'avoir fait partie du jury. Je remercie vivement M. le Professeur Xavier Marie qui m'a fait l'honneur de présider le Jury. Je remercie l'ensemble du jury pour ses questions pertinentes qui m'ont permis d'appréhender le sujet en profondeur.

Je remercie les équipes du Laboratoire des Solides Irradiées, Ecole Polytechnique et de l'Institut de Physique Fondamentale de l'Université Paris-Sud de m'avoir accueillie dans leurs lieux respectifs.

Je remercie en particulier Travis Wade pour les corrections de l'anglais concernant les articles et pour le manuscrit.

Je remercie Juliette Mangeney et ses deux doctorants Loïc Meignien et Matthieu Martin pour la grande gentillesse dont ils ont fait preuve avec leur co-

occupante de la pièce 124 à l'IEF, laquelle ne pouvait dire un mot de français lors de son arrivée.

Je remercie Thi-Phuong Ngo, Viet-Hung Nguyen, Eloy Ramirez-Garcia, Quang-Anh Nguyen, Mihaela-Cristina Ciornei, Feng Yang - mes amis à IEF et au LSI - pour les petits moments où on faisait une pause et parlait de notre travail. Grand merci à tous mes amis de l'X avec qui j'ai partagé la vie quotidienne pendant plus de trois années sur le « Plateau venteux » et qui m'ont beaucoup aidée à surmonter les moments difficiles.

Je remercie tous ceux et celles qui, malgré la distance et l'éloignement m'ont procurée leurs encouragements.

Je dédie enfin cette thèse à mon mari, et à ma famille qui m'ont beaucoup soutenue tout au long de cette thèse.

Table des matières

Introduction

La mécanique quantique a introduit des concepts nouveaux, sans équivalents dans la mécanique classique (newtonienne), tels l'effet tunnel et le spin. Schématiquement, l'effet tunnel consiste à envoyer des particules, qui seront dans le cas présent des électrons, d'un milieu A, dont le potentiel constant sera pris nul pour fixer les idées, vers un milieu B, appelée barrière, de potentiel positif et d'épaisseur finie terminée par un troisième milieu identique au milieu A pour simplifier. On considère le cas où l'énergie cinétique de l'électron est inférieure au potentiel du milieu B. Alors que la physique newtonienne interdit toute transmission, il n'en est pas de même en mécanique quantique où quelques électrons peuvent passer à travers la barrière, le pourcentage exact dépendant de l'énergie cinétique, de la hauteur du potentiel et de l'épaisseur du milieu B. Comme ni le principe ni le détail du calcul ne sont difficiles, ceci fait l'objet d'un des premiers exercices donnés aux étudiants qui voient ainsi que des idées simples conduisent, en mécanique quantique, à des résultats non triviaux et, en tous les cas, sans équivalent classique. D'un autre côté, le spin de l'électron, ou moment cinétique intrinsèque, n'étant pas un mouvement de rotation de l'électron sur lui-même, n'a pas non plus d'analogue classique. Le spin a deux états propres "haut" et "bas". Ces deux états sont orthogonaux dans l'espace des spins et ont des directions bien définies dans l'espace réel à trois dimensions, déterminées par la valeur moyenne des matrices de Pauli, moyenne effectuée sur l'état de spin considéré. Dans le cas où existe un champ magnétique, les deux états propres de l'hamiltonien décrivant le spin dans le champ magnétique sont orientés parallèlement au champ pour l'état "haut" et dans le sens opposé pour l'état "bas". De nouveau, les calculs étant très simples, ceci est l'objet d'un exercice de base pour étudiants qui peuvent ainsi comprendre que le fait d'appartenir à un certain espace à deux dimensions n'empêche pas un spin d'avoir une direction bien définie dans notre espace usuel à trois dimensions.

Comment ceci se traduit-il dans les semi-conducteurs ?

Regardons tout d'abord l'effet tunnel. Dans le cas le plus simple, le premier milieu est constitué d'un semi-conducteur A dont le bas de la bande de conduction, à laquelle appartient l'énergie de l'électron, est à une énergie plus basse que le bas de la bande de conduction du milieu barrière constitué d'un semi-conducteur B, l'énergie de l'électron étant dans la bande interdite de B, le troisième milieu étant également constitué du semi-conducteur A. Alors que dans le cas idéal, décrit au premier paragraphe, l'électron a la masse de l'électron libre, dans le cas d'un semi-conducteur l'électron a une masse effective définie par la parabole du bas de la bande de conduction. Si cette masse n'est pas la même dans les semi-conducteurs A et B, l'hamiltonien tenant compte d'une masse dépendant de la position est connu depuis 1966 grâce aux travaux de BenDaniel-Duke qui utilisèrent les résultats de Harrison parus en 1961. Cet hamiltonien n'entraîne pas de difficultés supplémentaires par rapport au cas de l'électron libre ou de l'électron à masse effective constante. Ceci étant, il est clair que l'utilisation de cet hamiltonien suppose que l'énergie des électrons incidents sur la barrière est proche à la fois de l'énergie du bas de la bande de conduction du semi-conducteur A et de l'énergie du bas de la bande de conduction du semi-conducteur B, tout comme, quand on calcule l'énergie d'un donneur en utilisant la masse effective de conduction, on suppose que l'énergie du donneur est proche de l'énergie du bas de la bande de conduction. Dans ce cas, un vecteur d'onde réel est suffisant pour décrire l'onde plane incidente via une exponentielle complexe dans le semi-conducteur A, l'opposé de ce vecteur est utile pour décrire la réflexion dans le premier milieu, un vecteur d'onde imaginaire décrit les ondes dans la barrière via les exponentielles réelles. Ceci ne diffère guère du cas modèle de l'électron libre. Le problème est simple parce que l'on sait très bien ce qui se passe dans chacun des milieux et qu'il suffit d'utiliser les conditions aux limites usuelles pour résoudre le problème.

Qu'en est-il maintenant si l'énergie de l'électron, tout en étant proche de celle du bas de la bande de conduction du semi-conducteur A, est nettement inférieure au bas de la bande de conduction du semi-conducteur B, par exemple si cette énergie se situe aux environs du milieu de la bande interdite du semi-conducteur B ? Il est clair que le problème change complètement et que l'hamiltonien de BenDaniel-Duke devient inutilisable. La première chose à faire est évidemment

d'arriver à décrire l'onde dans la bande interdite. Ce problème n'est pas récent et dans le cas modèle d'une bande de conduction et d'une bande de valence définissant une masse de conduction et une masse de valence, une simple matrice 2×2, ou hamiltonien H_2, dont la base est faite de la fonction de conduction et de la fonction de valence permet de connaître le vecteur d'onde quelle que soit l'énergie. Les éléments hors diagonale de cet hamiltonien permettent de décrire l'énergie dans la bande interdite. Si le vecteur d'onde est réel, l'énergie est soit celle d'un électron de conduction soit celle d'un électron de valence. Si le vecteur d'onde est imaginaire, l'énergie est dans la bande interdite. Pour un petit vecteur d'onde réel, la bande de conduction et la bande de valence sont toutes deux paraboliques définissant les masses effectives de conduction et de valence. Pour un vecteur d'onde imaginaire, on obtient un ovale qui joint le bas de la bande de conduction au sommet de la bande de valence et qui traverse donc toute la bande interdite. Ce n'est pas une ellipse car près de la bande de conduction, la courbure est la même que celle du bas de la bande de conduction et, près de la bande de valence, la courbure est la même que celle de la bande de valence. Au passage, notons que ceci est une justification supplémentaire de l'utilisation de la masse effective pour décrire les impuretés peu profondes, i.e. les impuretés (donneur ou accepteur) dont l'énergie est dans la bande interdite mais proche d'une bande de conduction ou de valence. Le détail sera donné au chapitre 1. Chacun sait cependant que les semi-conducteurs ne peuvent se résumer à la description simplette telle que l'on vient de la donner. Sans spin, la bande de conduction n'est pas dégénérée mais le sommet de bande de valence est dégénérée trois fois, avec le spin la bande de conduction est dégénérée deux fois et la bande de valence six fois. La matrice minimum pour décrire alors ce qui se passe autour de la bande interdite est une matrice 8×8, ou hamiltonien H_8, dit de Pidgeon-Brown. Cependant cet hamiltonien ne permet pas de décrire complètement les énergies dans la bande interdite car les trous lourds ne sont pas simplement couplés à la bande de conduction de sorte que, dans le but de décrire la bande interdite, manque, pour les trous lourds, l'équivalent des termes hors diagonale de l'hamiltonien H_2. Il faut donc, pour avoir l'équivalent de l'hamiltonien H_2 dans les semi-conducteurs réels utiliser un autre hamiltonien. On peut bien sûr utiliser un hamiltonien complet, en principe infini, mais nous verrons que l'hamiltonien utile, et aussi le plus petit possible, est l'hamiltonien qui tient compte de la seconde bande de conduction. Cet hamiltonien sera nommé H_{14} car c'est un hamiltonien 14×14 (la bande de valence est dégénérée trois fois, la bande de conduction une fois, la deuxième

bande de valence trois fois, le tout multiplié par deux pour tenir compte du spin). Nous verrons au chapitre 1 que cet hamiltonien a toutes les qualités pour décrire la bande interdite dans le cas qui nous occupe. Ceci acquis, on peut se dire que l'étude des ondes dans la bande interdite d'un semi-conducteur n'est qu'un cas particulier d'une étude qui se situerait dans le cadre plus général des propriétés des ondes évanescentes dans les solides, ce qui permettrait de guider les études dans les semi-conducteurs où la complexité est telle qu'il devient difficile de prévoir quelle va être la structure de bande à l'intérieur de la bande interdite. Ce problème a été abordé par Kohn dans les semi-conducteurs en 1959, et par Heine en 1963 et Jones en 1966 de façon générale bien que les exemples soient plutôt tirés de la physique des semi-conducteurs. Il en ressort que l'étude des branches dans la bande interdite doit être faite en fonction d'un vecteur d'onde complexe et non pas imaginaire pur comme le suggère l'image simple de l'électron libre dans l'effet tunnel. Ceci peut sembler étrange mais nous verrons au cours de cette étude qu'un vecteur d'onde purement imaginaire ne résout le problème que dans des cas particuliers. Le fait que le vecteur soit complexe entraîne d'ailleurs immédiatement d'autres problèmes : comment se fait-il qu'il n'y ait pas d'absorption associée, auquel cas ce ne serait plus un effet tunnel ? Un des objets de cette thèse est de résoudre cette contradiction apparente dans le cas tout à fait concret d'un barrière faite d'un semi-conducteur III-V. Les travaux des auteurs ci-dessus amènent bien d'autre résultats intéressants, comme par exemple le fait que, dans la bande interdite, une branche d'énergie ne peut se terminer sur un point d'arrêt mais relie forcément une branche à une autre, ce dont on a donné un exemple simple dans le cas de l'hamiltonien H_2, où l'ovale dans la bande interdite fait le pont entre la bande de conduction et la bande de valence. Si la branche est tout entière à l'intérieur de la bande interdite, elle a la forme d'un lacet et ne peut se terminer par un bout qui ne serait lié à rien. Nous verrons un exemple de cela au chapitre 1. Dans ce cadre, plus qu'utile pour ne pas aller à l'aveuglette, on peut s'intéresser à ce qui se passe dans la bande interdite des semi-conducteurs. Les études ont été menées dans les années 1980 par Chang (1982), Chang et Schulman (1982) et Schuurmans et 't Hooft (1985) qui ont utilisé la méthode des combinaisons linéaires d'orbitales atomiques pour obtenir les énergies dans la bande interdite. Ces auteurs s'intéressent au silicium en tenant compte du couplage spin-orbite puis à l'arséniure de gallium soit en tenant compte de l'absence d'inversion soit en tenant compte du couplage spin-orbite mais sans prendre en compte l'absence d'inversion. On retrouve évidemment leurs résultats via la théorie $\mathbf{k} \cdot \mathbf{p}$, utilisée

dans ce manuscrit, car ce qui compte est essentiellement le nombre de bandes que l'on utilise. Quel que soit le cadre utilisé (combinaisons linéaires d'orbitales atomiques ou théorie $\mathbf{k}\cdot\mathbf{p}$), une méthode numérique est nécessaire mais nous verrons que la théorie $\mathbf{k}\cdot\mathbf{p}$ permet de comprendre certains résultats curieux car elle permet de faire des calculs analytiques pour de faibles vecteurs d'onde même quand ceux-ci sont complexes.L'application de la théorie des groupes [KOS] à la construction des matrices $\mathbf{k}\cdot\mathbf{p}$ est détaillée dans la Ref. [GF].

Nous nous sommes intéressés au cas d'une barrière B composée d'un semiconducteur III-V où l'on tient compte à la fois de l'absence de centre d'inversion et du couplage spin-orbite. Il faut distinguer deux cas. Dans le premier, on s'occupe, dans l'espace des vecteurs d'onde, des directions de haute symétrie telles [100] ou [111] ; la dégénérescence de spin n'est pas levée et le fait de tenir compte de l'absence de centre d'inversion ne change pas grand chose ; le vecteur d'onde dans la bande interdite est purement imaginaire ; dans l'approximation de la masse effective, il suffit de remplacer le vecteur d'onde réel usuel par un vecteur d'onde imaginaire dont le carré est réel et on obtient simplement une énergie négative i.e., dans la bande interdite. Dans le deuxième cas on s'occupe des autre directions, [110] pour fixer les idées, et le problème change complètement. En effet il est connu, depuis les travaux de Dresselhaus en 1955 que la dégénérescence de spin est levée, la différence d'énergie étant proportionnelle au cube du vecteur d'onde. Dans le cas d'un vecteur d'onde réel et dans l'approximation de la masse effective, il suffit de remplacer le vecteur d'onde réel usuel par un vecteur d'onde imaginaire dont le carré est réel et on obtient simplement une énergie qui est la somme, à des coefficients près, du carré d'un vecteur réel et du cube d'un vecteur réel. Il est clair que le problème change complètement dans le cas d'un vecteur d'onde imaginaire où le terme proportionnel au cube du vecteur d'onde sera imaginaire et ne pourra s'éliminer en utilisant l'énergie cinétique négative certes mais purement réelle. Ce cas semble avoir complètement échappé à ceux qui ont fait les études de bande interdite dans les années 1980, dont les résultat ont été très brièvement rappelés dans le paragraphe ci-dessus. On voit donc que dans le cas où l'on a affaire à un effet tunnel où le spin intervient explicitement, autrement dit où la dégénérescence de spin est levée, les deux effets purement quantiques dont il a été question au début sont étroitement imbriqués. On est donc obligé, dans le cas de la direction [110], d'avoir recours à un vecteur complexe comme suggéré par Kohn, Heine et Jones. Naturellement la première chose à connaître,

avant de s'occuper de l'effet tunnel, est la structure de bande dans la bande interdite. Ce problème a été étudié dans l'équipe où ce travail de thèse a eu lieu et les principaux résultas seront rappelés au chapitre 1. Il faut cependant signaler que, en 2003, Perel' *et al.* ont étudié un cas très particulier, celui ou l'incidence est très proche de (mais non identique à) la direction [100] et que ce cas particulier permet d'éviter la majorité des difficultés évoquées ici.

Le but principal de cette thèse est précisément de s'attaquer au problème de l'effet tunnel dépendant du spin, au moins dans un cas simple qui est celui où les masses effectives ont un sens. Le principal problème est évidemment celui de la conservation du courant de probabilité. Nous verrons lors du chapitre 3, que nous avons réussi à donner une solution analytique à ce problème et que cela nécessite de revoir les conditions aux limites habituelles. Nous nous sommes également intéressés au problème étudié par Perel' *et al.* pour comprendre ce qui est sous-jacent dans leur étude. Enfin nous avons étudié le cas, qui sort du cadre de la masse effective, d'une onde qui se propage dans la barrière selon une direction plus générale que celle de Perel' *et al.* Comme dit précédemment les énergies possibles ont une structure en boucle, structure étudiée précédemment. En revanche ce qui n'avait pas été étudié concerne les deux états propres de spin. Dans le cas général l'hamiltonien H_{14} est nécessaire ce qui oblige à des calculs numériques dont nous verrons que les résultats ne sont pas conformes à ce qui est censé être bien connu en mécanique quantique, ce qui pourrait poser un problème d'interprétation. Cependant, pour de faibles valeurs du vecteur d'onde, la levée de dégénérescence se traduit simplement par un hamiltonien 2×2 dit hamiltonien H_{DP} de D'yakonov-Perel' (1971) qui décrit un champ magnétique interne et explique donc bien la différence d'énergie entre les spins "haut" et "bas". Cet hamiltonien dépend des composantes du vecteur d'onde. Le vecteur d'onde étant complexe dans la bande interdite, on peut se demander quelle est la direction de quantification du spin et tout simplement quelle signification peuvent revêtir les termes de "haut" et "bas". Comme cet hamiltonien est à deux dimensions, il est possible de faire des calculs analytiques ne dépassant pas quelques lignes et donnant des résultats très simples mais loin d'être intuitifs. Ce cas limite des faibles vecteurs d'onde complexes donne fort heureusement des résultats identiques à ce que donne l'hamiltonien H_{14} dans ce même cas limite et permet donc de donner un sens physique aux résultats numériques obtenus sur l'ensemble de la boucle. Ceci est décrit au chapitre 2. Enfin nous avons profité de ces résultats pour pro-

poser de construire un super-réseau qui permettrait de faire tourner les spins de façon différente selon leur état ("haut" ou "bas"), de sorte que les directions des deux spins dans l'espace réel forment un angle important.

Avant de rentrer dans le vif du sujet, donnons le plan du manuscrit. Le chapitre 1 rappelle quelques résultats de la théorie $\mathbf{k} \cdot \mathbf{p}$. Ce qui est connu de la structure de bande dans la bande interdite est aussi rappelé dans cette chapitre. Le cœur de ce travail est donné dans les chapitres 2 à 4. La conclusion met en évidence les principaux résultats. Enfin les annexes pourront être utiles aux lecteurs désireux de savoir plus précisément comment certains résultas ont été obtenus.

Chapitre 1

The main points of $\mathbf{k} \cdot \mathbf{p}$ theory

1.1 O_h and T_d groups

1.1.1 Brillouin zone

Crystals of diamond and zinc-blende semiconductors are constructed by two face-centered cubic (fcc) sublattices (A) and (B), shifted by one forth of the cube main diagonal. The atoms are placed at each sublattice point. If we take the Ox, Oy, and Oz axes and their corresponding unit vectors $\mathbf{e}_x$, $\mathbf{e}_y$, and $\mathbf{e}_z$ parallel to the [100], [010], and [001] directions of the crystal, an atom of sublattice (A) at the point $\mathbf{R}'_j = \mathbf{R}_j + \mathbf{a}$ has four nearest neighbors set at the points $\mathbf{R}_j + \mathbf{a}_n$, where $\mathbf{a} = a\,[1/4, 1/4, 1/4]\,; n = \{0, 1, 2, 3\} : \mathbf{a}_0 = 0$, $\mathbf{a}_1 = a\,(1/2, 1/2, 0)$, $\mathbf{a}_2 = a\,(1/2, 0, 1/2)$, and $\mathbf{a}_3 = a\,(0, 1/2, 1/2)$, where a is the length of of the unit cell. (See Fig. 1.1).

If the two atoms in the two sublattices are identical, we obtain the diamond structure. An inversion center exists in the middle of the segment joining these two atoms. These semiconductors belong to the O_h group. This is the case of the semiconductors of group IV such as Silicon, Gemanium, and Carbon.

If the two atoms in the two sublattices are different, we have the zinc-blende structure. This is the case of the III-V compounds such as GaAs, or II-VI such as ZnTe. These structures belong to the T_d group, where the inversion symmetry no longer exists.

The reciprocal lattice of this structure is the body-centered cubic lattice (bcc). Fig. 1.2 describes the common first Brillouin zone of the O_h and T_d groups, bounded by eight regular hexagonal faces and six square faces. Remarkable points

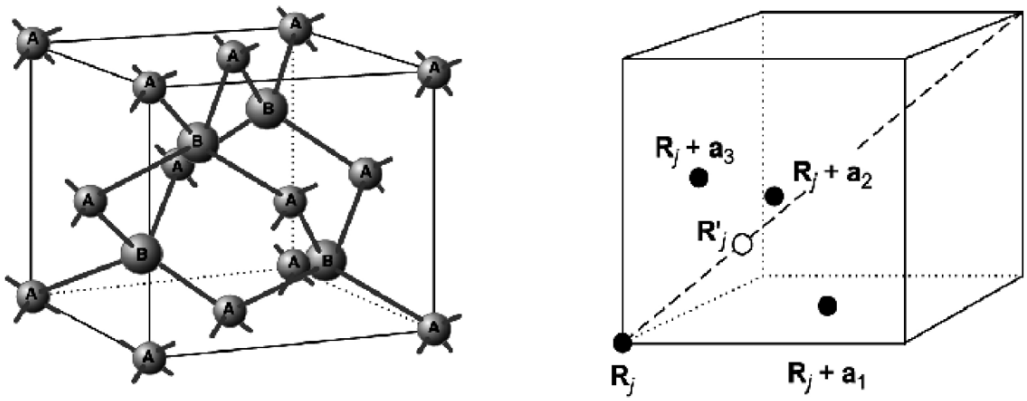

FIG. 1.1 – Left : two interpenetrating face-centered cubic sublattices form the diamond structure if the A and B atoms are identical and the zinc-blende structure if A and B are different. Right : four nearest neighbors of an atom in a zinc-blende structure.

are defined as follows

Γ	$(2\pi/a)\,(0,\ 0,\ 0)$	K'	$(2\pi/a)\,(1, 1/4, -1/4)$
X	$(2\pi/a)\,(1,\ 0,\ 0)$	U	$(2\pi/a)\,(1/4,\ 1,\ 1/4)$
L	$(2\pi/a)\,(1/2,\ 1/2,\ 1/2)$	W	$(2\pi/a)\,(1,\ 1/2,\ 0)$
K	$(2\pi/a)\,(3/4,\ 3/4,\ 0)$		

Γ is the center of the Brillouin zone. The K, K', and U points are equivalent from the point of view of crystallography. The Δ line connecting Γ and X, the Λ line connecting Γ and L, and the Σ line connecting Γ and K are three principal directions. Along the Δ direction, the first Brillouin zone lies in the interval $[-2\pi/a, 2\pi/a]$ with the width $4\pi/a$.

The present thesis tackles the spins in evanescent bands in GaAs, a semiconductor with T_d symmetry, but a starting point with O_h symmetry is necessary to understand the notations which are used.

1.1.2 Tight binding

Suppose that we have two identical atoms, A and A'. In the perfectly free state, their energy levels are given by E_s and E_p. When the spin is taken into account, E_s is two-fold degenerate with the corresponding atomic wave function s_a and E_p is six-fold degenerate, the corresponding atomic wave functions being

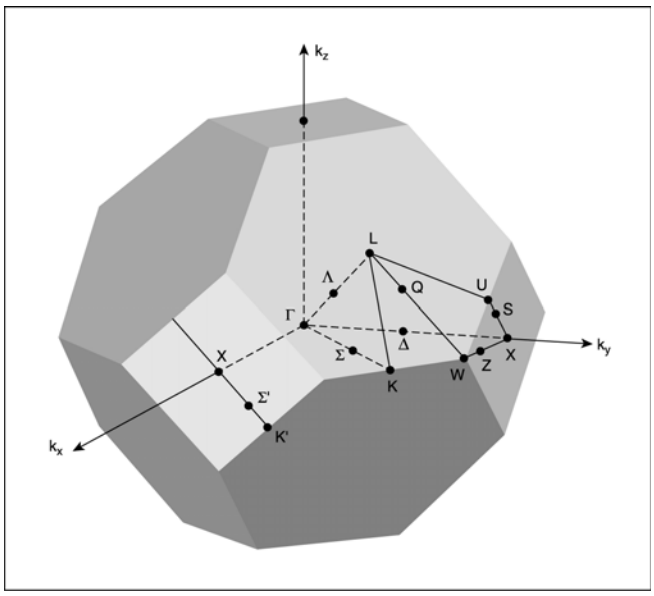

FIG. 1.2 – Common Brillouin zone of diamond and zinc-blende semiconductors.

$p_a = \{x_a, y_a, z_a\}$. If we put these two atoms together, at the points $\mathbf{R}_j$ and $\mathbf{R}'_j$, and at a near enough distance $d = \left|\mathbf{R}_j - \mathbf{R}'_j\right|$, there is a perturbation between the energy levels. The wave functions overlap and consequently, new energies levels are formed with the wave functions becoming linear combinations of the atomic functions s_a and p_a.

Fig. 1.3 represents the band structure resulting from tight-binding calculations for a semiconductor and a metal. The wave functions at the zone center are given hereafter :

$$\begin{array}{cccc} p(AB) & X_C = x_a + x'_a & p(B) & X = x_a - x'_a \\ p(AB) & Y_C = y_a + y'_a & p(B) & Y = y_a - y'_a \\ p_0(AB) & Z_C = z_a + z'_a & p_0(B) & Z = z_a - z'_a \\ s_0(AB) & S = s_a - s'_a & s_0(B) & S_V = s_a + s'_a \end{array}$$

The S, X_C, Y_C, and Z_C functions are antisymmetric, the S_V, X, Y, and Z functions are symmetric in the O_h group. Group theory shows that, in the O_h group, the S function has an xyz symmetry (the three axes play the same role), changing the sign when $\mathbf{r}$ is changed to $-\mathbf{r}$, the X, Y, and Z functions have respectively yz, zx, and xy symmetry (privileging the Ox, Oy and Oz axes respectively) which do not change their sign when $\mathbf{r}$ is changed to $-\mathbf{r}$; the function S_V has the s symmetry and the X_C, Y_C, and Z_C functions have x, y, and z symmetry under O_h operations.

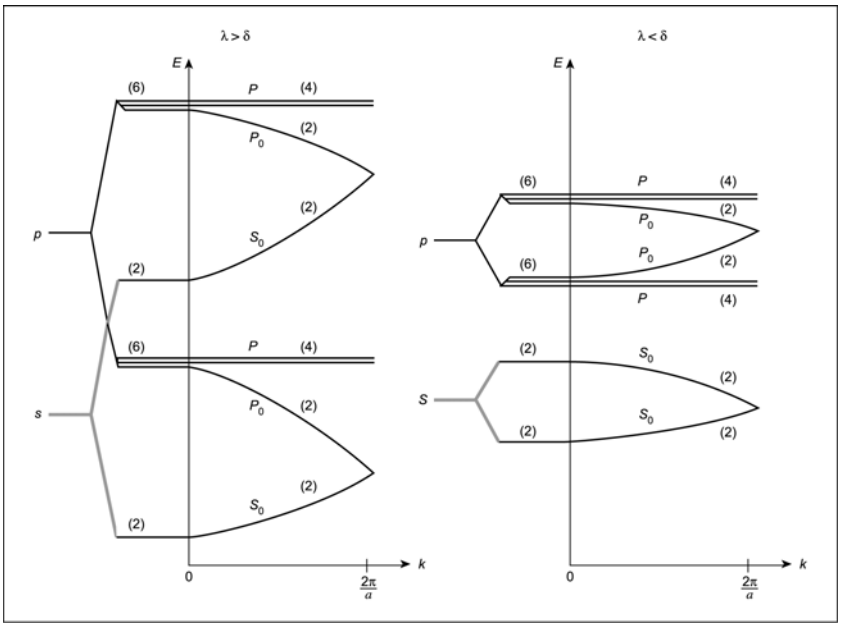

FIG. 1.3 – s and p free-electron energy levels are pertubed and give rise to the crystalline levels at $\mathbf{k} = \mathbf{0}$ when the two atoms become closer and closer. λ is the interaction energy between A and A' and $\delta = (E_p - E_s)/2$ is the half of the energy gap between the s and p atomic levels. We have a semiconductor (left) if $\lambda > \delta$ and a metal (right) if $\lambda < \delta$. For a semiconductor, from up to down : the antibonding conduction bands $p(AB)$, $p_0(AB)$, and $s_0(AB)$, and the bonding valence bands $p(B)$, $p_0(B)$, and $s_0(B)$ with their degeneracy degrees.

For materials without centro-symmetry, such as GaAs, which belongs to the T_d group - a group isomorphic to the O group of the cube, but where the inversion center is removed - the potential $\mathfrak{U}_d$ of T_d can be written : $\mathfrak{U}_d = \mathfrak{U}_{sym} + \mathfrak{U}_{antisym}$ where $\mathfrak{U}_{antisym}$ can be considered as a perturbation potential. The T_d wave functions are equal to those of O_h plus an additional part which arises from the perturbation potential. The energy correction is a second order term. The following table represents the T_d zone-center wave functions and their symmetry properties, where ε is a small coefficient. For T_d we keep the X_C, Y_C, Z_C, S, X, Y, Z, and S_V notations but now the S function is no longer strictly antisymmetric and the X, Y, and Z functions are not strictly symmetric.

	Band	Function	$LCAO$	Group	Symmetry
			(sp^3)		(sp^3)
BC	Γ_{5C}	X_C	$(x_a + x'_a) + \varepsilon(x_a - x'_a)$	Γ_5	$x + \varepsilon\, yz$
BC	Γ_{5C}	Y_C	$(y_a + y'_a) + \varepsilon(y_a - y'_a)$	Γ_5	$y + \varepsilon\, zx$
BC	Γ_{5C}	Z_C	$(z_a + z'_a) + \varepsilon(z_a - z'_a)$	Γ_5	$z + \varepsilon\, xy$
BC	Γ_1	S	$(s_a - s'_a) + \varepsilon(s_a + s'_a)$	Γ_1	$xyz + \varepsilon\, s$
BV	Γ_5	X	$(x_a - x'_a) + \varepsilon(x_a + x'_a)$	Γ_5	$yz + \varepsilon\, x$
BV	Γ_5	Y	$(y_a - y'_a) + \varepsilon(y_a + y'_a)$	Γ_5	$zx + \varepsilon\, y$
BV	Γ_5	Z	$(z_a - z'_a) + \varepsilon(z_a + z'_a)$	Γ_5	$xy + \varepsilon\, z$
BV	Γ_{1V}	S_V	$(s_a + s'_a) + \varepsilon(s_a - s'_a)$	Γ_1	$s + \varepsilon\, xyz$

Although the T_d wave functions and their symmetry resulting from tight binding calculation are approximative, they provide us a straightforward way to guess the non-zero coupling coefficient in the $\mathbf{k}\cdot\mathbf{p}$ framework [GF]. Group theory gives us the right symmetry because the perturbation from all the remote bands is automatically taken into account.

1.2 $\mathbf{k}\cdot\mathbf{p}$ Hamiltonian

1.2.1 Starting Hamiltonian

Taking into account the spin-orbit coupling, the Hamiltonian for an electron in the crystal writes

$$\begin{aligned} H_{SC} &= \frac{\mathbf{p}^2}{2m_0} + \mathfrak{U} + \frac{\hbar}{4m_0^2c^2}(\boldsymbol{\nabla}\mathfrak{U}\times\mathbf{p})\cdot\boldsymbol{\sigma} \\ &= H_{\mathfrak{U}} + H_{SO} \end{aligned} \tag{1.1}$$

where

$$H_{\mathfrak{U}} = \frac{\mathbf{p}^2}{2m_0} + \mathfrak{U} \qquad ; \qquad H_{SO} = \frac{\hbar}{4m_0^2c^2}(\boldsymbol{\nabla}\mathfrak{U} \times \mathbf{p}) \cdot \boldsymbol{\sigma} \tag{1.2}$$

$\mathfrak{U} = \mathfrak{U}(\mathbf{r})$ is the lattice periodic potential, m_0 is the free-electron mass, $\boldsymbol{\sigma} = \{\sigma_x, \sigma_y, \sigma_z\}$ is the Pauli operator, c is the speed of light. The wave function is the solution of the Schrödinger equation $H_{SC}\Psi = E\Psi$, having the Bloch's form $\Psi_{n,\mathbf{k}}(\mathbf{r}) = e^{i\mathbf{k}\cdot\mathbf{r}}\varphi_{n\mathbf{k}}(\mathbf{r})$. Let us consider the crystal Hamiltonian $H_{\mathfrak{U}}$, we have

$$\begin{aligned} H_{\mathfrak{U}}\left[e^{i\mathbf{k}\cdot\mathbf{r}}U_{n\mathbf{k}}(\mathbf{r})\right] &= \left\{\frac{\mathbf{p}^2}{2m_0} + \mathfrak{U}\right\}\left[e^{i\mathbf{k}\cdot\mathbf{r}}\varphi_{n\mathbf{k}}(\mathbf{r})\right] \\ &= e^{i\mathbf{k}\cdot\mathbf{r}}\left(\frac{\mathbf{p}^2}{2m_0} + \frac{\hbar}{m_0}\mathbf{k}\cdot\mathbf{p} + \breve{k}^2\right)\varphi_{n\mathbf{k}}(\mathbf{r}) + e^{i\mathbf{k}\cdot\mathbf{r}}\mathfrak{U}\varphi_{n\mathbf{k}}(\mathbf{r}) \\ &= e^{i\mathbf{k}\cdot\mathbf{r}}\left\{H_{\mathfrak{U}} + \breve{k}^2 + \frac{\hbar}{m_0}\mathbf{k}\cdot\mathbf{p}\right\}\varphi_{n\mathbf{k}}(\mathbf{r}) \end{aligned} \tag{1.3}$$

$\breve{k}^2 \equiv (\hbar^2/2m_0)\,k^2$ is the free-electron energy.

The term $H_{SO} = (\hbar/4m_0^2c^2)\,(\boldsymbol{\nabla}\mathfrak{U} \times \mathbf{p}) \cdot \boldsymbol{\sigma}$ represents the spin-orbit interaction

$$\begin{aligned} H_{SO}\Psi &= \left\{\frac{\hbar}{4m_0^2c^2}(\boldsymbol{\sigma} \times \boldsymbol{\nabla}\mathfrak{U}) \cdot \mathbf{p}\right\}\left[e^{i\mathbf{k}\cdot\mathbf{r}}\varphi_{n\mathbf{k}}(\mathbf{r})\right] \\ &= e^{i\mathbf{k}\cdot\mathbf{r}}\left\{\frac{\hbar}{4m_0^2c^2}(\boldsymbol{\sigma} \times \boldsymbol{\nabla}\mathfrak{U})\right\} \cdot [\hbar\mathbf{k} + \mathbf{p}]\,\varphi_{n\mathbf{k}}(\mathbf{r}) \\ &= e^{i\mathbf{k}\cdot\mathbf{r}}\left\{\frac{\hbar}{4m_0^2c^2}(\boldsymbol{\nabla}\mathfrak{U} \times \mathbf{p}) \cdot \boldsymbol{\sigma} + \frac{\hbar^2}{4m_0^2c^2}(\boldsymbol{\nabla}\mathfrak{U} \times \mathbf{k}) \cdot \boldsymbol{\sigma}\right\}\varphi_{n\mathbf{k}}(\mathbf{r}) \end{aligned} \tag{1.4}$$

so that

$$\begin{aligned} H_{SC}\Psi &= e^{i\mathbf{k}\cdot\mathbf{r}}\left[H_{\mathfrak{U}} + \breve{k}^2 + \frac{\hbar}{m_0}\mathbf{k}\cdot\mathbf{p} + \frac{\hbar}{4m_0^2c^2}(\boldsymbol{\nabla}\mathfrak{U} \times \mathbf{p}) \cdot \boldsymbol{\sigma} + \frac{\hbar^2}{4m_0^2c^2}(\boldsymbol{\nabla}\mathfrak{U} \times \mathbf{k}) \cdot \boldsymbol{\sigma}\right]\varphi_{n\mathbf{k}}(\mathbf{r}) \\ &= e^{i\mathbf{k}\cdot\mathbf{r}}\left[H_{SC} + \breve{k}^2 + \frac{\hbar}{m_0}\mathbf{k}\cdot\mathbf{p} + \frac{\hbar^2}{4m_0^2c^2}(\boldsymbol{\nabla}\mathfrak{U} \times \mathbf{k}) \cdot \boldsymbol{\sigma}\right]\varphi_{n\mathbf{k}}(\mathbf{r}) \end{aligned} \tag{1.5}$$

The Schrödinger equation becomes

$$\left[H_{SC} + \breve{k}^2 + \frac{\hbar}{m_0}\mathbf{k}\cdot\mathbf{p} + \frac{\hbar^2}{4m_0^2c^2}(\boldsymbol{\nabla}\mathfrak{U} \times \mathbf{k}) \cdot \boldsymbol{\sigma}\right]\varphi_{n\mathbf{k}}(\mathbf{r}) = E_{n\mathbf{k}}\varphi_{n\mathbf{k}}(\mathbf{r}) \tag{1.6}$$

In the T_d group, the last term $H_{SO}^{\mathbf{k}} = (\hbar^2/4m_0^2c^2)\,(\nabla\mathfrak{U} \times \mathbf{k}) \cdot \boldsymbol{\sigma}$ does not introduce new splittings. Furthermore its influence is negligible [KAN]. Finally we obtain

$$\left[H_{SC} + \breve{k}^2 + \frac{\hbar}{m_0}\mathbf{k}\cdot\mathbf{p}\right]\varphi_{n\mathbf{k}}(\mathbf{r}) = E_{n\mathbf{k}}\varphi_{n\mathbf{k}}(\mathbf{r}) \tag{1.7}$$

The functions $\varphi_{n\mathbf{k}}(\mathbf{r})$ at $\mathbf{k}=\mathbf{0}$ are supposed to be known through their symmetry properties. We denote $\varphi_n = \varphi_{n(\mathbf{k}=\mathbf{0})}(\mathbf{r})$ and $E_n = E_{n(\mathbf{k}=\mathbf{0})}$ with $H_{SC}\varphi_n = E_n\varphi_n$. The functions at $\mathbf{k}\neq\mathbf{0}$ can be expanded as series of φ_n

$$\varphi_{n\mathbf{k}}(\mathbf{r}) = \sum_{\mathbf{k}} C_{n\mathbf{k}}\varphi_n \tag{1.8}$$

Multiplying Eq. 1.7 with φ_m^* and integrating over the unit cell, we obtain the equation determining the $C_{n\mathbf{k}}$ coefficient

$$\left[\langle\varphi_m|\left(H_{SC}+\frac{\hbar}{m_0}\mathbf{k}\cdot\mathbf{p}\right)|\varphi_n\rangle + \breve{k}^2\delta_{mn} - E_{n\mathbf{k}}\delta_{mn}\right]C_{n\mathbf{k}} = 0 \tag{1.9}$$

$\{\varphi_n\}$ is the relevant set of basis functions, $\langle\varphi_m|A|\varphi_n\rangle = (1/V)\int_V \varphi_m^*(\mathbf{r})\,A\varphi_n(\mathbf{r})\,d\mathbf{r}$ where V is the crystal volume. The energy E is the solution of the secular equation $\det\left(H_{\mathbf{kp}} - E\mathbb{I}\right) = 0$, $\mathbb{I}$ being the identity matrix and

$$H_{\mathbf{kp}} = \langle\varphi_m|\left(H_{SC}+\frac{\hbar}{m_0}\mathbf{k}\cdot\mathbf{p}\right)|\varphi_n\rangle + \breve{k}^2\delta_{mn} \tag{1.10}$$

1.2.2 Basis functions

We first construct the Hamiltonian for GaAs inside the $\{\Gamma_{5C},\Gamma_1,\Gamma_5\}\times\{\uparrow,\downarrow\}$ space taking into account the spin-orbit interaction. The basis functions are formed from the functions $X_C\uparrow(\downarrow)$, $Y_C\uparrow(\downarrow)$, $Z_C\uparrow(\downarrow)$, $S\uparrow(\downarrow)$, $X\uparrow(\downarrow)$, $Y\uparrow(\downarrow)$, and $Z\uparrow(\downarrow)$. The atomic functions s_a and p_a resulting from the hydrogen atom solutions, are of the form $f(r)\mathcal{Y}_{\ell m}(\theta,\varphi)$, where $\ell = 1,2,3...$, $m = \{-\ell,-\ell+1,...\ell\}$ and $\mathcal{Y}_{\ell m}(\theta,\varphi)$ is the spherical harmonic. The s function corresponds to $\ell=0$ (and therefore $m=0$), $s\sim e^{-r/a_0}$, where a_0 is the Bohr radius. The p functions come from $\ell=1$ (therefore $m=\{1,0,-1\}$); x_a, y_a, and z_a are respectively proportional to the functions xe^{-r/a_0}, ye^{-r/a_0}, and ze^{-r/a_0}. We have $\mathcal{Y}_{11} = i\left(x_a+iy_a\right)/\sqrt{2}$, $\mathcal{Y}_{10} = iz_a$, and $\mathcal{Y}_{1-1} = i\left(x_a-iy_a\right)/\sqrt{2}$. If we add spin with $\mathbf{s}=1/2$, the total moment is defined as $\mathbf{j}=\mathbf{l}+\mathbf{s}$. The projection of $\mathbf{j}$ on the z axis takes the values $m=j_z\in\{-j,-j+1,...j\}$. We are interested in the $|j\ m\rangle$ states which satisfy $|j\ m\rangle = \sqrt{j(j+1)-m(m-1)}\,|j\ m-1\rangle$. For s_a, $\ell=0$ and $j=1/2$ we have two states $|s+\rangle = |1/2,1/2\rangle_s$ and $|s-\rangle = |1/2,-1/2\rangle_s$. For $\ell=1$, we have four states ($|3/2\ -3/2\rangle_a$, $|3/2\ -1/2\rangle_a$, $|3/2\ 1/2\rangle_a$, and $|3/2\ 3/2\rangle_a$) corresponding to $j=3/2$ and two states ($|1/2\ -1/2\rangle_a$, $|1/2\ 1/2\rangle_a$) corresponding to $j=1/2$ given

as follows

$$\begin{array}{lcl} |3/2\ 3/2\rangle_a & = & |\mathcal{Y}_{11}\uparrow\rangle \\ |3/2\ 1/2\rangle_a & = & \left|\sqrt{2/3}\,\mathcal{Y}_{10}\uparrow+\frac{1}{\sqrt{3}}\,\mathcal{Y}_{11}\downarrow\right\rangle \\ |3/2\ -1/2\rangle_a & = & \left|1/\sqrt{3}\,\mathcal{Y}_{1-1}\uparrow+\sqrt{2/3}\,\mathcal{Y}_{10}\downarrow\right\rangle \\ |3/2\ -3/2\rangle_a & = & |\mathcal{Y}_{1-1}\downarrow\rangle \\ |1/2\ 1/2\rangle_a & = & \left|1/\sqrt{3}\,\mathcal{Y}_{10}\uparrow-\sqrt{2/3}\,\mathcal{Y}_{11}\downarrow\right\rangle \\ |1/2\ -1/2\rangle_a & = & \left|\sqrt{2/3}\,\mathcal{Y}_{1-1}\uparrow-1/\sqrt{3}\,\mathcal{Y}_{10}\downarrow\right\rangle \end{array} \tag{1.11}$$

The electron in the lattice does not have a true-orbital momentum l but only a pseudo-orbital momentum "L". The S function corresponds to "L"$=0$ while X, Y, and Z correspond to "L"$=1$. The sum "$\mathbf{J}$"="$\mathbf{L}$"+$\mathbf{S}$ is no longer defined, but starting with "L"$=0$ we can write "J"$=1/2$ for the Γ_6 band, starting with "L"$=1$ we can write "J"$=1/2$ for the Γ_7 band, and "J"$=3/2$ for the Γ_8 band. By analogy to the hydrogen atom case, we construct semiconductor cubic functions, after replacing the spherical harmonic $\mathcal{Y}_{\ell m}$ by cubic harmonics $Y_{\ell m}$, the atomic functions x_a, y_a, and z_a being replaced by the X, Y, and Z functions. Therefore, we define

$$Y_{11}=i\frac{X+iY}{-\sqrt{2}},\quad Y_{10}=iZ,\quad Y_{1-1}=i\frac{X-iY}{\sqrt{2}} \tag{1.12}$$

And similarly to the functions given in Eq. 1.11, we write the functions which we will choose as the basis to expand the $\mathbf{k}\cdot\mathbf{p}$ matrix

$$\begin{array}{lcl} |c3/2\rangle & = & \left|i\left[-\left(1/\sqrt{2}\right)\ (X_C+iY_C)\uparrow\right]\right\rangle \\ |c1/2\rangle & = & \left|i\left[\sqrt{2/3}\,Z_C\uparrow-1/\sqrt{6}\ (X_C+iY_C)\downarrow\right]\right\rangle \\ |c-1/2\rangle & = & \left|i\left[1/\sqrt{6}\ (X_C-iY_C)\uparrow+\sqrt{2/3}\,Z_C\downarrow\right]\right\rangle \\ |c-3/2\rangle & = & \left|i\left[1/\sqrt{2}\ (X_C-iY_C)\downarrow\right]\right\rangle \\ |c7/2\rangle & = & \left|i\left[1/\sqrt{3}\,Z_C\uparrow+\sqrt{2/3}\ (X_C+iY_C)\downarrow\right]\right\rangle \\ |c-7/2\rangle & = & \left|i\left[\sqrt{1/3}\,(X_C-iY_C)\uparrow-1/\sqrt{3}\,Z_C\downarrow\right]\right\rangle \\ |+\rangle & = & |S\uparrow\rangle \\ |-\rangle & = & |S\downarrow\rangle \end{array} \tag{1.13}$$

$$
\begin{array}{lcl}
|3/2\rangle & = & \left| i\left[-\left(1/\sqrt{2}\right)\ (X+iY)\uparrow\right]\right\rangle \\
|1/2\rangle & = & \left| i\left[\sqrt{2/3}\ Z\uparrow - 1/\sqrt{6}\ (X+iY)\downarrow\right]\right\rangle \\
|-1/2\rangle & = & \left| i\left[1/\sqrt{6}\ (X-iY)\uparrow + \sqrt{2/3}\ Z\downarrow\right]\right\rangle \\
|-3/2\rangle & = & \left| i\left[1/\sqrt{2}\ (X-iY)\downarrow\right]\right\rangle \\
|7/2\rangle & = & \left| i\left[1/\sqrt{3}\ Z\uparrow + \sqrt{2/3}\ (X+iY)\downarrow\right]\right\rangle \\
|-7/2\rangle & = & \left| i\left[\sqrt{1/3}\,(X-iY)\uparrow - 1/\sqrt{3}\ Z\downarrow\right]\right\rangle
\end{array}
\tag{1.14}
$$

we have introduced the notations
$|cM\rangle$ instead of $|3/2\ M\rangle_{\Gamma_{8C}}$,
$|M\rangle$ instead of $|3/2\ M\rangle_{\Gamma_8}$,
$|c\pm 7/2\rangle$ instead of $|1/2\ \pm 1/2\rangle_{\Gamma_{7C}}$,
and $|\pm 7/2\rangle$ instead of $|1/2\ \pm 1/2\rangle_{\Gamma_7}$.
The 7/2 number only recalls that these functions have the Γ_7 symmetry.

The following table allows us to compare the notations and the symmetry properties of the wave functions of the T_d group in the case without spin and including spin.

Without spin	Γ	Ψ		With spin	Γ	Ψ
Γ_5	Γ_{5C}	$X_C,\ Y_C,\ Z_C$		Γ_8	Γ_{8C}	$\lvert cM\rangle$
Γ_5	Γ_{5C}	$X_C,\ Y_C,\ Z_C$		Γ_7	Γ_{7C}	$\lvert c\pm 7/2\rangle$
Γ_1	Γ_1	S		Γ_6	Γ_6	$\lvert\pm\rangle$
Γ_5	Γ_5	$X,\ Y,\ Z$		Γ_8	Γ_8	$\lvert M\rangle$
Γ_5	Γ_5	$X,\ Y,\ Z$		Γ_7	Γ_7	$\lvert\pm 7/2\rangle$

1.2.3 $\mathbf{k}\cdot\mathbf{p}$ term

We need a Hamiltonian which describes at least ten percent of the Brillouin zone, as we shall show in section 1.3. The smallest possible Hamiltonian is the 14×14 matrix. Taking the 14 $|\varphi_n\rangle$ functions (Eqs. 1.13 and 1.14) as basis functions, we are going to calculate the elements of the 14×14 $\mathbf{k}\cdot\mathbf{p}$ matrix. Note that $H_{SC} = H_{\mathfrak{U}} + H_{SO}$ and $\langle\varphi_m|H_{\mathfrak{U}}|\varphi_n\rangle = E_n\delta_{mn}$. As $H_{\mathfrak{U}}$ does not include the spin, E_n is the energy corresponding to the wave function in the simple group, i.e., $\langle cM|H_{\mathfrak{U}}|cM\rangle = \langle c\pm 7/2|H_{\mathfrak{U}}|\pm 7/2\rangle = E_{5C}$, $\langle\pm|H_{\mathfrak{U}}|\pm\rangle = E_1$, and $\langle M|H_{\mathfrak{U}}|M\rangle = \langle\pm 7/2|H_{\mathfrak{U}}|\pm 7/2\rangle = E_5$. Therefore, from Eq. 1.9, we have to determine two terms : $(\hbar/m_0)\,\langle\varphi_m|\mathbf{k}\cdot\mathbf{p}|\varphi_n\rangle$, the $\mathbf{k}\cdot\mathbf{p}$ term, and $\langle\varphi_m|H_{SO}|\varphi_n\rangle$, the spin-orbit term. We first consider the $\mathbf{k}\cdot\mathbf{p}$ term. Let $U_{n\sigma}$ be the set of func-

tions $\{X, Y, Z, S, X_C, Y_C, Z_C\} \times \{\uparrow, \downarrow\}$. From Eqs. 1.13 and 1.14, $|\varphi_n\rangle$ is a linear combination of $U_{n\sigma}$. This leads us to calculate $\langle U_{m\sigma}| \left(\hbar/m_0\right) \mathbf{k} \cdot \mathbf{p} |U_{n\sigma'}\rangle$. We have

$$\langle U_{m\sigma}| \frac{\hbar}{m_0} \mathbf{k} \cdot \mathbf{p} |U_{n\sigma'}\rangle = \langle U_m| \frac{\hbar}{m_0} \mathbf{k} \cdot \mathbf{p} |U_n\rangle \delta_{\sigma\sigma'} \tag{1.15}$$

This term is non-zero only when $\sigma = \sigma'$. Besides

$$\langle U_m| \frac{\hbar}{m_0} \mathbf{k} \cdot \mathbf{p} |U_n\rangle = \frac{\hbar}{m_0} \sum_{\alpha=x,y,z} \langle U_m| k_\alpha p_\alpha |U_n\rangle = \frac{\hbar}{m_0} \sum_{\alpha=x,y,z} k_\alpha \langle U_m| p_\alpha |U_n\rangle \tag{1.16}$$

Following group theory, if the Ψ_{Γ_n} functions have the Γ_n symmetry, Ψ_{Γ_p} the Γ_p symmetry, and the A_{Γ_m} operator the Γ_m symmetry, then the quantity

$$A = \langle \Psi_{\Gamma_n}| A_{\Gamma_m} |U_{n\sigma'}\rangle \quad \begin{cases} = 0 & \text{if } \Gamma_1 \notin (\Gamma_n \times \Gamma_m \times \Gamma_p) \\ \neq 0 & \text{if } \Gamma_1 \in (\Gamma_n \times \Gamma_m \times \Gamma_p) \end{cases} \tag{1.17}$$

Let us consider the term $\langle U_m| p_\alpha |U_n\rangle$ (Eq. 1.16) :

i) $\langle S| p_\alpha |S\rangle$.

We have $\Gamma_1 \notin [\Gamma_1 \times \Gamma_5 \times \Gamma_1 = \Gamma_5 \times \Gamma_1 = \Gamma_5]$

and therefore $\langle S| k_\alpha |S\rangle = 0$.

ii) $\langle S| p_\alpha |X, Y, Z, X_C, Y_C, Z_C\rangle$.

We have $\Gamma_1 \in [\Gamma_1 \times \Gamma_5 \times \Gamma_5 = \Gamma_5 \times \Gamma_5 = (\Gamma_1 + \Gamma_3 + \Gamma_4 + \Gamma_5)]$

so that $\langle S| p_\alpha |X, Y, Z, X_C, Y_C, Z_C\rangle$ may be non-zero. The coupling coefficients - Table 83 in the book by Koster [KOS] - give us

$\langle S| p_x |X\rangle = \langle S| p_y |Y\rangle = \langle S| p_z |Z\rangle$; $\langle S| p_x |X_C\rangle = \langle S| p_y |Y_C\rangle = \langle S| p_z |Z_C\rangle$

These quantities are pure-imaginary elements due to the properties of the orbital-like functions.

iii) $\langle X\,(Y, Z, X_C, Y_C, Z_C)\, |p_\alpha| X\,(Y, Z, X_C, Y_C, Z_C)\rangle$.

We have $\Gamma_5 \times \Gamma_5 \times \Gamma_5 = (\Gamma_1 + \Gamma_3 + \Gamma_4 + \Gamma_5) \times \Gamma_5$

$$= \Gamma_5 + (\Gamma_4 + \Gamma_5) + (\Gamma_2 + \Gamma_3 + \Gamma_4 + \Gamma_5) + (\Gamma_1 + \Gamma_3 + \Gamma_4 + \Gamma_5)$$
$$= (\Gamma_1 + \Gamma_2 + 2\Gamma_3 + 3\Gamma_4 + 4\Gamma_5)$$

so that $\Gamma_1 \in (\Gamma_5 \times \Gamma_5 \times \Gamma_5)$. Then $\langle X\,(Y, Z)\, |p_\alpha| X\,(Y, Z)\rangle$ may differ from 0.

The coupling coefficients - Table 83 of Koster [KOS] - give us :

$\langle X| p_y |Z\rangle = \langle X| p_z |Y\rangle = \langle Y| p_x |Z\rangle = \langle Y| p_z |X\rangle = \langle Z| p_x |Y\rangle = \langle Z| p_y |X\rangle = M$,

and

$\langle X| p_y |Z_C\rangle = \langle X| p_z |Y_C\rangle = \langle Y| p_x |Z_C\rangle$

$$= \langle Y| p_z |X_C\rangle = \langle Z| p_x |Y_C\rangle = \langle Z| p_y |X_C\rangle = M'$$

According to Dresselhauss [DRE.55] $M = 0$, $M' \neq 0$.

In summary, the non-zero $\mathbf{k}\cdot\mathbf{p}$ terms are

$$\begin{aligned}\langle S|p_x|iX\rangle &= \langle S|p_y|iY\rangle = \langle S|p_z|iZ\rangle = \varpi \qquad (1.18)\\ \langle S|p_x|iX_C\rangle &= \langle S|p_y|iY_C\rangle = \langle S|p_y|iZ_C\rangle = \varpi' \qquad (1.19)\end{aligned}$$

$$\begin{aligned}\langle X|p_y|iZ_C\rangle &= \langle X|p_z|iY_C\rangle = \langle Y|p_x|iZ_C\rangle\\ &= \langle Y|p_z|iX_C\rangle = \langle Z|p_x|iY_C\rangle\\ &= \langle Z|p_y|iX_C\rangle = -\varpi_X \qquad (1.20)\end{aligned}$$

where ϖ, ϖ', ϖ_X are real. We define the real $\mathbf{k}\cdot\mathbf{p}$ parameters

$$P = \frac{\hbar}{m_0}\varpi \qquad P' = \frac{\hbar}{m_0}\varpi' \qquad P_X = \frac{\hbar}{m_0}\varpi_X \qquad (1.21)$$

and the corresponding energies

$$E_P = \left(2m_0/\hbar^2\right)P^2 \qquad E_{P'} = \left(2m_0/\hbar^2\right)P'^2 \qquad E_{P_X} = \left(2m_0/\hbar^2\right)P_X^2 \qquad (1.22)$$

1.2.4 Spin-orbit coupling

Now, we determine the term describing the spin-orbit interaction

$$H_{SO} = \frac{\hbar^2}{4m_0^2c^2}(\nabla\mathfrak{U}\times\mathbf{k})\cdot\boldsymbol{\sigma} \qquad (1.23)$$

We denote $\zeta = \hbar/4m_0^2c^2$ and $\mathbf{G} = \boldsymbol{\nabla}\mathfrak{U}\times\mathbf{p}$, then $H_{SO} = \zeta\ \mathbf{G}\cdot\boldsymbol{\sigma}$. To calculate the terms of the type $\langle U_{m\sigma}|H_{SO}|U_{n\sigma'}\rangle$, we note that

a) $\zeta\langle U_m\uparrow|\mathbf{G}\cdot\boldsymbol{\sigma}|U_n\downarrow\rangle = \zeta\langle U_m\uparrow|\left(G_x\sigma_x + G_y\sigma_y + G_z\sigma_z\right)|U_n\downarrow\rangle$
$= \zeta\langle U_m\uparrow|\left(G_x - iG_y\right)||U_n\uparrow\rangle$

therefore

$$\zeta\langle U_m\uparrow|\mathbf{G}\cdot\boldsymbol{\sigma}|U_n\downarrow\rangle = \zeta\langle U_m|G_x|U_n\rangle - i\zeta\langle U_m|G_y|U_n\rangle \qquad (1.24)$$

b) $\zeta\langle U_m\uparrow|\mathbf{G}\cdot\boldsymbol{\sigma}|U_n\uparrow\rangle = \zeta\langle U_m\uparrow|\left(G_x\sigma_x + G_y\sigma_y + G_z\sigma_z\right)|U_n\uparrow\rangle$
$= \zeta\langle U_m\uparrow|G_z|U_n\uparrow\rangle$

therefore

$$\zeta\langle U_m\uparrow|\mathbf{G}\cdot\boldsymbol{\sigma}|U_n\uparrow\rangle = \zeta\langle U_m|G_z|U_n\rangle \qquad (1.25)$$

c) $\zeta\langle U_m\downarrow|\mathbf{G}\cdot\boldsymbol{\sigma}|U_n\uparrow\rangle = \zeta\langle U_m\downarrow|\left(G_x\sigma_x + G_y\sigma_y + G_z\sigma_z\right)|U_n\uparrow\rangle$
$= \zeta\langle U_m\downarrow|\left(G_x + iG_y\right)|U_n\downarrow\rangle$

therefore

$$\zeta\langle U_m\uparrow|\mathbf{G}\cdot\boldsymbol{\sigma}|U_n\uparrow\rangle = \zeta\langle U_m|G_x|U_n\rangle + i\zeta\langle U_m|G_y|U_n\rangle \qquad (1.26)$$

d) $\zeta\langle U_m \downarrow |\mathbf{G}\cdot\boldsymbol{\sigma}|U_n \downarrow\rangle = \zeta\langle U_m \downarrow |\left(G_x\sigma_x + G_y\sigma_y + G_z\sigma_z\right)|U_n \downarrow\rangle$
$= \zeta\langle U_m \downarrow |\left(-G_z\right)|U_n \downarrow\rangle$

therefore

$$\zeta\langle U_m \downarrow |\mathbf{G}\cdot\boldsymbol{\sigma}|U_n \uparrow\rangle = -\zeta\langle U_m|G_z|U_n\rangle \tag{1.27}$$

This leads us to calculate $\langle U_m|G_\alpha|U_n\rangle$, where $U_m = \{S, X, Y, Z, X_C, Y_C, Z_C\}$. In T_d, the G_α operator transforms like a pseudo-vector which belongs to Γ_4 representation. Consider

i) $\langle S|G_\alpha|S\rangle$.

We have $\Gamma_1 \notin [\Gamma_1 \times \Gamma_4 \times \Gamma_1 = \Gamma_4]$, so that $\langle S|G_\alpha|S\rangle = 0$.

ii) $\langle S|G_\alpha|X(Y, Z, X_C, Y_C, Z_C)\rangle$.

We have $\Gamma_1 \notin [\Gamma_1 \times \Gamma_4 \times \Gamma_5 = \Gamma_4 \times \Gamma_5 = (\Gamma_2 + \Gamma_3 + \Gamma_4 + \Gamma_5)]$,
so that $\langle S|G|X(YZ)\rangle = 0$.

iii) $\langle X(Y, Z, X_C, Y_C, Z_C)|G_\alpha|X(Y, Z, X_C, Y_C, Z_C)\rangle$.

We have $\Gamma_1 \in [\Gamma_5 \times \Gamma_4 \times \Gamma_5 = (\Gamma_2 + \Gamma_3 + \Gamma_4 + \Gamma_5) \times \Gamma_5]$,
so that $\langle X(Y, Z, X_C, Y_C, Z_C)|G_\alpha|X(Y, Z, X_C, Y_C, Z_C)\rangle$ may differ from 0.

The coupling coefficients - Table 83 of Koster [KOS] - give us

$$\langle X\,|G_y|\,Z\rangle = +\delta \qquad \langle Y\,|G_z|\,X\rangle = +\delta \qquad \langle Z\,|G_x|\,Y\rangle = +\delta \tag{1.28}$$
$$\langle X\,|G_z|\,Y\rangle = -\delta \qquad \langle Y\,|G_x|\,Z\rangle = -\delta \qquad \langle Z\,|G_y|\,X\rangle = -\delta \tag{1.29}$$
$$\Delta = 3i\zeta\,(-\delta)\,. \tag{1.30}$$

$$\langle X_C\,|G_y|\,Z_C\rangle = +\delta^C \qquad \langle Y_C\,|G_z|\,X_C\rangle = +\delta^C \qquad \langle Z_C\,|G_x|\,Y_C\rangle = +\delta^C \tag{1.31}$$
$$\langle X_C\,|G_z|\,Y_C\rangle = -\delta^C \qquad \langle Y_C\,|G_x|\,Z_C\rangle = -\delta^C \qquad \langle Z_C\,|G_y|\,X_C\rangle = -\delta^C \tag{1.32}$$
$$\Delta^C = 3i\zeta\left(-\delta^C\right). \tag{1.33}$$

$$\langle X\,|G_y|\,Z_C\rangle = +\delta' \qquad \langle Y\,|G_z|\,X_C\rangle = +\delta' \qquad \langle Z\,|G_x|\,Y_C\rangle = +\delta' \tag{1.34}$$
$$\langle X\,|G_z|\,Y_C\rangle = -\delta' \qquad \langle Y\,|G_x|\,Z_C\rangle = -\delta^C \qquad \langle Z\,|G_y|\,X_C\rangle = -\delta' \tag{1.35}$$
$$\Delta' = 3i\zeta\left(-\delta'\right). \tag{1.36}$$

In other words

$$\Delta^C = \left(\frac{3\hbar^2}{4m_0^2c^2}\right)\left\langle X_C\left|\frac{\partial\mathfrak{U}}{\partial x}p_y - \frac{\partial\mathfrak{U}}{\partial y}p_x\right|iY_C\right\rangle \tag{1.37}$$
$$\Delta = \left(\frac{3\hbar^2}{4m_0^2c^2}\right)\left\langle X\left|\frac{\partial\mathfrak{U}}{\partial x}p_y - \frac{\partial\mathfrak{U}}{\partial y}p_x\right|iY\right\rangle \tag{1.38}$$
$$\Delta' = \left(\frac{3\hbar^2}{4m_0^2c^2}\right)\left\langle X\left|\frac{\partial\mathfrak{U}}{\partial x}p_y - \frac{\partial\mathfrak{U}}{\partial y}p_x\right|iY_C\right\rangle \tag{1.39}$$

All the others terms of the form $\langle X\,|G_y|\,Y\rangle$ are equal to 0.

1.2.5 14×14 $\mathbf{k} \cdot \mathbf{p}$ matrix inside $\{\Gamma_{5C},\ \Gamma_1,\ \Gamma_5\}$

Now, the 14×14 $\mathbf{k}\cdot\mathbf{p}$ matrix elements can be easily calculated. Only the spin-orbit term contributes to the elements in the diagonal. These diagonal elements are :
$\langle cM|H_{\mathbf{kp}}\,|cM\rangle = E_{5C} + \Delta^C/3 + \breve{k}^2 = E_{8C} + \breve{k}^2$, where $E_{8C} = E_{5C} + \Delta^C/3$;
$\langle c\pm7/2|H_{\mathbf{kp}}\,|c\pm7/2\rangle = E_{5C} - 2\Delta^C/3 + \breve{k}^2 = E_{7C} + \breve{k}^2$ where $E_{7C} = E_{5C} - 2\Delta^C/3$;
$\langle\pm|H_{\mathbf{kp}}\,|\pm\rangle = E_1 + \breve{k}^2 = E_6 + \breve{k}^2$, where $E_6 = E_1$;
$\langle M|H_{\mathbf{kp}}\,|M\rangle = E_5 + \Delta/3 + \breve{k}^2 = E_8 + \breve{k}^2$, where $E_8 = E_5 + \Delta/3$;
$\langle\pm7/2|H_{\mathbf{kp}}\,|\pm7/2\rangle = E_5 - 2\Delta/3 + \breve{k}^2 = E_7 + \breve{k}^2$, where $E_7 = E_5 - 2\Delta/3$.

$\Delta^C = E_{8C} - E_{7C}$ (respectively $\Delta = E_8 - E_7$) is the spin-orbit splitting resulting from spin-orbit interaction inside $\{\Gamma_{7C}, \Gamma_{8C}\}$ (respectively $\{\Gamma_7, \Gamma_8\}$). In the presence of spin-orbit interactions, the energy level Γ_{5C} (respectively Γ_5) is split, two new levels E_{8C} and E_{7C} (respectively E_8 and E_7) are formed, separated by the quantity Δ^C (respectively Δ). The E_{8C} (respectively E_8) level is fourfold degenerate, the functions are $|cM\rangle$ (respectively $|M\rangle$). The E_{7C} (respectively E_7) level is twice degenerate, the functions are $|c \pm 7/2 >$ (respectively $| \pm 7/2 >$). The band schema is illustrated in the Fig. 1.4.

Due to the symmetry between $\{\Gamma_{7C}, \Gamma_{8C}\}$ and $\{\Gamma_{7C}, \Gamma_{8C}\}$, the $\langle cM|H_{\mathbf{kp}}\,|M\rangle$ and $\langle c \pm 7/2|H_{\mathbf{kp}}\,|\pm7/2\rangle$ also come from the spin-orbit term, we have :
$\langle cM|H\,|M\rangle = \Delta'/3$
$\langle c \pm 7/2|H\,|\pm7/2\rangle = -2\Delta'/3$.

Δ', proportional to $\langle cM|H\,|M\rangle$, is the interband spin-orbit energy. From a group theory point of view, Δ^C was born when we constructed the $\Gamma_{7C} + \Gamma_{8C}$ double group representation from Γ_{5C} simple group representation, Δ was born when we constructed the $\Gamma_7 + \Gamma_8$ double group representation from Γ_5 simple group representation while Δ' results from the fact that the eigen functions $|M\rangle$ and $|\pm7/2\rangle$ are built from the Γ_5 functions and are not the true functions of Γ_8 and Γ_7.

We denote $E_G = E_6 - E_8$; E_G is the width of the fundamental gap, $E^\Delta = E_{7C} - E_6$, $E^G = E^\Delta + \Delta^C$, and $E_\Delta = E_G + \Delta$. Let us choose E_8 as the energy origin. Then the 14×14 $\mathbf{k}\cdot\mathbf{p}$ Hamiltonian is written in Eq. 1.40, where $P^z = Pk_z$, $P^\pm = Pk_\pm$, $P_X^z = P_X k_z$, and $P_X^\pm = P_X k_\pm$; $\breve{E}_j = E_j + \breve{k}^2$ with $E_j = \{E_{8C}, E_{7C}, E_6\}$. The elements below the diagonal are complex conjugate (cc) of the elements above the diagonal, i.e., $(H_{\mathbf{kp}})_{ji} = (H_{\mathbf{kp}})^*_{ij}$. At $k = 0$, $H_{\mathbf{kp}} \equiv H_{SC}$. If the interband spin-orbit interaction is zero, i.e., $\Delta' = 0$, the 14×14 $\mathbf{k}\cdot\mathbf{p}$ is diagonalized : the

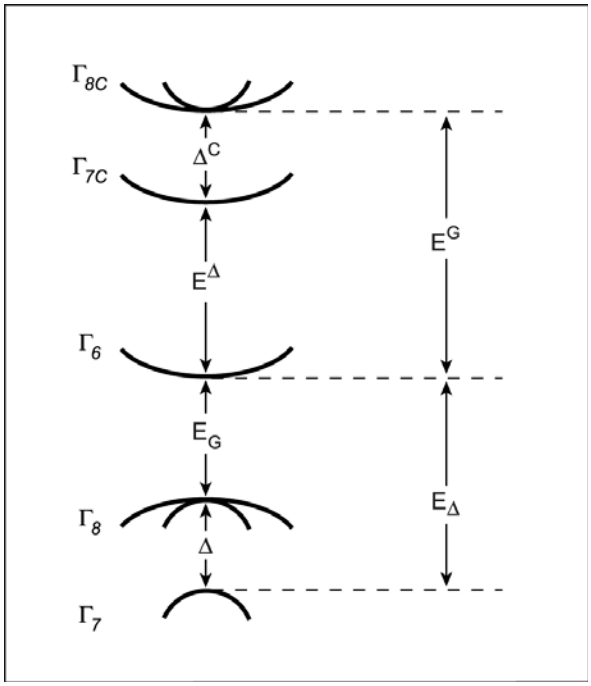

FIG. 1.4 – Band schema used in the construction of the 14×14 $\mathbf{k} \cdot \mathbf{p}$ Hamiltonian.

basis functions (Eqs. 1.13, 1.14) are eigenstates of the Hamiltonian H_{SC} (Eq. 1.1) at $\mathbf{k} = 0$.

$$
\begin{bmatrix}
\left|c\frac{3}{2}\right\rangle & \left|c\frac{1}{2}\right\rangle & \left|c\frac{-1}{2}\right\rangle & \left|c\frac{-3}{2}\right\rangle & \left|c\frac{7}{2}\right\rangle & \left|c\frac{-7}{2}\right\rangle & |+\rangle & |-\rangle & \left|\frac{3}{2}\right\rangle & \left|\frac{1}{2}\right\rangle & \left|\frac{-1}{2}\right\rangle & \left|\frac{-3}{2}\right\rangle & \left|\frac{7}{2}\right\rangle & \left|\frac{-7}{2}\right\rangle \\
\breve{E}_{8C} & 0 & 0 & 0 & 0 & 0 & \frac{-1}{\sqrt{2}}P'^{-} & 0 & \frac{\Delta'}{3} & \frac{1}{\sqrt{3}}P_X^{+} & \frac{1}{\sqrt{3}}P_X^{z} & 0 & \frac{1}{\sqrt{6}}P_X^{+} & \sqrt{\frac{2}{3}}P_X^{z} \\
0 & \breve{E}_{8C} & 0 & 0 & 0 & 0 & \sqrt{\frac{2}{3}}P'^{z} & \frac{-1}{\sqrt{6}}P'^{-} & \frac{-1}{\sqrt{3}}P_X^{-} & \frac{\Delta'}{3} & 0 & \frac{1}{\sqrt{3}}P_X^{z} & 0 & \frac{-1}{\sqrt{2}}P_X^{+} \\
0 & 0 & \breve{E}_{8C} & 0 & 0 & 0 & \frac{1}{\sqrt{6}}P'^{+} & \sqrt{\frac{2}{3}}P'^{z} & \frac{-1}{\sqrt{3}}P_X^{z} & 0 & \frac{\Delta'}{3} & \frac{-1}{\sqrt{3}}P_X^{+} & \frac{1}{\sqrt{2}}P_X^{-} & 0 \\
0 & 0 & 0 & \breve{E}_{8C} & 0 & 0 & 0 & \frac{1}{\sqrt{2}}P'^{+} & 0 & \frac{-1}{\sqrt{3}}P_X^{z} & \frac{1}{\sqrt{3}}P_X^{-} & \frac{\Delta'}{3} & \sqrt{\frac{2}{3}}P_X^{z} & \frac{-1}{\sqrt{6}}P_X^{-} \\
0 & 0 & 0 & 0 & \breve{E}_{7C} & 0 & \frac{1}{\sqrt{3}}P'^{z} & \frac{1}{\sqrt{3}}P'^{-} & \frac{-1}{\sqrt{6}}P_X^{-} & 0 & \frac{-1}{\sqrt{2}}P_X^{+} & -\sqrt{\frac{2}{3}}P_X^{z} & -\frac{2\Delta'}{3} & 0 \\
0 & 0 & 0 & 0 & 0 & \breve{E}_{7C} & \frac{1}{\sqrt{3}}P'^{+} & \frac{-1}{\sqrt{3}}P'^{z} & -\sqrt{\frac{2}{3}}P_X^{z} & \frac{1}{\sqrt{2}}P_X^{-} & 0 & \frac{1}{\sqrt{6}}P_X^{+} & 0 & -\frac{2\Delta'}{3} \\
cc & cc & cc & 0 & cc & cc & \breve{E}_{6} & 0 & \frac{-1}{\sqrt{2}}P^{+} & \sqrt{\frac{2}{3}}P^{z} & \frac{1}{\sqrt{6}}P^{-} & 0 & \frac{1}{\sqrt{3}}P^{z} & \frac{1}{\sqrt{3}}P^{-} \\
0 & cc & cc & cc & cc & cc & 0 & \breve{E}_{6} & 0 & \frac{-1}{\sqrt{6}}P^{+} & \sqrt{\frac{2}{3}}P^{z} & \frac{1}{\sqrt{2}}P^{-} & \frac{1}{\sqrt{3}}P^{+} & \frac{-1}{\sqrt{3}}P^{z} \\
\frac{\Delta'}{3} & cc & cc & 0 & cc & cc & cc & 0 & \breve{k}^2 & 0 & 0 & 0 & 0 & 0 \\
cc & \frac{\Delta'}{3} & 0 & cc & 0 & cc & cc & cc & 0 & \breve{k}^2 & 0 & 0 & 0 & 0 \\
cc & 0 & \frac{\Delta'}{3} & cc & cc & 0 & cc & cc & 0 & 0 & \breve{k}^2 & 0 & 0 & 0 \\
0 & cc & cc & \frac{\Delta'}{3} & cc & cc & 0 & cc & 0 & 0 & 0 & \breve{k}^2 & 0 & 0 \\
cc & 0 & cc & cc & \frac{-2\Delta'}{3} & 0 & cc & cc & 0 & 0 & 0 & 0 & -\Delta+\breve{k}^2 & 0 \\
cc & cc & 0 & cc & 0 & \frac{-2\Delta'}{3} & cc & cc & 0 & 0 & 0 & 0 & 0 & -\Delta+\breve{k}^2
\end{bmatrix}
\tag{1.40}
$$

1.2.6 Projection in the $\{\Gamma_6, \Gamma_8, \Gamma_7\}$ space

Using Luttinger-Kohn renormalization [LK], the projection matrix on the $\{\Gamma_6, \Gamma_8, \Gamma_7\}$ subspace can easily be calculated. Note that now the $\mathbf{k} \cdot \mathbf{p}$ term is exact in the $\{\Gamma_6, \Gamma_8, \Gamma_7\}$ subspace and it has to be considered as a perturbation potential when calculating the influence of the $\{\Gamma_{8C}, \Gamma_{7C}\}$ bands in this subspace. The perturbation caused by the spin-orbit coupling is negligible. The resulting matrix is expressed in Eq. 1.41

$$
\begin{array}{c}
\begin{array}{cccccccc}
|+\rangle & |-\rangle & |3/2\rangle & |1/2\rangle & |-1/2\rangle & |-3/2\rangle & |7/2\rangle & |-7/2\rangle
\end{array} \\
\left[\begin{array}{cccccccc}
E_{++} & 0 & \frac{-1}{\sqrt{2}}Pk_+ & \sqrt{\frac{2}{3}}Pk_z & \frac{1}{\sqrt{6}}Pk_- & 0 & \frac{1}{\sqrt{3}}Pk_z & \frac{1}{\sqrt{3}}Pk_- \\
0 & E_{--} & 0 & \frac{-1}{\sqrt{6}}Pk_+ & \sqrt{\frac{2}{3}}Pk_z & \frac{1}{\sqrt{2}}Pk_- & \frac{1}{\sqrt{3}}Pk_+ & \frac{-1}{\sqrt{3}}Pk_z \\
cc & 0 & \begin{array}{c}-\gamma_1^p\breve{k}^2 \\ +\mathfrak{A}^p\end{array} & \mathfrak{B}^p & \mathfrak{C}^p & 0 & \frac{1}{\sqrt{2}}\mathfrak{B}_\Delta^p & \sqrt{2}\mathfrak{C}_\Delta^p \\
cc & cc & cc & \begin{array}{c}-\gamma_1^p\breve{k}^2 \\ -\mathfrak{A}^p\end{array} & 0 & \mathfrak{C}^p & -\sqrt{2}\mathfrak{A}_\Delta^p & -\sqrt{\frac{3}{2}}\mathfrak{B}_\Delta^p \\
cc & cc & cc & 0 & \begin{array}{c}-\gamma_1^p\breve{k}^2 \\ -\mathfrak{A}^p\end{array} & -\mathfrak{B}^p & -\sqrt{\frac{3}{2}}\mathfrak{B}_\Delta^{p*} & \sqrt{2}\mathfrak{A}_\Delta^p \\
0 & cc & 0 & cc & cc & \begin{array}{c}-\gamma_1^p\breve{k}^2 \\ +\mathfrak{A}^p\end{array} & -\sqrt{2}\mathfrak{C}_\Delta^* & \frac{1}{\sqrt{2}}\mathfrak{B}_\Delta^{p*} \\
cc & cc & cc & cc & cc & cc & \begin{array}{c}-\Delta \\ -\gamma_{\Delta 1}^p\breve{k}^2\end{array} & 0 \\
cc & cc & cc & cc & cc & cc & 0 & \begin{array}{c}-\Delta \\ -\gamma_{\Delta 1}^p\breve{k}^2\end{array}
\end{array}\right]
\end{array}
\tag{1.41}
$$

where

$E_{++} = E_{--} = E_G + \left(1 + \gamma_C^{5C}\right)\breve{k}^2$

$\mathfrak{A}^p = \gamma_2^p\left(2\breve{k}_z^2 - \breve{k}_\rho^2\right) = \gamma_2^p\left(3\breve{k}_z^2 - \breve{k}^2\right)$

$\mathfrak{B}^p = 2\sqrt{3}\gamma_3^p\breve{k}_z\breve{k}_-$

$\mathfrak{C}^p = \sqrt{3}\left[\gamma_2^p\left(\breve{k}_x^2 - \breve{k}_y^2\right) - 2i\gamma_3^p\breve{k}_x\breve{k}_y\right]$

$\mathfrak{A}_\Delta^p = \gamma_{\Delta 2}^p\left(2\breve{k}_z^2 - \breve{k}_\rho^2\right) = \gamma_{\Delta 2}^p\left(3\breve{k}_z^2 - \breve{k}^2\right)$

$\mathfrak{B}_\Delta^p = 2\sqrt{3}\gamma_{\Delta 3}^p\breve{k}_z\breve{k}_-$

$\mathfrak{B}_\Delta^p = 2\sqrt{3}\gamma_{\Delta 3}^p\breve{k}_z\breve{k}_-$

$\mathfrak{C}_\Delta^p = \sqrt{3}\left[\gamma_{\Delta 2}^p\left(\breve{k}_x^2 - \breve{k}_y^2\right) - 2i\gamma_{\Delta 3}^p\breve{k}_x\breve{k}_y\right]$

The coefficients are given as follows, where $E_{m-n} \equiv E_m - E_n$

$$\gamma_C^{5C} = -\frac{E'_P}{3}\left(\frac{2}{E^G} + \frac{1}{E^\Delta}\right) \tag{1.42a}$$

$$\gamma_1^p = -1 + \frac{E_{PX}}{3}\left(\frac{1}{E_{8C-8}} + \frac{1}{E_{7C-8}}\right) \tag{1.42b}$$

$$\gamma_{\Delta 1}^p = -1 + \frac{2}{3}\frac{E_{PX}}{E_{8C-7}} \tag{1.42c}$$

$$\gamma_2^p = -\frac{1}{6}\frac{E_{PX}}{E_{7C-8}} \tag{1.42d}$$

$$\gamma_{\Delta 2}^p = -\frac{E_{PX}}{12}\left(\frac{1}{E_{8C-8}} + \frac{1}{E_{8C-7}}\right) \tag{1.42e}$$

$$\gamma_3^p = -\gamma_2^p \;\; ; \;\; \gamma_{\Delta 3}^p = -\gamma_{\Delta 2}^p \tag{1.42f}$$

1.2.7 Pidgeon-Brown Hamiltonian and Luttinger parameters

The 8×8 Pidgeon-Brown matrix [PB] is the 8×8 matrix given in Eq. 1.41 plus the perturbation which comes from the remote bands, i.e., the bands differ from $\{\Gamma_6,\ \Gamma_8,\ \Gamma_7\}$. It is useful to introduce

$$K' = \frac{2}{m_0}\sum_{n\neq 5C,1,5}\frac{\langle S|p_x|n\rangle\langle n|p_x|S\rangle}{E_1 - E_n} \tag{1.43a}$$

$$L' = \frac{2}{m_0}\sum_{n\neq 5C,1,5}\frac{\langle X|p_x|n\rangle\langle n|p_x|X\rangle}{E_5 - E_n} \tag{1.43b}$$

$$M' = \frac{2}{m_0}\sum_{n\neq 5C,1,5}\frac{\langle X|p_y|n\rangle\langle n|p_y|X\rangle}{E_5 - E_n} \tag{1.43c}$$

$$N' = \frac{2}{m_0}\sum_{n\neq 5C,1,5}\frac{\langle X|p_x|n\rangle\langle n|p_y|Y\rangle + \langle X|p_y|n\rangle\langle n|p_x|Y\rangle}{E_5 - E_n} \tag{1.43d}$$

We define the Pidgeon-Brown parameters by

$$\tilde{\gamma}_C \cong 1 + \gamma_C^{5C} + K' \tag{1.44a}$$
$$\tilde{\gamma}_1 \cong \gamma_1^p - (L' + 2M')/3 \tag{1.44b}$$
$$\tilde{\gamma}_2 \cong \gamma_2^p - (L' - M')/6 \tag{1.44c}$$
$$\tilde{\gamma}_3 \cong -\gamma_2^p - N'/6 \tag{1.44d}$$
$$\tilde{\gamma}_{\Delta 1} \cong \gamma_{\Delta 1}^p - (L' + 2M')/3 \tag{1.44e}$$
$$\tilde{\gamma}_{\Delta 2} \cong \gamma_{\Delta 2}^p - (L' - M')/6 \tag{1.44f}$$
$$\tilde{\gamma}_{\Delta 3} \cong -\gamma_2^p - N'/6 \tag{1.44g}$$

The Pidgeon-Brown matrix is obtained from Eq. 1.41 by replacing γ_C^{5C} (respectively γ_1^p, γ_2^p, γ_3^p, $\gamma_{\Delta 1}^p$, $\gamma_{\Delta 2}^p$, and $\gamma_{\Delta 3}^p$) by $\tilde{\gamma}_C$ (respectively $\tilde{\gamma}_1$, $\tilde{\gamma}_2$, $\tilde{\gamma}_3$, $\tilde{\gamma}_{\Delta 1}$, $\tilde{\gamma}_{\Delta 2}$, and $\tilde{\gamma}_{\Delta 3}$). The Luttinger parameters which are well known and determined by cyclotron resonance [VMR], relate to Pidgeon-Brown parameters as follows

$$\gamma_C = \tilde{\gamma}_C + \frac{E_P}{3}\left(\frac{2}{E_G} + \frac{1}{E_\Delta}\right) \tag{1.45a}$$
$$\gamma_1 = \tilde{\gamma}_1 + \frac{E_P}{3E_G} \tag{1.45b}$$
$$\gamma_2 = \tilde{\gamma}_2 + \frac{E_P}{6E_G} \tag{1.45c}$$
$$\gamma_3 = \tilde{\gamma}_3 + \frac{E_P}{6E_G} \tag{1.45d}$$
$$\gamma_{\Delta 1} = \tilde{\gamma}_{\Delta 1} + \frac{E_P}{3E_\Delta} \tag{1.45e}$$
$$\gamma_{\Delta 2} = \tilde{\gamma}_{\Delta 2} + \frac{E_P}{12}\left(\frac{1}{E_G} + \frac{1}{E_\Delta}\right) \tag{1.45f}$$
$$\gamma_{\Delta 3} = \tilde{\gamma}_{\Delta 2} + \frac{E_P}{12}\left(\frac{1}{E_G} + \frac{1}{E_\Delta}\right) \tag{1.45g}$$

1.2.8 The 14×14 $\mathbf{k} \cdot \mathbf{p}$ Hamiltonian

The full 14×14 $\mathbf{k} \cdot \mathbf{p}$ matrix, i.e., with the perturbation of all remote bands, can be expressed through Luttinger parameters. We use the notations
$E_{8C}^H = E'_{8C} - \gamma'_{C1}\breve{k}^2 + \mathfrak{A}'_C$;
$E_{8C}^L = E'_{8C} - \gamma'_{C1}\breve{k}^2 - \mathfrak{A}'_C$;
$E_{7C}^k = E'_{7C} - \gamma'_{C\Delta 1}\breve{k}^2$;
$E_6^k = E_6 + \gamma'_C\breve{k}^2$;
$E_8^H = E'_8 - \gamma'_1\breve{k}^2 + \mathfrak{A}'$;

$E_8^L = E_8' - \gamma_1' \breve{k}^2 - \mathfrak{A}'$;
$E_7^k = E_7' - \gamma_{\Delta 1}' \breve{k}^2$;
$\mathfrak{A}_C' = \gamma_{C2}' \left(2\breve{k}_z^2 - \breve{k}_\rho^2 \right)$;
$\mathfrak{A}_{C\Delta}' = \gamma_{C\Delta 2}' \left(2\breve{k}_z^2 - \breve{k}_\rho^2 \right)$;
$\mathfrak{B}_C' = 2\sqrt{3}\, \gamma_{C3}' \breve{k}_z \breve{k}_-$;
$\mathfrak{B}_{C\Delta}' = 2\sqrt{3}\, \gamma_{C\Delta 3}' \breve{k}_z \breve{k}_-$;
$\mathfrak{C}_C' = \sqrt{3} \left[\gamma_{C2}' \left(\breve{k}_x^2 - \breve{k}_y^2 \right) - 2i\gamma_{C3}' \breve{k}_x \breve{k}_y \right]$;
$\mathfrak{C}_{C\Delta}' = \sqrt{3} \left[\gamma_{C\Delta 2}' \left(\breve{k}_x^2 - \breve{k}_y^2 \right) - 2i\gamma_{C\Delta 3}' \breve{k}_x \breve{k}_y \right]$;
$\mathfrak{A}' = \gamma_2' \left(2\breve{k}_z^2 - \breve{k}_\rho^2 \right)$;
$\mathfrak{A}_\Delta' = \gamma_{\Delta 2}' \left(2\breve{k}_z^2 - \breve{k}_\rho^2 \right)$;
$\mathfrak{B}' = 2\sqrt{3} \gamma_3' \breve{k}_z \breve{k}_-$;
$\mathfrak{B}_\Delta' = 2\sqrt{3} \gamma_{\Delta 3}' \breve{k}_z \breve{k}_-$;
$\mathfrak{C}' = \sqrt{3} \left[\gamma_2' \left(\breve{k}_x^2 - \breve{k}_y^2 \right) - 2i\gamma_3' \breve{k}_x \breve{k}_y \right]$;
$\mathfrak{C}_\Delta' = \sqrt{3} \left[\gamma_{\Delta 2}' \left(\breve{k}_x^2 - \breve{k}_y^2 \right) - 2i\gamma_3' \breve{k}_x \breve{k}_y \right]$.

The presence of γ_{Cj}' and $\gamma_{C\Delta j}'$ is due to the symmetry between the subspaces $\{\Gamma_{7C},\ \Gamma_{8C}\}$ and $\{\Gamma_7,\ \Gamma_8\}$. The parameters γ_C', γ_j', and $\gamma_{\Delta j}'$ ($j = 1,\ 2,\ 3$) are related to measurable Luttinger parameters γ_C, γ_j, and $\gamma_{\Delta j}$ by

$$\gamma_C' = \gamma_C - \frac{E_P}{3} \left(\frac{2}{E_G} + \frac{1}{E_\Delta} \right) + \frac{E_P'}{3} \left(\frac{2}{E^G} + \frac{1}{E^\Delta} \right) \tag{1.46a}$$

$$\gamma_1' = \gamma_1 - \frac{E_P}{3E_G} - \frac{E_{PX}}{3} \left(\frac{1}{E_{7C-8}} + \frac{1}{E_{8C-8}} \right) \tag{1.46b}$$

$$\gamma_2' = \gamma_2 - \frac{E_P}{6E_G} + \frac{E_{PX}}{6E_{7C-8}} \tag{1.46c}$$

$$\gamma_3' = \gamma_3 - \frac{E_P}{6E_G} - \frac{E_{PX}}{6E_{7C-8}} \tag{1.46d}$$

$$\gamma_{C1}' = \gamma_{C1} + \frac{E_P'}{3E^G} + \frac{E_{PX}}{3} \left(\frac{1}{E_{8C-8}} + \frac{1}{E_{8C-7}} \right) \tag{1.46e}$$

$$\gamma_{C2}' = \gamma_{C2} + \frac{E_P'}{6E^G} - \frac{E_{PX}}{6E_{8C-7}} \tag{1.46f}$$

$$\gamma_{C3}' = \gamma_{C3} + \frac{E_P'}{6E^G} + \frac{E_{PX}}{6E_{8C-7}} \tag{1.46g}$$

$\gamma_{\Delta 1}' \cong \gamma_1'$; $\quad \gamma_{\Delta 2}' \cong \gamma_2'$; $\quad \gamma_{\Delta 3}' \cong \gamma_3'$; $\quad \gamma_{C\Delta j}' = \gamma_{Cj}'$
$\gamma_{C\Delta 1}' \cong \gamma_{C1}'$; $\quad \gamma_{C\Delta 2}' \cong \gamma_{C2}'$; $\quad \gamma_{C\Delta 3}' \cong \gamma_{C3}'$

$$
\begin{bmatrix}
\left|c\frac{3}{2}\right\rangle & \left|c\frac{1}{2}\right\rangle & \left|c\frac{-1}{2}\right\rangle & \left|c\frac{-3}{2}\right\rangle & \left|c\frac{7}{2}\right\rangle & \left|c\frac{-7}{2}\right\rangle & |+\rangle & |-\rangle & \left|\frac{3}{2}\right\rangle & \left|\frac{1}{2}\right\rangle & \left|\frac{-1}{2}\right\rangle & \left|\frac{-3}{2}\right\rangle & \left|\frac{7}{2}\right\rangle & \left|\frac{-7}{2}\right\rangle \\
E_{8C}^{H} & \mathfrak{B}'_{C} & \mathfrak{C}'_{C} & 0 & \frac{1}{\sqrt{2}}\mathfrak{B}'_{C\Delta} & \sqrt{2}\mathfrak{C}'_{C\Delta} & \frac{-1}{\sqrt{2}}P'^{-} & 0 & \frac{1}{3}\Delta' & \frac{1}{\sqrt{3}}P_X^{+} & \frac{1}{\sqrt{3}}P_X^{z} & 0 & \frac{1}{\sqrt{6}}P_X^{+} & \sqrt{\frac{2}{3}}P_X^{z} \\
\mathfrak{B}'^{*}_{C} & E_{8C}^{L} & 0 & \mathfrak{C}'_{C} & -\sqrt{2}\mathfrak{A}'_{C\Delta} & -\sqrt{\frac{3}{2}}\mathfrak{B}'_{C\Delta} & \sqrt{\frac{2}{3}}P'^{z} & \frac{-1}{\sqrt{6}}P'^{-} & \frac{-1}{\sqrt{3}}P_X^{-} & \frac{1}{3}\Delta' & 0 & \frac{1}{\sqrt{3}}P_X^{z} & 0 & \frac{-1}{\sqrt{2}}P_X^{+} \\
\mathfrak{C}'^{*}_{C} & 0 & E_{8C}^{L} & -\mathfrak{B}'_{C} & -\sqrt{\frac{3}{2}}\mathfrak{B}'^{*}_{C\Delta} & \sqrt{2}\mathfrak{A}'_{C\Delta} & \frac{1}{\sqrt{6}}P'^{+} & \sqrt{\frac{2}{3}}P'^{z} & \frac{-1}{\sqrt{3}}P_X^{z} & 0 & \frac{1}{3}\Delta' & \frac{-1}{\sqrt{3}}P_X^{+} & \frac{1}{\sqrt{2}}P_X^{-} & 0 \\
0 & \mathfrak{C}'^{*}_{C} & -\mathfrak{B}'^{*}_{C} & E_{8C}^{H} & -\sqrt{2}\mathfrak{C}'^{*}_{C\Delta} & \frac{1}{\sqrt{2}}\mathfrak{B}'^{*}_{C\Delta} & 0 & \frac{1}{\sqrt{2}}P'^{+} & 0 & \frac{-1}{\sqrt{3}}P_X^{z} & \frac{1}{\sqrt{3}}P_X^{-} & \frac{1}{3}\Delta' & \sqrt{\frac{2}{3}}P_X^{z} & \frac{-1}{\sqrt{6}}P_X^{-} \\
\frac{1}{\sqrt{2}}\mathfrak{B}'^{*}_{C\Delta} & -\sqrt{2}\mathfrak{A}'_{C\Delta} & -\sqrt{\frac{3}{2}}\mathfrak{B}'_{C\Delta} & -\sqrt{2}\mathfrak{C}'_{C\Delta} & E_{7C}^{k} & 0 & \frac{1}{\sqrt{3}}P'^{z} & \frac{1}{\sqrt{3}}P'^{-} & \frac{-1}{\sqrt{6}}P_X^{-} & 0 & \frac{-1}{\sqrt{2}}P_X^{+} & -\sqrt{\frac{2}{3}}P_X^{z} & \frac{-2}{3}\Delta' & 0 \\
\sqrt{2}\mathfrak{C}'^{*}_{C\Delta} & -\sqrt{\frac{3}{2}}\mathfrak{B}'^{*}_{C\Delta} & \sqrt{2}\mathfrak{A}'_{C\Delta} & \frac{1}{\sqrt{2}}\mathfrak{B}'_{C\Delta} & 0 & E_{7C}^{k} & \frac{1}{\sqrt{3}}P'^{+} & \frac{-1}{\sqrt{3}}P'^{z} & -\sqrt{\frac{2}{3}}P_X^{z} & \frac{1}{\sqrt{2}}P_X^{-} & 0 & \frac{1}{\sqrt{6}}P_X^{+} & 0 & \frac{-2}{3}\Delta' \\
\frac{-1}{\sqrt{2}}P'^{+} & \sqrt{\frac{2}{3}}P'^{z} & \frac{1}{\sqrt{6}}P'^{-} & 0 & \frac{1}{\sqrt{3}}P'^{z} & \frac{1}{\sqrt{3}}P'^{-} & E_{6}^{k} & 0 & \frac{-1}{\sqrt{2}}P^{+} & \sqrt{\frac{2}{3}}P^{z} & \frac{1}{\sqrt{6}}P^{-} & 0 & \frac{1}{\sqrt{3}}P^{z} & \frac{1}{\sqrt{3}}P^{-} \\
0 & \frac{-1}{\sqrt{6}}P'^{+} & \sqrt{\frac{2}{3}}P'^{z} & \frac{1}{\sqrt{2}}P'^{-} & \frac{1}{\sqrt{3}}P'^{+} & \frac{-1}{\sqrt{3}}P'^{z} & 0 & E_{6}^{k} & 0 & \frac{-1}{\sqrt{6}}P^{+} & \sqrt{\frac{2}{3}}P^{z} & \frac{1}{\sqrt{2}}P^{-} & \frac{1}{\sqrt{3}}P^{+} & \frac{-1}{\sqrt{3}}P^{z} \\
\frac{1}{3}\Delta' & \frac{-1}{\sqrt{3}}P_X^{+} & \frac{-1}{\sqrt{3}}P_X^{z} & 0 & \frac{-1}{\sqrt{6}}P_X^{+} & -\sqrt{\frac{2}{3}}P_X^{z} & \frac{-1}{\sqrt{2}}P^{-} & 0 & E_{8}^{H} & \mathfrak{B}' & \mathfrak{C}' & 0 & \frac{1}{\sqrt{2}}\mathfrak{B}'_{\Delta} & \sqrt{2}\mathfrak{C}'_{\Delta} \\
\frac{1}{\sqrt{3}}P_X^{-} & \frac{1}{3}\Delta' & 0 & \frac{-1}{\sqrt{3}}P_X^{z} & 0 & \frac{1}{\sqrt{2}}P_X^{+} & \sqrt{\frac{2}{3}}P^{z} & \frac{-1}{\sqrt{6}}P^{-} & \mathfrak{B}'^{*} & E_{8}^{L} & 0 & \mathfrak{C}' & -\sqrt{2}\mathfrak{A}' & -\sqrt{\frac{3}{2}}\mathfrak{B}'_{\Delta} \\
\frac{1}{\sqrt{3}}P_X^{z} & 0 & \frac{1}{3}\Delta' & \frac{1}{\sqrt{3}}P_X^{+} & \frac{-1}{\sqrt{2}}P_X^{-} & 0 & \frac{1}{\sqrt{6}}P^{+} & \sqrt{\frac{2}{3}}P^{z} & \mathfrak{C}'^{*} & 0 & E_{8}^{L} & -\mathfrak{B}' & -\sqrt{\frac{3}{2}}\mathfrak{B}'^{*}_{\Delta} & \sqrt{2}\mathfrak{A}'_{\Delta} \\
0 & \frac{1}{\sqrt{3}}P_X^{z} & \frac{-1}{\sqrt{3}}P_X^{-} & \frac{1}{3}\Delta' & -\sqrt{\frac{2}{3}}P_X^{z} & \frac{1}{\sqrt{6}}P_X^{-} & 0 & \frac{1}{\sqrt{2}}P^{+} & 0 & \mathfrak{C}'^{*} & -\mathfrak{B}'^{*} & E_{8}^{H} & -\sqrt{2}\mathfrak{C}'^{*}_{\Delta} & \frac{1}{\sqrt{2}}\mathfrak{B}'^{*}_{\Delta} \\
\frac{1}{\sqrt{6}}P_X^{-} & 0 & \frac{1}{\sqrt{2}}P_X^{+} & \sqrt{\frac{2}{3}}P_X^{z} & \frac{-2}{3}\Delta' & 0 & \frac{1}{\sqrt{3}}P^{z} & \frac{1}{\sqrt{3}}P^{-} & \frac{1}{\sqrt{2}}\mathfrak{B}'^{*}_{\Delta} & -\sqrt{2}\mathfrak{A}' & -\sqrt{\frac{3}{2}}\mathfrak{B}'_{\Delta} & -\sqrt{2}\mathfrak{C}'_{\Delta} & E_{7}^{k} & 0 \\
\sqrt{\frac{2}{3}}P_X^{z} & \frac{-1}{\sqrt{2}}P_X^{-} & 0 & \frac{-1}{\sqrt{6}}P_X^{+} & 0 & \frac{-2}{3}\Delta' & \frac{1}{\sqrt{3}}P^{+} & \frac{-1}{\sqrt{3}}P^{z} & \sqrt{2}\mathfrak{C}'^{*}_{\Delta} & -\sqrt{\frac{3}{2}}\mathfrak{B}'^{*}_{\Delta} & \sqrt{2}\mathfrak{A}'_{\Delta} & \frac{1}{\sqrt{2}}\mathfrak{B}'_{\Delta} & 0 & E_{7}^{k}
\end{bmatrix}
\tag{1.47}
$$

1.2.9 k^3 term

Now, using the projection of the Hamiltonian (Eq. 1.47) on the $\Gamma_6 = \{|S\uparrow\rangle, |S\downarrow\rangle\}$ subspace by third- and fourth-order perturbations, we obtain the Hamiltonian for the conduction band

$$H_C = \gamma'_C \breve{k}^2 \mathbb{I} \quad + \quad \mathfrak{H}_3 \tag{1.48}$$

where $\mathbb{I}$ is the unitary matrix and

$$\mathfrak{H}_3 = -\gamma \begin{bmatrix} & |S\uparrow\rangle & & |S\downarrow\rangle \\ & k_z\left(k_x^2 - k_y^2\right) & & k_x\left(k_y^2 - k_z^2\right) - ik_y\left(k_z^2 - k_x^2\right) \\ & k_x\left(k_y^2 - k_z^2\right) + ik_y\left(k_z^2 - k_x^2\right) & & -k_z\left(k_x^2 - k_y^2\right) \end{bmatrix} \tag{1.49}$$

with

$$\gamma = \gamma^{(3)} + \gamma^{(4)} \tag{1.50}$$

$$\gamma^{(3)} = \frac{4}{9} P_X P P' \frac{\Delta\left(E^G + 2E^\Delta\right) + \Delta^C\left(E_G + 2E_\Delta\right)}{E_G E_\Delta E^G E^\Delta} \tag{1.51}$$

$$\gamma^{(4)} = -\frac{4}{9} P_X \Delta' \frac{P^2\left(2E^G + E^\Delta\right) + P'^2\left(E_G + 2E_\Delta\right)}{E_G E_\Delta E^G E^\Delta} \tag{1.52}$$

$\gamma^{(3)}$ is obtained via third-order perturbation and $\gamma^{(4)}$ via fourth-order perturbation. In GaAs, Δ' is negative so that $\gamma^{(3)}$ and $\gamma^{(4)}$ are added in absolute value (the matrix elements are positive). On the other hand, $|\gamma^{(4)}|$ is much larger than $|\gamma^{(3)}|$, this means that the fourth-order contribution is more important than the third-order contribution. This shows the difficulty to guess to what order of perturbation we have to stop in this kind of problem.

We define the $\boldsymbol{\chi}$ vector

$$\boldsymbol{\chi} = \left[\chi_x = k_x\left(k_y^2 - k_z^2\right),\ \chi_y = k_y\left(k_z^2 - k_x^2\right),\ \chi_z = k_z\left(k_x^2 - k_y^2\right)\right] \tag{1.53}$$

Eq. 1.49 writes $\mathfrak{H}_3 = -\gamma\boldsymbol{\chi}\cdot\boldsymbol{\sigma} = -2\gamma\boldsymbol{\chi}\cdot\mathbf{S}$ with $\mathbf{S} = \boldsymbol{\sigma}/2$, or

$$\mathfrak{H}_3 = -\gamma\boldsymbol{\chi}\cdot\boldsymbol{\sigma} = -2\gamma\boldsymbol{\chi}\cdot\mathbf{S} = -\gamma \begin{bmatrix} & |S\uparrow\rangle & & |S\downarrow\rangle \\ & \chi_z & & \chi_x - i\chi_y \\ & \chi_x + i\chi_y & & -\chi_z \end{bmatrix} \tag{1.54}$$

$\mathfrak{H}_3$ is the so-called the D'yakonov-Perel' Hamiltonian. The expression $\mathfrak{H}_3 = -\gamma\boldsymbol{\chi}\cdot\boldsymbol{\sigma}$ shows that the electron spin feels a magnetic field proportional to $\boldsymbol{\chi}$, which depends on the $\mathbf{k}-$direction. $\boldsymbol{\chi}$ is called the internal magnetic field or D'yakonov-Perel' field. The internal magnetic field varies both in magnitude and

direction and this is known to lead to a spin relaxation mechanism of conduction electrons (D'yakonov-Perel' mechanism) [DP].

The energies of the conduction electrons, eigenvalues of H_C, can be written in different ways :

$$E = \gamma'_C \breve{k}^2 \pm \gamma \sqrt{\chi_x^2 + \chi_y^2 + \chi_z^2} \tag{1.55}$$

or

$$E_\pm = \gamma'_C \breve{k}^2 \pm \gamma \sqrt{\left[\left(k_x^2 - k_y^2\right) k_z\right]^2 + \left[\left(k_y^2 - k_z^2\right) k_x\right]^2 + \left[\left(k_z^2 - k_x^2\right) k_y\right]^2} \tag{1.56a}$$

$$= \gamma'_C \breve{k}^2 \pm \gamma \sqrt{\left(k_x^2 + k_y^2\right)\left(k_y^2 + k_z^2\right)\left(k_z^2 + k_x^2\right) - 8k_x^2 k_y^2 k_z^2} \tag{1.56b}$$

$$= \gamma'_C \breve{k}^2 \pm \gamma \sqrt{k^2\left(k_x^2 k_y^2 + k_y^2 k_z^2 + k_z^2 k_x^2\right) - 9k_x^2 k_y^2 k_z^2} \tag{1.56c}$$

This in agreement with the energy dispersion of the Γ_6 conduction band to third order in $\mathbf{k}$ calculated by G. Dresselhaus [DRE.55].

$$E = C_0 k^2 \pm C_1 \left[k^2\left(k_x^2 k_y^2 + k_y^2 k_z^2 + k_z^2 k_x^2\right) - 9k_x^2 k_y^2 k_z^2\right]^{1/2} \tag{1.57}$$

When taking account of the lack of inversion symmetry and the spin-orbit interaction, the degeneracy of the conduction band is lifted in all but [001] and [111] directions. In the [110] direction, the splitting is maximum with a value proportional to k^3.

1.2.10 Kramers conjugate

Time reversal in quantum mechanics is explained for instance in the books by Schiff [SCH], Messiah [MES], and Abragam and Bleaney [AB]. Application to Bloch functions can be found in the book by Kittel [KIT]. When the spin is not included, the time reversal operator is the complex conjugation, represented by $\hat{K}_0$ operator. Under the action of $\hat{K}_0$, $\mathbf{r}$ remains unchanged while $\mathbf{p}$ is changed into $-\mathbf{p}$, i.e., the orbital angular momentum is transformed into its opposite. $\hat{K}_0$ changes a wave function to its complex conjugate $\hat{K}_0\Psi = \Psi^*$.

When the spin is included, the time reversal operator $\hat{K}$ has the same properties as $\hat{K}_0$, and moreover, it reverses the spin $\mathbf{S}$. Following the demonstration given in Ref. [MES], the explicit form of the time reversal operator, for the 1/2 spin case is

$$\hat{K} = -i\sigma_y \hat{K}_0 \tag{1.58}$$

where σ_y is the $y-$component of the Pauli operator. We easily see that

$$\hat{K}^2 = -\mathbb{I} \quad ; \quad \hat{K} \uparrow = \downarrow \quad ; \quad \hat{K} \downarrow = -\uparrow \tag{1.59}$$

It is shown in Ref. [KIT] that, in the absence of external magnetic field, if Ψ is an eigenstate of Hamiltonian H, $\hat{K}\Psi$ is also an eigenstate of H at the same energy. $\hat{K}\Psi$ is called the Kramers' conjugate of Ψ and is orthogonal to Ψ, i.e., $\langle \Psi | K\Psi \rangle = 0$. From Eqs. 1.58 and 1.59, we have $\hat{K}\left[f(\mathbf{r}) \uparrow + g(\mathbf{r}) \downarrow\right] = f^*(\mathbf{r}) \downarrow - g^*(\mathbf{r}) \uparrow$. For example, the basis functions of the 14×14 $\mathbf{k} \cdot \mathbf{p}$ Hamiltonian (Eq. 1.14) are pairs of Kramers' conjugate

$$\begin{aligned} \hat{K} \left| \pm 3/2 \right\rangle &= \pm \left| \mp 3/2 \right\rangle \\ \hat{K} \left| \pm 1/2 \right\rangle &= \mp \left| \mp 1/2 \right\rangle \\ \hat{K} \left| \pm 7/2 \right\rangle &= \pm \left| \mp 7/2 \right\rangle \end{aligned} \tag{1.60}$$

Note that, these functions are atomic-like states, which are transformed by Kramers' operator according to the rule $\hat{K}|j,m\rangle = (-1)^{j-m}|j,-m\rangle$ ([MES], note 6, p. 445).

Concerning the Bloch function, the states $\hat{K}\Psi^B_{\mathbf{k},\uparrow} = \Psi^B_{-\mathbf{k},\downarrow}$ are associated to the wave vector $-\mathbf{k}$. Kramers' operator acts only on the spin and on the $\mathbf{k}-$dependent part of the wave function, e. g., for the plane wave $\hat{K}\left(e^{i\mathbf{kr}} \uparrow\right) = e^{i(-\mathbf{k})\mathbf{r}} \downarrow$. It is worth to keep in mind that, when we apply the Kramers' conjugation to a wave function, it is sufficient to change $\mathbf{k}$ to $-\mathbf{k}$, $\uparrow$ to $\downarrow$, and $\downarrow$ to $-\uparrow$, while the space part remains unchanged. For example, the Pidgeon-Brown Hamiltonian (Subsec. 1.2.7) gives us the conduction wave functions at $\mathbf{k} \neq \mathbf{0}$, under first-order perturbation and second-order renormalization

$$\begin{aligned} |+,\mathbf{k}\rangle = |+\rangle \\ + P\left[\frac{-3\sqrt{2}k_- \left|\frac{3}{2}\right\rangle + 2\sqrt{6}k_z \left|\frac{1}{2}\right\rangle + \sqrt{6}k_+ \left|\frac{-1}{2}\right\rangle}{6E_G} + \frac{\sqrt{3}k_z \left|\frac{7}{2}\right\rangle + \sqrt{3}k_+ \left|\frac{-7}{2}\right\rangle}{3\left(E_G + \Delta\right)}\right] \end{aligned} \tag{1.61a}$$

$$\begin{aligned} |-,\mathbf{k}\rangle = |-\rangle \\ + P\left[\frac{-\sqrt{6}k_- \left|\frac{1}{2}\right\rangle + 2\sqrt{6}k_z \left|\frac{-1}{2}\right\rangle + 3\sqrt{2}k_+ \left|\frac{-3}{2}\right\rangle}{6E_G} + \frac{\sqrt{3}k_- \left|\frac{7}{2}\right\rangle - \sqrt{3}k_z \left|\frac{-7}{2}\right\rangle}{3\left(E_G + \Delta\right)}\right] \end{aligned} \tag{1.61b}$$

From Eq. 1.60, and noting that $\hat{K}k_\pm = k_\mp$, $\hat{K}k_z = k_z$, we have

$$\hat{K}\,|+,\mathbf{k}\rangle = |-,-\mathbf{k}\rangle \tag{1.62}$$

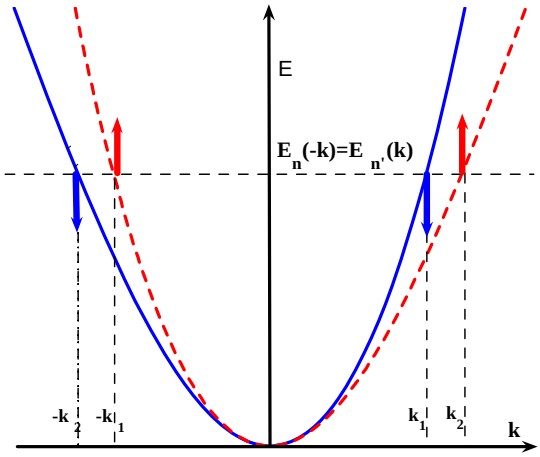

FIG. 1.5 – Kramers' degeneracy : $E_n(-\mathbf{k}) = E_{n'}(\mathbf{k})$, where E_n corresponds to the function $\psi_k(\mathbf{r})$ (dashed line), and $E_{n'}$ corresponds to $\hat{K}\psi_k(\mathbf{r})$ (solid line).

Because, as stated above, $\Psi^B_{\mathbf{k},\uparrow}$ and $\hat{K}\Psi^B_{\mathbf{k},\uparrow}$, i.e., $\Psi^B_{\mathbf{k},\uparrow}$ and $\Psi^B_{-\mathbf{k},\downarrow}$ correspond to the same energy, we can write

$$E_\uparrow(\mathbf{k}) = E_\downarrow(-\mathbf{k}) \qquad ; \qquad E_\downarrow(\mathbf{k}) = E_\uparrow(-\mathbf{k}) \tag{1.63}$$

The bands keep their two-fold degeneracy, but not at the same wave vector. This is the Kramers' degeneracy. The usual degeneracy $E_\uparrow(\mathbf{k}) = E_\downarrow(\mathbf{k})$ (spin degeneracy) is restored only when the Hamiltonian has a space-inversion center, i.e., $V(\mathbf{r}) = V(-\mathbf{r})$.

In a more general case, for the wave function $\psi_k(\mathbf{k}) = [f(\mathbf{r})\uparrow + g(\mathbf{r})\downarrow]$, we have

$$E_{\psi_k}(\mathbf{k}) = E_{\hat{K}\psi_k}(-\mathbf{k}) \tag{1.64}$$

or, in short

$$E_n(\mathbf{k}) = E_{n'}(-\mathbf{k}) \tag{1.65}$$

n, and n' may or may not refer to the same band. The Kramers' degeneracy always applies (Fig. 1.5) without external magnetic field.

Lastly, let us consider an illustration of Kramers' degeneracy in T_d semiconductor. Recall that the energy splitting of the conduction band, given in Eq. 1.55, is k^3 dependent. Along the [110] direction, where the energy splitting is maximum,

we have

$$\begin{aligned} E_{\pm}(k) &= \gamma'_C \breve{k}^2 \pm \gamma k^3 \\ E_{\pm}(-k) &= \gamma'_C \breve{k}^2 \mp \gamma k^3 \end{aligned} \tag{1.66}$$

so that

$$E_{\pm}(k) = E_{\mp}(-\mathbf{k}) \tag{1.67}$$

1.3 Evanescent states

While a real wave vector describes a propagating state, a complex wave vector describes an evanescent state. Such states are localized close to the crystal surface or in the forbidden bandgap of a bulk semiconductor [SHO]. We are interested in the latter case, evanescent states with wave functions decaying exponentially in the bulk, which are relevant for superlattice barriers.

1.3.1 2×2 $\mathbf{k} \cdot \mathbf{p}$ Hamiltonian

We consider the one-electron Schrödinger equation $H\Psi_{n,k}(r) = E_n(k)\,\Psi_{n,k}(r)$. When the wave vector is complex, the Hamiltonian is no longer Hermitian and $E_n(k)$ can be a complex quantity. But along certain lines in this complex-wave-vector space, the energies are real. These lines, called real-energy lines, define the possible evanescent states. In the $\mathbf{k} \cdot \mathbf{p}$ framework, the evanescent states are found by solving the secular equation $\det(H_{\mathbf{kp}} - E\mathbb{I}) = 0$ at a real energy E and at a complex wave vector $\mathbf{k}$. To highlight this, let us first begin with a two-bands "toy" model, introduced by the 2×2 $\mathbf{k} \cdot \mathbf{p}$ matrix

$$\hat{H} = \frac{\hbar^2 k^2}{2m_0}\mathbb{I} + \begin{bmatrix} E_G & Pk \\ Pk & 0 \end{bmatrix} \tag{1.68}$$

where the spin is not taken into account. This matrix is written in a basis including a $|C\rangle$ (respectively the $|V\rangle$) state which describes the conduction (respectively the valence) band. We choose the phase such that $\langle \mathbf{r}\,|C\rangle$ (respectively $\langle \mathbf{r}\,|V\rangle$) is real (respectively purely imaginary). The energy origin is set at the top of the valence band. P is the parameter representing the coupling between $|C\rangle$ and $|V\rangle$: $P = (\hbar/m)\,\langle C|p_x|V\rangle$ is real. The energy E is solution of the secular equation

$$E = \lambda + \frac{\hbar^2 k^2}{2m_0} \tag{1.69}$$

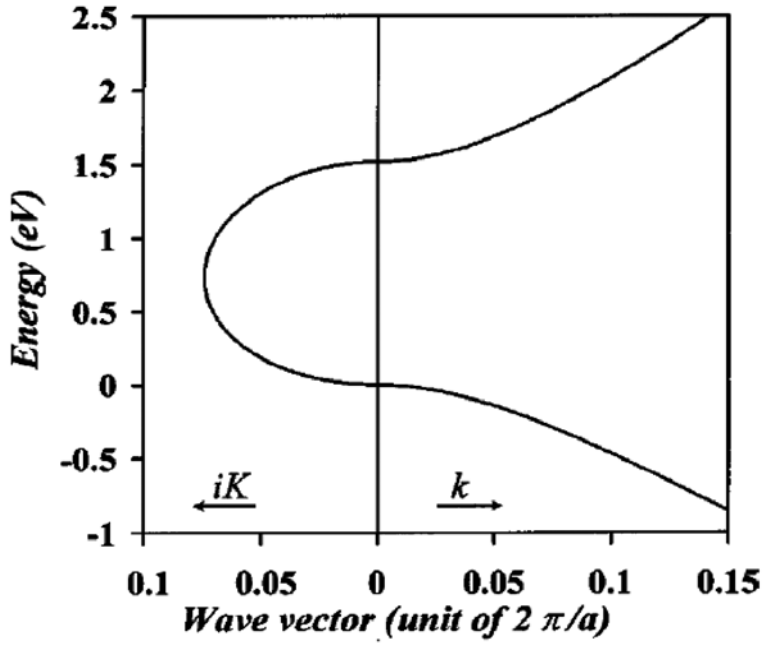

FIG. 1.6 – The two-bands model : evanescent states connect the conduction band to the valence band through the $\mathbf{k} \cdot \mathbf{p}$ interaction.

where λ satisfies

$$\lambda^2 + E_G\lambda - (Pk)^2 = 0 \tag{1.70}$$

or

$$\lambda = E_G/2 \pm \sqrt{E_G + 4\,(Pk)^2} \tag{1.71}$$

For the evanescent states, k is a pure-imaginary wave vector, i.e., $k = iK$, where K is real, so that we have

$$\lambda = E_G/2 \pm \sqrt{E_G - 4P^2K^2} \tag{1.72}$$

E is real only if $|K| \leq E_G/2P$. For GaAs, $P = 9.3$ eV Å and $E_G = 1.52$ eV, then $|K| \lesssim 0.1$ Å^{-1} : the evanescent states are localized within about 0.1 Å $^{-1}$, i.e., the extension of evanescent states is only a small region of the K-space (Fig. 1.6).

Note that, when $k = iK$, the Hamiltonian becomes

$$\hat{H} = -\frac{\hbar^2K^2}{2m_0}\mathbb{I} + \begin{bmatrix} E_G & iPK \\ iPK & 0 \end{bmatrix} \tag{1.73}$$

which is not Hermitian.

1.3.2 Realistic models

In the framework of group theory, Heine [HEI] carefully studied the general properties of the real-energy lines for the diamond structure (O_h group). He proved several theorems for these real-energy lines. Neither the real-energy lines can branch nor terminate, nor can they coalesce more than one time. They can cross each other only at real wave vector k . Energies at the crossing point are extrema of E when plotted in real-wave-vector space. He concluded that there are only two possibilities for the evanescent states, one is that the real-energy line crosses the bandgap, connecting the maximum of one band to the minimum of a higher band, another is that these lines monotonically vary and run to infinity. This prediction was confirmed by Jones [JON], who performed a numerical calculation for determining the evanescent states of silicon, taking into account only the bands in the neighborhood of the band gap. The energy E was fixed at a real value and the wave vector was found by iteratively solving the secular equation, until $\det(H - E\mathbb{I}) = 0$.

By using the 10-bands nearest-neighbor tight binding model, Y.-C. Chang [CHA] calculated the structure of evanescent states in several materials with diamond structure (O_h) or with zinc-blende structure (T_d), but without taking into account the spin-orbit coupling (Fig. 1.7). In 1985, Schuurmans and 't Hooft [SH] studied the band structure of GaAs and AlAs (T_d) via the Kane model [KAN]. The spin-orbit coupling was taken into account in the simplest way, but these authors supposed that the k^3 contribution to the bands is minor, and they disregarded the linear k term in the band dispersion, so GaAs and AlAs were considered as if they belonged to the O_h group. The results are shown in Fig. 1.7 and 1.8. The evanescent states are spin degenerate, no splitting is found for evanescent states in any direction.

The spin-orbit coupling and the absence of inversion symmetry were both taken into account for the first time in a band structure calculation by Richard *et. al.,* [RDRF] and Rougemaille *et. al.,* [RDRFS], using the 14×14 and 30×30 $\mathbf{k} \cdot \mathbf{p}$ matrices. An original topology of evanescent states was found along the direction $[\tan\theta, 0, i]$ (see Fig. 1.9, where $\theta = \xi/K$). We reproduced this result in diagonalizing the 14×14 $\mathbf{k} \cdot \mathbf{p}$ Hamiltonian (Eq. 1.47) which includes both the spin-orbit coupling and the lack of the inversion center. The $\mathbf{k} \cdot \mathbf{p}$ parameters are taken from Jancu's papers [JSAL].

A numerical calculation shows that the evolution of the evanescent lines is

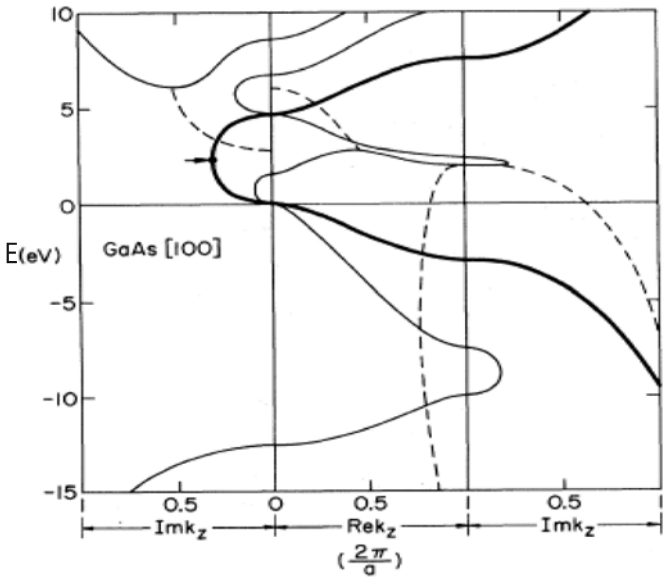

FIG. 1.7 – Real-energy lines from 10-bands tight-binding calculation for complex band structure by Y.-C. Chang [CHA]. Solid lines : real wave vector (i.e., $\mathrm{Im}(k_z) = 0$), imaginary wave vector (i.e., $\mathrm{Re}\,(k_z) = 0$), complex wave vector (i.e., $\mathrm{Re}\,(k_z) = 2\pi/a$, $\mathrm{Im}(k_z) \neq 0$) correspond to the midle, left, and right part respectively. Broken lines : neither the real part nor the imaginary part of the wave vector are equal to zero (i.e., $\mathrm{Re}(k_z) \cdot \mathrm{Im}\,(k_z) \neq 0$).

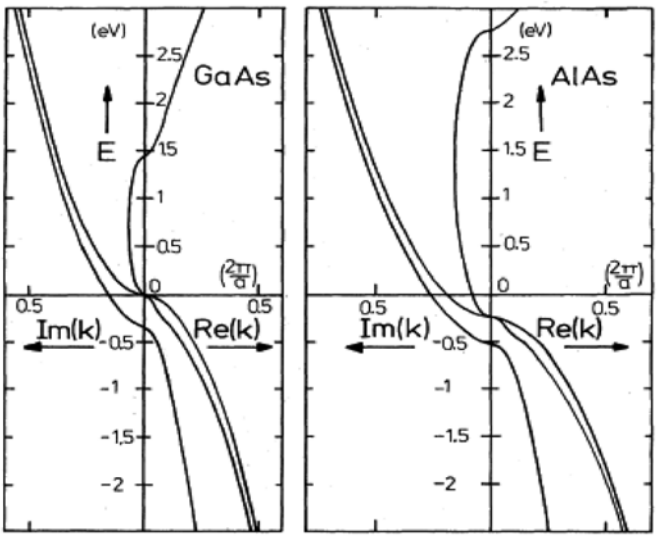

FIG. 1.8 – Evanescent states in the forbidden bandgap of GaAs and AlAs in the Kane model [SH].

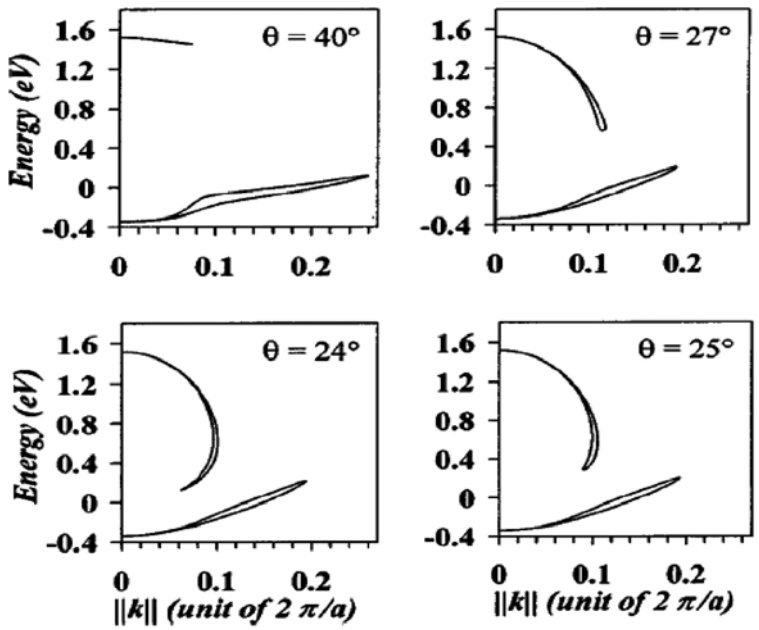

FIG. 1.9 – Evanescent states in the fundamental bangap along the $[\tan\theta, 0, i]$ direction (where $\theta = \xi/K$, i.e., $k = [\xi, 0, iK]$) via the 14×14 $\mathbf{k} \cdot \mathbf{p}$ calculation [RDRF]. The presence of the spin-orbit coupling and the lack of an inversion center leads to a splitting in the complex band structure when $\theta \neq 0$.

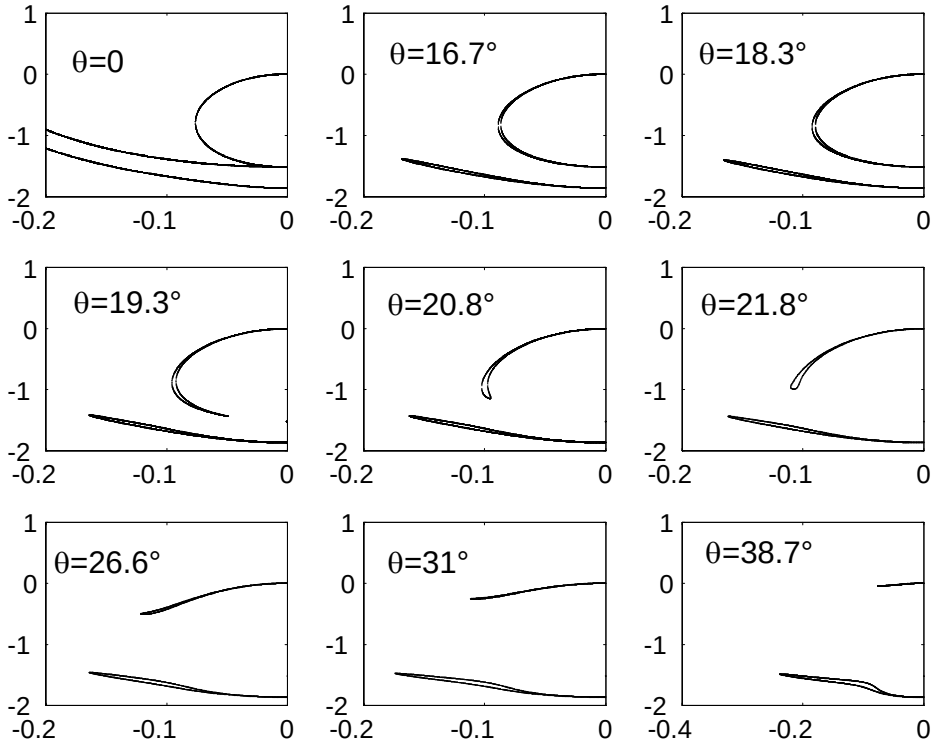

FIG. 1.10 – 14×14 $\mathbf{k} \cdot \mathbf{p}$ calculation : Evanescent energies are plotted versus the wave-vector modulus $||\mathbf{k}||$ in $2\pi/a$ unit, a is the cubic-lattice parameter. The $\mathbf{k} \cdot \mathbf{p}$ parameters used are $E_G = 1.519$ eV, $P = 9.88$ eVÅ, $P' = 0.41$eVÅ, $P_X = 6.68$eVÅ, $\Delta = 0.341$eVÅ, $E_\Delta = 2.969$ eV, $\Delta^C = 0.171$ eV, and $\Delta' = -0.17$ eV.

strikingly dependent on θ (see Fig. 1.10). When $\theta = 0$, i.e., in the [001] direction, we find an evanescent loop connecting the Γ_6 conduction band and Γ_8 light-hole bands, with two-fold degeneracy. When increasing θ ($\theta > 0$ but small), there appears the D'yakonov-Perel' field, leading to a small energy splitting. The evanescent line is now a loop that connects two spins subbands inside the forbidden band. The splitting between these two evanescent subbands increases when θ increases, until $\theta \approx 19°$, an angle beyond which the evanescent state extension begins to decrease. An energy region where no states are allowed exists in the band gap : a (new) forbidden band gap appears inside the bangap. The evanescent loop no longer reaches the valence band. At larger θ, we observe a smaller extension of the evanescent loops in wave-vector space and energy. The loop totally disappears at the value $\theta = 45^{\circ}$. Such band diagrams are the consequence of the spin-orbit coupling and of the lack of inversion symmetry, and have no equivalent in real-band structure.

The 14×14 $\mathbf{k} \cdot \mathbf{p}$ matrix is the smallest possible Hamiltonian to describe the splitting of the bands for (real or imaginary) wave vectors smaller than 0.2 Å^{-1}, but larger than 0.1 Å^{-1}, which is necessary to describe the evanescent states. Following Ref. [HEI], for a complex wave vector $\mathbf{k}$ we have $E(\mathbf{k}^*) = [E(\mathbf{k})]^*$. For evanescent states $E(\mathbf{k}^*) = E(\mathbf{k})$. Then, with Kramers' conjugate, we find four states $[(\mathbf{k}, |s>), (-\mathbf{k}^*, |-s>), (\mathbf{k}^*, |s'>)$, and $(-\mathbf{k}, |-s'>)]$ at the same energy. The wave vectors $[\xi, 0, iK]$ we have used above correspond to a situation which is important for applications since they describe an off-normal tunneling process through a barrier oriented along the [001] crystallographic direction. This situation will be studied in chapter 3.

Chapitre 2

Trajectoire du spin le long d'une boucle évanescente

La prise en compte de l'interaction spin orbite et de l'absence de symmétrie d'inversion conduit, nous l'avons vu au chapitre 1, à une topologie particulièrement originale des états évanescents. Dans ce chapitre, on explore les propriétés de spin de la structure en boucle des états évanescents dans la bande interdite, décrite pour des vecteurs d'onde de la forme $[\xi, 0, iK]$. Rappelons que de tels vecteurs d'ondes correspondent à une situation importante pour les applications puisqu'ils décrivent un processus tunnel sous incidence oblique pour une barrière orientée selon la direction cristallographique [001]. Un phénomène marquant est l'évolution de ces boucles en fonction de l'angle θ ($\tan\theta = \xi/K$) : lorque $\theta = 0$ (on est sous incidence normale), il n'y a aucune levée de dégénérescence de spin et la boucle est l'ovale habituel qui relie le bas de la bande de conduction au sommet de la bande de valence au travers de la bande interdite ; lorque θ augmente, il y a apparition d'un champ D'yakonov-Perel' conduisant à un dédoublement et à une structure en boucle qui connecte deux sous bandes de spins différents - mais pas opposés - en centre de zone. Ces boucles n'atteignent pas la bande de valence. Au fur et à mesure que θ augmente, leur extension en k et en énergie se restreint, les boucles disparaissant fnalement lorsque θ atteint 45°. La question de l'évolution du vecteur spin le long de telles boucles est intriguante. Au voisinage du centre de zone de Brillouin, tant que le cristal est décrit via l'Hamiltonien D'yakonov-Perel', les branches restent des états purs de spin, le spin n'évolue pas. A un certain point, lorsque les branches se "rejoignent" pour former la boucle, les spins doivent évidemment être parallèles, mais il se pourrait que le module du spin ait

varié fortement. On pourrait même imaginer qu'il s'annule... Cette structure fermée, qui survient à une certaine distance du centre de zone (mais cette distance est d'autant plus petite que θ est voisin de 45°) résulte clairement de l'interaction avec les bandes éloignées et son étude nécessite d'utiliser une description basée sur l'Hamiltonien 14×14 introduit au chapitre 1. Les résultats de ce travail ont été publiés dans l'artice "Spin trajectory along an evanescent loop" [T. L. Hoai Nguyen, H.-J. Drouhin, and G. Fishman, Phys. Rev. B**80**, 075207, 2009]. Il est apparu instructif de visualiser les résultats comme un mouvement du spin sur la sphère unité, le module du vecteur spin restant quasi-constant . Dans cette représentation "géographique", les sous-bandes obtenues dans la limite du modèle D'yakonov-Perel' (et que nous désignons par le terme de "sous-bande DP"), se réduisent à deux localités, à des positions symmétriques dans l'hémisphère nord et dans l'hémisphère sud. Elles sont d'autant plus près de l'équateur que θ est grand. La trajectoire du spin est un chemin qui relie ces localités en suivant un méridien. Lorsque θ approche 45°, nous avons vu que la longueur de la boucle évanescente tend vers 0 et nous constatons sur cette représentation que le trajet dans l'espace des spins tend aussi vers zéro. Cette représentation permet du même coup de définir le point de rencontre des branches : l'un des trajets est situé dans l'hémisphère nord, alors que l'autre est situé dans l'hémisphère sud. Une des branches correspond ainsi à un spin "plutôt haut" et l'autre à un spin "plutôt bas". Finalement, et c'est une surprise, durant une bonne partie de la boucle, le module et la direction du spin varient peu, la rotation s'accélérant en bout de boucle. Ceci a des conséquences pour les applications puisque les propriétés de filtrage à spin - qui surviennent selon un axe correspondant à l'axe nord-sud de la sphère - peuvent persister pour d'assez grands vecteurs d'ondes, bien au-delà de la limite de validité du modèle D'yakonov-Perel'. Une représentation imagée du processus tunnel est également exposée, basée sur l'analogie - dans une bonne partie du domaine - entre boucle et bandes dédoublées : si l'on interprétait les deux branches comme deux sous bandes de spin opposé (ce qui n'est pas vrai), à énergie donnée, on déduirait immédiatement deux vecteurs d'ondes évanescents différents selon le sens du spin, et les propriétés de filtrage de spin en résultant.

Spin trajectory along an evanescent loop in zinc-blende semiconductors

T. L. Hoai Nguyen,[1,2] Henri-Jean Drouhin,[1,*] and Guy Fishman[2]
[1]*Ecole Polytechnique, LSI, CNRS and CEA/DSM/IRAMIS, Palaiseau F-91128, France*
[2]*Université Paris-Sud, IEF, CNRS, Orsay F-91405, France*
(Received 20 May 2009; revised manuscript received 8 July 2009; published 21 August 2009)

Due to the absence of inversion symmetry, spin-orbit interaction leads to a very particular topology of the evanescent states in zinc-blende semiconductors, which may consist of loops connecting different spin sub-bands at the zone center. The spin-vector motion along such loops is analytically or numerically studied. A surprising picture emerges from this detailed analysis. Namely, the two spin sub-bands do *not* correspond to opposite spin states near the Brillouin-zone center and merge with identical spins at larger wave vector. This determines the spin-filtering capabilities of the semiconductor barrier.

DOI: 10.1103/PhysRevB.80.075207 PACS number(s): 72.25.Dc, 73.40.Gk, 71.20.Mq

I. INTRODUCTION

Spin-dependent tunneling is of growing importance in spintronics.[1] Fundamental properties of tunneling phenomena in solids are intensively investigated and the structure of the evanescent states is crucial in determining the tunneling scheme. In pioneering papers, Heine[2] and Jones[3] have derived general properties of the complex bands. The evanescent states, which are associated with complex wave vectors, have to be visualized in a real six-dimensional vectorial space, instead of the familiar three-dimensional representation of the real band structure. A careful study of the evanescent band structure inside the band gap of zinc-blende semiconductors can be found in Refs. 4 and 5. This semiconductor family, which is of great technological importance, is a paradigm for fundamental spin physics because a very accurate analytical description of the relevant bands can be obtained. Due to the absence of inversion symmetry, it is well-known that the spin-orbit interaction removes the spin degeneracy of the bands.[6] Concerning the evanescent states, a particular structure arises with a deeply directional dependent nature. Its implications for tunneling have been extensively investigated in Ref. 7, paving the way to spin-orbit engineering of heterostructures. There, it was also shown that even the familiar notion of probability current has to be revisited in the presence of a D'yakonov-Perel' (DP) field,[8] as well as the matching conditions of the wave function at the boundaries. Perel' *et al.*[9] pointed out that a [001]-oriented tunnel barrier under off-normal incidence presents spin-filtering capabilities. These properties are related to the particular topology of the evanescent states in the fundamental band gap which, along the relevant directions, consist of loops connecting two different spin sub-bands at the zone center.[4,5] In the present paper we study the spin properties and especially the spin-vector trajectory along such loops. This provides us with a tractable case where a number of general considerations[2,3] find illuminating illustrations and it emphasizes that, when dealing with spin-dependent tunneling properties, one has to be extremely cautious because the regular representations do not apply.

In zinc-blende semiconductors, the spin splitting of the first conduction band is usually studied near the Brillouin-zone center and described through an effective (2×2) Hamiltonian, referred to as the DP Hamiltonian.[8] In Ref. 4, the evanescent band structure of GaAs was calculated within the $\mathbf{k}\cdot\mathbf{p}$ framework, incorporating an increasing number of bands. Starting with the DP Hamiltonian the evanescent band structure was finally calculated through a (30×30) Hamiltonian formalism which had been shown to yield an accurate description of the first and second real conduction bands and of the three upper real valence bands over the whole Brillouin zone. Concerning the evanescent states in the fundamental band gap (between the top of the upper valence bands and the bottom of the first conduction band) we are interested in, because their wave-vector extension is limited—less than about 10 % of the Brillouin zone—it is sufficient to use a (14×14) Hamiltonian[4] which is also the smallest possible which can include the matrix elements responsible for the spin splitting. This description takes into account seven orbital states, the three *p*-like bonding states which give rise to the three upper valence bands (Γ_{5V}), the *s*-like antibonding states which give rise to the first conduction band (Γ_1), and the three *p*-like antibonding states which correspond to the second conduction band (Γ_{5C}). For directions of the type $[\xi,0,iK]$ $(\xi,K\geq 0)$, referred to the cubic crystallographic axes, the evanescent states consist of loops as shown in Fig. 1, provided that $0\leq\theta<45°$ where $\tan\theta=\xi/K$.[4] The loop extension in wave-vector space decreases when θ increases, tending to zero when θ approaches 45°.

The purpose of the present paper is to study the direction of the two spin states along a whole loop. This is simple and analytical near the Brillouin-zone center (in a small energy domain just below the bottom of the first conduction band), where the (2×2) DP Hamiltonian is sufficient, while the (14×14) Hamiltonian, needed to describe the whole loop, needs numerical resolution.

II. SPIN-VECTOR CALCULATION

The general expression of a normalized pure spin state is $|\phi\rangle=a\uparrow+b\downarrow$, $|a|^2+|b|^2=1$, a combination with complex scalar coefficients of $\uparrow$, $\downarrow$, which are the eigenvectors of $\hat{\sigma}_z$, the z component of the Pauli operator $\hat{\boldsymbol{\sigma}}$. The spin vector is given by the mean value of the Pauli operator $\hat{\boldsymbol{\sigma}}$ in the state $|\phi\rangle$, i.e., $\langle\phi|\hat{\sigma}_j|\phi\rangle$, $j=x,y,z$, with $\langle\phi|\hat{\boldsymbol{\sigma}}|\phi\rangle^2=\Sigma_j\langle\phi|\hat{\sigma}_j|\phi\rangle^2=1$.

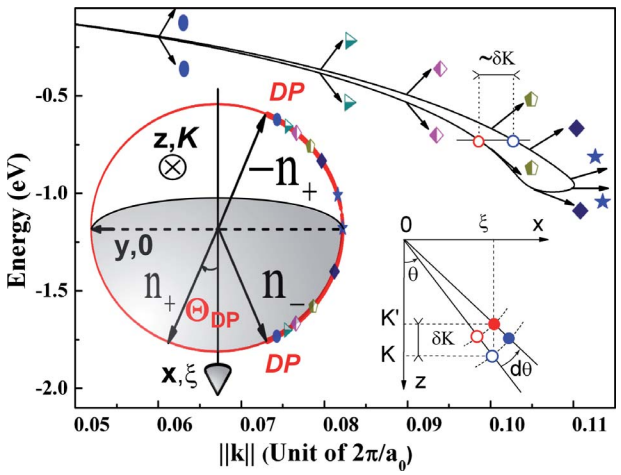

FIG. 1. (Color online) Evanescent loop in the wave vector—energy plane. The energy origin is set at the bottom of the first conduction band. The wave-vector $\mathbf{k}$ lies along the $[\tan\theta,0,i]$ direction, at $\eta=\xi/K=0.4$ ($\theta=21.8°$). The spin vector, in the xOy plane, is represented, after a numerical calculation, for several pairs of points (identical symbols) related to the two sub-bands at a given wave vector. For small wave vectors—in the D'yakonov-Perel limit (out of the representation domain)—the spin vector is given by n_- (respectively, $-n_+$) for the lower-(respectively, upper-) energy band. Lower right inset: top view of the intercepts of two evanescent loops with a constant energy plane determining the evanescent components of the wave-vector K and K' at constant ξ. To the first order, the wave-vector change δK can be directly measured on the loop in the main figure. Lower left inset: the unit sphere allows a simple visualization of the spin-direction trajectory along the loop (take care that the sphere is pointing down to the north hemisphere, the axis being along Ox, the spin-filter axis). The imaginary (in-plane) component of the wave vector, K (ξ) lies along Oz (Ox). The calculated path, with the symbols referring to the points on the loop, connects two symmetrical spots where the D'yakonov-Perel' sub-bands collapse (DP symbols), located in the north (shaded area) and south hemispheres. The departure location in the north hemisphere lies at the colatitude Θ_{DP}.

Now, let us consider the state $|\psi\rangle=|f\rangle\uparrow+|g\rangle\downarrow$ where $|f\rangle$ and $|g\rangle$ are two kets in r-space, i.e., $\langle\mathbf{r}|f\rangle=f(\mathbf{r})$, $\langle\mathbf{r}|g\rangle=g(\mathbf{r})$, and $\psi(r,\sigma)=\langle\mathbf{r}|\psi\rangle=f(\mathbf{r})\uparrow+g(\mathbf{r})\downarrow$. The normalization of the wave vector implies $\langle\psi|\psi\rangle=\langle f|f\rangle+\langle g|g\rangle=1$. We have $\langle\hat{\sigma}_j\rangle=\int\psi^*(r,\sigma)\hat{\sigma}_j\psi(r,\sigma)\mathrm{d}^3\mathbf{r}$, so that

$$\langle\psi|\hat{\boldsymbol{\sigma}}|\psi\rangle^2=1+4[|\langle f|g\rangle|^2-\|f\|^2\|g\|^2]\geq 0. \quad (1)$$

The Cauchy-Schwartz inequality states that $|\langle f|g\rangle|-\|f\|\|g\|\leq 0$ so that the modulus of the spin vector in a mixed state is, in general, smaller than 1. Its norm remains equal to unity if and only if the (f,g) family is not free, i.e., in a pure spin state.

In many usual cases—for instance when f and g relate to different bands of the Hamiltonian without spin—f and g are orthogonal, then

$$\langle\psi|\hat{\boldsymbol{\sigma}}|\psi\rangle^2=1-4\|f\|^2\|g\|^2=4\left(\|f\|^2-\frac{1}{2}\right)^2. \quad (2)$$

If $\|f\|=\|g\|$, we have $\langle\psi|\hat{\boldsymbol{\sigma}}|\psi\rangle^2=0$. This means that, if a band associated with a given spin becomes fully hybridized with another band of opposite spin, with an equal weight for each of the two spin bands, the mean spin modulus becomes zero.

Assume that $|f\rangle$ and $|g\rangle$ belong to a vectorial subspace $\mathcal{E}_n$ with $\dim\mathcal{E}_n=n$, sustended by the orthonormal basis $\mathcal{B}_n$. More formally, the Pauli operator $\hat{\mathfrak{S}}=\hat{\boldsymbol{\sigma}}\otimes\widehat{I_n}$, where $\widehat{I_n}$ is the identity operator acting over $\mathcal{E}_n$, is to be used to calculate the spin vector with $\langle\psi|\hat{\boldsymbol{\sigma}}|\psi\rangle=\langle\psi|\hat{\mathfrak{S}}|\psi\rangle$. The calculation could be performed in the basis $\{\uparrow,\downarrow\}\otimes\mathcal{B}_n$, and in this tensorial-product basis, the matrix representing $\hat{\mathfrak{S}}_j$ is the $(2n\times 2n)$ matrix consisting of n (2×2) identical diagonal blocs, each of them being equal to σ_j. When the spin-orbit coupling is taken into account, $\{\uparrow,\downarrow\}\otimes\mathcal{B}_n$ is not a convenient basis and, depending on the Hamiltonian, another basis involving hybridized states will be used instead. Then, the matrices $\mathfrak{S}_j$ representing $\hat{\mathfrak{S}}$ in this basis will take a more complicated form but, obviously verify the same commutation relations as well as $\mathrm{Tr}\,\mathfrak{S}_j=n\,\mathrm{Tr}\,\sigma_j=0$ and $\det\mathfrak{S}_j=(\det\sigma_j)^n=(-1)^n$.

To study the spin motion along an evanescent band, we calculate the mean value of the Pauli operator in the eigenvector $|\psi\rangle$ corresponding to the energy E. The energy is calculated from the (14×14) Hamiltonian and the eigenvector can be written $|\psi\rangle=\Sigma_{\ell=1}^{14}c_\ell|\Phi_\ell\rangle$ where $\{|\Phi_\ell\rangle\}$ is the set of normalized vectors allowing us to express the (14×14) Hamiltonian. The $|\Phi_\ell\rangle$ are spinors which may be expanded on the $\{\uparrow,\downarrow\}$ basis. The orbital part is written in the basis $\{X,Y,Z,S,X_C,Y_C,Z_C\}$ where X, Y, and Z refer to Γ_{5V}, S refers to Γ_1 symmetry, and X_C, Y_C, and Z_C refer to Γ_{5C}. The detail of the $\mathbf{k}\cdot\mathbf{p}$ matrices up to (30×30) is given in Ref. 10. For convenience, the (14×14) Hamiltonian—similar to the expression derived by Pfeffer and Zawadzki[11] but not identical because the basis differs—is reproduced in the Appendix. We have

$$\langle\psi|\hat{\mathfrak{S}}|\psi\rangle=\sum_{\ell,n=1}^{14}c_\ell^*c_n\langle\Phi_\ell|\hat{\mathfrak{S}}|\Phi_n\rangle=\sum_j\mathbf{e}_j\sum_{\ell,n=1}^{14}c_\ell^*\mathfrak{S}_j^{\ell,n}c_n, \quad (3)$$

where $\mathbf{e}_j$ is the unit vector in the j direction. From the wave functions, the $\mathfrak{S}_j^{\ell,n}$ matrix elements can be straightforwardly calculated. We express them using the (14×14) $[\mathfrak{S}_j]^{\ell,n}$ matrices

$$\mathfrak{S}_j=\begin{pmatrix}\sigma_j^A & 0 & 0\\ 0 & \sigma_j^C & 0\\ 0 & 0 & \sigma_j^B\end{pmatrix}. \quad (4)$$

Here, $\sigma_j^C=\sigma_j$ acts in the conduction (C) $\Gamma_1\otimes\{\uparrow,\downarrow\}=\{|S\rangle\uparrow,|S\rangle\downarrow\}$ subset; σ_j^A acts in the antibonding (A) $\Gamma_{5C}\otimes\{\uparrow,\downarrow\}$ subset, whereas $\sigma_j^B=\sigma_j^A$ acts in the bonding (B) $\Gamma_{5V}\otimes\{\uparrow,\downarrow\}$ subset. For $j=x$ or y, we find

$$\sigma_j^{A,B} = \begin{pmatrix} 0 & e^{-i\varphi_j}/\sqrt{3} & 0 & 0 & -\sqrt{2/3}e^{-i\varphi_j} & 0 \\ e^{i\varphi_j}/\sqrt{3} & 0 & 2e^{-i\varphi_j}/3 & 0 & 0 & -\sqrt{2}e^{-i\varphi_j}/3 \\ 0 & 2e^{i\varphi_j}/3 & 0 & e^{-i\varphi_j}/\sqrt{3} & \sqrt{2}e^{i\varphi_j}/3 & 0 \\ 0 & 0 & e^{i\varphi_j}/\sqrt{3} & 0 & 0 & \sqrt{2/3}e^{i\varphi_j} \\ -\sqrt{2/3}e^{i\varphi_j} & 0 & \sqrt{2}e^{-i\varphi_j}/3 & 0 & 0 & -e^{-i\varphi_j}/3 \\ 0 & -\sqrt{2}e^{i\varphi_j}/3 & 0 & \sqrt{2/3}e^{-i\varphi_j} & -e^{i\varphi_j}/3 & 0 \end{pmatrix} \tag{5}$$

with $\varphi_x=0$ and $\varphi_y=\pi/2$. For $j=z$, we obtain

$$\sigma_z^{A,B} = \begin{pmatrix} 1 & 0 & 0 & 0 & 0 & 0 \\ 0 & 1/3 & 0 & 0 & 2\sqrt{2}/3 & 0 \\ 0 & 0 & -1/3 & 0 & 0 & 2\sqrt{2}/3 \\ 0 & 0 & 0 & -1 & 0 & 0 \\ 0 & 2\sqrt{2}/3 & 0 & 0 & -1/3 & 0 \\ 0 & 0 & 2\sqrt{2}/3 & 0 & 0 & 1/3 \end{pmatrix}. \tag{6}$$

The results need a numerical calculation because $\{c_n\}$ is to be determined. However, for complex wave vectors with a small modulus, analytical solutions can be derived and it is illuminating to consider this case. Near the Brillouin-zone center, the energy dispersion of the first conduction band is accurately described by the DP Hamiltonian, $\hat{H}_{DP}$, which can be obtained from the (14×14) Hamiltonian performing a third-order perturbation expansion from remote bands

$$\hat{H}_{DP} = \gamma_c \mathbf{k}^2 + \gamma \boldsymbol{\chi} \cdot \hat{\boldsymbol{\sigma}}, \tag{7}$$

where γ is the coupling parameter and $\gamma_c=\hbar^2/2m$, with m being the effective mass; $\boldsymbol{\chi}=\boldsymbol{\chi}(\mathbf{k})$ is a vector representing the internal field, $[\chi_x,\chi_y,\chi_z]=[k_x(k_y^2-k_z^2),k_y(k_z^2-k_x^2),k_z(k_x^2-k_y^2)]$. The H_{DP} matrix is expressed in the $\{|S\rangle\uparrow,|S\rangle\downarrow\}$ basis. The evanescent states that we are studying correspond to wave vectors of the form $\{\alpha(\boldsymbol{\xi}+i\beta\mathbf{K})=\alpha(\xi\mathbf{e}_x+i\beta K\mathbf{e}_z);\alpha,\beta=\pm 1\}$. Note that α and β only take the values +1 or −1: $\alpha=1$, $\beta=1(-1)$ refer to the wave-vector $\mathbf{k}$ ($\mathbf{k}^*$) whereas $\alpha=-1$, $\beta=1(-1)$ refer to the wave vector $-\mathbf{k}$ ($-\mathbf{k}^*$). We use the notation $\eta=\xi/K=\tan\theta$ so that $\mathbf{k}=K[\alpha\eta,0,i\alpha\beta]$. Now, the DP field is $\boldsymbol{\chi}=K^3[\alpha\eta,0,i\alpha\beta\eta^2]$ and H_{DP} can be written as

$$H_{DP} = \begin{bmatrix} \gamma_c k^2 + i\alpha\beta\gamma\eta^2K^3 & \alpha\gamma\eta K^3 \\ \alpha\gamma\eta K^3 & \gamma_c k^2 - i\alpha\beta\gamma\eta^2K^3 \end{bmatrix}. \tag{8}$$

For a given wave-vector $\mathbf{k}$, H_{DP} has the two eigenvalues $\lambda_\pm=\gamma_c k^2+\epsilon\gamma\eta\sqrt{1-\eta^2}K^3$, $\epsilon=\pm 1$ correspond to the two energies of two spin states, we shall see the meaning of which just below. Observe that on a real-energy line we have $\eta<1$ (i.e., $\theta<45°$). The components of the corresponding eigenstates are $a=1/\sqrt{2}$ and $b=(\epsilon\alpha\sqrt{1-\eta^2}-i\beta\eta)/\sqrt{2}$. We calculate $\langle\hat{\sigma}_x\rangle=\epsilon\alpha\sqrt{1-\eta^2}$, $\langle\hat{\sigma}_y\rangle=-\beta\eta$, and $\langle\hat{\sigma}_z\rangle=0$. This shows that the spin remains in the xOy plane, perpendicular to the z-quantization axis. In GaAs, γ is a negative quantity[12] so that $\epsilon=-1$ ($\epsilon=+1$) corresponds to the higher- (lower-) energy sub-band. Let us define $\mathbf{n}_\pm=[\sqrt{1-\eta^2},\pm\eta,0]$. The unit vector $\mathbf{n}_+$ makes the angle Θ_{DP} with respect to Ox, with $\sin\Theta_{DP}=\eta=\tan\theta$. The result is summed up in Table I, which indicates $\langle\hat{\boldsymbol{\sigma}}\rangle$ for a given wave vector at a given ϵ.

These two spins are not collinear unless $\eta=0$ (and, in this latter case, the spin splitting of the evanescent states vanishes). Note that in the DP case the quantum state is $|\varphi\rangle=a|S\rangle\uparrow+b|S\rangle\downarrow$ and then the norm of the spin vector is equal to 1.

When going off the Brillouin-zone center, H_{DP} can no longer be used so that a numerical calculation has to be performed as explained above. The GaAs $\mathbf{k}\cdot\mathbf{p}$ parameter values used in the present calculation are $P=9.88$ eV.Å, $P'=0.41$ eV.Å, $E_G=1.519$ eV, $\Delta_C=E_{\Gamma_{8C}}-E_{\Gamma_{7C}}=0.171$ eV, $Q=8.68$ eV.Å, $\Delta=0.341$ eV, $E_\Delta=E_{\Gamma_{7C}}-E_{\Gamma_6}=2.969$ eV, and $\Delta'=-0.17$ eV.[13] This parameter set yields $\gamma=-24$ eV.Å^3. To obtain an image of the spin evolution, it is convenient to plot the spin vector along the loop as shown in Fig. 1. In the upper part, the evanescent loop describes the energy for $\eta=\xi/K=0.4$ ($\theta=21.8°$). All the spin vectors drawn on the curve result from numerical calculation, the DP limit being out of the representation domain. In the lower part, the spin path is drawn on the sphere, the spin modulus being almost constant within an accuracy of 3%. As underlined in Sec. II, it is not obvious that the spin motion can be represented on the unit sphere because, in an hybridized band, the spin vector has a modulus smaller than 1, and possibly 0. The quasiconservation of the modulus is essential for applications to spintronics. Near the Brillouin-zone center, the spin-vector $\mathbf{n}_-$ in the lower-energy sub-band ($\epsilon=+1$) starts from a direction at the polar angle Θ_{DP} with respect to Ox. More precisely, on the unit sphere with the north pole defined by Ox and the longitude of 0° corresponding to the Oy axis, $\mathbf{n}_-$ is defined by the colatitude Θ_{DP} and a longitude of 180°. When increasing the wave-vector modulus, the spin vector rotates at a constant longitude to make the angle Θ with respect to Ox. Starting from the $\Theta=\Theta_{DP}$ in the DP regime, Θ increases up to a point where the spin vector lies along Oy ($\Theta=90°$). Having in mind a movement on the sphere, the path first occurs in the north hemisphere (shaded area). It starts from a point at the colatitude Θ_{DP} which increases versus θ ($\Theta_{DP}\approx\theta$ within an accuracy of 10% up to about 25°, and $\Theta_{DP}=90°$ for $\theta=45°$, the maximum possible value) to reach the equatorial plane $\Theta=90°$. When θ is small but nonzero, the departure point lies near the north pole, but never exactly at the pole. Crossing the

TABLE I. Spin vector $\langle\hat{\boldsymbol{\sigma}}\rangle$ in the D'yakonov-Perel' sub-bands ($\epsilon=\pm1$) and relevant wave vectors. $\mathbf{n}_{\pm}$ are unit vectors that are not collinear.

	$\epsilon=+1$	$\epsilon=-1$
$\mathbf{k}$	$\mathbf{n}_{-}$	$-\mathbf{n}_{+}$
$-\mathbf{k}$	$-\mathbf{n}_{+}$	$\mathbf{n}_{-}$
$\mathbf{k}^{*}$	$\mathbf{n}_{+}$	$-\mathbf{n}_{-}$
$-\mathbf{k}^{*}$	$-\mathbf{n}_{-}$	$\mathbf{n}_{+}$

equatorial plane, the x component of the spin vector becomes negative and the path lies in the south hemisphere: the spin continues to rotate to reach a point which is symmetrical to the departure position with respect to the equatorial plane. This last location is reached in the small-wave-vector regime for $\epsilon=-1$ and the spin vector is $-\mathbf{n}_{+}$. Alternatively, one may think of two spin sub-bands near the zone center which extend off the zone center to connect at the equator. At large θ, not far from 45°, the departure and arrival locations come close to the equator: the length of the path becomes shorter and shorter, tending to zero and it can be seen that, correlatively, the length of the evanescent loop decreases to zero.[4] In Ref. 7, tunneling of electrons under off-normal incidence on a [001]-oriented barrier (z axis) was analyzed, taking ξ along Ox. Then, the tunnel scheme involves two evanescent loops in the xOz plane, because, at a given energy the ξ component of the wave vector has to be conserved, leading to two different θ angles corresponding to wave-vector components K and K' in each "spin" sub-band. As a result, and in agreement with the calculation by Perel' *et al.*,[9] the barrier acts as a spin filter. Fig. 1 in the present paper is also drawn with reference to this very situation: the Oz axis is the tunneling direction—the loop lies in the xOz plane, and Ox is the "spin-filter axis." Roughly speaking, the transmission asymmetry, which is also the transmitted beam polarization when the primary beam is unpolarized, is equal to $\tanh[(aK)(\delta K/K)]$.[7] In this expression (aK) determines the barrier transmission and $(\delta K/K)$ is the "initial" polarization of the sub-bands. We have the relation $d\theta=-\cos^2\theta(\xi/K)(dK/K)$, which shows that, when the ratio ξ/K is small, $d\theta$ is a second-order term which can be neglected. Therefore, δK simply corresponds to the distance between the two branches of the loop at a given energy, restoring a familiar picture. In Fig. 1, it can be shown that, along the loop, $\delta K/K$ starts from the value $(\gamma/\gamma_c)K\tan\theta$ to reach about 7% at $\|\mathbf{k}\|=K/\cos\theta\approx0.1(2\pi/a_0)$ while the spin vector only slightly changes. Therefore, it can be expected that transmission asymmetries as large as 20 % could be achieved, instead of 2 % in the DP limit for a 40 Å-thick barrier. In GaSb, the ratio (γ/γ_c) is about five times larger than in GaAs (Ref. 13) so that extremely high polarizations might be expected.

III. CONCLUSION

In conclusion, the loop structure of the spin sub-bands along $[\tan\theta,0,i]$ directions is responsible for the spin-filtering capability of a [001]-oriented GaAs barrier under off-normal incidence. The θ angle defines the in-plane component ξ of the wave vector—a quantity which is conserved in the tunnel process—through the relation $\tan\theta=\xi/K$, where K is the imaginary component of the wave vector in the barrier. This peculiar topology is a consequence of the spin-orbit interaction in the absence of inversion symmetry. A complete analysis of the spin-vector trajectory has been performed and, if the result is simple, it is far from intuitive. For a wave-vector K $[\tan\theta,0,i]$ at a fixed θ value, the two sub-bands which originate from the diagonalization of the D'yakonov-Perel' Hamiltonian, that we call the DP sub-bands, do not correspond to opposite spin states, even infinitely close to the Brillouin-zone center. Representing the spin vector on the unit sphere, these DP sub-bands reduce to two points located at the same longitude, which are symmetrical with respect to the equatorial plane. Their colatitude Θ_{DP} which varies between 0 and 90°, depends on θ, which varies between 0 and 45°: at small angles $\Theta_{DP}\approx\theta$ whereas Θ_{DP} rapidly increases at large θ. The loops in the dispersion relation of the evanescent bands correspond to paths which connect these two DP spots at the equator when K is large enough. The spin tag allows us to define properly the point where the two sub-bands, which might be thought as up- and down-spin sub-bands near the zone center, connect because one path entirely lies into the north hemisphere (along this path, the spin is rather up than down) whereas the other entirely lies into the south hemisphere (in this region, the spin is rather down than up). In the tunneling geometry, at a fixed energy, the wave with wave-vector $\mathbf{k}$ has to be associated to the wave with wave-vector $\mathbf{k}^{*}$ and it is obvious that these two waves do not correspond to identical spin states so that a two spin-channel tunneling model has to be used to account for electron transmission.[7] Besides, when going off the zone center, the bands hybridize, the spin is no longer a good quantum number and the modulus of the spin vector is slightly reduced. These peculiarities correspond to a situation that appears to be quite general in solids.

ACKNOWLEDGMENT

We thank Travis Wade for a critical reading of the manuscript.

APPENDIX: THE (14×14) HAMILTONIAN

Let X, Y, and Z be the orbital functions of the Γ_{5V} valence band (at $\mathbf{k}=\mathbf{0}$, without spin-orbit interaction) in Koster's notations.[14] Due to spin-orbit interaction the Γ_{5V} level splits into Γ_{8V} and Γ_{7V} subsets. To save place, the four Γ_{8V} functions are referred to as $|M\rangle$ with $M=\pm\frac{3}{2},\pm\frac{1}{2}$ while the two Γ_{7V} functions are written as $|\pm\frac{7}{2}\rangle$, a mnemonic notation recalling that these last two functions belong to Γ_{7V}. S is the orbital function of the first conduction-band Γ_1. X_C, Y_C, and Z_C are the orbital functions of the second conduction-band Γ_{5C}. Due to spin-orbit interaction the Γ_{5C} level splits into Γ_{8C} and Γ_{7C} subsets. The four Γ_{8C} functions are written as

$|cM\rangle$ and the two Γ_{7C} functions are written as $|c\frac{\pm 7}{2}\rangle$.

When one has to deal with time-reversal operator $\hat{\mathbf{K}} = -i\sigma_y \hat{K}_0$, where σ_y is the relevant Pauli matrix and $\hat{K}_0$ is the operation of taking the complex conjugate—as done in Ref. 7—it is preferable to use the basis defined in Ref. 15. Thus, we construct the basis given in Table II where the atomic functions φ_s, φ_{p_x}, φ_{p_y}, and φ_{p_z} of Ref. 15 are substituted with S, X, Y, and Z. Then, the (14×14) Hamiltonian writes:

$$
\begin{array}{c}
\begin{array}{cccccccccccccc}
\left|c\frac{3}{2}\right\rangle & \left|c\frac{1}{2}\right\rangle & \left|c\frac{-1}{2}\right\rangle & \left|c\frac{-3}{2}\right\rangle & \left|c\frac{7}{2}\right\rangle & \left|c\frac{-7}{2}\right\rangle & |+\rangle & |-\rangle & \left|\frac{3}{2}\right\rangle & \left|\frac{1}{2}\right\rangle & \left|\frac{-1}{2}\right\rangle & \left|\frac{-3}{2}\right\rangle & \left|\frac{7}{2}\right\rangle & \left|\frac{-7}{2}\right\rangle
\end{array}
\\
\left[\begin{array}{cccccccccccccc}
E_{8C}^H & \mathfrak{B}_C & \mathfrak{C}_C & 0 & \frac{1}{\sqrt{2}}\mathfrak{B}_C & \sqrt{2}\mathfrak{C}_C & \frac{-1}{\sqrt{2}}P'^- & 0 & \frac{1}{3}\Delta' & \frac{1}{\sqrt{3}}P_X^+ & \frac{1}{\sqrt{3}}P_X^z & 0 & \frac{1}{\sqrt{6}}P_X^+ & \sqrt{\frac{2}{3}}P_X^z \\
\mathfrak{B}_C^* & E_{8C}^L & 0 & \mathfrak{C}_C & -\sqrt{2}\mathfrak{A}_C & -\sqrt{\frac{3}{2}}\mathfrak{B}_C & \sqrt{\frac{2}{3}}P'^z & \frac{-1}{\sqrt{6}}P'^- & \frac{-1}{\sqrt{3}}P_X^- & \frac{1}{3}\Delta' & 0 & \frac{1}{\sqrt{3}}P_X^z & 0 & \frac{-1}{\sqrt{2}}P_X^+ \\
\mathfrak{C}_C^* & 0 & E_{8C}^L & -\mathfrak{B}_C & -\sqrt{\frac{3}{2}}\mathfrak{B}_C^* & \sqrt{2}\mathfrak{A}_C & \frac{1}{\sqrt{6}}P'^+ & \sqrt{\frac{2}{3}}P'^z & \frac{-1}{\sqrt{3}}P_X^z & 0 & \frac{1}{3}\Delta' & \frac{-1}{\sqrt{3}}P_X^+ & \frac{1}{\sqrt{2}}P_X^- & 0 \\
0 & \mathfrak{C}_C^* & -\mathfrak{B}_C^* & E_{8C}^H & -\sqrt{2}\mathfrak{C}_C^* & \frac{1}{\sqrt{2}}\mathfrak{B}_C^* & 0 & \frac{1}{\sqrt{2}}P'^+ & 0 & \frac{-1}{\sqrt{3}}P_X^z & \frac{1}{\sqrt{3}}P_X^- & \frac{1}{3}\Delta' & \sqrt{\frac{2}{3}}P_X^z & \frac{-1}{\sqrt{6}}P_X^- \\
\frac{1}{\sqrt{2}}\mathfrak{B}_C^* & -\sqrt{2}\mathfrak{A}_C & -\sqrt{\frac{3}{2}}\mathfrak{B}_C & -\sqrt{2}\mathfrak{C}_C & E_{7C}^k & 0 & \frac{1}{\sqrt{3}}P'^z & \frac{1}{\sqrt{3}}P'^- & \frac{-1}{\sqrt{6}}P_X^- & 0 & \frac{-1}{\sqrt{2}}P_X^+ & -\sqrt{\frac{2}{3}}P_X^z & \frac{-2}{3}\Delta' & 0 \\
\sqrt{2}\mathfrak{C}_C^* & -\sqrt{\frac{3}{2}}\mathfrak{B}_C^* & \sqrt{2}\mathfrak{A}_C & \frac{1}{\sqrt{2}}\mathfrak{B}_C & 0 & E_{7C}^k & \frac{1}{\sqrt{3}}P'^+ & \frac{-1}{\sqrt{3}}P'^z & -\sqrt{\frac{2}{3}}P_X^z & \frac{1}{\sqrt{2}}P_X^- & 0 & \frac{1}{\sqrt{6}}P_X^+ & 0 & \frac{-2}{3}\Delta' \\
\frac{-1}{\sqrt{2}}P'^+ & \sqrt{\frac{2}{3}}P'^z & \frac{1}{\sqrt{6}}P'^- & 0 & \frac{1}{\sqrt{3}}P'^z & \frac{1}{\sqrt{3}}P'^- & E_6^k & 0 & \frac{-1}{\sqrt{2}}P^+ & \sqrt{\frac{2}{3}}P^z & \frac{1}{\sqrt{6}}P^- & 0 & \frac{1}{\sqrt{3}}P^z & \frac{1}{\sqrt{3}}P^- \\
0 & \frac{-1}{\sqrt{6}}P'^+ & \sqrt{\frac{2}{3}}P'^z & \frac{1}{\sqrt{2}}P'^- & \frac{1}{\sqrt{3}}P'^+ & \frac{-1}{\sqrt{3}}P'^z & 0 & E_6^k & 0 & \frac{-1}{\sqrt{6}}P^+ & \sqrt{\frac{2}{3}}P^z & \frac{1}{\sqrt{2}}P^- & \frac{1}{\sqrt{3}}P^+ & \frac{-1}{\sqrt{3}}P^z \\
\frac{1}{3}\Delta' & \frac{-1}{\sqrt{3}}P_X^+ & \frac{-1}{\sqrt{3}}P_X^z & 0 & \frac{-1}{\sqrt{6}}P_X^+ & -\sqrt{\frac{2}{3}}P_X^z & \frac{-1}{\sqrt{2}}P^- & 0 & E_8^H & \mathfrak{B} & \mathfrak{C} & 0 & \frac{1}{\sqrt{2}}\mathfrak{B} & \sqrt{2}\mathfrak{C} \\
\frac{1}{\sqrt{3}}P_X^- & \frac{1}{3}\Delta' & 0 & \frac{-1}{\sqrt{3}}P_X^z & 0 & \frac{1}{\sqrt{2}}P_X^+ & \sqrt{\frac{2}{3}}P^z & \frac{-1}{\sqrt{6}}P^- & \mathfrak{B}^* & E_8^L & 0 & \mathfrak{C} & -\sqrt{2}\mathfrak{A} & -\sqrt{\frac{3}{2}}\mathfrak{B} \\
\frac{1}{\sqrt{3}}P_X^z & 0 & \frac{1}{3}\Delta' & \frac{1}{\sqrt{3}}P_X^+ & \frac{-1}{\sqrt{2}}P_X^- & 0 & \frac{1}{\sqrt{6}}P^+ & \sqrt{\frac{2}{3}}P^z & \mathfrak{C}^* & 0 & E_8^L & -\mathfrak{B} & -\sqrt{\frac{3}{2}}\mathfrak{B}^* & \sqrt{2}\mathfrak{A} \\
0 & \frac{1}{\sqrt{3}}P_X^z & \frac{-1}{\sqrt{3}}P_X^- & \frac{1}{3}\Delta' & -\sqrt{\frac{2}{3}}P_X^z & \frac{1}{\sqrt{6}}P_X^- & 0 & \frac{1}{\sqrt{2}}P^+ & 0 & \mathfrak{C}^* & -\mathfrak{B}^* & E_8^H & -\sqrt{2}\mathfrak{C}^* & \frac{1}{\sqrt{2}}\mathfrak{B}^* \\
\frac{1}{\sqrt{6}}P_X^- & 0 & \frac{1}{\sqrt{2}}P_X^+ & \sqrt{\frac{2}{3}}P_X^z & \frac{-2}{3}\Delta' & 0 & \frac{1}{\sqrt{3}}P^z & \frac{1}{\sqrt{3}}P^- & \frac{1}{\sqrt{2}}\mathfrak{B}^* & -\sqrt{2}\mathfrak{A} & -\sqrt{\frac{3}{2}}\mathfrak{B} & -\sqrt{2}\mathfrak{C} & E_7^k & 0 \\
\sqrt{\frac{2}{3}}P_X^z & \frac{-1}{\sqrt{2}}P_X^- & 0 & \frac{-1}{\sqrt{6}}P_X^+ & 0 & \frac{-2}{3}\Delta' & \frac{1}{\sqrt{3}}P^+ & \frac{-1}{\sqrt{3}}P^z & \sqrt{2}\mathfrak{C}^* & -\sqrt{\frac{3}{2}}\mathfrak{B}^* & \sqrt{2}\mathfrak{A} & \frac{1}{\sqrt{2}}\mathfrak{B} & 0 & E_7^k
\end{array}\right]
\end{array}
\tag{A1}
$$

In Eq. (A1), the parameters are the following:

$$P = (\hbar/m_0)\langle S|p_x|iX\rangle;$$

$$P_X = (\hbar/m_0)\langle X_C|p_y|iZ\rangle;$$

$$P' = (\hbar/m_0)\langle S|p_x|iX_C\rangle.$$

m_0 is the free-electron mass. P, P_X, and P' are real.

$$P_\alpha^\pm = P_\alpha(k_x \pm ik_y), \quad P_\alpha^z = P_\alpha k_z$$

with $P_\alpha = P$ or P_X or P'.

$$E_{P\alpha} = (2m_0/\hbar^2)P_\alpha^2.$$

$$\Delta = (3\hbar/4m_0^2c^2)\langle X|(\partial\mathfrak{U}/\partial x)p_y - (\partial\mathfrak{U}/\partial y)p_x|iY\rangle;$$

$$\Delta_C = (3\hbar/4m_0^2c^2)\langle X_C|(\partial\mathfrak{U}/\partial x)p_y - (\partial\mathfrak{U}/\partial y)p_x|iY_C\rangle;$$

$$\Delta' = (3\hbar/4m_0^2c^2)\langle X|(\partial\mathfrak{U}/\partial x)p_y - (\partial\mathfrak{U}/\partial y)p_x|iY_C\rangle.$$

$\mathfrak{U}$ is the periodic potential in the Bloch Hamiltonian $\mathbf{p}^2/2m_0 + \mathfrak{U}(\mathbf{r})$. Δ, Δ_C, and Δ' are, respectively, the spin-orbit-coupling energy of the Γ_{5V} valence band which results in Γ_{8V} and Γ_{7V}, the spin-orbit-coupling energy of the second Γ_{5C} conduction band which results in Γ_{8C} and Γ_{7C}, and the interband spin-orbit-coupling energy between Γ_{5V} and Γ_{5C}.

P' and Δ' vanish in O_h group but are nonzero in T_d group.

$$E_{8C}^H = E'_{8C} - \gamma'_{C1}\check{k}^2 + \mathfrak{A}_C; \quad E_{8C}^L = E'_{8C} - \gamma'_{C1}\check{k}^2 - \mathfrak{A}_C;$$
$$E_{7C}^k = E'_{7C} - \gamma'_{C1}\check{k}^2; \quad E'_{8C} - E'_{7C} = \Delta_C;$$

$$E_6^k = E_6 + \gamma'_C\check{k}^2;$$

$$E_8^H = E'_8 - \gamma'_1\check{k}^2 + \mathfrak{A}; \quad E_8^L = E'_8 - \gamma'_1\check{k}^2 - \mathfrak{A};$$
$$E_7^k = E'_7 - \gamma'_1\check{k}^2; \quad E'_8 - E'_7 = \Delta.$$

$$\mathfrak{A}_C = \gamma'_{C2}(2\check{k}_z^2 - \check{k}_\rho^2); \quad \mathfrak{B}_C = 2\sqrt{3}\gamma'_{C3}\check{k}_z\check{k}_-;$$
$$\mathfrak{C}_C = \sqrt{3}[\gamma'_{C2}(\check{k}_x^2 - \check{k}_y^2) - 2i\gamma'_{C3}\check{k}_x\check{k}_y];$$

TABLE II. The basis wave functions of the (14×14) Hamiltonian. These functions are pairs of Kramers conjugates. For example, $\hat{\mathbf{K}}|+\rangle=|-\rangle$ or $\hat{\mathbf{K}}|\frac{3}{2}\rangle=|\frac{-3}{2}\rangle$.

$\|+\rangle=\|S\uparrow\rangle$	$\|-\rangle=\|S\downarrow\rangle$
$\|c\frac{3}{2}\rangle=\|i[-\sqrt{1/2}(X_C+iY_C)\uparrow]\rangle$	$\|\frac{3}{2}\rangle=\|i[-\sqrt{1/2}(X+iY)\uparrow]\rangle$
$\|c\frac{1}{2}\rangle=\|i[\sqrt{2/3}Z_C\uparrow-\sqrt{1/6}(X_C+iY_C)\downarrow]\rangle$	$\|\frac{1}{2}\rangle=\|i[\sqrt{2/3}Z\uparrow-\sqrt{1/6}(X+iY)\downarrow]\rangle$
$\|c\frac{-1}{2}\rangle=\|i[\sqrt{1/6}(X_C-iY_C)\uparrow+\sqrt{2/3}Z_C\downarrow]\rangle$	$\|\frac{-1}{2}\rangle=\|i[\sqrt{1/6}(X-iY)\uparrow+\sqrt{2/3}Z\downarrow]\rangle$
$\|c\frac{-3}{2}\rangle=\|i[\sqrt{1/2}(X_C-iY_C)\downarrow]\rangle$	$\|\frac{-3}{2}\rangle=\|i[\sqrt{1/2}(X-iY)\downarrow]\rangle$
$\|c\frac{7}{2}\rangle=\|i[\sqrt{1/3}Z_C\uparrow+\sqrt{1/3}(X_C+iY_C)\downarrow]\rangle$	$\|\frac{7}{2}\rangle=\|i[\sqrt{1/3}Z\uparrow+\sqrt{1/3}(X+iY)\downarrow]\rangle$
$\|c\frac{-7}{2}\rangle=\|i[\sqrt{1/3}(X_C-iY_C)\uparrow-\sqrt{1/3}Z_C\downarrow]\rangle$	$\|\frac{-7}{2}\rangle=\|i[\sqrt{1/3}(X-iY)\uparrow-\sqrt{1/3}Z\downarrow]\rangle$

$$\mathfrak{A}=\gamma_2'(2\check{k}_z^2-\check{k}_\rho^2);\quad \mathfrak{B}=2\sqrt{3}\gamma_3'\check{k}_z\check{k}_-;$$

$$\mathfrak{C}=\sqrt{3}[\gamma_2'(\check{k}_x^2-\check{k}_y^2)-2i\gamma_3'\check{k}_x\check{k}_y].$$

$$\check{k}_w=\sqrt{\hbar^2/2m_0}k_w \quad \text{with} \quad w=x,y,z.$$

$$\check{k}_\pm=\check{k}_x\pm i\check{k}_y,\ \check{k}_\rho^2=\check{k}_x^2+\check{k}_y^2.$$

E_{8C}', E_{7C}', E_8', and E_7' would, respectively, be the energies $E(\Gamma_{8C})$, $E(\Gamma_{7C})$, $E(\Gamma_{8V})$, and $E(\Gamma_{7V})$ at $\mathbf{k}=\mathbf{0}$ if the Δ' interband spin-orbit coupling were equal to zero.

Furthermore,

$$\gamma_C'=\gamma_C-\frac{E_P}{3}\left(\frac{2}{E_G}+\frac{1}{E_G+\Delta}\right)+\frac{E_P'}{3}\left(\frac{2}{E_{8C-6}}+\frac{1}{E_{7C-6}}\right),$$

$$\gamma_1'=\gamma_1-\frac{E_P}{3E_G}-\frac{E_{PX}}{3}\left(\frac{1}{E_{7C-8}}+\frac{1}{E_{8C-8}}\right),$$

$$\gamma_2'=\gamma_2-\frac{E_P}{6E_G}+\frac{E_{PX}}{6E_{7C-8}},$$

$$\gamma_3'=\gamma_3-\frac{E_P}{6E_G}-\frac{E_{PX}}{6E_{7C-8}}, \tag{A2}$$

where E_G is the band-gap energy and $E_{n-m}=E(\Gamma_n)-E(\Gamma_m)$.

As quoted in Ref. 11, γ_j' $(j=1,2,3)$ are Luttinger-like parameters, in which the $\mathbf{k}\cdot\mathbf{p}$ interaction inside $\{\Gamma_{8C},\Gamma_{7C},\Gamma_6,\Gamma_{8V},\Gamma_{7V}\}$ has been subtracted. γ_j are Luttinger parameters. The same holds for γ_{Cj}'. However and for the sake of simplicity we take γ_{Cj}' equal to zero which does not change any significant result for the spin splitting in the forbidden band gap as shown in Ref. 4. In the same way, γ_C' is linked to γ_c with $\gamma_C=m_0/m_C$ where m_C is the conduction effective mass.

*henri-jean.drouhin@polytechnique.edu

[1] W. H. Butler, X.-G. Zhang, T. C. Schulthess, and J. M. MacLaren, Phys. Rev. B **63**, 054416 (2001); Phys. Rev. B **63**, 092402 (2001).

[2] V. Heine, Proc. Phys. Soc. London **81**, 300 (1963).

[3] R. O. Jones, Proc. Phys. Soc. London **89**, 443 (1966).

[4] S. Richard, H.-J. Drouhin, N. Rougemaille, and G. Fishman, J. Appl. Phys. **97**, 083706 (2005).

[5] N. Rougemaille, H.-J. Drouhin, S. Richard, G. Fishman, and A. K. Schmid, Phys. Rev. Lett. **95**, 186406 (2005).

[6] G. Dresselhaus, Phys. Rev. **100**, 580 (1955).

[7] T. L. Hoai Nguyen, H.-J. Drouhin, J.-E. Wegrowe, and G. Fishman, Phys. Rev. B **79**, 165204 (2009).

[8] M. D'yakonov and V. I. Perel', Zh. Eksp. Teor. Fiz. **60**, 1954 (1971); [Sov. Phys. JETP **33**, 1053 (1971)]; M. D'yakonov and V. I. Perel', Fiz. Tverd. Tela (Leningrad) **13**, 3581 (1971); [Sov. Phys. Solid State **13**, 3023 (1972)].

[9] V. I. Perel', S. A. Tarasenko, I. N. Yassievich, S. D. Ganichev, V. V. Bel'kov, and W. Prettl, Phys. Rev. B **67**, 201304(R) (2003).

[10] G. Fishman, *Semi-conducteurs: les bases de la théorie* $\mathbf{k}\cdot\mathbf{p}$ (Les Éditions de l'École Polytechnique, Palaiseau, 2009).

[11] P. Pfeffer and W. Zawadzki, Phys. Rev. B **53**, 12813 (1996).

[12] B. Jusserand, D. Richards, G. Allan, C. Priester, and B. Etienne, Phys. Rev. B **51**, 4707 (1995).

[13] J.-M. Jancu, R. Scholz, E. A. de Andrada e Silva, and G. C. La Rocca, Phys. Rev. B **72**, 193201 (2005). Δ^- and Δ_0' in the article by Jancu *et al.* are, respectively, written as Δ' and Δ_C in the present article.

[14] G. F. Koster, J. O. Dimmock, G. Wheeler, and R. G. Statz, *Properties of the Thirty-Two Point Groups* (MIT Press, Cambridge, Massachusetts, 1963).

[15] A. Messiah, *Mécanique Quantique* (Dunod, Paris, 1995), p. 445.

Chapitre 3

Effet tunnel dépendant du spin

La description de l'effet tunnel au travers d'une barrière semi-conductrice est un problème clé dès lors qu'on s'intéresse à la physique des hétérostructures. Tout ceci est bien sûr directement lié à la notion d'Hamiltonien effectif et aux techniques de fonction-enveloppe, sujets difficiles et encore partiellement ouverts [BDM]. La description du transport électronique dans un milieu dont la périodicité est brisée est un problème fort ancien, citons entre autres les contributions de J. C. Slater [SLA] et de J. M. Luttinger et W. Kohn [LK]. Harrison [HAR] a étudié le problème du transport quantique dans un matériau hétérogène et a introduit de nouvelles conditions de discontinuité de la fonction enveloppe et de sa dérivée, dans une approche très générale, bien au delà de la physique des semi-conducteurs. Un pas décisif fut franchi par BenDaniel et Duke [BDD] qui introduisirent les conditions de raccord de la fonction enveloppe à l'interface entre deux milieux de masses effectives différentes, grâce à la construction d'un hamiltonien effectif garantissant la conservation du courant de probabilité. Dans ces processus de transport, c'est bien la notion de courant de probabilité qui joue un rôle central, le courant étant la quantité conservative du problème. Cette approche a été adaptée et généralisée au traitement des hétérostructures par Bastard, Altarelli et Foreman [GB]. Elle est devenue la procédure standard de calcul pour les hétérostructures. Dans ce chapitre, basé sur l'article "Spin rotation, spin filtering, and spin transfer in directional tunneling through barriers in noncontrosymmetric semiconducteurs" [T. L. Hoai Nguyen, H.-J. Drouhin, J.-E. Wegrowe, and G. Fishman, Phys. Rev. B **79**, 165204-1 à 21 (2009)], nous considérons une barrière faite de GaAs, un semi-conducteur ne possédant pas de symétrie d'inversion. Dans ce cas, outre les possibles discontinuités de masses effectives, l'hétérostructure est

caractérisée par des discontinuités de l'interaction spin-orbite - et plus précisément par des discontinuités de champ D'yakonov-Perel', qui dépend du vecteur d'onde électronique. Le processus tunnel va donc devenir fortement dépendant de la direction cristallographique et potentiellement compliqué. En effet, si l'on réalise que l'Hamiltonien d'interaction spin-orbite est en $\boldsymbol{\nabla} V \times \mathbf{p}$, on comprend bien que, pour une simple barrière rectangulaire (V contenant des fonctions d'Heaviside), le potentiel n'est pas *a priori* borné ($\boldsymbol{\nabla} V$ contient des distributions de Dirac). On s'attend par conséquent à devoir, en général, renoncer à la continuité de la dérivée de la fonction d'onde. De fait, l'équation de Schrödinger associée au problème recèle des difficultés mathématiques. Dans le traitement proposé ici, on s'affranchit de ces pathologies en considérant que, dans les régions propagatives, l'énergie cinétique est très faible, de sorte que la levée de dégénérescence de spin est négligeable, quelle que soit la valeur du coefficient de proportionnalité (γ) définissant le champ interne. Au contraire, dans la barrière, si l'effet tunnel survient significativement en dessous du sommet de la barrière, la levée de dégénérescence de spin sera appréciable. On considère donc pour simplifier un système dans lequel le coefficient γ est supposé comme constant (on évite les discontinuités de γ). De même, on n'oublie pas que l'expression classique du champ interne résulte d'un calcul de perturbation et, partant des solutions du problème que l'on connaît bien en l'absence de champ interne ($\gamma = 0$), on cherche les nouvelles solutions lorsqu'on branche le champ effectif en se limitant aux corrections du premier ordre seulement. En pratique, on focalise l'étude sur deux cas particuliers importants : i) le tunneling sous incidence non-normale sur une barrière orientée selon la direction [001] ; ii) le tunneling sous incidence normale pour une barrière orientée selon la direction [110]. Dans le premier cas, on retrouve un processus tunnel quasi "classique". Les conditions de raccord sont la continuité de la fonction d'onde et de sa dérivée aux deux interfaces, projetées sur chaque canal de spin. Au final, nous obtenons un système linéaire de 8 équations couplées à 8 inconnues. Cette situation conduit à un filtrage en spin, l'axe du filtre à spin étant un direction située dans le plan de la barrière, et correspond à un cas étudié par Perel' et al. en utilisant une approche différente [PER]. Le deuxième cas est beaucoup plus surprenant car l'Hamiltonien effectif n'est pas quadratique (il contient des termes cubiques). Il est tout d'abord nécessaire de redéfinir la notion de courant de probabilité et ceci constitue un résultat important (présenté dans l'Appendice B de l'article). Partant de l'équation de Schrödinger effective, les conditions de discontinuité de la dérivée de la fonction d'onde sont établies. Au final, les deux

canaux de spin sont découplés et, s'il n'y a aucun filtrage de spin - ce qui est curieux puisque c'est selon cette direction que la levée de dégénérescence de spin est maximum dans la bande de conduction - la fonction d'onde transmise subit des déphasages opposés selon le sens du spin (quantifié le long de la direction du champ D'yakonov-Perel', dans le plan de la barrière). Partant d'un spin incident situé dans le plan perpendiculaire au champ, on observe une précession de spin autour du champ complexe au cours du processus tunnel. Divers développements sont détaillés dans l'annexe C. Il s'agit en particulier de la construction de combinaisons de fonctions d'ondes de la barrière qui correspondent à la notion usuelle de courant de probabilité (pour un électron libre) et de la structure mathématique de ces solutions (espace vectoriel sur $\mathbb{R}$ et pas sur $\mathbb{C}$). Cette notion est utile pour fabriquer des situations qui ont des analogues classiques et aussi pour aborder le cas d'une barrière séparant deux matériaux dans lesquels l'électron est libre : il s'agira bien ici de conserver le courant usuel. Un certain nombre de calculs du cas i), liés à la résolution approchée du système 8×8, sont utiles mais assez fastidieux : ils sont eux aussi explicités dans l'annexe E. Enfin, la notion de filtre à spin, importante en spintronique, est rarement discutée : quelques réflexions sont rassemblées dans l'annexe D.

Spin rotation, spin filtering, and spin transfer in directional tunneling through barriers in noncentrosymmetric semiconductors

T. L. Hoai Nguyen,[1,2] Henri-Jean Drouhin,[1,*] Jean-Eric Wegrowe,[1] and Guy Fishman[2]
[1]*Ecole Polytechnique, LSI, CNRS and CEA/DSM/IRAMIS, Palaiseau F-91128, France*
[2]*Université Paris-Sud, IEF, CNRS, Orsay F-91405, France*
(Received 20 February 2008; revised manuscript received 12 November 2008; published 10 April 2009)

We discuss possible tunneling phenomena associated with complex wave vectors along directions where the spin degeneracy is lifted in noncentrosymetric semiconductors. We show that the result drastically depends on the direction. In the [110] direction, no solution can be calculated in the usual way assuming that the wave function and its derivative are continuous. A method for obtaining physical solutions is given and consequences are drawn. As a result, there is no spin filtering in such a direction but the spin undergoes a precession through the barrier with the rotation angle being proportional to the barrier thickness. In a direction close to [001] we find a spin-filter effect in close agreement with the model discussed by Perel' *et al.* [Phys. Rev. B **67**, 201304(R) (2003)].

DOI: 10.1103/PhysRevB.79.165204 PACS number(s): 72.25.Dc, 73.40.Gk, 71.20.Mq

I. INTRODUCTION

Understanding spin-dependent tunneling through semiconductor barriers is a fundamental problem in semiconductor physics. A description of this coherent process is crucial for spin-subband engineering of semiconductor heterostructures and superlattices. Moreover, spin-dependent tunneling through crystalline barriers has also become a topic of major interest in spintronics.[1,2] This paper thus lies at the interface between general semiconductor physics and spintronics. Regarding semiconductor physics, it has close connections with open problems in the envelope function theory.[3] Harrison[4] studied the problem of heterogeneous materials and introduced the conditions of discontinuity of the envelope function, taking a general viewpoint, well beyond the semiconductor area. A decisive step in semiconductors was performed by BenDaniel and Duke[5] who defined specific discontinuity conditions of the derivative of the envelope function between two media with different effective masses, based on the conservation of the probability current. This approach has been successfully applied to heterostructures by Bastard[6] and has become the standard calculation routine, yielding very accurate energy positions of the energy bands, in perfect agreement with the experimental data.[7] Hereafter, analogously, we deal with periodic lattices which are perturbed by a spin-orbit potential and where, due to the absence of space-inversion symmetry, the spin degeneracy of the bands is lifted through a wave-vector-dependent "exchange" field.[8,9] We show that the matching conditions of the derivative of envelope function at the boundaries cannot be "as usual." Thus, the basic tunneling equations are not known.

First of all, dealing with tunneling phenomena requires an accurate knowledge of the energy structure in the forbidden band gap, i.e., of the complex band structure of the barrier material. In pioneering articles, Heine[10] and Jones[11] derived general properties of the evanescent states and showed their complexity over six-dimensional wave-vector space, consisting of complex vectors associating a pure imaginary component to a real propagating one. It might be thought that the electrons will tunnel through such complex-wave-vector states as they would do through usual evanescent states (with pure imaginary wave vectors), and this intuitive explanation would be supported by our familiarity with the tunneling of electrons located in semiconductor side valleys (e.g., in the conduction band of silicon). Hereafter, we deal with spin-dependent tunneling of conduction electrons through a gallium arsenide barrier, a compound with no inversion symmetry.[12] Such processes were investigated by Perel' *et al.*[13] in a stimulating article using the effective-mass approximation and under simplifying assumptions; quite large spin-filter effects were predicted. Although the complex band structure of GaAs was expected to be well known, we have recently found that, in fact, the spin-orbit interaction and the absence of inversion symmetry had never been taken into account simultaneously throughout the Brillouin zone.[14,15] The evanescent band structure was calculated by several authors. Chang[16] considered semiconductors oriented in the [100], [111], and [110] directions, with space-inversion centers (O_h group) or without space-inversion centers (T_d group), but without taking into account the spin-orbit coupling. Chang and Schulman[17] performed a detailed calculation of the band structure of silicon, which belongs to the O_h group. Schuurmans and t'Hooft[18] studied semiconductors belonging to the T_d group but explicitly discarded terms which lead to odd k terms, so that essentially they studied GaAs and AlAs as if they belonged to the O_h group. In Ref. 15 the evanescent band structure in the fundamental gap of GaAs-like III-V semiconductors, including both the spin-orbit coupling and the lack of inversion symmetry, was carefully calculated within a 14×14 and a 30×30 $\mathbf{k}\cdot\mathbf{p}$ Hamiltonian framework. Then it was demonstrated that the evanescent states in the fundamental gap present an original topology, with loops connecting nearly-opposite spin states at the center of the Brillouin zone.[14] This very structure has strong consequences for electron tunneling. Here, in order to remove any unnecessary complexity, we start dealing with electrons with a unique effective mass m, inside and outside the barrier—an approximation used in numerical applications in Ref. 13. The spin splitting in the barrier is described

via the D'yakonov-Perel' (DP) Hamiltonian.[8] We thus revisit a classic in elementary quantum mechanics—the tunneling of free electrons through a square potential barrier—but in a case where the evanescent states in the barrier are spin split. From general considerations, we derive relevant boundary conditions which are sensitive on the crystallographic direction. We demonstrate that the tunneling process can become rather involved: the case of loop-shaped real-energy lines correspond to wave vectors which have both an imaginary component, which defines the tunneling direction, and an *orthogonal* real component, so that one has to deal, so to say, with a "classical" tunneling effect in the sense where it is possible to recover almost usual tunneling properties—analogous to off-normal tunneling of free electrons—but in a subtle way. In the case of one-dimensional tunneling with a complex (neither real nor purely imaginary) wave vector, the tunnel effect seems to be "anomalous:" a spin precession occurs around a "complex magnetic field." We show that the derivative of the envelope function, which is the solution of the Schrödinger equation, undergoes discontinuities at the barrier plane—usually, in semiconductor heterostructures, discontinuities of the derivative arise *as a consequence of the different effective masses* in the well and in the barrier material[6]—and we propose a treatment of heterostructures. After entangling the two spin channels, it is possible to recover a situation which has strong analogy with standard tunneling and where the discontinuity of a "magnetic current" can be viewed as the result of a kinetic-momentum transfer at the barrier interfaces. The spin-orbit-split barrier exerts a torque on the electron spin, similar to spin-torque phenomena in ferromagnetic junctions as predicted by Slonczewski[9] and Berger,[19] but in the case considered by these authors, as the barrier is constituted of magnetic material, a spin transfer occurs between the tunneling electrons and the magnetization.

The layout of this paper is as follows. In Sec. II, we give the background relative to the spin splitting and to the conservation of the probability current which will be used afterward. We show how the spin splitting can lead to complex (not strictly imaginary) wave vectors in the barrier and we analyze the consequences on the probability current. In Sec. III, we study a barrier normal to [110] and in Sec. IV we look in detail the case of an incident wave whose direction is almost normal to a [001] barrier. A summary is given in Sec. V.

II. BACKGROUND

A. Symmetry

Let us present the notations used throughout the present paper (see Fig. 1). $\mathbf{e}$ is a unit vector. The direction of the axes, defined by $\mathbf{e}_x$, $\mathbf{e}_y$, $\mathbf{e}_z$ with respect to crystal axes, will be given in each case. $\mathbf{e}_z$ is normal to the barrier. $\mathbf{e}_z=\mathbf{e}_{110}$ in Sec. III and $\mathbf{e}_z=\mathbf{e}_{001}$ in Sec. IV. We define $\mathbf{k}_{\mathrm{I}}=\boldsymbol{\xi}+\mathbf{q}$, $\mathbf{k}_{\mathrm{II}}=\boldsymbol{\xi}+\mathbf{Q}+i\mathbf{K}$ ($\boldsymbol{\xi}$, $\mathbf{q}$, $\mathbf{Q}$, and $\mathbf{K}$ are all real vectors), and $\mathbf{k}_{\mathrm{III}}=\boldsymbol{\xi}+\mathbf{q}$. We also use the following notations: $\boldsymbol{\rho}=x\mathbf{e}_x+y\mathbf{e}_y$, $\boldsymbol{\xi}=\xi_x\mathbf{e}_x+\xi_y\mathbf{e}_y$, $\mathbf{q}=q\mathbf{e}_z$, $\mathbf{Q}=Q\mathbf{e}_z$, $\mathbf{K}=K\mathbf{e}_z$, $\mathbf{k}_{\mathrm{I}}\cdot\mathbf{r}=\mathbf{k}_{\mathrm{III}}\cdot\mathbf{r}=\xi_x x+\xi_y y+qz$, and $\mathbf{k}_{\mathrm{II}}\cdot\mathbf{r}=\xi_x x+\xi_y y+(Q+iK)z$. Without spin, the wave function of the incident plane wave and in the barrier should be written as $e^{i(\boldsymbol{\xi}\cdot\boldsymbol{\rho}+qz)}$ and $e^{i[\boldsymbol{\xi}\cdot\boldsymbol{\rho}+(\mathbf{Q}+i\mathbf{K})z]}$, respectively.

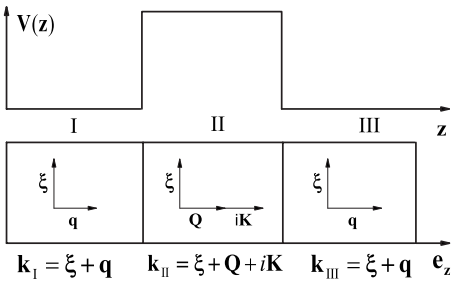

FIG. 1. Sketch of the tunnel geometry with definition of notations. The spin-orbit-split barrier material of thickness a (medium II) is located between two free-electronlike materials (media I and III). The tunnel axis, normal to the barrier, is the z axis. In the free-electronlike materials, the real electron wave vector in the z direction is referred to as $\mathbf{q}$. In the barrier material, the evanescent wave vector along the z axis is referred to as $\mathbf{Q}+i\mathbf{K}$, where $\mathbf{Q}$ and $\mathbf{K}$ are real quantities. The transverse wave-vector component, in the barrier plane, $\boldsymbol{\xi}$ is conserved in the tunnel process. Then, the overall wave vectors in the three media are, respectively, $\mathbf{k}_{\mathrm{I}}=\mathbf{k}_{\mathrm{III}}=\boldsymbol{\xi}+\mathbf{q}$ and $\mathbf{k}_{\mathrm{II}}=\boldsymbol{\xi}+\mathbf{Q}+i\mathbf{K}$.

To describe the structure of the evanescent states, we use the $\mathbf{k}\cdot\mathbf{p}$ method. In a n-band model, the energy dispersion curves result from the diagonalization of a $(n\times n)$ $\mathbf{k}\cdot\mathbf{p}$ Hamiltonian $\hat{H}$, but $\mathbf{k}$ is a complex vector, so that $\hat{H}$ is no longer Hermitian and the evanescent states are associated only to real eigenvalues E.[14,15] To find the energy dispersion curves, we have to solve the secular equation $\det M(\mathbf{k})=\det[\hat{H}-E\hat{I}]$, where $\hat{I}$ is the identity. Because the Hamiltonian is Hermitian when $\mathbf{k}$ is a real vector, we have the relation $M(\mathbf{k})^{t*}=M(\mathbf{k}^*)$. Thus, $\det M(\mathbf{k}^*)=[\det M(\mathbf{k})^t]^*=[\det M(\mathbf{k})]^*$. It follows that $E_n(\mathbf{k})=E_{n'}(\mathbf{k}^*)$, where the band indices n and n' may or may not refer to the same band.[10,11] Moreover, Kramers conjugates correspond to the same energy, so that the state associated to $(\mathbf{k},|\mathrm{up}\rangle)$ and the state associated to $(-\mathbf{k},|\mathrm{down}\rangle)$ are degenerate.[20,21] Let us recall that Kramers-conjugate states are obtained by application of $\hat{K}$, the time-reversal operator $\hat{K}=-i\sigma_y\hat{K}_0$, where σ_y is the relevant Pauli matrix and $\hat{K}_0$ is the operation of taking the complex conjugate.[20] Thus in GaAs, the spin degeneracy is lifted and we expect that the four states $[(\mathbf{k},|s\rangle)$, $(\mathbf{k}^*,|s'\rangle)$, $(-\mathbf{k}^*,|-s\rangle)$, and $(-\mathbf{k},|-s'\rangle)]$ be degenerate, with $|s\rangle$ and $|s'\rangle$ being up-spin states in directions which, generally, are not parallel (Fig. 2). We are going to see a concrete example in Sec. II B, where $|s\rangle$ and $|s'\rangle$ are quantized in the same direction, and in Sec. IV, where $|s\rangle$ and $|s'\rangle$ are not quantized in the same direction.

B. Energy levels

In Sec. I, we mentioned that the evanescent band structure is deeply altered when the lack of inversion symmetry is taken into account together with the spin-orbit splitting. A particular topology consisting of loops connecting Kramers-conjugate spin states near the zone center was shown along directions of type $K[\xi/K,0,i]$ when the ratio $\xi/K=\tan\theta$ is fixed. Such loop structure can be expected to arise as it is

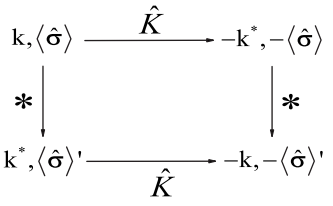

FIG. 2. This figure illustrates transformations which, starting from a state of wave vector **k** and with a mean value of the Pauli operator $\langle\hat{\boldsymbol{\sigma}}\rangle$, construct degenerate states. $\hat{K}_0$ is the complex conjugation and $\hat{K}=-i\sigma_y\hat{K}_0$ is the Kramers time-reversal operator. $\hat{K}$ yields a state with the wave vector $-\mathbf{k}^*$ and with the mean spin $-\langle\hat{\boldsymbol{\sigma}}\rangle$. The state of wave vector $\mathbf{k}^*$ may be associated to another spin state, corresponding to the mean value $\langle\hat{\boldsymbol{\sigma}}\rangle'$. Applying $\hat{K}$ to this state, we form a degenerate state with the wave vector $-\mathbf{k}$ and associated to the mean spin $-\langle\hat{\boldsymbol{\sigma}}\rangle'$. Four states are finally obtained.

known that a band cannot stop.[10] Depending on θ, we obtain the different pictures shown in Fig. 3. The spin vector along a loop is defined by the mean value of the Pauli operator $\hat{\boldsymbol{\sigma}}$. In the small-$k$ and small-θ limit, we get two nearly-opposite spin vectors. When going off the zone center, a numerical calculation shows that the two spin vectors rotate to become parallel at the point where the two subbands are connecting. The appearance of these loops is the fingerprint of a strong band mixing of the first conduction band and of the three upper valence bands with remote bands (more precisely with the second conduction band). Indeed, as long as the wave

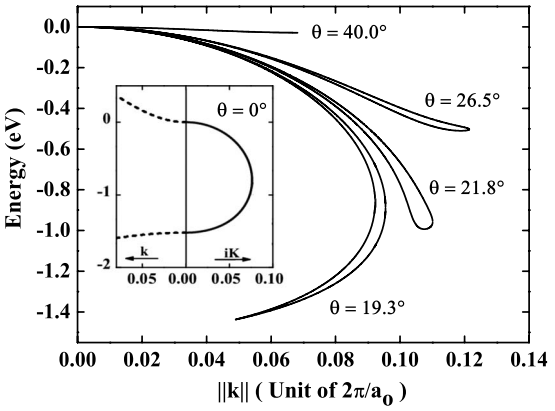

FIG. 3. Plot of the real-energy lines inside the gap for $\mathbf{k}=[\xi,0,iK]$, where K and ξ are real and positive and $\tan\theta=\xi/K$. The calculation is performed using a 14×14 $\mathbf{k}\cdot\mathbf{p}$ Hamiltonian. The loops are drawn versus $\|\mathbf{k}\|$ in $2\pi/a_0$ units, where a_0 is the cubic lattice parameter. In all these directions, the spin degeneracy is lifted. Their shape and extension sharply depend on θ. For $\theta=43.2°$, the two branches are too close to be resolved at this scale. The parameters used in the calculation are $P=9.88$ eV Å, $P'=0.41$ eV Å, $E_G=1.519$ eV, $\Delta_c=E_{\Gamma8c}-E_{\Gamma7c}=0.171$ eV, $P_X=8.68$ eV Å, $\Delta=0.341$ eV, $E_\Delta=E_{\Gamma7c}-E_{\Gamma6c}=2.969$ eV, and $\Delta'=-0.17$ eV (see Ref. 30 for a complete discussion). Inset: real-band structure (left, dashed line; for clarity, only a valence band which is connected to the evanescent branch is drawn) and evanescent band across the band gap (right, full line) along the [001] direction ($\theta=0$) where the DP exchange field is zero (no spin splitting).

vector remains in some vicinity of Γ, the energy levels are well described by the DP Hamiltonian, where the spin states in the subbands only depend on θ (see Sec. IV). Observe, in Fig. 3, that—because the extension of the loop tends to zero when θ tends to 45°—the portion of the loops which can be described in this analytical model also has an extension which can become vanishingly small. Hereafter, we stay in the framework of the DP model, which allows analytical calculations.

Throughout the present paper, we take the origin of the energy at the bottom of the conduction band, so that the relevant Hamiltonian is written as

$$\hat{H}=\hat{H}_0+\hat{H}_{\mathrm{DP}},$$

$$\hat{H}_0=\frac{\hat{\mathbf{p}}^2}{2m}=\frac{-\hbar^2}{2m}\boldsymbol{\nabla}^2=-\gamma_c\boldsymbol{\nabla}^2,$$

$$\hat{H}_{\mathrm{DP}}=\gamma\boldsymbol{\chi}\cdot\hat{\boldsymbol{\sigma}}, \tag{2.1}$$

where m is the effective mass. $\hat{H}_{\mathrm{DP}}$ is the DP Hamiltonian which describes the k^3 spin splitting:[8] $\boldsymbol{\chi}=\boldsymbol{\chi}(\mathbf{k})=[\chi_x,\chi_y,\chi_z]=[k_x(k_y^2-k_z^2),k_y(k_z^2-k_x^2),k_z(k_x^2-k_y^2)]$. When $\mathbf{k}$ is real, the energy levels are pure spin states, quantized along $\boldsymbol{\chi}$, in the plane perpendicular to $\mathbf{k}$. Note that the two eigenvalues of $\boldsymbol{\chi}\cdot\hat{\boldsymbol{\sigma}}$ are opposite, equal to the square roots of $\bar{\chi}^2=\chi_x^2+\chi_y^2+\chi_z^2$. We designate by $\bar{\chi}_+$ ($\bar{\chi}_-$) the square roots of $\bar{\chi}^2$ ($\bar{\chi}_+$ with a positive real part and $\bar{\chi}_-$ with a negative real part, if relevant). $\bar{\chi}_+$ ($\bar{\chi}_-$) will be used in Eqs. (2.6) and (2.8). The eigenvalues of $\hat{H}$ are written as $\mathcal{E}(\mathbf{k})$.

Inside a finite-width barrier, the incident plane wave e^{iqz} is usually to be replaced with $e^{\mp Kz}$ which corresponds to an imaginary wave vector $\pm iK$.

(a) If the incident wave vector $\mathbf{k}_{\mathrm{I}}$ is in the [001] direction ($\mathbf{k}_{\mathrm{I}}=[0,0,q]$), the wave vector in the barrier is $\mathbf{k}_{\mathrm{II}}=[0,0,\pm iK]$ and the degenerate eigenvalues of $\hat{H}$ are $\mathcal{E}(\mathbf{k})=-\gamma_cK^2$ which is the (real) energy $E(\mathbf{k})$ in the forbidden band gap. If $\mathbf{k}_{\mathrm{I}}$ is almost in the [001] direction ($\mathbf{k}_{\mathrm{I}}=[\xi,0,q]$ with $\xi\ll q$), $\mathbf{k}_{\mathrm{II}}=[\xi,0,\pm iK]$ and the eigenvalues of $\hat{H}$ are $\mathcal{E}(\mathbf{k})=-\gamma_c(K^2-\xi^2)\pm\gamma\xi K\sqrt{K^2-\xi^2}$ which is the energy $E(\mathbf{k})$ in the forbidden band gap as well.

(b) If $\mathbf{k}_{\mathrm{I}}$ is in the [110] direction ($\mathbf{k}_{\mathrm{I}}=\frac{q}{\sqrt{2}}[110]$), a simple idea would be to take $\mathbf{k}_{\mathrm{II}}=\pm\frac{iK}{\sqrt{2}}[110]$ which leads to $\mathcal{E}(\mathbf{k})=-\gamma_cK^2\pm i\frac{\gamma}{2}K^3$. This quantity is not real and cannot be an energy $E(\mathbf{k})$.[22] We are therefore led to consider a wave vector such that $\mathbf{k}_{\mathrm{II}}=\frac{1}{\sqrt{2}}(Q\pm iK)[110]$.

The calculation is given in Appendix A. The resulting band is plotted in Fig. 4, over a very broad energy domain to reveal its general structure. We are only interested in evanescent states located in the forbidden band gap, i.e., states with a small negative energy. For our purposes, a key point is that, at a given energy, we have *exactly* four possible states, with wave vectors $(Q\pm iK)$ for spin ↑ and $(-Q\pm iK)$ for spin ↓, the latter being obtained from the former through $\hat{K}$. In short,

$$E_\uparrow(\mathbf{k})=E_\uparrow(\mathbf{k}^*)=E_\downarrow(-\mathbf{k})=E_\downarrow(-\mathbf{k}^*). \tag{2.2}$$

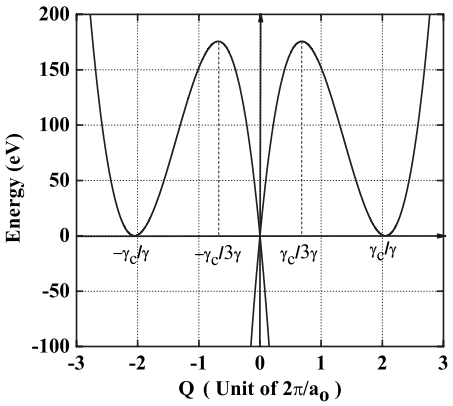

FIG. 4. Mathematical plot of the real-energy lines for **k** along [110] as a function of the real part of the wave vector Q in the barrier. The calculation is performed for a ratio $\gamma/\gamma_c=0.438$ Å. We are only concerned with negative energies, which refer to evanescent states. More precisely, the physical states are located within a very small energy domain below the origin. The domain $Q>0$ refers to up-spin states, whereas the domain $Q<0$ refers to down-spin states. In each case, the imaginary component of the wave vector can take the values $\pm K$. Thus, at a given energy, we have exactly the *four* possible states $(Q\pm iK)\uparrow$ and $(-Q\pm iK)\downarrow$. The down-spin states are Kramers conjugates of the up-spin states.

Equation (2.2) provides us with a concrete example of the ideas developed by Jones[11] who showed that $E(\mathbf{k})=E(\mathbf{k}^*)$. The corresponding four plane waves are $e^{i(Q\pm iK)}\uparrow$ and $e^{i(-Q\pm iK)}\downarrow$ or $e^{\mp Kz}e^{iQz}\uparrow$ and $e^{\mp Kz}e^{-iQz}\downarrow$ (this is schematically shown in Fig. 5). This leads us to define

$$\Uparrow = e^{iQz}\uparrow, \quad \Downarrow = e^{-iQz}\downarrow, \tag{2.3}$$

so that the four plane waves write $e^{\mp Kz}\Uparrow$ and $e^{\mp Kz}\Downarrow$.

In the following, $\uparrow$ and $\downarrow$ are the up and down spins when the $\boldsymbol{\chi}$ vector, which plays the role of a magnetic field, lies along a real direction which is taken as quantization axis. When $\boldsymbol{\chi}$ is not collinear to any real direction, the spin eigenstates are $\uparrow_{\mathbf{k}}$ and $\downarrow_{\mathbf{k}}$. In Sec. IV A, we shall see that $\uparrow_{\mathbf{k}}$ and $\downarrow_{\mathbf{k}}$ are no longer orthogonal. The implications of a wave vector $k=Q\pm iK$ in the [110] direction will be considered in detail in Sec. III.

C. Probability current

1. Free-electron probability current

We consider a spin-orbit-split barrier separating two regions where the electron states are described by plane waves

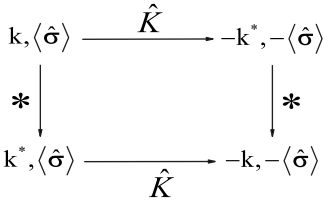

FIG. 5. This figure is a special case of Fig. 2, when the DP field $\boldsymbol{\chi}$ lies along a real direction **n**. Following the same procedure, four degenerate states are constructed, which now have their spins quantized along the *same* direction **n** (i.e., $\langle\hat{\boldsymbol{\sigma}}\rangle=\langle\hat{\boldsymbol{\sigma}}\rangle'$).

and where the potential is taken equal to zero, as shown in Fig. 1. The barrier potential is assumed to be a positive constant. When dealing with tunneling phenomena through crystalline barriers, the wave-vector component $\boldsymbol{\xi}$ parallel to the barrier plane has to be conserved. For an incident plane wave, which has a real wave-vector component parallel to the surface plane, this implies that the imaginary component of the wave vector inside the barrier has to be orthogonal to the barrier plane. Then, the imaginary component of the wave vector inside the barrier defines the tunneling direction. To analyze the tunneling processes, we distinguish two different mechanisms: (i) the wave vector has collinear real and imaginary components along the normal to the barrier (we refer to this mechanism as *para* type) and (ii) the real and imaginary components of the wave vector in the barrier are orthogonal (we refer to this mechanism as *ortho* type). We would point out that a plane wave with the real (imaginary) wave vector $(\boldsymbol{\xi}+\mathbf{Q})$ $(i\mathbf{K})$ is associated with the "classical" probability current, e.g., calculated for a free electron, $\mathbf{J}^f=\hbar(\boldsymbol{\xi}+\mathbf{Q})/m$ $(\mathbf{0})$. Such currents, with a zero divergence, conserve the local probability in any domain located in the barrier. On the contrary, a plane wave with the wave vector $(\boldsymbol{\xi}+\mathbf{Q})+i\mathbf{K}$ is associated to $\mathbf{J}^f=e^{-2\mathbf{K}\cdot\mathbf{r}}\hbar(\boldsymbol{\xi}+\mathbf{Q})/m$. It looks as if the local probability were to be no longer conserved in a domain located in the barrier, unless $\mathbf{Q}=\mathbf{0}$, because $\boldsymbol{\nabla}\cdot\mathbf{J}^f=-(2\hbar/m)(\mathbf{K}\cdot\mathbf{Q})e^{-2\mathbf{K}\cdot\mathbf{r}}$. The case $Q=0$, results in a laminar free-electron probability flux. The loops in the complex band structure which have been studied in Ref. 15 correspond to orthotunneling, the normal to the barrier plane lying along [001], a direction where the spin splitting is zero. On the contrary, tunneling along the [110] direction, a direction where the DP field is maximum, is a paraprocess. More precisely, the definition of the free-electron current of probability

$$\mathbf{J}^f[\psi]=\mathrm{Re}\left[\psi^*\frac{\hat{\mathbf{p}}}{m}\psi\right]=\frac{\hbar}{m}\mathrm{Im}[\psi^*\,\boldsymbol{\nabla}\,\psi] \tag{2.4}$$

is obtained from the conservation of the local probability when the potential in the Schrödinger equation is real.[23] Obviously, the equations expressing the conservation of the probability have to be re-examined carefully in our case, where the Hermitian potential is nonreal due to the spin-orbit interaction. The detailed derivation of the relevant current operator which allows one to calculate the true currents of probability $\mathbf{J}_\pm$ and $\mathbf{J}=\mathbf{J}_+ + \mathbf{J}_-$ is given in Appendix B. There, it is shown how to extend the usual procedure, which consists defining the velocity $\hat{v}$ from the relation

$$\hat{v}=\frac{\partial\hat{H}}{\partial p}. \tag{2.5}$$

2. Ortho- and paraprocesses

Coming back to the specific case of the GaAs-type barrier, let us derive a few basic results and present some definitions. The orbital part of the wave function of the conduction band is S in usual Kane's notation[24] and we write $\psi_+=S\uparrow(\mathbf{k})$ and

$\psi_-=S\downarrow(\mathbf{k})$, where $\uparrow(\mathbf{k})=\uparrow$ [see (i) below] or $\uparrow(\mathbf{k})=\uparrow_{\mathbf{k}}$ [see (ii) below] and $\downarrow(\mathbf{k})=\downarrow$ [(i)] or $\downarrow(\mathbf{k})=\downarrow_{\mathbf{k}}$ [(ii)]. The corresponding Schrödinger equation is

$$i\hbar\frac{\partial\psi_\pm}{\partial t}=\frac{\hat{\mathbf{p}}^2}{2m}\psi_\pm+\gamma\bar{\chi}_\pm(\mathbf{k})\psi_\pm. \tag{2.6}$$

(i) *Orthoprocess*. Let us assume that $\mathbf{k}_{\mathrm{II}}=\boldsymbol{\xi}+i\mathbf{K}$ (i.e., $\mathrm{Re}\,\mathbf{k}_{\mathrm{II}}\cdot\mathrm{Im}\,\mathbf{k}_{\mathrm{II}}=\boldsymbol{\xi}\cdot\mathbf{K}=0$) is a possible evanescent state. Because $E=\frac{\hbar^2}{2m}(\xi^2-K^2)$ is real on a real-energy line, the terms $\bar{\chi}_\pm(\mathbf{k})$ originating from the spin part of the Hamiltonian are also to be real. We follow the usual procedure to derive the expression of the probability current. $\uparrow_{\mathbf{k}}$ and $\downarrow_{\mathbf{k}}$ are no longer orthogonal but in any case the real spin term disappears, so that we obtain

$$\frac{\partial|\psi_\pm|^2}{\partial t}=-\boldsymbol{\nabla}\cdot\mathbf{J}^f[\psi_\pm], \tag{2.7}$$

which is the usual relation for probability conservation. Care has to be taken that the relation $\boldsymbol{\nabla}\cdot\mathbf{J}^f[\psi_\pm]=\boldsymbol{\nabla}\cdot\mathbf{J}[\psi_\pm]$ does not mean that $\mathbf{J}^f[\psi_\pm]=\mathbf{J}[\psi_\pm]$. However, in such a case, a number of classical results derived for free electrons will be recovered.

(ii) *Paraprocess*. In the case of one-dimensional tunneling along the $\mathbf{n}$ direction, where $\mathbf{n}$ is a unit vector normal to the barrier, which involves a complex wave vector $\mathbf{k}=(Q+iK)\mathbf{n}$, $\boldsymbol{\chi}(\mathbf{k})=(Q+iK)^3\boldsymbol{\chi}(\mathbf{n})$, we quantize the spin along the direction of $\boldsymbol{\chi}(\mathbf{n})$ which is a real non-normalized vector. $\bar{\chi}_\pm(\mathbf{k})$ are no longer real. We follow the same procedure to derive the expression of the probability current and we obtain

$$\frac{\partial|\psi_\pm|^2}{\partial t}=-\boldsymbol{\nabla}\cdot\mathbf{J}^f[\psi_\pm]+\frac{2}{\hbar}\gamma\,\mathrm{Im}\,\bar{\chi}_\pm|\psi_\pm|^2. \tag{2.8}$$

These equations could suggest an interpretation in terms of two-channel transport with a generation-recombination rate, analogous to Giant magnetoresistance phenomena.[25] In such a case, we would classically expect a spin mixing and we will show that, indeed, a formal analogy exists. However, care has to be taken that, at a given $\mathbf{k}$, ψ_+ and ψ_- do not correspond to the same energy except when $\bar{\chi}$ is zero.

3. [110] direction

More specifically, we will deal with electron tunneling along the [110] direction, a direction where the spin splitting is maximum in the real conduction band. On this example, we illustrate the preceding considerations. Let us consider for instance the up-spin channel, where a possible wave vector is $\mathbf{k}=(Q+iK)\mathbf{e}_{110}$ as shown in Sec. II B, with the wave function

$$\psi_+(z)=e^{i(Q+iK)z} \tag{2.9}$$

and the DP field

$$\bar{\chi}_+=\frac{1}{2}(Q+iK)^3. \tag{2.10}$$

The free-electron current is

$$\mathbf{J}^f[\psi_+]=\frac{\hbar}{m}\mathrm{Im}\,\psi_+^*\boldsymbol{\nabla}\psi_+=\frac{\hbar Q}{m}e^{-2Kz}, \tag{2.11}$$

$$\boldsymbol{\nabla}\cdot\mathbf{J}^f[\psi_+]=-\frac{2\hbar}{m}KQe^{-2Kz}. \tag{2.12}$$

On a real-energy line [see Eq. (A5)],

$$\frac{\partial|\psi_+|^2}{\partial t}=-\boldsymbol{\nabla}\cdot\mathbf{J}_+[\psi_+]=\frac{2\hbar}{m}KQe^{-2Kz}+\frac{\gamma}{\hbar}\mathrm{Im}(Q+iK)^3e^{-2Kz}$$
$$=\frac{2K}{\hbar}\left[2\gamma_cQ+\frac{1}{2}\gamma(3Q^2-K^2)\right]e^{-2Kz}=0. \tag{2.13}$$

Along the real-energy line, the eigenstates of the Schrödinger equation comply, as expected, with the continuity equation, with the current $\mathbf{J}_+$ to be identified. Here, it is easy to show that (see Appendix B)

$$\mathbf{J}_\pm[\psi_\pm]=\mathbf{J}^f[\psi_\pm]\pm\frac{\gamma}{2\hbar}\left(3\left|\frac{\partial}{\partial z}\psi_\pm\right|^2-\frac{\partial^2}{\partial z^2}|\psi_\pm|^2\right). \tag{2.14}$$

In the real conduction band, taking $\psi_\pm=e^{iqz}$, we obtain

$$\mathbf{J}_\pm[e^{iqz}]=\frac{2\gamma_c}{\hbar}q\pm\frac{3}{2}\frac{\gamma}{\hbar}q^2=\frac{1}{\hbar}\frac{\partial}{\partial q}\left[\gamma_cq^2\pm\frac{1}{2}\gamma q^3\right]=\frac{1}{\hbar}\frac{\partial}{\partial q}E(q). \tag{2.15}$$

Concerning an evanescent wave $\psi_\pm=e^{(K\pm iQ)z}$, it is easy to check that $\mathbf{J}_\pm[e^{(K\pm iQ)z}]=0$ on a real-energy line.

4. Waves conserving the free-electron probability current

The waves which conserve the free-electron current of probability play a special role: they appear to be "quasiclassical states" which allow us to build solutions yielding intuitive physical interpretations. The waves involved in an orthoprocess verify $\mathrm{Re}\,\mathbf{k}\cdot\mathrm{Im}\,\mathbf{k}=0$ and we have seen in Sec. II C 2 that this condition ensures the conservation of $\mathbf{J}^f$. In the case of a paraprocess, with a paradigm of tunneling along [110], $\mathbf{J}^f$ is not conserved in a given spin channel. Therefore, it is necessary to consider an intricated wave function $\psi(\mathbf{r})=\psi_+(\mathbf{r})\uparrow+\psi_-(\mathbf{r})\downarrow=\psi_+\uparrow+\psi_-\downarrow=\psi_\uparrow\uparrow+\psi_\downarrow\downarrow$. In the following, we indifferently use the notation ψ_+ and ψ_- or $\psi_\uparrow$ and $\psi_\downarrow$.

The free-electron probability current is given by[20] $\mathbf{J}^f[\psi]=(1/m)\mathrm{Re}\langle\psi^*\hat{\mathbf{p}}\psi\rangle_\sigma$, where the index σ means a summation (partial trace) on the spin or $\mathbf{J}^f[\psi]=(1/m)\mathrm{Re}(\psi_+^*\hat{\mathbf{p}}\psi_+ +\psi_-^*\hat{\mathbf{p}}\psi_-)=\mathbf{J}^f[\psi_+]+\mathbf{J}^f[\psi_-]$. Due to Kramers symmetry, the wave functions in the barriers $\psi_{\mathrm{II}+}$ and $\psi_{\mathrm{II}-}$ can be written as

$$\psi_{\mathrm{II}+}(z)=A_2e^{i(Q+iK)}+B_2e^{i(Q-iK)z},$$

$$\psi_{\mathrm{II}-}(z)=\tilde{A}_2e^{i(-Q+iK)}+\tilde{B}_2e^{i(-Q-iK)z}. \tag{2.16}$$

The free-electron probability current carried by the function of the type $\phi=(A_2e^{-Kz}+B_2e^{Kz})e^{i\epsilon Qz}$ is ($\epsilon=\pm1$)

$$\mathbf{J}^f[\phi] = \frac{\hbar}{m}[2K \text{ Im } A_2^* B_2 + \epsilon Q(2 \text{ Re } A_2 B_2^* + |A_2|^2 e^{-2Kz} + |B_2|^2 e^{2Kz})]. \tag{2.17}$$

In the barrier, let us write $\Psi_{\text{II}} = \Psi_{\text{II}+}\uparrow + \Psi_{\text{II}-}\downarrow$, so we have

$$\mathbf{J}^f[\Psi_{\text{II}}] = \frac{\hbar}{m}\{2Q[\text{Re } B_2 A_2^* - \text{Re } \tilde{B}_2 \tilde{A}_2^*] + 2K[\text{Im } B_2 A_2^* + \text{Im } \tilde{B}_2 \tilde{A}_2^*] + Q[e^{-2Kz}(|A_2|^2 - |\tilde{A}_2|^2) + e^{2Kz}(|B_2|^2 - |\tilde{B}_2|^2)]\}. \tag{2.18}$$

We see that the free-electron probability current in the barrier is constant if and only if $|A_2| = |\tilde{A}_2|$ and $|B_2| = |\tilde{B}_2|$. This leads to $A_2 = \mathcal{A}e^{i\theta_A}$, $\tilde{A}_2 = \mathcal{A}e^{-i\theta_A}$, $B_2 = \mathcal{B}e^{i\theta_B}$, and $\tilde{B}_2 = \mathcal{B}e^{-i\theta_B}$, where $\mathcal{A}$ and $\mathcal{B}$ are two complex numbers. So the general expression of a wave *sustaining a constant* $\mathbf{J}^f$ inside the barrier is

$$\Psi_{\text{II}} = \Psi_{\text{II}}(z) = \mathcal{A}e^{-Kz}[e^{i\theta_A}\Uparrow + e^{-i\theta_A}\Downarrow] + \mathcal{B}e^{Kz}[e^{i\theta_B}\Uparrow + e^{-i\theta_B}\Downarrow]. \tag{2.19}$$

It is useful to write

$$\Psi_{\text{II}}(z) = \mathcal{A}e^{-Kz}S_{\exp i\theta_A} + \mathcal{B}e^{Kz}S_{\exp i\theta_B}, \tag{2.20}$$

where

$$S_\lambda = S_\lambda(z) = \lambda\Uparrow + \lambda^*\Downarrow. \tag{2.21}$$

The Kramers conjugate of S_λ is $\hat{S}_\lambda = \hat{K}S_\lambda$, where $\hat{K}$ is the time-reversal transformation. Observe that S_λ and $\hat{S}_\lambda$ are eigenstates of the helicity operator $(\hat{\mathbf{p}}\cdot\hat{\boldsymbol{\sigma}})$ for the eigenvalue $\hbar Q$.

Let us look at the spin direction defined by S_λ. Recall that the spin quantization direction is along the $\boldsymbol{\chi}(\mathbf{e}_{110})$ vector. We call Oz' the direction parallel to $\boldsymbol{\chi}(\mathbf{e}_{110})$; Ox' and Oy' are in the $\boldsymbol{\Pi}_{\boldsymbol{\chi}}$ plane normal to $\boldsymbol{\chi}(\mathbf{e}_{110})$. The spin direction is defined via $\langle\sigma_{x'}\rangle$, $\langle\sigma_{y'}\rangle$, and $\langle\sigma_{z'}\rangle$. First of all we note that $\langle\sigma_{z'}\rangle = 0$ while $\langle\sigma_{x'}\rangle = 2 \text{ Re } \lambda^2$ and $\langle\sigma_{y'}\rangle = -2 \text{ Im } \lambda^2$ for $S_\lambda(0)$. The spin is in the $\boldsymbol{\Pi}_{\boldsymbol{\chi}}$ plane. Any spin direction in the $\boldsymbol{\Pi}_{\boldsymbol{\chi}}$ plane, which we call an *in-plane* direction, can be described by a suited value of λ. For instance with $\lambda = \exp i\theta_\lambda$, $\langle\sigma_{x'}\rangle = \cos 2\theta_\lambda$ and $\langle\sigma_{y'}\rangle = -\sin 2\theta_\lambda$, apart from a common factor, with θ_λ being the angle between the Ox' axis and the spin direction.

It can be shown that the largest vectorial space consisting of $\mathbf{J}^f$-conserving waves at a given energy is $\mathfrak{E} = \{\Psi_{\alpha,\beta}\}$, where

$$\Psi_{\alpha,\beta} = (\alpha\mathcal{A}e^{-Kz} + \beta\mathcal{B}e^{Kz})\Uparrow + (\alpha^*\mathcal{A}e^{-Kz} + \beta^*\mathcal{B}e^{Kz})\Downarrow \tag{2.22}$$

with α and $\beta \in \mathbb{C}$. $\mathfrak{E}$ is a vectorial space over $\mathbb{R}$, but not over $\mathbb{C}$.

Moreover, the existence of a superposition principle implies that any linear combination with real coefficients of two solutions with a current of probability of a given sign has to be a solution associated to a current of probability of the same sign. This is a strong constraint which is verified over $\mathfrak{E}_0 = \{\Phi_{\mathcal{A},\mathcal{B}}\} \otimes \{S_\alpha\} = \{(\mathcal{A}e^{-Kz} + \mathcal{B}e^{Kz})S_\alpha\}$, a vectorial subspace of $\mathfrak{E}$ (in this subspace $\mathbf{J}^f[\Phi_{\mathcal{A},\mathcal{B}}S_\alpha] = 2|\alpha|^2\mathbf{J}^f[\Phi_{\mathcal{A},\mathcal{B}}]$), or in $\{(\Phi_{\mathcal{A},\mathcal{B}}S)_{\lambda,\theta} = \cos\theta\,\Phi_{\mathcal{A},\mathcal{B}}S_\lambda + \sin\theta\frac{1}{K}\frac{\partial}{\partial z}\Phi_{\mathcal{A},\mathcal{B}}(i\hat{S}_\lambda)\}_\theta$—at fixed θ—which is also vectorial subspace (in this subspace $\mathbf{J}^f[(\Phi_{\mathcal{A},\mathcal{B}}S)_{\lambda,\theta}] = 2|\alpha|^2\mathbf{J}^f[\Phi_{\mathcal{A},\mathcal{B}}]\cos 2\theta$).

D. Standard tunneling case

The standard tunneling case is to be recovered when γ is zero; therefore, we build our analysis in close relation with it. A crucial point is that the probability current has to be constant, so that $R+T=1$, where R (T) is the reflection (transmission) coefficient.

We shall need the standard (without spin) function $\psi^{(0)}(z)$ defined as

$$\psi^{(0)}(z) = \begin{cases} \psi_{\text{I}}^{(0)}(z) = a_1 e^{iqz} + b_1 e^{-iqz} & (z<0), \\ \psi_{\text{II}}^{(0)}(z) = a_2 e^{-Kz} + b_2 e^{Kz} & (0<z<a), \\ \psi_{\text{III}}^{(0)}(z) = a_3 e^{iqz} & (a<z), \end{cases} \tag{2.23}$$

where $z<0$, $0<z<a$, and $a<z$, respectively, correspond to the incident wave (index I), to the wave in the barrier (index II), and to the transmitted wave (index III), as illustrated in Fig. 1. $\psi^{(0)}(z)$, a C^1 function, meets the boundary conditions

$$\psi^{(0)}(z_{0-}) = \psi^{(0)}(z_{0+}), \quad \frac{\partial\psi^0(z_{0-})}{\partial z} = \frac{\partial\psi^{(0)}(z_{0+})}{\partial z}, \quad z_0 = 0 \text{ or } a, \tag{2.24}$$

$$\frac{b_1}{a_1} = \frac{2(q^2+K^2)\sinh Ka}{D} \approx \frac{(q^2+K^2)}{(q+iK)^2}, \tag{2.25a}$$

$$\frac{a_2}{a_1} = \frac{2q(q+iK)e^{Ka}}{D} \approx 2\frac{q}{(q+iK)}, \tag{2.25b}$$

$$\frac{b_2}{a_1} = \frac{2q(-q+iK)e^{-Ka}}{D} \approx 2\frac{q(-q+iK)}{(q+iK)^2}e^{-2Ka}, \tag{2.25c}$$

$$\frac{a_3}{a_1} = \frac{4iKq}{D}e^{-iqa} \approx 4i\frac{qKe^{-iqa}}{(q+iK)^2}e^{-Ka}, \tag{2.25d}$$

$$D = (q+iK)^2e^{Ka} - (q-iK)^2e^{-Ka}. \tag{2.25e}$$

The approximations hold when $\exp Ka \gg 1$. The function $\psi^{(0)}(z)$ is such that the probability current $\mathbf{J}^f[\psi^{(0)}]$ is constant. The reflection coefficient $R = |b_1/a_1|^2$ and the transmission coefficient $T = |a_3/a_1|^2$ are such that $R+T=1$.

Also observe that, if we multiply $\psi^{(0)}$ by any C^1 function $f(\mathbf{r},\uparrow,\downarrow)$, the product and its derivative are continuous at the interfaces, satisfying the initial boundary conditions. Consider the case where the incident wave is $e^{i\mathbf{q}\cdot\mathbf{r}}$. If we take $f(\mathbf{r},\uparrow,\downarrow) = e^{i\boldsymbol{\xi}\cdot\mathbf{r}}\uparrow$ or $f(\mathbf{r},\uparrow,\downarrow) = e^{i\boldsymbol{\xi}\cdot\mathbf{r}}\downarrow$, we obtain a solution to the tunneling problem if, and only if, the incident component $e^{i(\mathbf{q}+\boldsymbol{\xi})\cdot\mathbf{r}}$ and the reflected component $e^{i(-\mathbf{q}+\boldsymbol{\xi})\cdot\mathbf{r}}$ correspond to the same energy.[26]

III. PARAPROCESS: [110]-ORIENTED BARRIER UNDER NORMAL INCIDENCE

A. General considerations

In the case where the wave vector is parallel to the [110] direction and the $\hat{H}_{\mathrm{DP}}$ Hamiltonian is taken into account, we have seen in Sec. II B that the wave vector is to be of the form $(\epsilon Q \pm iK)\mathbf{e}_{110}$ to get a real eigenvalue (an energy) of the Hamiltonian. But in such case, $\mathbf{J}^f$ is not conserved [Eq. (2.17)] and even not constant inside the barrier, so that the standard calculation routine to find the solution (i.e., the continuity of the wave function and of its derivative) cannot apply.

We could try to build a solution according to the usual procedure, but with a wave in the barrier involving the two spin channels, which can give a constant $\mathbf{J}^f$ [see Eq. (2.19)]

$$\Psi(z) = \begin{cases} \Psi_{\mathrm{I}}(z) = (A_1 e^{iqz} + B_1 e^{-iqz})\uparrow + \tilde{B}_1 e^{-iqz}\downarrow, \\ \Psi_{\mathrm{II}}(z) = (A_2 e^{-Kz} + B_2 e^{Kz}) \Uparrow + (\tilde{A}_2 e^{-Kz} + \tilde{B}_2 e^{Kz}) \Downarrow, \\ \Psi_{\mathrm{III}}(z) = A_3 e^{iqz}\uparrow + \tilde{A}_3 e^{iqz}\downarrow, \end{cases} \tag{3.1}$$

where $\Uparrow$ and $\Downarrow$ are defined in Eq. (2.3). The usual boundary conditions (C^1 function) for the down-spin channel, for instance, yield four equations determining $\tilde{B}_1$, $\tilde{A}_2$, $\tilde{B}_2$, and $\tilde{A}_3$,

$$\begin{aligned} \tilde{B}_1 &= \tilde{B}_2 + \tilde{A}_2, \\ q\tilde{B}_1 &= (Q - iK)\tilde{A}_2 + (Q + iK)\tilde{B}_2, \\ \tilde{A}_2 e^{-i(Q-iK)a} + \tilde{B}_2 e^{-i(Q+iK)a} &= \tilde{A}_3 e^{iqa}, \\ \tilde{A}_2(Q - iK)e^{-i(Q-iK)a} + \tilde{B}_2(Q + iK)e^{-i(Q+iK)a} &= -\tilde{A}_3 q e^{iqa}. \end{aligned} \tag{3.2}$$

They only provide a nontrivial solution if the determinant of the system is equal to zero which gives the relation

$$(q^2 - Q^2 - K^2)\sinh Ka + 2iKq \cosh Ka = 0. \tag{3.3}$$

The only solution is $K=0$ but it is not relevant to our problem.

B. Solutions to the tunneling problem

1. Constant-γ case

We go back to the Schrödinger equation to determine the proper boundary conditions and, to avoid any unnecessary mathematical complexity, here we assume that γ is constant over the three regions. Along the [110] direction, with $\mathbf{k} = (1/\sqrt{2})k[110]$, the DP Hamiltonian writes

$$H_{\mathrm{DP}} = \gamma_c k^2 \pm \frac{1}{2}\gamma k^3, \tag{3.4}$$

where the + (−) sign applies to the up (down) spin, quantized along the DP field. As usual, we obtain the effective Hamiltonian by substituting $\mathbf{k}$ with $-i\boldsymbol{\nabla}$, i.e., k with $-i\frac{\partial}{\partial z}$;

$$H_{\mathrm{DP}} = -\gamma_c \frac{\partial^2}{\partial z^2} \pm \frac{i}{2}\gamma \frac{\partial^3}{\partial z^3}. \tag{3.5}$$

Thus, we have the two equations

$$\begin{aligned} \left[-\gamma_c \frac{\partial^2}{\partial z^2} + \frac{1}{2} i\gamma \frac{\partial^3}{\partial z^3}\right]\psi_\uparrow &= [E - V(z)]\psi_\uparrow, \\ \left[-\gamma_c \frac{\partial^2}{\partial z^2} - \frac{1}{2} i\gamma \frac{\partial^3}{\partial z^3}\right]\psi_\downarrow &= [E - V(z)]\psi_\downarrow, \end{aligned} \tag{3.6}$$

where $V(z)=V$ when $0 \le z \le a$ and $V(z)=0$ outside. Because the DP Hamiltonian was obtained using the perturbation theory, we will look for a solution to the effective Schrödinger equation to the first order in γ only. Let us consider the up-spin channel. We write

$$\psi_\uparrow = \psi^{(0)} + \psi_\uparrow^{(1)}, \tag{3.7}$$

where $\psi^{(0)}$ is the standard function [obtained for $\gamma=0$ and defined by Eq. (2.23); it is a C^1 function, with a discontinuous second derivative]. $\psi_\uparrow^{(1)}$ is a first-order term in γ, so that the Schrödinger equation to the first order writes

$$-\gamma_c \frac{\partial^2 \psi_\uparrow}{\partial z^2} + \frac{1}{2} i\gamma \frac{\partial^3 \psi^{(0)}}{\partial z^3} = [E - V(z)]\psi_\uparrow. \tag{3.8}$$

We integrate this equation from one side of the interface to the other, i.e.,

$$-\gamma_c \left[\frac{\partial \psi_\uparrow}{\partial z}\right]_{z_0-\varepsilon}^{z_0+\varepsilon} + \frac{1}{2} i\gamma \left[\frac{\partial^2 \psi_\uparrow^{(0)}}{\partial z^2}\right]_{z_0-\varepsilon}^{z_0+\varepsilon} = \int_{z_0-\varepsilon}^{z_0+\varepsilon} [E - V(z)]\psi_\uparrow dz. \tag{3.9}$$

Then

$$\lim_{\varepsilon \to 0} \left\{ -\gamma_c \left[\frac{\partial \psi_\uparrow}{\partial z}\right]_{z_0-\varepsilon}^{z_0+\varepsilon} + \frac{1}{2} i\gamma \left[\frac{\partial^2 \psi^{(0)}}{\partial z^2}\right]_{z_0-\varepsilon}^{z_0+\varepsilon} \right\} = 0. \tag{3.10}$$

Taking the standard function [Eq. (2.23)] and referring to the limit at z_0 inside the barrier and inside the well, respectively, as z_0^B and z_0^W, we obtain

$$\left[\frac{\partial^2 \psi^{(0)}}{\partial z^2}\right]_{z_0^W} = -q^2 \psi^{(0)}(z_0^W) \tag{3.11}$$

outside the barrier and

$$\left[\frac{\partial^2 \psi^{(0)}}{\partial z^2}\right]_{z_0^B} = K^2 \psi^{(0)}(z_0^B) \tag{3.12}$$

inside the barrier. At the interfaces $\psi^{(0)}(z_0^B) = \psi^{(0)}(z_0^W) = \psi^{(0)}(z_0)$, then

$$\gamma_c \left[\frac{\partial \psi_\uparrow}{\partial z}\right]_{z_0-\varepsilon}^{z_0+\varepsilon} = \frac{1}{2} i\gamma (K^2 + q^2)\psi^{(0)}(z_0). \tag{3.13}$$

This provides us with the jump of the derivative at the interfaces. To the first order in q/K,

$$\left[\frac{\partial\psi_\uparrow}{\partial z}\right]_{z_0^W}^{z_0^B} = \frac{1}{2}i\frac{\gamma}{\gamma_c}(K^2+q^2)\psi^{(0)}(z_0) \approx \frac{1}{2}i\frac{\gamma}{\gamma_c}K^2\psi^{(0)}(z_0) = 2iQ_\uparrow\psi^{(0)}(z_0) \tag{3.14}$$

after Eq. (A9).

Similarly, for a down spin $Q_\downarrow = -Q_\uparrow$, and we have

$$\left[\frac{\partial\psi_\downarrow}{\partial z}\right]_{z_0^W}^{z_0^B} = 2iQ_\downarrow\psi^{(0)}(z_0). \tag{3.15}$$

It is worth remarking that this very discontinuity condition was found in a quite different situation, involving Rashba-split quantum wells.[27]

Now let us assume that $Q_\uparrow = Q$. The wave function constructed from the eigenstates in the three regions is

$$\psi(z) = \begin{cases} \psi_{\mathrm{I}}(z) = A_1 e^{iqz} + B_1(q,K,Q)e^{-iqz} & (z<0), \\ \psi_{\mathrm{II}}(z) = A_2(q,K,Q)e^{-Kz}e^{iQz} + B_2(q,K,Q)e^{Kz}e^{iQz} & (0<z<a), \\ \psi_{\mathrm{III}}(z) = A_3(q,K,Q)e^{iqz} & (a<z) \end{cases} \tag{3.16}$$

with the coefficients $B_1(q,K,Q)$, $A_2(q,K,Q)$, $B_2(q,K,Q)$, and $A_3(q,K,Q)$ to be determined.

To the first order in Q, the solution can be expanded as

$$\psi_{\mathrm{I}}(z) = (a_1 e^{iqz} + b_1 e^{-iqz}) + \beta_1 Q e^{-iqz},$$

$$\psi_{\mathrm{II}}(z) = (a_2 e^{-Kz} + b_2 e^{Kz})e^{iQz} + Q(\alpha_2 e^{-Kz} + \beta_2 e^{Kz})e^{iQz},$$

$$\psi_{\mathrm{III}}(z) = a_3 e^{iqz}e^{iQa} + \alpha_3' Q e^{iqz} \tag{3.17}$$

with

$$\beta_1 = \left[\frac{dB_1(q,K,Q)}{dQ}\right]_{Q=0}, \tag{3.18}$$

$$\alpha_2 = \left[\frac{dA_2(q,K,Q)}{dQ}\right]_{Q=0}, \quad \beta_2 = \left[\frac{dB_2(q,K,Q)}{dQ}\right]_{Q=0}, \tag{3.19}$$

and

$$\alpha_3 = \left[\frac{dA_3(q,K,Q)}{dQ}\right]_{Q=0} = iaa_3 + \alpha_3'. \tag{3.20}$$

We write

$$\psi = \varphi^S + \varphi^{\hat{S}}, \tag{3.21}$$

where

$$\varphi^S(z) = \begin{cases} \varphi_{\mathrm{I}}^S(z) = a_1 e^{iqz} + b_1 e^{-iqz} & (z<0), \\ \varphi_{\mathrm{II}}^S(z) = (a_2 e^{-Kz} + b_2 e^{Kz})e^{iQz} & (0<z<a), \\ \varphi_{\mathrm{III}}^S(z) = a_3 e^{iqz}e^{iQa} & (a<z), \end{cases} \tag{3.22}$$

$$\varphi^{\hat{S}}(z) = \begin{cases} \varphi_{\mathrm{I}}^{\hat{S}}(z) = \beta_1 Q e^{-iqz} & (z<0), \\ \varphi_{\mathrm{II}}^{\hat{S}}(z) = Q(\alpha_2 e^{-Kz} + \beta_2 e^{Kz})e^{iQz} & (0<z<a), \\ \varphi_{\mathrm{III}}^{\hat{S}}(z) = \alpha_3' Q e^{iqz} & (a<z). \end{cases} \tag{3.23}$$

φ^S is a continuous function but its derivative is not. To the first order, its jump at the interfaces is

$$\left[\frac{\partial\varphi^S}{\partial z}\right]_{z_0^W}^{z_0^B} = iQ\psi_{\mathrm{II}}^{(0)}(z_0) \tag{3.24}$$

As we have derived that the jump of the derivative of the wave function ψ is $2iQ\psi_{\mathrm{II}}^{(0)}(z_0)$, we deduce that $\varphi^{\hat{S}}$ is a continuous function and that the jump of its derivative at the interfaces is

$$\left[\frac{\partial\varphi^{\hat{S}}}{\partial z}\right]_{z_0^W}^{z_0^B} = iQ\psi_{\mathrm{II}}^{(0)}(z_0). \tag{3.25}$$

This provides us with the following four equations which determine the four coefficients β_1, α_2, β_2, and α_3':

$$\beta_1 - \alpha_2 - \beta_2 = 0,$$

$$\alpha_2 e^{-Ka} + \beta_2 e^{Ka} - \alpha_3' e^{iqa} = 0,$$

$$iq\beta_1 - K\alpha_2 + K\beta_2 = i\psi_{\mathrm{II}}^{(0)}(0),$$

$$K\alpha_2 e^{-Ka} - K\beta_2 e^{Ka} + iq\alpha_3' e^{iqa} = -i\psi_{\mathrm{II}}^{(0)}(a). \tag{3.26}$$

The solution of this system is

$$\beta_1 = -\frac{i}{K}a_3 e^{iqa}\sinh aK = \frac{4q}{D}a_1 \sinh aK,$$

$$\alpha_2 = -ia_3 e^{iqa}\frac{e^{Ka}}{2K} = \frac{a_2}{q+iK},$$

$$\beta_2 = ia_3 e^{iqa}\frac{e^{-Ka}}{2K} = \frac{b_2}{q - iK},$$

$$\alpha_3' = 0. \tag{3.27}$$

In the following, we consider $Q/K = \gamma K/4\gamma_c$ and also q/K as first order terms and we look for solutions up to the first order. The term in the reflected wave function arising from $Q\beta_1 = 2(q/K)(Q/K)$ is a second-order contribution which has to be neglected. Note that, in region I, if the incident wave has the wave vector q, the reflected wave should have the wave vector $-q'$, where $q = q_0 - \delta q$ and $q' = q_0 + \delta q$. From Eq. (B27), it can be verified that $\delta q = (\gamma/4\gamma_c)q_0^2 = (q_0/K)^2 Q$. Then δq is a second-order term which has to be neglected, so that media I and III have no sizable spin splitting. This indicates that the solution we obtain in the case of a constant γ also constitutes a plausible physical solution when γ is a step function, with $\gamma = 0$ outside the barrier. Also note that, at this level of approximation, $\varphi^{\hat{S}}$ is a wave which only exists inside the barrier and is not coupled to the free-electron waves outside the barrier. Because $A_3 = a_3 e^{iQa}$, we see that there is a pure dephasing between the up- $(Q_\uparrow = Q)$ and the down- $(Q_\downarrow = -Q)$ spin channels.

We have to be sure that, in our treatment, the probability current is conserved along the tunnel process. The wave in the barrier, in the up-spin channel, is of the form $\psi(z) = (A_2 e^{-Kz} + B_2 e^{Kz})e^{iQz} = \phi(z)e^{iQz}$ with $A_2 = a_2(1 - i\frac{Q}{K})$ and $B_2 = b_2(1 + i\frac{Q}{K})$. Let us calculate $\mathbf{J}$ to the first order in Q by making use of Eq. (2.14),

$$\mathbf{J}[\psi] = \mathbf{J}_+[\psi] = \mathbf{J}^f[\psi] + \frac{\gamma}{2\hbar}\left[3\left|\frac{\partial}{\partial z}\psi\right|^2 - \frac{\partial^2}{\partial z^2}|\psi|^2\right]. \tag{3.28}$$

It is sufficient to evaluate the term in the bracket to the zeroth order, substituting ψ with $\psi^{(0)}$. One finds

$$\begin{aligned}\mathbf{J}[\psi] &= \mathbf{J}^f[\psi] + \frac{\gamma}{2\hbar}\left[\left|\frac{\partial\psi^{(0)}}{\partial z}\right|^2 - \psi^{(0)*}\frac{\partial^2}{\partial z^2}\psi^{(0)} - \psi^{(0)}\frac{\partial^2}{\partial z^2}\psi^{(0)*}\right] \\ &\approx \mathbf{J}^f[\psi] + 2\frac{\gamma_c}{\hbar K}\frac{Q}{K}\left[\left|\frac{\partial\psi^{(0)}}{\partial z}\right|^2 - 2K^2|\psi^{(0)}|^2\right] = \mathbf{J}^f[\psi] \\ &\quad - 2\frac{\gamma_c}{\hbar}Q[|\psi^{(0)}|^2 + 2(a_2^* b_2 + a_2 b_2^*)]\end{aligned} \tag{3.29}$$

with

$$\mathbf{J}^f[\psi] = \mathrm{Im}\left(\psi^*\frac{\hbar}{m}\frac{\partial\psi}{\partial z}\right) = \frac{2\gamma_c}{\hbar}\mathrm{Im}\left(\phi^*\frac{\partial\phi}{\partial z}\right) + \frac{2\gamma_c}{\hbar}Q|\psi^{(0)}|^2, \tag{3.30}$$

$$\begin{aligned}\mathbf{J}^f[\psi] &= \frac{2\gamma_c}{\hbar}\mathrm{Im}\left(\psi^{(0)*}\frac{\partial\psi^{(0)}}{\partial z}\right) + \frac{4\gamma_c}{\hbar}Q(a_2^* b_2 + a_2 b_2^*) \\ &\quad + \frac{2\gamma_c}{\hbar}Q|\psi^{(0)}|^2.\end{aligned} \tag{3.31}$$

By comparing these expressions, one obtains

$$\mathbf{J}[\psi] = \frac{2\gamma_c}{\hbar}\mathrm{Im}\left(\psi^{(0)*}\frac{\partial\psi^{(0)}}{\partial z}\right) = \mathbf{J}^f[\psi^{(0)}]. \tag{3.32}$$

This definitely establishes current conservation in the tunnel process.

Starting with an incident spin state $|\varphi_0\rangle$, the transmission asymmetry $\mathcal{T}$ in the spin-dependent tunneling process can be expressed as

$$\mathcal{T} = \frac{\|T(|\varphi_0\rangle)\|^2 - \|T(\hat{K}|\varphi_0\rangle)\|^2}{\|T(|\varphi_0\rangle)\|^2 + \|T(\hat{K}|\varphi_0\rangle)\|^2}. \tag{3.33}$$

In the present case, we find $\mathcal{T} = 0$. Whatever the incident spin, the tunnel barrier acts as a pure spin rotator, without any spin filter effect. The cases of a spin-split quantum well confined between infinite walls and grown along the [110] direction is discussed in Appendix B, Sec. B 2.

2. Unified description

Let us now consider transport in the real conduction band, in region I or III. In the case $\gamma = 0$, the solution of the Schrödinger equation is $\psi(z) = \psi^{(0)}(z) = a_j e^{iq_0 z} + b_j e^{-iq_0 z}$, where $j = 1$ or 3 and $b_3 = 0$. When γ is nonzero, the wave function, in the up-spin channel, has to be of the form

$$\psi(z) = e^{i\vartheta}\left[a_j\left(1 + \alpha\frac{\delta q}{q_0}\right)e^{iq_0 z} + b_j\left(1 + \beta\frac{\delta q}{q_0}\right)e^{-iq_0 z}\right]e^{-i\delta q z}, \tag{3.34}$$

where $e^{i\vartheta}$ is a phase factor. Here again, let us calculate $\mathbf{J}$ to the first order in δq by making use of Eq. (3.28). Substituting ψ with $\psi^{(0)}$ in the bracket, one obtains

$$\begin{aligned}\mathbf{J}[\psi] &\approx \mathbf{J}^f[\psi] + \frac{\gamma}{2\hbar}\left[\left|\frac{\partial\psi^{(0)}}{\partial z}\right|^2 + 2q_0^2|\psi^{(0)}|^2\right] = \mathbf{J}^f[\psi] \\ &\quad + 2\frac{\gamma_c}{\hbar}\delta q[3|\psi^{(0)}|^2 - 2(a_j^* b_j e^{2iq_0 z} + a_j b_j^* e^{-2iq_0 z})],\end{aligned} \tag{3.35}$$

$$\begin{aligned}\mathbf{J}^f[\psi] &= \mathbf{J}^f[\psi^{(0)}] + 4\frac{\gamma_c}{\hbar}\delta q(|a_j|^2 \mathrm{Re}\ \alpha - |b_j|^2 \mathrm{Re}\ \beta) \\ &\quad - 2\frac{\gamma_c}{\hbar}\delta q|\psi^{(0)}|^2.\end{aligned} \tag{3.36}$$

For Re $\alpha = -$Re β, one finds

$$\begin{aligned}\mathbf{J}^f[\psi] &= \mathbf{J}^f[\psi^{(0)}] + 4\frac{\gamma_c}{\hbar}\delta q\ \mathrm{Re}\ \alpha(|a_j|^2 + |b_j|^2) - 2\frac{\gamma_c}{\hbar}\delta q|\psi^{(0)}|^2 \\ &= \mathbf{J}^f[\psi^{(0)}] + 4\frac{\gamma_c}{\hbar}\delta q\ \mathrm{Re}\ \alpha[|\psi^{(0)}|^2 - (a_j^* b_j e^{2iq_0 z} \\ &\quad + a_j b_j^* e^{-2iq_0 z})] - 2\frac{\gamma_c}{\hbar}\delta q|\psi^{(0)}|^2.\end{aligned} \tag{3.37}$$

Taking Re $\alpha = -1$ and Im $\alpha =$ Im $\beta = 0$,

$$\mathbf{J}[\psi] = \mathbf{J}^f[\psi^{(0)}]. \tag{3.38}$$

In the barrier, we consider (cf. Sec. III B 1)

$$\psi_B(z) = \left[a_2\left(1 - i\frac{Q}{K}\right)e^{-Kz} + b_2\left(1 + i\frac{Q}{K}\right)e^{Kz}\right]e^{iQz}, \tag{3.39}$$

$$\psi_B(z_0)e^{-iQz_0} = (a_2e^{-Kz_0} + b_2e^{Kz_0}) - i\frac{Q}{K}(a_2e^{-Kz_0} - b_2e^{Kz_0}), \tag{3.40}$$

$$\psi_B(z_0) = e^{iQz_0}\left[\psi^{(0)}(z_0) + i\frac{Q}{K^2}\frac{\partial\psi_B^{(0)}(z_0)}{\partial z}\right] = e^{iQz_0}\left[\psi^{(0)}(z_0) + i\frac{\gamma_2}{4\gamma_{2c}}\frac{\partial\psi_B^{(0)}(z_0)}{\partial z}\right]. \tag{3.41}$$

In the well, let us take [cf. Eq. (3.34)]

$$\psi_W(z) = e^{iQz_0}\left[a_j\left(1 - \frac{\delta q_j}{q_{j0}}\right)e^{iq_{j0}z} + b_j\left(1 + \frac{\delta q_j}{q_{j0}}\right)e^{-iq_{j0}z}\right]e^{-i\delta q_j(z-z_0)}, \tag{3.42}$$

where z_0 is the boundary relevant to the region of the well (e.g., $z_0=0$ in region I and $z_0=a$ in region III). Although we are still dealing with a unique effective mass and a constant γ, for the subsequent discussion, it is convenient to refer to γ (γ_c) as γ_2 (γ_{2c}) or γ_j (γ_{jc}), where $j=1$ or 3 in the different regions, and to the wave vectors as $q_{j0}-\delta q_j$ and $-(q_{j0}+\delta q_j)$;

$$\psi_W(z_0) = e^{iQz_0}\left[(a_je^{iq_{j0}z_0} + b_je^{-iq_{j0}z_0}) + \frac{\delta q_j}{q_{j0}}(-a_je^{iq_{j0}z_0} + b_je^{-iq_{j0}z_0})\right] \tag{3.43}$$

$$\psi_W(z_0) = e^{iQz_0}\left[\psi^{(0)}(z_0) + i\frac{\delta q_j}{q_{j0}^2}\frac{\partial\psi_W^{(0)}(z_0)}{\partial z}\right] = e^{iQz_0}\left[\psi^{(0)}(z_0) + i\frac{\gamma_j}{4\gamma_{jc}}\frac{\partial\psi_W^{(0)}(z_0)}{\partial z}\right] \tag{3.44}$$

We obtain

$$\psi_B(z_0) - \psi_W(z_0) = e^{iQz_0}\left[i\frac{\gamma_2}{4\gamma_{2c}}\frac{\partial\psi_B^{(0)}(z_0)}{\partial z} - i\frac{\gamma_j}{4\gamma_{jc}}\frac{\partial\psi_W^{(0)}(z_0)}{\partial z}\right] = e^{iQz_0}\frac{i}{4\gamma_{jc}}\frac{\partial\psi_B^{(0)}(z_0)}{\partial z}\left(\frac{\gamma_2\gamma_{jc}}{\gamma_{2c}} - \frac{\gamma_j\gamma_{2c}}{\gamma_{jc}}\right) = e^{iQz_0}\frac{i}{4\gamma_{2c}}\frac{\partial\psi_W^{(0)}(z_0)}{\partial z}\left(\frac{\gamma_2\gamma_{jc}}{\gamma_{2c}} - \frac{\gamma_j\gamma_{2c}}{\gamma_{jc}}\right). \tag{3.45}$$

Here, we have used the relation

$$\gamma_{2c}\frac{\partial\psi_B^{(0)}(z_0)}{\partial z} = \gamma_{jc}\frac{\partial\psi_W^{(0)}(z_0)}{\partial z} \tag{3.46}$$

which originates from the usual relation expressing current conservation in the absence of DP field.[6] When γ and γ_c (i.e., m) are constant, $\psi_B(z_0)-\psi_W(z_0)=0$, which establishes the continuity of the wave function.

Now, let us examine the matching conditions of the derivative,

$$\psi_B(z) = \left[a_2\left(1 - i\frac{Q}{K}\right)e^{-Kz} + b_2\left(1 + i\frac{Q}{K}\right)e^{Kz}\right]e^{iQz}, \tag{3.47}$$

$$\frac{\partial\psi_B(z_0)}{\partial z} = e^{iQz_0}\left\{\left[-Ka_2\left(1 - i\frac{Q}{K}\right)e^{-Kz_0} + Kb_2\left(1 + i\frac{Q}{K}\right)e^{Kz_0}\right] + iQ(a_2e^{-Kz_0} + b_2e^{Kz_0})\right\} = e^{iQz_0}\left[\frac{\partial\psi_B^{(0)}(z_0)}{\partial z} + 2iQ\psi^{(0)}(z_0)\right], \tag{3.48}$$

$$\frac{\partial\psi_W(z_0)}{\partial z} = e^{iQz_0}\left\{iq_j\left[a_j\left(1 - \frac{\delta q_j}{q_{j0}}\right)e^{iq_{j0}z_0} - b_j\left(1 + \frac{\delta q_j}{q_{j0}}\right)e^{-iq_{j0}z_0}\right] - i\delta q_j\psi^{(0)}(z_0)\right\} = e^{iQz_0}\left[\frac{\partial\psi_W^{(0)}(z_0)}{\partial z} - 2i\delta q_j\psi^{(0)}(z_0)\right]. \tag{3.49}$$

$$\gamma_{2c}\frac{\partial\psi_B(z_0)}{\partial z} - \gamma_{jc}\frac{\partial\psi_W(z_0)}{\partial z} = e^{iQz_0}\left\{\left[\gamma_{2c}\frac{\partial\psi_B^{(0)}(z_0)}{\partial z} - \gamma_{jc}\frac{\partial\psi_W^{(0)}(z_0)}{\partial z}\right] + 2i(\gamma_{2c}Q + \gamma_{jc}\delta q_j)\psi^{(0)}(z_0)\right\} = \frac{1}{2}i(\gamma_2K^2 + \gamma_jq_{j0}^2)e^{iQz_0}\psi^{(0)}(z_0). \tag{3.50}$$

This is exactly the jump of the derivative calculated in Eq. (3.14), up to the second-order terms. Thus, starting from the standard solution, we have constructed in a very simple way a wave function which is continuous, associated to the constant current of probability $\mathbf{J}^f[\psi^{(0)}]$, and which is the solution to the tunneling problem.

3. Insight into the step-function case

The case where $\gamma(z)=\gamma g(z)$ is not a constant raises difficult questions. The problem is not to solve Eq. (3.6) but to define a proper Hamiltonian, which has to be Hermitian: this would not be the case simply by substituting γ with $\gamma(z)$ in these equations and there are several ways to symmetrize this Hamiltonian. This is in line with the BenDaniel-Duke (BDD)[5] approach when dealing with a heterostructure where $m=m(z)$, i.e., where m depends on z; for instance, $m=m_1$ in region I and $m=m_2$ in region II.[6,7] In that case, the starting point is the Hamiltonian

$$\hat{H} = -\frac{\hbar^2}{2m(z)}\frac{\partial^2}{\partial z^2} + V. \tag{3.51}$$

The key idea is to transform this equation by defining the BBD Hamiltonian

$$\hat{H}_{\mathrm{BDD}} = \frac{\hbar}{2i}\frac{\partial}{\partial z}\hat{v} + V, \tag{3.52}$$

where $\hat{v}$ is defined in Eq. (2.5). Then, an integration of the Schrödinger equation around the origin, exactly as performed above, will allow us to show that $\mathbf{J}=\psi^*\hat{v}\psi$ is continuous because ψ and $\frac{1}{m(z)}\frac{\partial\psi}{\partial z}$ are continuous. The BDD Hamiltonian guarantees probability-current conservation and the problem receives sound foundations. Unfortunately, the more complicated form of the current of probability given in Eq. (2.14), in particular due to the $|\frac{\partial\psi_\pm}{\partial z}|^2$ term, makes an analogous transformation not obvious, so that the general case still remains an open question. However, let us point out that, when the masses and the DP-field coefficients are not very different over the three regions—a frequent situation in heterostructures—through the procedure described in Sec. III B 2, we are able to construct a wave which is continuous at the boundaries and that conserves the current of probability. Therefore, this wave is a plausible solution. The principle is first to solve the envelope-function problem in the absence of DP field, i.e., $g(z)=0$, taking into account the mass discontinuities in framework of the BDD formalism. This determines the standard function $\psi^{(0)}(z)$. Second, the wave functions in the different regions are modified according to the rules defined in Sec. III B 2 [Eqs. (3.39) and (3.42)]. The current of probability remains equal to $J^f[\psi^{(0)}]$ in the three regions. Concerning the continuity of the wave function at the boundaries, we have at $z_0=0$

$$\frac{\partial\psi_W^{(0)}(0)}{\partial z} \approx 2iq_1a_1,$$

$$\delta q \approx \frac{\gamma_1\gamma_{2c}}{\gamma_2\gamma_{1c}}\frac{\gamma_2}{4\gamma_{2c}}q_1^2, \quad Q \approx \frac{\gamma_2}{4\gamma_{2c}}K^2. \tag{3.53}$$

Thus [see Eq. (3.45)]

$$\psi_B(0)-\psi_W(0) = -\frac{1}{2}\frac{q_1a_1}{\gamma_{2c}}\left(\frac{\gamma_2\gamma_{jc}}{\gamma_{2c}} - \frac{\gamma_j\gamma_{2c}}{\gamma_{jc}}\right). \tag{3.54}$$

We use

$$\gamma_{j,2} = \frac{\gamma_j+\gamma_2}{2}, \quad \delta\gamma_{j,2} = \frac{\gamma_j-\gamma_2}{2},$$

$$\gamma_j = \gamma_{j,2}+\delta\gamma_{j,2}, \quad \gamma_2 = \gamma_{j,2}-\delta\gamma_{j,2} \tag{3.55}$$

$$\Gamma_{j,2} = \frac{\gamma_{jc}+\gamma_{2c}}{2}, \quad \delta\Gamma_{j,2} = \frac{\gamma_{jc}-\gamma_{2c}}{2},$$

$$\gamma_{jc} = \Gamma_{j,2}+\delta\Gamma_{j,2}, \quad \gamma_{2c} = \Gamma_{j,2}-\delta\Gamma_{j,2}, \tag{3.56}$$

$$\begin{aligned}\psi_B(0)-\psi_W(0) &= -\frac{1}{2}\frac{q_1a_1}{\gamma_{2c}}\gamma_{1,2}\left[\frac{\left(1-\frac{\delta\gamma_{1,2}}{\gamma_{1,2}}\right)\left(1+\frac{\delta\Gamma_{1,2}}{\Gamma_{1,2}}\right)}{1-\frac{\delta\Gamma_{1,2}}{\Gamma_{1,2}}}\right.\\ &\left. - \frac{\left(1+\frac{\delta\gamma_{1,2}}{\gamma_{1,2}}\right)\left(1-\frac{\delta\Gamma_{1,2}}{\Gamma_{1,2}}\right)}{1+\frac{\delta\Gamma_{1,2}}{\Gamma_{1,2}}}\right] = \frac{q_1a_1}{\gamma_{2c}}\gamma_{1,2}\left(\frac{\delta\gamma_{1,2}}{\gamma_{1,2}}\right.\\ &\left. - 2\frac{\delta\Gamma_{1,2}}{\Gamma_{1,2}}\right) \approx \frac{q_1a_1}{\gamma_{2c}}\gamma_2\left(\frac{\delta\gamma_{1,2}}{\gamma_{1,2}} - 2\frac{\delta\Gamma_{1,2}}{\Gamma_{1,2}}\right)\\ &= 4a_1\frac{q_1}{K}\frac{Q}{K}\left(\frac{\delta\gamma_{1,2}}{\gamma_{1,2}} - 2\frac{\delta\Gamma_{1,2}}{\Gamma_{1,2}}\right).\end{aligned} \tag{3.57}$$

At $z_0=a$, the situation is similar with

$$\frac{\partial\psi_W^{(0)}(a)}{\partial z} = iq_3a_3e^{iQa}e^{iq_3a}. \tag{3.58}$$

In the case where $\frac{\delta\gamma_{j,2}}{\gamma_{j,2}}$ and $\frac{\delta\Gamma_{j,2}}{\Gamma_{j,2}}$ are small and considered as first-order terms, the discontinuities are third-order terms which can be safely neglected.

4. Quasiclassical picture (regions I and III without sizable spin splitting)

In the case where regions I and III have no sizable spin splitting, we develop a quasiclassical picture of the tunneling process. For an up spin $Q=Q_\uparrow$, the wave function in the barrier writes as

$$\begin{aligned}\psi_{\mathrm{II}+}(z) &= \left[a_2\left(1-\frac{iQ}{K}\right)e^{-Kz} + b_2\left(1+\frac{iQ}{K}\right)e^{Kz}\right]e^{iQz}\\ &= \psi_{\mathrm{II}}^{(0)}(z)e^{iQz} + \left(\frac{iQ}{K}\frac{1}{K}\frac{\partial}{\partial z}\psi_{\mathrm{II}}^{(0)}(z)\right)e^{iQz}.\end{aligned} \tag{3.59}$$

The wave function for the down spin is obtained by replacing Q with $-Q$. We can combine the two spin channels to build the quasiclassical solution $\psi^c(z)$ corresponding to an incident wave with a spin lying in the plane perpendicular to the DP field,

$$\psi_{\mathrm{I}}^c(z) = (\lambda\uparrow+\lambda^*\downarrow)\psi_{\mathrm{I}}^{(0)}(z) = S_\lambda(0)\psi_{\mathrm{I}}^{(0)}(z) \tag{3.60}$$

which yields

$$\psi_{\mathrm{II}}^c(z) = \psi_{\mathrm{II}}^{(0)}(z)S_\lambda(z) - \frac{Q}{K}\frac{1}{K}\frac{\partial}{\partial z}\psi_{\mathrm{II}}^{(0)}(z)i\hat{K}S_\lambda(z). \tag{3.61}$$

Defining

$$\tan\theta = \frac{Q}{K} \approx \theta \tag{3.62}$$

we can write to the first order

$$\psi_{\mathrm{II}}^c(z) = \cos\theta\psi_{\mathrm{II}}^{(0)}(z)S_\lambda(z) - \sin\theta\frac{1}{K}\frac{\partial}{\partial z}\psi_{\mathrm{II}}^{(0)}(z)i\hat{K}S_\lambda(z). \tag{3.63}$$

The transmitted wave is

$$\psi^{c}_{\mathrm{III}} = (\lambda e^{iQa}\uparrow + \lambda^{*} e^{-iQa}\downarrow) a_3 e^{iqz} = S_{\lambda}(a)\psi^{(0)}_{\mathrm{III}}. \quad (3.64)$$

The incident wave corresponds to a spin lying in the $\mathbf{\Pi}_{\chi}$ plane, normal to $\chi(\mathbf{e}_{110})$. An important result is that the transmitted wave has the spin $S_{\alpha}(a)$, i.e., rotated by the angle $-2Qa$. We can estimate the angle $2Qa \approx 0.2(K/1\ \text{Å}^{-1})^2(a/1\ \text{Å})$ in GaAs along the [110] direction, with the largest reasonable value of K being smaller than $0.1\ \text{Å}^{-1}$, a value beyond which the spin splitting in k^3 is no longer valid. The spin-split barrier appears to exert a spin torque which produces a rotation of the spin of the transmitted electron around the quantization axis, which is the direction of the DP field. There is no spin transmission asymmetry. The spin-orbit-split barrier acts as a spin rotator inside the $\mathbf{\Pi}_{\chi}$ plane. This has some analogies with the reflection of a neutron beam on a ferromagnetic mirror discussed in Ref. 28 which physically results from spin precession during the time spent by the evanescent wave inside the barrier. But, in this example, this straightforwardly arises from the difference in the reflection and transmission coefficients for the two spin eigenstates. Anyway, this spin precession provides an estimation of the tunnel time τ, by using this built-in Larmor clock.[29] The effective field is determined through $\hbar\Omega \approx 2\gamma|\bar{\chi}|$ whereas $\Omega\tau = 2Qa \approx |a\gamma\bar{\chi}_e/\gamma_c|K^2$. We find $\tau \approx |a\hbar/2\gamma_c||\bar{\chi}_e/\bar{\chi}|K^2$. In the [110] direction, $\bar{\chi}_e = 1/2$ (see Sec. II B), so that $\tau \approx |a\hbar/4\gamma_c K| \approx 10^{-18}(a/1\ \text{Å})(1\ \text{Å}^{-1}/K)$ s.

We recognize that the in-plane solution belongs to the subspace of free-electron-current conserving waves studied in Sec. II C 4. In that sense, we have restored a classical tunneling process. Note that $\mathbf{J} = \mathbf{J}^f$ is a constant, but the classical magnetic current in region II, $\delta\mathbf{J}^f(z) = \mathbf{J}^f_{\uparrow}(z) - \mathbf{J}^f_{\downarrow}(z)$, is not and undergoes a discontinuity at the boundaries. Quite generally for any two-component spinor $\psi = \psi_+\uparrow + \psi_-\downarrow$ with $\psi_+ = \Phi e^{iQz}$ and $\psi_- = \Phi e^{iQz}$

$$\mathbf{J}^f[\psi_{\pm}] = \frac{\hbar}{m}\mathrm{Im}[\psi^{*}_{\pm} \nabla \psi_{\pm}], \quad (3.65a)$$

$$\delta\mathbf{J}^f = \mathbf{J}^f[\psi_+] - \mathbf{J}^f[\psi_-] = \frac{\hbar}{m}\mathrm{Im}[\psi^{*}_{+} \nabla \psi_{+} - \psi^{*}_{-} \nabla \psi_{-}], \quad (3.65b)$$

$$\delta\mathbf{J}^f = \frac{\hbar}{m}\mathrm{Im}[(\psi_+\uparrow - \psi_-\downarrow)^{\dagger} \nabla (\psi_+\uparrow + \psi_-\downarrow)] = \frac{1}{m}\mathrm{Re}[\psi^{\dagger}(\hat{\mathbf{p}}\cdot\hat{\boldsymbol{\sigma}})\psi]. \quad (3.65c)$$

Thus, the jump of $\delta\mathbf{J}^f$ is

$$[\delta\mathbf{J}^f]^{z_0^B}_{z_0^W} = \frac{\hbar}{m}\mathrm{Im}\{(\hat{\sigma}_z\psi)^{\dagger}_{z_0}[\nabla\psi]^{z_0^B}_{z_0^W}\} = \frac{1}{m}\mathrm{Re}[\psi^{\dagger}(\hat{\mathbf{p}}\cdot\hat{\boldsymbol{\sigma}})\psi]^{z_0^B}_{z_0^W}. \quad (3.66)$$

More explicitly, we have $\delta\mathbf{J}^f_{\mathrm{I}} = \delta\mathbf{J}^f_{\mathrm{III}} = 0$, $\delta\mathbf{J}^f_{\mathrm{II}}(z) \simeq 2\frac{\hbar Q}{m}|\lambda|^2|\frac{1}{K}\frac{\partial\Phi_{\mathrm{II}}(z)}{\partial z}|^2$. This can be viewed as a kinetic-momentum transfer along the internal-field direction during the tunnel process, in strong analogy with the spin transfer resulting from spin torque in ferromagnetic structures, as introduced by Slonczewski[9] and Berger.[19]

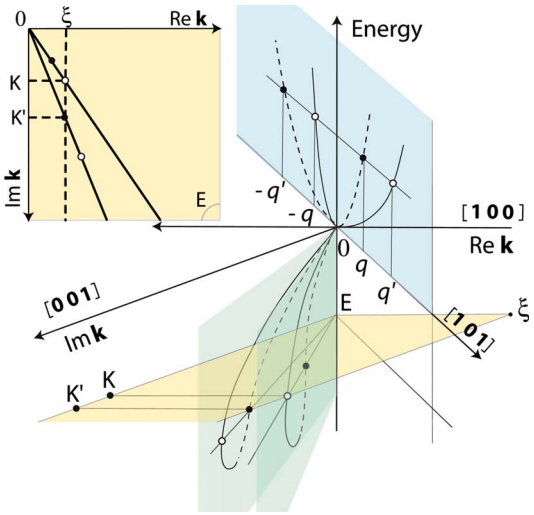

FIG. 6. (Color online) The lower part of this figure illustrates the spin-dependent tunneling scheme in the case of a [001]-oriented barrier (Perel's case). The horizontal plane describes the electron wave vector in the barrier; **K** is taken along the [001] axis and $\boldsymbol{\xi}$ lies in the barrier plane, along [100]. The upper part of the figure ($E > 0$) corresponds to the real conduction band—the wave vectors are real quantities—and the parabolalike curves describing spin-split states along the [101] direction are drawn. An up-spin state (full line, open circle) with the wave vector $\mathbf{q}'$ is degenerate with a down-spin state at the wave vector $\mathbf{q}$ (dotted line, dark circle) and also with up- and down-spin states at the wave vectors $-\mathbf{q}$ and $-\mathbf{q}'$, respectively. This is useful for the calculation of a quantum well, given in Appendix B, Sec. B 2. Concerning the evanescent states, in a naive effective-mass picture, one may think of evanescent states being mirrors of these real states (in the $E < 0$ domain) with imaginary wave vectors. Then up- and down-spin electrons at the energy E would tunnel with the two different wave vectors $i\mathbf{q}'$ and $i\mathbf{q}$, thus resulting in a spin-filter effect. However, our calculation shows that, concerning evanescent states (lower part of the figure, $E < 0$), the situation is not so simple. In the negative-energy region, the **K** axis refers to the imaginary wave-vector component and $\boldsymbol{\xi}$ refers to the real wave-vector component. Real-energy lines are found only when $\tan\theta = \xi/K < 1$. These real-energy lines, when drawn for a given θ, consist of loops connecting nearly-opposite spin states at the zone center ("up" spin: full curve and "down" spin: dotted curve). Obviously, when going off the zone center, the spin no longer remains a good quantum number—in fact, it can be calculated that its average value rotates along the loop—but it has to be pointed out that, in the D'yakonov and Perel' description, the energy eigenvectors are pure spin states which depend on the θ ratio. Two of these loops are drawn here. Let us consider a tunneling process at the energy E (horizontal gray plane or yellow plane in the online edition) of an electron with the wave-vector component $\boldsymbol{\xi}$ in the barrier plane, which has to be conserved in the tunneling process. It can be observed here that the two states marked on the loops by a dark circle ($\mathbf{K}'$) and an open circle ($\mathbf{K}$)—which are energy degenerate—are associated to the same real wave-vector component $\boldsymbol{\xi}$. However, they correspond to two different θ as they are, respectively, associated to the imaginary components $i\mathbf{K}$ and $i\mathbf{K}'$, along the tunneling direction. The difference between K and K' results in a spin-filter effect. Inset (upper left): top view of the plane at energy E showing the intercepts with the loops which determine the relevant wave vectors **K** and $\mathbf{K}'$.

IV. ORTHOPROCESS: [001]-ORIENTED BARRIER UNDER ALMOST NORMAL INCIDENCE

It is not possible to stay in simple band schemes, like in Fig. 3, as $\boldsymbol{\xi}$ has to be conserved: the relevant scheme is drawn in Fig. 6. To simplify without altering the physics of interest, the component of the wave vector normal to [001] is taken parallel to [100]. The spin is quantized along the Oz axis, taken parallel to [001]. As shown below, the eigenstates of the spin are in a direction normal to Oz. The energy writes

$$E = -\gamma_c(\mathcal{K}^2 - \xi^2) \pm \gamma\xi\mathcal{K}\sqrt{\mathcal{K}^2 - \xi^2}, \tag{4.1}$$

$$[E + \gamma_c(\mathcal{K}^2 - \xi^2)]^2 = (\gamma\xi\mathcal{K})^2(\mathcal{K}^2 - \xi^2), \tag{4.2}$$

where the generic wave vector is $\xi\mathbf{e}_{100} + i\mathcal{K}\mathbf{e}_{001}$. This equation may admit four real roots $\pm K$ and $\pm K'$. The states of the four wave vectors $(\xi,0,iK)\uparrow_{\mathbf{k}}$, $(\xi,0,-iK)\uparrow_{\mathbf{k}^*}$, $(\xi,0,iK')\downarrow_{\mathbf{k}'}$, and $(\xi,0,-iK')\downarrow_{\mathbf{k}'^*}$ have the same energies: K and K' are such that $E\uparrow(K) = E\downarrow(K')$. Note that Kramers conjugate states, which would involve $-\xi$, are not relevant because ξ is conserved. We use $K_0 = (K' + K)/2$ and $\delta K = K' - K$ (note that this definition differs by a factor of 2 of the definition used in Sec. III, where $2\delta q = q' - q$; the choice made in the present section makes the comparison easier with the results derived in Ref. 13). We assume that $K' > K > 0$, so that $\delta K > 0$. Moreover, as in Ref. 13, the incident-wave energy is smaller than half of the barrier energy, which means that $q < K$.

As recognized by Perel' *et al.*, the tunneling problem admits simple C^1 solutions under the approximation $\xi/K_0 \ll 1$. Besides, the spin asymmetry which originates from the spin-orbit interaction is characterized by the ratio $\delta K/K_0$, which, from band-structure calculations[30] and from spin-precession experiments,[31,32] is known to be small, i.e., $\delta K/K_0 \ll 1$. We further assume that aK_0 is not small compared to unity, which corresponds to a barrier of small transparency, and consequently we have $\exp(-2aK_0) \ll 1$. These three quantities, ξ/K_0, $\delta K/K_0$, and $\exp(-2aK_0)$, will be hereafter taken as first-order quantities and we will look for solutions to the first order only. This does not imply that the quantity $a\delta K = (aK_0)(\delta K/K_0)$, which is of crucial interest as it characterizes the spin selectivity of the barrier (as illustrated by the simple evaluation indicated below), is smaller than unity. In the physical problem, we consider electron tunneling under off-normal incidence and the angle of incidence is significant only when q and ξ are of the same order, which means $q/K_0 \ll 1$. We shall use this additional approximation only when it will be necessary to get analytical expressions of the wave vectors (Sec. IV C). Intuitively, if we start with an unpolarized electron beam, the up- (down-) spin electrons merge from the barrier with an amplitude of probability almost proportional to $\exp(-aK)$ $[\exp(-aK')]$, so that the current asymmetry—which, in this case, is also the polarization Π of the current—is given by

$$\Pi \approx \frac{e^{-2aK} - e^{-2aK'}}{e^{-2aK} + e^{-2aK'}} = \tanh a\delta K. \tag{4.3}$$

Indeed, in Ref. 13, it is found that the polarization $\mathcal{P}$ of the transmitted current, when the primary beam is not polarized, is $\mathcal{P} \approx \tanh a\delta K$ [see below Eq. (4.15)]. In practical cases, $a\delta K$ cannot be larger than a (often small) fraction of unity. Nevertheless, in the calculation, we do not put any restrictive assumption on $a\delta K$ (which is not assumed to be a first-order quantity) and we will calculate eigenvectors, when required, as a power expansion in $a\delta K$; but, obviously, we keep in mind that the first-order term will generally be sufficient to reach a reasonable accuracy.

A. Zeroth-order wave functions

The wave vectors K and K' are related through the equation ($K' > K$ and assuming $\gamma > 0$ for the sake of simplicity)

$$-\gamma_c(K^2 - \xi^2) - \gamma\xi K\sqrt{K^2 - \xi^2} = -\gamma_c(K'^2 - \xi^2) + \gamma\xi K'\sqrt{K'^2 - \xi^2} \tag{4.4}$$

or

$$\gamma_c(K'^2 - K^2) = \gamma\xi(K\sqrt{K^2 - \xi^2} + K'\sqrt{K'^2 - \xi^2}). \tag{4.5}$$

Up to the first order in $\delta K/K_0$, Eq. (4.5) writes as

$$2\gamma_c K_0\delta K = 2\gamma\xi K_0\sqrt{(K_0^2 - \xi^2)} \tag{4.6}$$

or

$$\delta K = \frac{\gamma\xi K_0}{\gamma_c}\sqrt{\left(1 - \frac{\xi^2}{K^2}\right)} \approx \frac{\gamma\xi K_0}{\gamma_c}. \tag{4.7}$$

We now calculate the eigenvectors. Let us write $k = (\xi, 0, \eta i\mathcal{K})$ with $\eta = \pm 1$, $\mathcal{K} = K$ or K', ξ, K, and $K' > 0$. $\boldsymbol{\chi} = \mathcal{K}\xi(K, 0, i\eta\xi)$. The eigenvalues of $\hat{\boldsymbol{\sigma}}\cdot\boldsymbol{\chi} = \begin{bmatrix} \chi_z & \chi_x - i\chi_y \\ \chi_x + i\chi_y & -\chi_z \end{bmatrix}$ are $\pm\xi\mathcal{K}\sqrt{\mathcal{K}^2 - \xi^2}$. To the first order in ξ/K_0, the normalized eigenvectors $c_1\uparrow + c_2\downarrow = \begin{bmatrix} c_1 \\ c_2 \end{bmatrix}$ are such that

$$\begin{array}{lcccc} \text{wave} & \begin{bmatrix} \xi \\ 0 \\ iK \end{bmatrix} & \begin{bmatrix} \xi \\ 0 \\ -iK \end{bmatrix} & \begin{bmatrix} \xi \\ 0 \\ iK' \end{bmatrix} & \begin{bmatrix} \xi \\ 0 \\ -iK' \end{bmatrix} \\ \text{vector} & & & & \\ \text{spin} \times \sqrt{2} & \begin{bmatrix} 1 + \dfrac{i\xi}{2K} \\ 1 - \dfrac{i\xi}{2K} \end{bmatrix} & \begin{bmatrix} 1 - \dfrac{i\xi}{2K} \\ 1 + \dfrac{i\xi}{2K} \end{bmatrix} & \begin{bmatrix} 1 - \dfrac{i\xi}{2K'} \\ -\left(1 + \dfrac{i\xi}{2K'}\right) \end{bmatrix} & \begin{bmatrix} 1 + \dfrac{i\xi}{2K'} \\ -\left(1 - \dfrac{i\xi}{2K'}\right) \end{bmatrix} \end{array}. \tag{4.8}$$

Observe that $\uparrow_{\mathbf{k}}$ and $\downarrow_{\mathbf{k}}$ are not orthogonal (even in a first-order calculation—compare the first term to the third one after substituting K' with K). Inside the barrier the wave function is of the shape $\Psi^{\mathrm{II}}(\mathbf{r})=e^{i\boldsymbol{\xi}\cdot\boldsymbol{\rho}}\Psi^{\mathrm{II}}(z)$ and

$$\begin{aligned}\Psi^{\mathrm{II}}(z) &= A_2\begin{bmatrix}1+\frac{i\xi}{2K}\\ 1-\frac{i\xi}{2K}\end{bmatrix}e^{-Kz}+B_2\begin{bmatrix}1-\frac{i\xi}{2K}\\ 1+\frac{i\xi}{2K}\end{bmatrix}e^{Kz}\\ &+\tilde{A}_2\begin{bmatrix}1-\frac{i\xi}{2K'}\\ -\left(1+\frac{i\xi}{2K'}\right)\end{bmatrix}e^{-K'z}+\tilde{B}_2\begin{bmatrix}1+\frac{i\xi}{2K'}\\ -\left(1-\frac{i\xi}{2K'}\right)\end{bmatrix}e^{K'z}\\ &=\left[A_2e^{-Kz}+B_2e^{Kz}+\frac{i\xi}{2K'}(-\tilde{A}_2e^{-K'z}+\tilde{B}_2e^{K'z})\right]\begin{bmatrix}1\\1\end{bmatrix}\\ &+\left[\frac{i\xi}{2K}(A_2e^{-Kz}-B_2e^{Kz})+\tilde{A}_2e^{-K'z}+\tilde{B}_2e^{K'z}\right]\begin{bmatrix}1\\-1\end{bmatrix}.\end{aligned} \tag{4.9}$$

Outside the barrier, we are looking for the solution of the shape

$$\begin{aligned}\Psi^{\mathrm{I}}(z) &= A_1\begin{bmatrix}1\\1\end{bmatrix}e^{iqz}+B_1\begin{bmatrix}1\\1\end{bmatrix}e^{-iqz}+\tilde{A}_1\begin{bmatrix}1\\-1\end{bmatrix}e^{iqz}\\ &+\tilde{B}_1\begin{bmatrix}1\\-1\end{bmatrix}e^{-iqz}\end{aligned} \tag{4.10}$$

and

$$\Psi^{\mathrm{III}}(z)=A_3\begin{bmatrix}1\\1\end{bmatrix}e^{iqz}+\tilde{A}_3\begin{bmatrix}1\\-1\end{bmatrix}e^{iqz}. \tag{4.11}$$

The wave function writes as

$$\Psi^{\mathrm{I}}(z)=[A_1e^{iqz}+B_1e^{-iqz}][1\quad 1]^t+[\tilde{A}_1e^{iqz}+\tilde{B}_1e^{-iqz}][1\quad -1]^t, \tag{4.12a}$$

$$\begin{aligned}\Psi^{\mathrm{II}}(z) &= \left[A_2e^{-Kz}+B_2e^{Kz}+\frac{i\xi}{2K'}(-\tilde{A}_2e^{-K'z}+\tilde{B}_2e^{K'z})\right][1\quad 1]^t\\ &+\left[\frac{i\xi}{2K}(A_2e^{-Kz}-B_2e^{Kz})+\tilde{A}_2e^{-K'z}+\tilde{B}_2e^{K'z}\right]\\ &\times[1\quad -1]^t,\end{aligned} \tag{4.12b}$$

$$\Psi^{\mathrm{III}}(z)=[A_3e^{iqz}][1\quad 1]^t+[\tilde{A}_3e^{iqz}][1\quad -1]^t. \tag{4.12c}$$

The continuity of the wave function [Eq. (4.12)] and of its derivative at $z=0$ and $z=a$ provides a linear system of eight equations. A full discussion is given in Appendix C. This calculation has strong similarities with Slonczewski's[9] approach of the tunneling between two ferromagnets separated by a barrier, because we deal with two coupled spin channels.

B. Polarization

The transmission asymmetry $\mathcal{T}$ is

$$\mathcal{T}=\frac{|t^+|^2-|t^-|^2}{|t^+|^2+|t^-|^2} \tag{4.13}$$

with $|t^+|^2$ (resp. $|t^-|^2$) $=|\Psi^{\mathrm{III}}|^2$, calculated when $A_1=1$ and $\tilde{A}_1=0$ (resp. $A_1=0$, $\tilde{A}_1=1$). All the coefficients A_j and $\tilde{A}_j$ are calculated in Appendix C.

To the zeroth order in ξ/K_0, $t^{\pm}=t_0^{\pm}$, and $\mathcal{T}=T_0$, now

$$|t_0^+|^2=\left|\frac{4qKe^{-Ka}}{(K-iq)^2}\right|^2,\quad |t_0^-|^2=\left|\frac{4qK'e^{-K'a}}{(K'-iq)^2}\right|^2 \tag{4.14}$$

and we get the result of Ref. 13, namely,

$$\mathcal{T}_0=\tanh a\delta K. \tag{4.15}$$

Up to the first order in ξ/K_0, $t^{\pm}=t_1^{\pm}$, and $\mathcal{T}=\mathcal{T}_1$, $|t_1^{\pm}|^2=(|A_3^{\pm}|^2+|\tilde{A}_3^{\pm}|^2)$ but $|\tilde{A}_3^{+}|^2$ and $|A_3^{-}|^2$ are of second order in ξ/K_0, so that, *up to the first order in* ξ/K_0, *the result is the same as for the zeroth order:* $\mathcal{T}_0=\mathcal{T}_1$.

It is easy to show that this transmission asymmetry is nothing but the spin polarization of the transmitted beam when the primary beam is unpolarized, $\mathcal{T}_0=\mathcal{T}_1=\mathcal{P}$. As we have only assumed that $q<K_0$, we may wonder why the ratio q/K_0 does not appear in $\mathcal{P}$. The answer is given if we perform the calculation 1 order further in $\delta K/K_0\ll 1$. Then, a lengthy calculation leads to

$$\mathcal{P}=\frac{\tanh a\delta K+\frac{K_0-q}{K_0+q}\frac{\delta K}{K_0}}{1+\frac{K_0-q}{K_0+q}\frac{\delta K}{K_0}\tanh a\delta K}. \tag{4.16}$$

In the limit where $\delta K/K_0$ is negligible, $\mathcal{P}=\tanh a\delta K$ is recovered.

Let us consider the transmission of a primary electron beam with an initial current polarization P_i through a spin-filtering structure characterized by the transmission coefficients $e^{-2aK'}$ (e^{-2aK}) for up- (down-) spin electrons. As the incident up- (down-) spin current is proportional to $1+\mathcal{P}_i$ ($1-\mathcal{P}_i$), the current polarization of the emerging beam is simply given by $\mathcal{P}$,

$$\mathcal{P}=\frac{(1+\mathcal{P}_i)e^{-2aK}-(1-\mathcal{P}_i)e^{-2aK'}}{(1+\mathcal{P}_i)e^{-2aK}+(1-\mathcal{P}_i)e^{-2aK'}}=\frac{\mathcal{P}_i+\Pi}{1+\Pi\mathcal{P}_i}, \tag{4.17}$$

where Π is given by Eq. (4.3). The above formula yielding the polarization of the transmitted beam is a standard expression for spin filters (in spin polarimetry, Π is referred to as the Sherman function).[33] Thus, $\mathcal{P}$ in Eq. (4.16) appears to result from the combination of a primary-electron-beam polarization $\mathcal{P}_i\approx-\delta K/K_0$ when $q/K_0\ll 1$, which does not depend on the barrier thickness, with the spin asymmetry of the material, $\Pi=\tanh(a\delta K)$. The initial polarization $-\delta K/K_0$ could be straightforwardly understood as resulting from the band mismatch, an interface effect. If this analogy provides us with a useful physical insight, it must, however, be realized that the above calculation is only valid when $\exp aK_0$

$\geqslant 1$ and cannot be extrapolated to $a=0$. In any case, it is clear that P_i builds up in the early stage of the transport process.

C. ξ/K_0 first-order wave function

It is shown in Appendix C that there is no ξ/K_0 first-order term in A_2, A_3, B_1, and B_2. We are therefore going to calculate ξ/K_0 first-order terms in $\tilde{B}_1$, $\tilde{A}_2$, $\tilde{B}_2$, and $\tilde{A}_3$. To be consistent with Sec. IV A, we assume that $A_1 \neq 0$ and $\tilde{A}_1=0$. We obviously have to invert the role of K and K' if we start from $A_1=0$ and $\tilde{A}_1 \neq 0$. Let us recall that the calculation is performed with $\delta K/K_0 \ll 1$ which is always true and $\xi/K_0 \ll 1$.

Equations (C1e)–(C1h) give

$$-\tilde{A}_2\left(1-\frac{iq}{K'}\right)+\tilde{B}_2\left(1+\frac{iq}{K'}\right)=\frac{i\xi}{2K'}\left(1-\frac{iq}{K}\right)A_2+\frac{i\xi}{2K'}\left(1+\frac{iq}{K}\right)B_2, \quad (4.18a)$$

$$-\tilde{A}_2\left(1+\frac{iq}{K'}\right)e^{-K'a}+\tilde{B}_2\left(1-\frac{iq}{K'}\right)e^{K'a}=\frac{i\xi}{2K'}\left(1+\frac{iq}{K}\right)A_2e^{-Ka}+\frac{i\xi}{2K'}\left(1-\frac{iq}{K}\right)B_2e^{Ka}. \quad (4.18b)$$

The determinant of the system defined by Eq. (4.18) is

$$\mathrm{Det}=\left(1+\frac{iq}{K'}\right)^2e^{-K'a}-\left(1-\frac{iq}{K'}\right)^2e^{K'a} \quad (4.19)$$

which differs from zero; therefore, $\tilde{A}_2$ and $\tilde{B}_2$ can be calculated.

We assume $a \neq 0$ (the case $a=0$ has no interest) and we obtain

$$\tilde{A}_2=-\frac{i\xi}{2K'}\left[A_2e^{a\delta K/2}\frac{\sinh(K_0a)}{\sinh(K'a)}+B_2e^{K_0a}\frac{\sinh(a\delta K/2)}{\sinh(K'a)}\right] \quad (4.20)$$

and

$$\tilde{B}_2=\frac{i\xi}{2K'}\left[A_2e^{-K_0a}\frac{\sinh(a\delta K/2)}{\sinh(K'a)}+B_2e^{-a\delta K/2}\frac{\sinh(K_0a)}{\sinh(K'a)}\right]. \quad (4.21)$$

Noticing that (i) $\xi/K'=\xi/K_0(1+\delta K/2K)\approx(\xi/K_0)(1-\delta K/2K_0)\approx\xi/K_0$ (the same result holds for $\xi/K\approx\xi/K_0$), (ii) $a\delta K \ll aK$, (iii) $A_2 \propto A_1$ [Eq. (2.25b)], and (iv) $B_2 \propto A_1\exp(-2Ka)$ [Eq. (2.25c)], we get

$$\tilde{A}_2\approx-\frac{i\xi}{2K_0}A_2e^{a\delta K/2}\frac{\sinh(K_0a)}{\sinh(K'a)}, \quad (4.22a)$$

$$\tilde{B}_2=\frac{i\xi}{2K_0}\left[A_2e^{-K_0a}\frac{\sinh(a\delta K/2)}{\sinh(K'a)}+B_2e^{-a\delta K/2}\frac{\sinh(K_0a)}{\sinh(K'a)}\right]. \quad (4.22b)$$

From now on we assume that $\exp K_0a \gg 1$, so that $\sinh(K_0a)/\sinh(K'a)=\exp(-a\delta K/2)$ and

$$\tilde{A}_2\approx-\frac{i\xi}{2K_0}A_2. \quad (4.23)$$

A lengthy calculation shows that

(i) $\tilde{B}_1$ is proportional to $(\xi/K_0)(\delta K/K_0)$ and therefore is negligible. However, we can note that $\tilde{B}_1$ is not strictly equal to zero so that the reflected wave has a $[1\ \ -1]^t$ component even though the incident wave has only a $[1\ \ 1]^t$ component.

(ii)

$$\tilde{B}_2\approx\frac{i\xi}{2K_0}e^{-a\delta K}\left[2\frac{iK+q}{iK-q}e^{-a\delta K/2}\sinh\frac{a\delta K}{2}+1\right]B_2. \quad (4.24)$$

We furthermore assume that $q/K_0 \ll 1$, so that

$$\tilde{B}_2\approx\frac{i\xi}{2K_0}e^{-a\delta K}[2-e^{-a\delta K}]B_2 \quad (4.25)$$

and eventually

$$\tilde{A}_3=\frac{i\xi}{2K_0}\left(\sinh\frac{a\delta K}{2}-2\sinh^2\frac{a\delta K}{2}\right)A_3. \quad (4.26)$$

There is no assumption on $a\delta K$ in Eq. (4.26).

We note that, as $\tilde{A}_3$ differs from zero, the incident wave with only a $[1\ \ 1]^t$ spin component is transmitted with a component along the $[1\ \ -1]^t$ spin direction. This means there is no pure spin-filter effect along the x-quantization axis.[34]

V. CONCLUSION

Electron tunneling in a semiconductor with no inversion symmetry and in the presence of spin-orbit coupling involves complex wave vectors in the barrier. In directions where the D'yakonov-Perel' (DP) field is nonzero, the problem becomes highly nontrivial. We have distinguished two particular types of tunnel processes: para-type process where we have one-dimensional tunneling with a complex wave vector and ortho-type process associated with a complex wave vector with orthogonal real and imaginary components. For a paraprocess, the DP field is a complex vector, but it remains collinear to a real direction, so that the eigenvectors are orthogonal spin states. We have shown that, along the [110] direction no C^1 solution exists. The expression of the current of probability is re-examined, proper boundary conditions are derived, and a treatment of heterostructures is proposed. Quasiclassical states are shown to be in-plane solutions, which imply a pure spin rotation of the transmitted beam around the direction of the DP field. In the [110] direction, there is no spin-filter effect. This contrasts with the situation in the real conduction band where the spin splitting is maximum along [110]. For an orthoprocess, the DP field is a complex vector, which is not collinear to any real direction, and the eigenvectors of the Hamiltonian are no longer orthogonal spin states. Moreover, the evanescent eigenvectors are not associated with the same spin depending whether

they propagate from left to right or from right to left. In this case, we have derived a first-order solution to the tunnel problem, which has strong similarities with standard off-normal tunneling, and an almost pure spin-filter effect was demonstrated, a conclusion consistent with the result of Perel' *et al.*[13] whose expression for the transmitted polarization has been corrected by the introduction of an initial interface polarization.

All these questions should now be addressed experimentally and we think that experiments are within reach. For instance, further developments of the study of the polarization of a reflected spin-polarized electron beam can be considered, in line with the measurements reported in Ref. 35. Polarized-luminescence experiments in quantum wells grown along the [110] axis could also bring valuable information, as well as measurements on resonant-tunneling devices or photogavalnic-effect measurements in coupled quantum wells.[36–39] The results derived in the present paper provide insight in spin-dependent tunneling in solids whereas they also open stimulating perspectives for spin manipulation in tunnel devices.

ACKNOWLEDGMENTS

We are deeply indebted to Michel Dyakonov for an illuminating discussion. We thank Catherine Bouton-Drouhin, Henri Jaffrès, and André Rougé for useful advice, and Jean-Noël Chazalviel and Travis Wade for a careful reading of the manuscript.

APPENDIX A: EVANESCENT BAND IN THE [110] DIRECTION

Let us write $\mathbf{k}=(Q+iK)\mathbf{e}$, having in mind $\mathbf{e}$ along the [110] direction: $\mathbf{e}=\mathbf{e}_{110}=\frac{1}{\sqrt{2}}[110]$. We have to find the relation between Q and K to get a real eigenvalue of the Hamiltonian $\hat{H}$. This real eigenvalue is the energy. The Hamiltonian $\hat{H}$ writes as

$$\hat{H}=\gamma_c(Q+iK)^2+\gamma\hat{\boldsymbol{\sigma}}\cdot\boldsymbol{\chi}=\gamma_c(Q+iK)^2+\gamma\bar{\chi}_{\mathbf{e}}(Q+iK)^3\hat{\boldsymbol{\sigma}}\cdot\mathbf{e}_{\boldsymbol{\chi}}, \tag{A1}$$

where $\mathbf{e}_{\boldsymbol{\chi}}=\boldsymbol{\chi}/\|\boldsymbol{\chi}\|$ (provided $\|\boldsymbol{\chi}\|\neq 0$). $\bar{\chi}_e$, a dimensionless parameter, depends on the direction. If $\mathbf{e}=\mathbf{e}_{110}$, $\boldsymbol{\chi}$ is parallel to $\mathbf{e}_{1\bar{1}0}$ with $\bar{\chi}_{\mathbf{e}}=1/2$.

The eigenvalues are

$$\mathcal{E}(\mathbf{k})=\gamma_c(Q+iK)^2+\epsilon\bar{\chi}_{\mathbf{e}}\gamma(Q+iK)^3. \tag{A2}$$

The spin is quantized along $\gamma\mathbf{e}_{\boldsymbol{\chi}}$, so that $\epsilon\gamma>0$ corresponds to the spin $\uparrow$ and $\epsilon\gamma<0$ corresponds to the spin $\downarrow$. Separating the real and imaginary parts of the eigenvalue, we obtain

$$\mathrm{Re}\,\mathcal{E}(\mathbf{k})=\gamma_c(Q^2-K^2)+\epsilon\bar{\chi}_{\mathbf{e}}\gamma(Q^3-3QK^2), \tag{A3}$$

$$\mathrm{Im}\,\mathcal{E}(\mathbf{k})=2\gamma_cQK+\epsilon\bar{\chi}_{\mathbf{e}}\gamma(3Q^2K-K^3). \tag{A4}$$

Looking for the real-energy lines, we have the equation

$$\mathrm{Im}\,\mathcal{E}(\mathbf{k})=0\Rightarrow 2\gamma_cQ+\epsilon\bar{\chi}_{\mathbf{e}}\gamma(3Q^2-K^2)=0, \tag{A5}$$

$$K^2=3Q^2+2\epsilon\frac{\gamma_c}{\gamma\bar{\chi}_{\mathbf{e}}}Q \quad \left(=3Q^2+\epsilon 4\frac{\gamma_c}{\gamma}Q \text{ if } \mathbf{e}=\mathbf{e}_{110}\right). \tag{A6}$$

Equation (A6) is the relation between Q and K we were looking for. The energy is

$$E_\varepsilon(Q)=-\epsilon 8\bar{\chi}_{\mathbf{e}}\gamma Q^3-8\gamma_cQ^2-\epsilon 2\frac{\gamma_c^2}{\gamma\bar{\chi}_{\mathbf{e}}}Q=-\epsilon 4\gamma Q^3-8\gamma_cQ^2-\epsilon 4\frac{\gamma_c^2}{\gamma}Q \text{ if } \mathbf{e}=\mathbf{e}_{110}. \tag{A7}$$

For a given $E(Q)$ value, we have *two* possible choices of K,

$$K=\pm\sqrt{3Q^2+2\epsilon\frac{\gamma_c}{\gamma\bar{\chi}_{\mathbf{e}}}Q} \quad \left(=\pm\sqrt{3Q^2+\epsilon 4\frac{\gamma_c}{\gamma}Q} \text{ if } \mathbf{e}=\mathbf{e}_{110}\right). \tag{A8}$$

Let us note that $|\epsilon 4(\gamma/\gamma_c)Q|\gg 3Q^2$, so that $|Q|\ll|K|$ and

$$K\approx\pm\sqrt{(4\epsilon\gamma_c/\gamma)Q}. \tag{A9}$$

The sign of $\epsilon\gamma$ determines the sign of Q ($\gamma_c>0$). As stated above $\epsilon\gamma>0$, which corresponds to spin $\uparrow$, gives $Q>0$ whereas $\epsilon\gamma<0$, which corresponds to spin $\downarrow$, gives $Q<0$.

We have the symmetry property

$$E_\pm(Q)=E_\mp(-Q). \tag{A10}$$

The study of the function $E(Q)$ is straightforward and we take $\epsilon=-1$ in the following, with the other case being deduced by symmetry,

$$\frac{dE_-(Q)}{dQ}=24\bar{\chi}_e\gamma Q^2-16\gamma_cQ+2\frac{\gamma_c^2}{\gamma\bar{\chi}_{\mathbf{e}}} \quad \left(=12\gamma Q^2-16\gamma_cQ+4\frac{\gamma_c^2}{\gamma} \text{ if } \mathbf{e}=\mathbf{e}_{110}\right). \tag{A11}$$

The roots Q_1 and Q_2 of the derivative are

$$Q_1=\frac{\gamma_c}{2\gamma\bar{\chi}_{\mathbf{e}}}, \quad Q_2=\frac{\gamma_c}{6\gamma\bar{\chi}_{\mathbf{e}}},$$

$$Q_1=\frac{\gamma_c}{\gamma}, \quad Q_2=\frac{\gamma_c}{3\gamma} \text{ if } \mathbf{e}=\mathbf{e}_{110}. \tag{A12}$$

Incidentally we note that

$$E_-(Q_1)=0. \tag{A13}$$

The corresponding curve is plotted in Fig. 4. It must be realized that we are only dealing with evanescent states, which correspond to a negative energy. Thus, for a given energy $E<0$, we have two possible Q values ($\pm Q$), each associated with a given spin subband.

Finally, we find that, at a given energy, we have exactly four possible states, with wave vectors $(Q\pm iK)$ for spin $\uparrow$

and $(-Q \pm iK)$ for spin $\downarrow$, with the latter obtained from the former through $\hat{K}$. In short

$$E_{\uparrow}(\mathbf{k}) = E_{\uparrow}(\mathbf{k}^*) = E_{\downarrow}(-\mathbf{k}) = E_{\downarrow}(-\mathbf{k}^*). \tag{A14}$$

APPENDIX B: CONTINUITY EQUATION AND DEFINITION OF THE PROBABILITY CURRENT

1. Definition of the probability current

Consider a Hamiltonian given by

$$\hat{H} = \sum_j a_j \hat{p}_j + \sum_{j,k} b_{jk} \hat{p}_j \hat{p}_k + \sum_{j,k,l} c_{jkl} \hat{p}_j \hat{p}_k \hat{p}_l + V, \tag{B1}$$

where a_j, b_{jk}, and c_{jkl} are Hermitian matrices, invariant under permutation of the indices i, j, and k, and where V is real. We define the velocity operator

$$\hat{v}_j = \frac{\partial \hat{H}}{\partial p_j} = a_j + 2\sum_k b_{jk} \hat{p}_k + 3\sum_{k,l} c_{jkl} \hat{p}_k \hat{p}_l. \tag{B2}$$

It will be useful to take the following notations:

$$|\psi) = \psi_1(\mathbf{r})\uparrow + \psi_2(\mathbf{r})\downarrow = \begin{bmatrix} \psi_1(\mathbf{r}) \\ \psi_2(\mathbf{r}) \end{bmatrix},$$

$$|\phi) = \phi_1(\mathbf{r})\uparrow + \phi_2(\mathbf{r})\downarrow = \begin{bmatrix} \phi_1(\mathbf{r}) \\ \phi_2(\mathbf{r}) \end{bmatrix},$$

$$(\psi| = [\psi_1^*(\mathbf{r}) \quad \psi_2^*(\mathbf{r})], \quad (\phi| = [\phi_1^*(\mathbf{r}) \quad \phi_2^*(\mathbf{r})], \quad (\phi|\psi) = \phi_1^*(\mathbf{r})\psi_1(\mathbf{r}) + \phi_2^*(\mathbf{r})\psi_2(\mathbf{r}),$$

$$(\psi|\psi) = \psi_1^*(\mathbf{r})\psi_1(\mathbf{r}) + \psi_2^*(\mathbf{r})\psi_2(\mathbf{r}) = |\psi(\mathbf{r})|^2 = |\psi|^2,$$

$$|\hat{p}\psi) = \begin{bmatrix} \hat{p}\psi_1(\mathbf{r}) \\ \hat{p}\psi_2(\mathbf{r}) \end{bmatrix}, \quad (\hat{p}\phi| = [\hat{p}^*\phi_1^*(\mathbf{r}) \quad \hat{p}^*\phi_2^*(\mathbf{r})] = [-\hat{p}\phi_1^*(\mathbf{r}) \quad -\hat{p}\phi_2^*(\mathbf{r})],$$

$$(\hat{p}\phi|\hat{p}\psi) = [\hat{p}^*\phi_1^*(\mathbf{r})][\hat{p}\psi_1(\mathbf{r})] + [\hat{p}^*\phi_2^*(\mathbf{r})][\hat{p}\psi_2(\mathbf{r})] = [-\hat{p}\phi_1^*(\mathbf{r})][\hat{p}\psi_1(\mathbf{r})] + [-\hat{p}\phi_2^*(\mathbf{r})][\hat{p}\psi_2(\mathbf{r})]. \tag{B3}$$

The Schrödinger equation is

$$i\hbar \frac{\partial |\psi)}{\partial t} = \sum_j a_j \hat{p}_j |\psi) + \sum_{j,k} b_{jk} \hat{p}_j \hat{p}_k |\psi) + \sum_{j,k,l} c_{jkl} \hat{p}_j \hat{p}_k \hat{p}_l |\psi)$$

$$-i\hbar \frac{\partial (\psi|}{\partial t} = \sum_j (\hat{p}_j\psi| a_j + \sum_{j,k} (\hat{p}_j\hat{p}_k\psi| b_{jk} + \sum_{j,k,l} (\hat{p}_j\hat{p}_k\hat{p}_l\psi| c_{jkl}. \tag{B4}$$

The continuity equation can be written as

$$i\hbar\left[\left(\psi|\frac{\partial}{\partial t}\psi\right) + \left(\frac{\partial}{\partial t}\psi|\psi\right)\right] = i\hbar\frac{\partial|\psi|^2}{\partial t} = \sum_j [(\psi|a_j\hat{p}_j\psi) - (\hat{p}_j\psi|a_j\psi)] + \sum_{j,k} [(\psi|b_{jk}\hat{p}_j\hat{p}_k\psi) - (\hat{p}_j\hat{p}_k\psi|b_{jk}\psi)] + \sum_{j,k,l} [(\psi|c_{jkl}\hat{p}_j\hat{p}_k\hat{p}_l\psi) - (\hat{p}_j\hat{p}_k\hat{p}_l\psi|b_{jk}\psi)]. \tag{B5}$$

Note that

$$(\psi|a_j\hat{p}_j\psi) = (a_j\hat{p}_j\psi|\psi)^* = (\hat{p}_j\psi|a_j\psi)^* \tag{B6}$$

or

$$(\hat{p}_j\psi|a_j\psi) = (\psi|a_j\hat{p}_j\psi)^*. \tag{B7}$$

Similarly

$$(\hat{p}_j\hat{p}_k\psi|b_{jk}\psi) = (\psi|b_{jk}\hat{p}_j\hat{p}_k\psi)^*, \quad (\hat{p}_j\hat{p}_k\hat{p}_l\psi|b_{jk}\psi) = (\psi|c_{jkl}\hat{p}_j\hat{p}_k\hat{p}_l\psi)^*. \tag{B8}$$

Therefore

$$\frac{\partial|\psi|^2}{\partial t} = \frac{2}{\hbar}\mathrm{Im}\left[\sum_j (\psi|a_j\hat{p}_j\psi) + \sum_{j,k} (\psi|b_{jk}\hat{p}_j\hat{p}_k\psi) + \sum_{j,k,l} (\psi|c_{jkl}\hat{p}_j\hat{p}_k\hat{p}_l\psi)\right]. \tag{B9}$$

The probability current $\mathbf{J}$ has to satisfy

$$\boldsymbol{\nabla}\cdot\mathbf{J} = -\frac{2}{\hbar}\mathrm{Im}\left[\sum_j (\psi|a_j\hat{p}_j\psi) + \sum_{j,k} (\psi|b_{jk}\hat{p}_j\hat{p}_k\psi) + \sum_{j,k,l} (\psi|c_{jkl}\hat{p}_j\hat{p}_k\hat{p}_l\psi)\right] = \boldsymbol{\nabla}\cdot\mathbf{J}^{(1)} + \boldsymbol{\nabla}\cdot\mathbf{J}^{(2)} + \boldsymbol{\nabla}\cdot\mathbf{J}^{(3)}. \tag{B10}$$

From the expression of the velocity operator, we tentatively define the j component of the probability current as

$$\tilde{\mathbf{J}}_j = \left[\frac{1}{2}(\psi|a_j\psi) + \sum_k (\psi|b_{jk}\hat{p}_k\psi) + \frac{3}{2}\sum_{k,l} (\hat{p}_k\psi|c_{jkl}\hat{p}_l\psi)\right] + \text{c.c.}, \tag{B11}$$

where c.c. refers to the complex conjugate. We calculate

$$\boldsymbol{\nabla}\cdot\tilde{\mathbf{J}} = \sum_j \boldsymbol{\nabla}_j\tilde{\mathbf{J}}_j = \frac{i}{\hbar}\sum_j \hat{p}_j\tilde{\mathbf{J}}_j. \tag{B12}$$

Let us consider the first term

$$\tilde{\mathbf{J}}_j^{(1)} = \frac{1}{2}(\psi|a_j\psi) + \text{c.c.} = (\psi|a_j\psi), \tag{B13}$$

$$\sum_j \nabla_j \tilde{\mathbf{J}}_j^{(1)} = \frac{i}{\hbar}\sum_j \hat{p}_j(\psi|a_j\psi) = \frac{i}{\hbar}\sum_j (\psi|a_j\hat{p}_j\psi) - (\hat{p}_j\psi|a_j\psi)$$
$$= -\frac{2}{\hbar}\mathrm{Im}\sum_j (\psi|a_j\hat{p}_j\psi) = \boldsymbol{\nabla}\cdot\mathbf{J}^{(1)}. \quad \text{(B14)}$$

The second term gives

$$\tilde{\mathbf{J}}_j^{(2)} = \sum_k (\psi|b_{jk}\hat{p}_k\psi) + \text{c.c.} = \sum_k [(\psi|b_{jk}\hat{p}_k\psi) + (\hat{p}_k\psi|b_{jk}\psi)], \quad \text{(B15)}$$

$$\sum_j \nabla_j \tilde{\mathbf{J}}_j^{(2)} = \frac{i}{\hbar}\sum_{j,k} [(\psi|b_{jk}\hat{p}_j\hat{p}_k\psi) - (\hat{p}_j\psi|b_{jk}\hat{p}_k\psi) + (\hat{p}_k\psi|b_{jk}\hat{p}_j\psi)$$
$$- (\hat{p}_j\hat{p}_k\psi|b_{jk}\psi)] = -\frac{2}{\hbar}\mathrm{Im}\sum_j (\psi|b_{jk}\hat{p}_j\hat{p}_k\psi)$$
$$= \boldsymbol{\nabla}\cdot\mathbf{J}^{(2)}. \quad \text{(B16)}$$

Concerning the third term

$$\tilde{\mathbf{J}}_j^{(3)} = \frac{3}{2}\sum_{k,l} (p_k\psi|c_{jkl}\hat{p}_l\psi) + \text{c.c.} = 3\sum_{k,l} (p_k\psi|c_{jkl}\hat{p}_l\psi), \quad \text{(B17)}$$

$$\sum_j \nabla_j \tilde{\mathbf{J}}_j^{(3)} = \frac{3i}{\hbar}\sum_{k,l} [(\hat{p}_k\psi|c_{jkl}\hat{p}_j\hat{p}_l\psi) - (\hat{p}_j\hat{p}_k\psi|c_{jkl}\hat{p}_l\psi)]$$
$$\neq \boldsymbol{\nabla}\cdot\mathbf{J}^{(3)}. \quad \text{(B18)}$$

Let us now consider the quantity

$$\sum_{jkl} \hat{p}_j\hat{p}_k\hat{p}_l(\psi|c_{jkl}\psi) = \sum_{jkl} [(\psi|c_{jkl}\hat{p}_j\hat{p}_k\hat{p}_l\psi) - (\hat{p}_j\hat{p}_k\hat{p}_l\psi|c_{jkl}\psi)]$$
$$- 3\sum_{jkl} [(\hat{p}_j\psi|c_{jkl}\hat{p}_k\hat{p}_l\psi) - (\hat{p}_j\hat{p}_k\psi|c_{jkl}\hat{p}_l\psi)]$$
$$= \sum_j \hat{p}_j \sum_{kl} \hat{p}_k\hat{p}_l(\psi|c_{jkl}\psi)$$
$$= \frac{\hbar}{i}\sum_j \nabla_j \sum_{kl} \hat{p}_k\hat{p}_l(\psi|c_{jkl}\psi). \quad \text{(B19)}$$

We have

$$\sum_j \nabla_j \left[\sum_{k,l} \hat{p}_k\hat{p}_l(\psi|c_{jkl}\psi) + \tilde{\mathbf{J}}_j^{(3)}\right] = -\frac{2}{\hbar}\mathrm{Im}\sum_{j,k,l} (\psi|c_{jkl}\hat{p}_j\hat{p}_k\hat{p}_l\psi)$$
$$= \boldsymbol{\nabla}\cdot\mathbf{J}^{(3)}. \quad \text{(B20)}$$

Thus, we can define

$$\mathbf{J}_j^{(3)} = \tilde{\mathbf{J}}_j^{(3)} + \sum_{k,l} \hat{p}_k\hat{p}_l(\psi|c_{jkl}\psi). \quad \text{(B21)}$$

Finally, the j component of the probability current can be taken as

$$\mathbf{J}_j = \left[\frac{1}{2}(\psi|a_j\psi) + \sum_k (\psi|b_{jk}\hat{p}_k\psi) + \frac{3}{2}\sum_{k,l} (\hat{p}_k\psi|c_{jkl}\hat{p}_l\psi)\right.$$
$$\left. + \frac{1}{2}\sum_{k,l} \hat{p}_k\hat{p}_l(\psi|c_{jkl}\psi)\right] + \text{c.c.} \quad \text{(B22)}$$

or

$$\mathbf{J}_j = \mathbf{J}_j^f + (\psi|a_j\psi) + 3\sum_{k,l} (\hat{p}_k\psi|c_{jkl}\hat{p}_l\psi) + \sum_{k,l} \hat{p}_k\hat{p}_l(\psi|c_{jkl}\psi). \quad \text{(B23)}$$

2. Quantum well grown in the [110] direction

To illustrate some simple consequences, we apply the preceding results to the practical case of quantum wells grown in the [110] direction. First, let us point out that, in this case, a direct calculation of the current of probability is straightforward;

$$i\hbar\frac{\partial\psi_\pm}{\partial t} = -\gamma_c\frac{\partial^2\psi_\pm}{\partial z^2} \pm \frac{1}{2}i\gamma\frac{\partial^3\psi_\pm}{\partial z^3},$$
$$-i\hbar\frac{\partial\psi_\pm^*}{\partial t} = -\gamma_c\frac{\partial^2\psi^\pm}{\partial z^2} \mp \frac{1}{2}i\gamma\frac{\partial^3\psi_\pm^*}{\partial z^3}. \quad \text{(B24)}$$

Multiplying the first equation by $\psi_\pm^*$, the second equation by $\psi_\pm$ and subtracting them, we obtain

$$i\hbar\left(\psi_\pm^*\frac{\partial\psi_\pm}{\partial t} + \psi_\pm\frac{\partial\psi_\pm^*}{\partial t}\right)$$
$$= -\gamma_c\left(\psi_\pm^*\frac{\partial^2\psi_\pm}{\partial z^2} - \psi_\pm\frac{\partial^2\psi_\pm^*}{\partial z^2}\right)$$
$$\pm \frac{1}{2}i\gamma\left(\psi_\pm^*\frac{\partial^3\psi_\pm}{\partial z^3} + \psi_\pm\frac{\partial^3\psi_\pm^*}{\partial z^3}\right) \quad \text{(B25)}$$

or

$$-\boldsymbol{\nabla}\cdot\mathbf{J}_\pm = \frac{\partial|\psi|^2}{\partial t} = -\frac{\gamma_c}{i\hbar}\left(\psi_\pm^*\frac{\partial^2\psi_\pm}{\partial z^2} - \psi_\pm\frac{\partial^2\psi_\pm^*}{\partial z^2}\right)$$
$$+ \frac{1}{2}\frac{\gamma}{\hbar}\left(\psi_\pm^*\frac{\partial^3\psi_\pm}{\partial z^3} + \psi_\pm\frac{\partial^3\psi_\pm^*}{\partial z^3}\right) =$$
$$-\boldsymbol{\nabla}\cdot\left[\mathbf{J}_\pm^f \pm \frac{\gamma}{2\hbar}\left(3\left|\frac{\partial}{\partial z}\psi_\pm\right|^2 - \frac{\partial^2}{\partial z^2}|\psi_\pm|^2\right)\right]. \quad \text{(B26)}$$

We consider a well made of a spin-split semiconductor (GaAs) confined between infinite walls located at $z=0$ and $z=a$. At energy E, for a given spin, the wave function $\phi(z)$ consists of a combination of eigenstates associated to the wave vectors $q(E)$ and $-q'(E)$ (see Fig. 6, upper part) which satisfy

$$\gamma_c q^2 + \frac{1}{2}\gamma q^3 = \gamma_c q'^2 - \frac{1}{2}\gamma q'^3. \quad \text{(B27)}$$

The wave function writes

$$\phi(z) = Ae^{iqz} + Be^{-iq'z} \tag{B28}$$

and verifies the boundary condition $\phi(0)=\phi(a)=0$, so that $A=-B$ and $q+q'=n\frac{2\pi}{a}$ or

$$\phi(z) = 2iA\ \sin\left(\frac{n\pi}{a}z\right)e^{-i\delta qz}. \tag{B29}$$

A straightforward calculation gives

$$-\boldsymbol{\nabla}\cdot\mathbf{J} = \frac{\partial|\phi|^2}{\partial t} = -\frac{2}{\hbar}|A|^2\sin\{(q+q')z\}\left[\gamma_c(q^2-q'^2) + \frac{1}{2}\gamma(q'^3+q^3)\right] = 0 \tag{B30}$$

due to the energy expression [Eq. (B27)]. The probability current $\mathbf{J}$ is conserved as it should. However, a calculation of $\mathbf{J}$ according to Eq. (B26) yields

$$\mathbf{J}_{\pm} = \pm\frac{1}{2\hbar}\boldsymbol{\gamma}|\mathbf{A}|^2(q+q')^2. \tag{B31}$$

Obviously, we should have $\mathbf{J}_{\pm}=0$. This inconsistency arises due to a lack in the modelization relative to the singular case of infinite wall. Note that, if dealing with a finite barrier, $(\gamma/2\hbar)|\mathbf{A}|^2(q+q')^2=(2\gamma_c/\hbar)|\mathbf{A}|^2\mathbf{Q}(q+q')^2/K^2$, where q and Q are small. In the case of an infinite well, we are in a situation where K tends to infinity. Because of this inconsistency (the infinite well cannot meet the criteria used in our approximations), this term should certainly be discarded. The problem can also be circumvented when building the function

$$\Phi = \phi\uparrow + \hat{K}(\phi\uparrow) = \phi\uparrow + \phi^*\downarrow = 2\ \sin\left(\frac{n\pi}{a}z\right)[iAe^{-i\delta qz}\uparrow + (iA)^*e^{i\delta qz}\downarrow] \tag{B32}$$

which properly describes a solution with a spin lying in the plane perpendicular to the DP field and for which $\mathbf{J}=0$.

APPENDIX C: [100]-ORIENTED BARRIER ZEROTH-ORDER WAVE-FUNCTION COEFFICIENTS

The continuity of the wave function defined by Eq. (4.12) and of its derivative at $z=0$ and $z=a$ for the two spin channels provides the following linear system:

$$-B_1 + A_2 + B_2 - \frac{i\xi}{2K'}\tilde{A}_2 + \frac{i\xi}{2K'}\tilde{B}_2 = A_1, \tag{C1a}$$

$$i\frac{q}{K}B_1 - A_2 + B_2 + \frac{i\xi}{2K}\tilde{A}_2 + \frac{i\xi}{2K}\tilde{B}_2 = i\frac{q}{K}A_1, \tag{C1b}$$

$$A_2e^{-Ka} + B_2e^{Ka} - \frac{i\xi}{2K'}\tilde{A}_2e^{-K'a} + \frac{i\xi}{2K'}\tilde{B}_2e^{K'a} - A_3e^{iqa} = 0, \tag{C1c}$$

$$-A_2e^{-Ka} + B_2e^{Ka} + \frac{i\xi}{2K}\tilde{A}_2e^{-K'a} + \frac{i\xi}{2K}\tilde{B}_2e^{K'a} - i\frac{q}{K}A_3e^{iqa} = 0, \tag{C1d}$$

$$-\tilde{B}_1 + \frac{i\xi}{2K}A_2 - \frac{i\xi}{2K}B_2 + \tilde{A}_2 + \tilde{B}_2 = \tilde{A}_1, \tag{C1e}$$

$$i\frac{q}{K'}\tilde{B}_1 - \frac{i\xi}{2K'}A_2 - \frac{i\xi}{2K'}B_2 - \tilde{A}_2 + \tilde{B}_2 = i\frac{q}{K'}\tilde{A}_1, \tag{C1f}$$

$$\frac{i\xi}{2K}A_2e^{-Ka} - \frac{i\xi}{2K}B_2e^{Ka} + \tilde{A}_2e^{-K'a} + \tilde{B}_2e^{K'a} - \tilde{A}_3e^{iqa} = 0, \tag{C1g}$$

$$-\frac{i\xi}{2K'}A_2e^{-Ka} - \frac{i\xi}{2K'}B_2e^{Ka} - \tilde{A}_2e^{-K'a} + \tilde{B}_2e^{K'a} - i\frac{q}{K'}\tilde{A}_3e^{iqa} = 0. \tag{C1h}$$

The coefficients A_1 and $\tilde{A}_1$ which define the intensity of the two spin components of the incident wave are known (initial conditions). It could be verified that the determinant of this system is nonzero. We can calculate the eight coefficients B_1, $\tilde{B}_1$, A_2, B_2, $\tilde{A}_2$, $\tilde{B}_2$, A_3, and $\tilde{A}_3$ from the eight relations [Eq. (C1)]. We begin to solve these eight equations to the zeroth order in ξ/K_0 or, in other words, by writing $\xi/K_0=0$. We note that the eight equations are then divided into two sets: the first four equations are uncoupled to the last four ones.

The first four equations are related to the spin $[1\ \ 1]^t$ and write as

$$A_1 = -B_1 + A_2 + B_2, \tag{C2a}$$

$$iqA_1 = iqB_1 - KA_2 + KB_2, \tag{C2b}$$

$$A_3e^{iqa} = A_2e^{-Ka} + B_2e^{Ka}, \tag{C2c}$$

$$iqA_3e^{iqa} = -KA_2e^{-Ka} + KB_2e^{Ka}, \tag{C2d}$$

and the last four ones are related to the spin $[1\ \ -1]^t$. The equations are the same by altering (A_1,B_1,A_2,B_2,K) into $(\tilde{A}_1,\tilde{B}_1,\tilde{A}_2,\tilde{B}_2,K')$. This is the usual formulation of the tunnel effect. Because Eq. (C1) is written to the first order in ξ/K_0, we are looking for a solution to the same order.

To give an example, we look for the results when the incident wave has a spin $[1\ \ 1]^t$ $(A_1\neq 0,\ \tilde{A}_1=0)$. Considering Eq. (2.25), we note that the approximation given by the last term of each equation is almost valid as soon as $Ka>2$. In Ref. 13, K is of the order of magnitude of 0.1 Å^{-1} which gives a of the order of magnitude of 20 Å in order that the inequality holds, a value which is quite reasonable.

As $\tilde{A}_1=0$, this shows that to the zeroth order in ξ/K_0, the results may be summarized by

$$A_2/A_1 = f_2^{(0)}, \quad \tilde{A}_2 = 0,$$

$$A_3/A_1 = f_3^{(0)}, \quad \tilde{A}_3 = 0,$$

$$B_1/A_1 = g_1^{(0)}, \quad \tilde{B}_1 = 0,$$

$$B_2/A_1 = g_2^{(0)}, \quad \tilde{B}_2 = 0, \tag{C3}$$

where $f_j^{(0)}=f_j^{(0)}(q,K)$ and $g_j^{(0)}=g_j^{(0)}(q,K)$ correspond to the standard case (Sec. II D) and can be deduced from Eq. (2.25). This means that, up to the first order in ξ/K_0, the results are of the shape

$$A_2/A_1 = f_2^{(0)} + (\xi/K) f_2^{(1)}, \quad \tilde{A}_2/A_1 = (\xi/K)\tilde{f}_2^{(1)},$$

$$A_3/A_1 = f_3^{(0)} + (\xi/K) f_3^{(1)}, \quad \tilde{A}_3/A_1 = (\xi/K)\tilde{f}_3^{(1)},$$

$$B_1/A_1 = g_1^{(0)} + (\xi/K) g_1^{(1)}, \quad \tilde{B}_1/A_1 = (\xi/K)\tilde{g}_1^{(1)},$$

$$B_2/A_1 = g_2^{(0)} + (\xi/K) g_2^{(1)}, \quad \tilde{B}_2/A_1 = (\xi/K)\tilde{g}_2^{(1)}, \tag{C4}$$

where the factors of $f_j^{(1)}=f_j^{(1)}(q,K,K')$, $g_j^{(1)}=g_j^{(1)}(q,K,K')$, $\tilde{f}_j^{(1)}=\tilde{f}_j^{(1)}(q,K,K')$, and $\tilde{g}_j^{(1)}=\tilde{g}_j^{(1)}(q,K,K')$ may be equal to zero. In fact, a calculation up to the first order in ξ/K_0 via Eq. (C1) involves terms of $(\xi/K)\tilde{A}_2$ type, which are of second order in ξ/K_0. Therefore $f_j^{(1)}=g_j^{(1)}=0$ and Eq. (C4) writes as

$$A_2/A_1 = f_2^{(0)} + (\xi/K)^2 f_2^{(2)}, \quad \tilde{A}_2/A_1 = (\xi/K)\tilde{f}_2^{(1)},$$

$$A_3/A_1 = f_3^{(0)} + (\xi/K)^2 f_3^{(2)}, \quad \tilde{A}_3/A_1 = (\xi/K)\tilde{f}_3^{(1)},$$

$$B_1/A_1 = g_1^{(0)} + (\xi/K)^2 g_1^{(2)}, \quad \tilde{B}_1/A_1 = (\xi/K)\tilde{g}_1^{(1)},$$

$$B_2/A_1 = g_2^{(0)} + (\xi/K)^2 g_2^{(2)}, \quad \tilde{B}_2/A_1 = (\xi/K)\tilde{g}_2^{(1)}, \tag{C5}$$

where $f_j^{(2)}=f_j^{(2)}(q,K,K')$ and $g_j^{(2)}=g_j^{(2)}(q,K,K')$.

Of course if $A_1=0$ and $\tilde{A}_1\neq 0$, the results are to be inverted. $f_j^{(2)}$ ($g_j^{(2)}$) is comparable to, or smaller than, $f_j^{(0)}$ ($g_j^{(0)}$). In Sec. IV C, it can be seen that $\tilde{f}_j^{(1)}A_1$ is of the order of magnitude of A_j and $\tilde{g}_j^{(1)}A_1$ is of the order of magnitude of B_j.

*henri-jean.drouhin@polytechnique.edu

[1] W. H. Butler, X.-G. Zhang, T. C. Schulthess, and J. M. MacLaren, Phys. Rev. B **63**, 054416 (2001); W. H. Butler, X.-G. Zhang, T. C. Schulthess, and J. M. MacLaren, *ibid.* **63**, 092402 (2001).

[2] M. Elsen, H. Jaffrès, R. Mattana, L. T. Thevenard, A. Lemaître, and J.-M. George, Phys. Rev. B **76**, 144415 (2007).

[3] J. M. Luttinger and W. Kohn, Phys. Rev. **97**, 869 (1955).

[4] W. Harrison, Phys. Rev. **123**, 85 (1961).

[5] B. J. BenDaniel and C. B. Duke, Phys. Rev. **152**, 683 (1966).

[6] G. Bastard, *Wave Mechanics Applied to Semiconductor Heterostructures (Les Éditions de Physique)* (Les Ulis, France, 1996).

[7] Note that, however, it was shown in subsequent papers that the BenDaniel and Duke Hamiltonian is not the only possible choice; see R. Balian, D. Bessis, and G. A. Mezinsescu, Phys. Rev. B **51**, 17624 (1995); J. Phys. I **6**, 1377 (1996).

[8] M. D'yakonov and V. I. Perel', Zh. Eksp. Teor. Fiz. **60**, 1954 (1971); [Sov. Phys. JETP **33**, 1053 (1971)]; Fiz. Tverd. Tela (Leningrad) **13**, 3581 (1971); [Sov. Phys. Solid State **13**, 3023 (1972)].

[9] J. C. Slonczewski, Phys. Rev. B **39**, 6995 (1989).

[10] V. Heine, Proc. Phys. Soc. London **81**, 300 (1963).

[11] R. O. Jones, Proc. Phys. Soc. London **89**, 443 (1966).

[12] G. Dresselhaus, Phys. Rev. **100**, 580 (1955).

[13] V. I. Perel', S. A. Tarasenko, I. N. Yassievich, S. D. Ganichev, V. V. Bel'kov, and W. Prettl, Phys. Rev. B **67**, 201304(R) (2003).

[14] N. Rougemaille, H.-J. Drouhin, S. Richard, G. Fishman, and A. K. Schmid, Phys. Rev. Lett. **95**, 186406 (2005).

[15] S. Richard, H.-J. Drouhin, N. Rougemaille, and G. Fishman, J. Appl. Phys. **97**, 083706 (2005).

[16] Y. C. Chang, Phys. Rev. B **25**, 605 (1982).

[17] Y. C. Chang and J. N. Schulman, Phys. Rev. B **25**, 3975 (1982).

[18] M. F. H. Schuurmans and G. W. 't Hooft, Phys. Rev. B **31**, 8041 (1985).

[19] L. Berger, Phys. Rev. B **54**, 9353 (1996).

[20] A. Messiah, *Mécanique Quantique* (Dunod, Paris, 1995).

[21] C. Kittel, *Quantum Theory of Solids* (Wiley, New York, 1987).

[22] The imaginary part of $\mathcal{E}(\mathbf{k})$ has no physical meaning and should not be confused with the self-energy related to the lifetime, e.g., in many-electron calculations.

[23] C. Cohen-Tannoudji, B. Diu, and F. Laloë, *Mécanique Quantique* (Hermann, Paris, 1996), p. 238.

[24] E. O. Kane, J. Phys. Chem. Solids **1**, 249 (1957).

[25] T. Valet and A. Fert, Phys. Rev. B **48**, 7099 (1993).

[26] This straightforwardly explains, for instance, how tunneling occurs for electrons located in semiconductor side valleys (the spin-orbit interaction is not considered here). Indeed, the states associated to the wave vectors $\boldsymbol{\zeta}+\mathbf{q}$, where $\boldsymbol{\zeta}$ corresponds to the center of the considered valley, and to $\boldsymbol{\zeta}-\mathbf{q}$ are energy degenerate (in this example, we have not necessarily $\boldsymbol{\zeta}\cdot\mathbf{q}=0$). To solve such a problem, we only have to find usual formal solutions dealing with plane waves of vectors $\pm\mathbf{q}$ outside the barrier and $\pm i\mathbf{K}$ in the barrier, respectively. This provides us with the reflection and transmission coefficients. Then, we obtain the true wave functions by multiplying the formal solutions by $e^{i\boldsymbol{\zeta}\cdot\mathbf{r}}$.

[27] E. A. de Andrada e Silva, G. C. La Rocca, and F. Bassani, Phys. Rev. B **55**, 16293 (1997).

[28] C. Cohen-Tannoudji, B. Diu, and F. Laloë, *Mécanique Quantique* (Hermann, Paris, 1996), p. 980.

[29] M. Büttiker and R. Landauer, Phys. Rev. Lett. **49**, 1739 (1982).

[30] J.-M. Jancu, R. Scholz, E. A. de Andrada e Silva, and G. C. La Rocca, Phys. Rev. B **72**, 193201 (2005); Δ^-, Δ_0', and Q in the paper by Jancu *et al.* are, respectively, written as Δ', Δ_C, and P_X in the present paper.

[31] B. Jusserand, D. Richards, G. Allan, C. Priester, and B. Etienne, Phys. Rev. B **51**, 4707 (1995).

[32] H. Riechert, H.-J. Drouhin, and C. Hermann, Phys. Rev. B **38**, 4136 (1988).

[33] H.-J. Drouhin, A. J. van der Sluijs, Y. Lassailly, and G. Lampel, J. Appl. Phys. **79**, 4734 (1996).

[34] For a pure spin filter along a given quantization axis, the transmission operator is a diagonal 2×2 matrix with eigenvalues of

different moduli. Then, we deal with two uncoupled spin channels with a nonzero transmission asymmetry.

[35] L. Joly, J. K. Ha, M. Alouani, J. Kortus, and W. Weber, Phys. Rev. Lett. **96**, 137206 (2006).

[36] M. I. Katsnelson, K. S. Novoselov, and A. K. Geim, Nat. Phys. **2**, 620 (2006).

[37] H. Diehl, V. A. Shalygin, V. V. Bel'kov, Ch. Hoffmann, S. N. Danilov, T. Herrle, S. A. Tarasenko, D. Schuh, Ch. Gerl, W. Wegscheider, W. Prettl, and S. D. Ganichev, New. J. Phys. **9**, 349 (2007).

[38] M. M. Glazov, P. S. Alekseev, M. A. Odnoblyudov, V. M. Chistyakov, S. A. Tarasenko, and I. N. Yassievich, Phys. Rev. B **71**, 155313 (2005).

[39] R. Romo and S. E. Ulloa, Phys. Rev. B **72**, 121305(R) (2005).

Chapitre 4

Ingénierie spin-orbite d'hétérostructures : le cas d'un déphaseur à spins

Il est important de déterminer des situations expérimentales dans lesquelles les phénomènes que nous avons étudiés jouent un rôle important et d'imaginer d'éventuelles applications. C'est de cet exercice que résulte le "composant" décrit dans le présent chapitre. Son principe a été publié dans l'article "Spin-orbit engineering of heterostructures : a quantum-phase shifter" [T. L. Hoai Nguyen, H.-J. Drouhin, J.-E. Wegrowe, and G. Fisman, Appl. Phys. Lett. **95**, 802108 (2009)]. On y montre qu'il est possible de manipuler le spin dans des solides en utilisant l'effet tunnel. Il s'agit d'utiliser la précession d'un spin incident situé dans le plan perpendiculaire au champ D'yakonov-Perel' durant le processus tunnel. C'est exactement l'analogue de la précession classique dans un champ magnétique, mais le champ complexe qui résulte de l'interaction spin-orbite est exclusivement confiné dans la barrière. Pour lutter contre l'atténuation du courant tout en amplifiant l'effet recherché, nous proposons d'utiliser un empilement de plusieurs barrières tunnel résonantes. Il est très simple de montrer que les effets de déphasage se cumulent. Ceci résulte du caractère impair en k du champ D'yakonov-Perel', qui conduit à des précessions opposées pour un spin se propageant de gauche à doite et de droite à gauche. Nous avons montré qu'en utilisant une structure à base de GaSb, semi-conducteur dans lequel le coefficient γ du champ D'yakonov-Perel' est environ 5 fois plus grand que dans GaAs, des rotations de 90° peuvent être obtenues dans des structures dont la longueur n'excèdent pas la trentaine de nm,

compatibles avec la maintien de la cohérence quantique.

Spin-orbit engineering of semiconductor heterostructures: A spin-sensitive quantum-phase shifter

T. L. Hoai Nguyen,[1,2] Henri-Jean Drouhin,[1,a)] Jean-Eric Wegrowe,[1] and Guy Fishman[2]
[1]*Ecole Polytechnique, LSI, CNRS and CEA/DSM/IRAMIS, Palaiseau F-91128, France*
[2]*Université Paris-Sud, IEF, CNRS, Orsay F-91405, France*

(Received 26 June 2009; accepted 1 August 2009; published online 27 August 2009)

In noncentrosymmetric semiconductors with zinc-blende structure grown along the [110] crystallographic direction, electrons with up- and down-spins undergo different quantum-phase shifts upon tunneling, which can be viewed as resulting from spin precession around a complex magnetic field. There is no spin filtering but a pure spin dephasing. The phase shift of the transmitted wave is proportional to the overall barrier-material thickness. We show that a device incorporating a number of resonant tunnel barriers constitutes an efficient quantum-phase shifter. © *2009 American Institute of Physics*. [DOI: 10.1063/1.3211118]

Spin-dependent tunneling through a crystalline barrier is presently an active field of research with challenging applications related to the improvement of hard-disk read heads.[1] In these cases, the devices use different transmission coefficients for up- and down-spins, leading to a spin-filter effect and thus to an enhanced spin asymmetry of the tunnel process. Gallium arsenide is a model case of spin-orbit-split barriers because, due the absence of inversion symmetry, the spin degeneracy of the bands is lifted. The first conduction band is described by the well-known D'yakonov–Perel' (DP) Hamiltonian and the spin splitting appears to result from a wave-vector-dependent internal magnetic field, the DP field.[2] This DP field is maximum along crystallographic directions equivalent to [110]. Recently, we have shown that tunneling through a [110]-oriented barrier cannot be described in the usual way because the derivative of the wave function cannot be continuous at the boundaries.[3] Contrary to the case studied by Perel' *et al.*[4]—off-normal tunneling near the [100] direction, where there is a spin filter effect—along the [110] no spin-filter effect occurs upon tunneling, the spin-orbit-split barrier acting as a pure spin rotator. Hereafter, we show that the spin dephasing is proportional to the overall barrier-material thickness, whatever the number of barriers, so that we suggest the use of resonant tunnel barriers to control the relative phase of spin states.

We consider a barrier of thickness a made of a zinc-blende semiconductor separating two well materials of similar nature (Fig. 1). The spin splitting of the conduction band is described by the DP Hamiltonian H_{DP}: $\hat{H}_{\mathrm{DP}}=\gamma_j \chi \cdot \hat{\sigma}$, where γ_j is a coupling parameter (the index values $j=1$ and 3 refer to the well material, whereas $j=2$ corresponds to the barrier material), and $\chi=\chi(\mathbf{k})=[\chi_x,\chi_y,\chi_z]=[k_x(k_y^2-k_z^2),k_y(k_z^2-k_x^2),k_z(k_x^2-k_y^2)]$ allows one to define the DP field. When $\mathbf{k}$ is collinear to a real direction, the energy levels are up and down-spin states, which are quantized along χ, in the plane perpendicular to $\mathbf{k}$. Specifically, along the [110] direction, with the wave vector $\mathbf{k}=(1/\sqrt{2})k[110]$, the energy dispersion in the j material is

$$E=\gamma_{jc}k^2+V_j\pm\tfrac{1}{2}\gamma_j k^3, \tag{1}$$

where the + (−) sign applies to the up- (down-) spin, quantized along the DP field and where V_j is the potential; the γ_{jc} parameter is related to the effective mass. In the barrier material, the evanescent states are associated with complex wave vectors. To obtain a real energy, the wave vectors associated with up or down spins should be chosen as $k=(1/\sqrt{2})[Q_{\uparrow,\downarrow}+iK,Q_{\uparrow,\downarrow}+iK,0]$, where $K\approx\sqrt{(V-E)/\gamma_c}$ defines the attenuation. To the first order, $Q_\uparrow=-Q_\downarrow=Q$, where $Q=\gamma K^2/4\gamma_c$. Then, through the procedure described in Ref. 3, we construct a solution to the tunneling problem which is continuous at the boundaries and that conserves the current of probability. The discontinuity of its derivative at the boundaries is proportional to Q. The principle is first to solve the envelope-function problem in the absence of DP field, taking into account the mass discontinuities in the framework of the well-known BenDaniel–Duke formalism. This determines the standard solution $\psi^{(0)}(z)$, which conserves the free-electron probability current. Second, with turning the

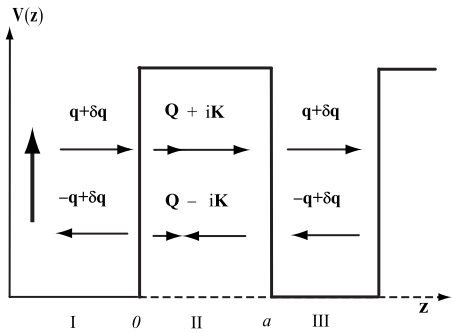

FIG. 1. Sketch of the tunnel geometry in the up-spin channel for a [110]-oriented zinc-blende semiconductor structure. The spin-orbit-split barriers of thickness a (medium II) are located between two identical free-electron-like spacers (media I and III). The tunnel axis, normal to the barrier, is the z axis. The wave vectors in the three media are, respectively, $k_{\mathrm{I}}=k_{\mathrm{III}}=\pm q+\delta q$ and $k_{\mathrm{II}}=Q_\uparrow\pm iK$. In the barrier, the energy for the up-spin electrons is $\gamma_c k^2+(1/2)\gamma k^3$ which requires the use of a complex k_{II} in order to have a real term; Re $k_{\mathrm{II}}=Q_\uparrow$ does not correspond to any absorption. Upon tunneling, a coherent spin dephasing builds up between the up- ($Q_\uparrow=+Q$) and down- ($Q_\downarrow=-Q$) spin channels. For such a nonquadratic Hamiltonian, the notion of current of probability has to be redefined (Ref. 3).

a)Electronic mail: henri-jean.drouhin@polytechnique.edu.

DP field on, the wave functions in the different regions are modified as indicated hereafter.

In the barrier, we take

$$\psi_B(z_0) = e^{iQz_0}\left[\psi^{(0)}(z_0) + i\frac{\gamma_2}{4\gamma_{2c}}\frac{\partial\psi^{(0)}(z_0)}{\partial z}\right], \tag{2}$$

where $z_0=0$ or $z_0=a$. In the well material, for the up channel

$$\psi_W(z) = e^{iQz_0}\left[a_j\left(1-\frac{\gamma_j}{4\gamma_{jc}}q_{j0}\right)e^{iq_{j0}z} + b_j\left(1+\frac{\gamma_j}{4\gamma_{jc}}q_{j0}\right)e^{-iq_{j0}z}\right]e^{-i\delta q_j(z-z_0)}, \tag{3}$$

where q_{j0} is the wave vector if the DP field were turned off ($\gamma_j=0$) and $\delta q_j=(\gamma_j/4\gamma_{jc})q_{j0}^2$. It can be shown that these functions are continuous up to third-order terms involving q/K, Q/K, effective masses, and DP-field coefficient relative jumps. Care has to be taken that, when the Hamiltonian is *nonquadratic*, the current of probability no longer coincides with the free-electron probability current $\mathbf{J}^f=(2\gamma_c/\hbar^2)\mathrm{Re}(\psi^*\hat{\mathbf{p}}\psi)$ and has to be properly redefined: considering the general form of the Hamiltonian

$$\hat{H} = \sum_j a_j\hat{p}_j + \sum_{j,k} b_{jk}\hat{p}_j\hat{p}_k + \sum_{j,k,l} c_{jkl}\hat{p}_j\hat{p}_k\hat{p}_l + V, \tag{4}$$

where a_j, b_{jk}, and c_{jkl} are Hermitian matrices, invariant under permutation of the indices j, k, and $l\in\{x,y,z\}$, and where V is real. The key point is that the j component of the probability current is

$$\mathbf{J}_j = \mathbf{J}_j^f + (\psi|a_j\psi) + 3\sum_{k,l}(\hat{p}_k\psi|c_{jkl}\hat{p}_l\psi) + \sum_{k,l}\hat{p}_k\hat{p}_l(\psi|c_{jkl}\psi). \tag{5}$$

In the case of the [110] direction that we consider here

$$\mathbf{J}_\pm = \mathbf{J}_\pm^f \pm \frac{\gamma}{2\hbar}\left(3\left|\frac{\partial}{\partial z}\psi_\pm\right|^2 - \frac{\partial^2}{\partial z^2}|\psi_\pm|^2\right). \tag{6}$$

Furthermore, it was shown that the current of probability remains equal to $J^f[\psi^{(0)}]$ in the three regions. We have the strong result that turning the DP field on does not change the current.

Hereafter, we use the transfer-matrix technique in this situation where the spin degeneracy of the bands is removed and where a two spin-channel transport model applies. First, we consider electron tunneling through a single barrier. Let us deal with the up-spin channel and assume that in regions I and III, the following wave functions are solutions of the Schrödinger equation:

$$\psi_{\mathrm{I}}(r)\uparrow = (A\psi_i + B\psi_r)\uparrow,$$

$$\psi_{\mathrm{III}}(r)\uparrow = (C\psi_t + D\tilde{\psi})\uparrow, \tag{7}$$

where ψ_i and ψ_r (ψ_t and $\tilde{\psi}$) are the incident and reflected (transmitted and reflected) plane waves in medium I (III). There are linear relations between the wave function coefficients, which can be summarized as

$$\begin{pmatrix} C \\ D \end{pmatrix} = M_\uparrow \begin{pmatrix} A \\ B \end{pmatrix}, \tag{8}$$

where $M_\uparrow$ is the transfer matrix

$$M_\uparrow = M = \begin{pmatrix} a & b \\ c & d \end{pmatrix}. \tag{9}$$

Similarly, in the down-spin channel, we have

$$M_\downarrow = \bar{M} = \begin{pmatrix} \bar{a} & \bar{b} \\ \bar{c} & \bar{d} \end{pmatrix}. \tag{10}$$

At a given energy, out of the barrier (regions I and III), the wave vectors associated with an up-spin (down-spin) are $\pm q+\delta q$ ($\pm q-\delta q$), whereas in the barrier (region II), the possible wave vectors are $Q\pm iK$ ($-Q\pm iK$). The elements of the transfer matrix depend on δq and Q

$$a = a(\delta q, Q), \quad b = b(\delta q, Q)\cdots. \tag{11}$$

The $\bar{a}$, $\bar{b}$, $\bar{c}$, and $\bar{d}$ coefficients are related to a, b, c, and d by changing δq to $-\delta q$ and Q to $-Q$.

$$\bar{a} = a(-\delta q, -Q), \quad \bar{b} = b(-\delta q, -Q)\cdots. \tag{12}$$

The Hamiltonian $\hat{H}$ is invariant under time reversal, i.e., under the action of the Kramers operator $\hat{K}$: if $\psi_{\mathrm{I}}\uparrow=(A\psi_i+B\psi_r)\uparrow$ is a solution, then $\psi_{\mathrm{I}}^*\downarrow=(A^*\psi_i^*+B^*\psi_r^*)\downarrow$ is also a solution, the transfer matrix remaining unchanged,

$$\begin{pmatrix} C \\ D \end{pmatrix} = \begin{pmatrix} a & b \\ c & d \end{pmatrix}\begin{pmatrix} A \\ B \end{pmatrix}, \tag{13}$$

$$\begin{pmatrix} D^* \\ C^* \end{pmatrix} = \begin{pmatrix} \bar{a} & \bar{b} \\ \bar{c} & \bar{d} \end{pmatrix}\begin{pmatrix} B^* \\ A^* \end{pmatrix}. \tag{14}$$

These two sets of equations yield $d=\bar{a}^*$ and $c=\bar{b}^*$. So that we obtain

$$M = \begin{pmatrix} a & b \\ \bar{b}^* & \bar{a}^* \end{pmatrix}. \tag{15}$$

The wave transmitted through the barrier in region III verifies $D=0$,

$$D = \bar{b}^*A + \bar{a}^*B = 0, \quad C = aA + bB \tag{16}$$

so $B=-(\bar{b}^*/\bar{a}^*)A$ and $C=aA-(\bar{b}^*/\bar{a}^*)bA=(a\bar{a}^*-b\bar{b}^*)/\bar{a}^*A=(\det M/\bar{a}^*)A$. When calculating the transmitted wave through a [110]-oriented barrier, neglecting the precession in the wells (i.e., $\delta q=0$) because the kinetic energy is small, we have shown[3] that $B=rA$ and $C=te^{iQa}A$, with r and t being the standard transmission and reflection amplitudes,

$$r = -(\bar{b}^*/\bar{a}^*)te^{iQa} = \det M/\bar{a}^*. \tag{17}$$

We deduce

$$\bar{a} = (1/t^*)e^{iQa}(\det M)^*, \quad \bar{b} = -(r^*/t^*)e^{iQa}\det M^* \tag{18}$$

and using the relation $\det\bar{M}=\det M^*$,

$$a = (1/t^*)e^{-iQa}(\det\bar{M})^* = (1/t^*)e^{-iQa}\det M,$$

$$b = -(r^*/t^*)e^{-iQa}(\det\bar{M})^* = -(r^*/t^*)e^{-iQa}\det M, \tag{19}$$

so that

$$M = \begin{pmatrix} (1/t^*)e^{-iQa} \det M & -(r^*/t^*)e^{-iQa} \det M \\ -(r/t)e^{-iQa} \det M & (1/t)e^{-iQa} \det M \end{pmatrix}$$
$$= (\det M)e^{-iQa}M_0/\det M_0, \quad (20)$$

where M_0 is the standard transfer matrix obtained when $Q=0$. We have the relation $\det M = e^{-2iQa}(\det M)^2/\det M_0$ which yields $\det M = e^{2iQa} \det M_0$. Finally,

$$M = e^{iQa}M_0. \quad (21)$$

The same result holds for the down-spin channel, substituting Q with $-Q$. If we describe a succession of barriers by means of transfer matrices, we see that the phase factor propagates from well to well so that the dephasing of the transmitted wave is the sum of the dephasing undergone in each barrier.

Let us consider a device including n resonant tunnel barriers—to achieve a good transmission in some energy regions—with an overall barrier-material thickness of na. In GaAs, the γ parameter value is equal to -24 eV Å^3. Numerically, $Qa \approx 0.1[K/(1\ \text{Å}^{-1})]^2[a/(1\ \text{Å})]$ so that for $K=0.1$ Å^{-1}, a value beyond which the k^3 spin splitting is no longer valid, and $a=20$ Å, $Qa=0.02$ rad$\approx 1°$. To achieve a large spin dephasing (e.g., 90° between the two spin states), a superlattice with about 45 periods would be required for an overall material thickness of the order of 1 500 Å, a distance over which coherent processes can still be expected. Other III-V semiconductor compounds could be used instead. As $Q=\gamma K^2/4\gamma_c \approx \gamma(V-E)/4\gamma_c^2$, the ratio (γ/γ_c) determines the efficiency at fixed K. Table II of Ref. 5 allows one to see that the largest value of (γ/γ_c) is obtained in GaSb, where Qa is five times larger than that in GaAs so that an overall material thickness of about 300 Å would be sufficient to achieve a dephasing of 90°. A [110] superlattice such as GaSb/InAs, where GaSb is the barrier material and InAs is the quantum well material, could be a good candidate for these experiments.

For zinc-blende semiconductor barriers grown along the [110] crystallographic axis, the spin-dependent tunnel scheme is "extraordinary." This arises because the effective Hamiltonian is nonquadratic, including the k^3 terms. Upon tunneling through a single barrier, a spin dephasing builds up between the up- and down-spin waves. Considering tunneling through a number of consecutive barriers, the resulting dephasing is the sum of the individual dephasing. This property is a consequence of the expression of the DP field, which is an odd power of the wave vector components: changing k to $-k$ changes the direction of the field so that the dephasing experienced by forward and backward propagating waves cancels. The reflected wave does not experience any dephasing and behaves as if there was no field. Then, a short GaAs superlattice, including an overall thickness of barrier material of less than 1500 Å, is able to produce a relative dephasing between the up- and down-spin states as large as 90°. Other III-V semiconductor compounds with larger internal fields and, in particular, GaSb, could be used to optimize the effect with only a few barriers. An experimental scheme to measure this effect could make use of a special magnetic tunnel junction: the emitter, for instance, a ferromagnetic layer, would have an in-plane magnetization perpendicular to the DP field, the insulator would be the tunnel-junction stack, and optical detection of the polarization vector of the transmitted electrons would be performed in a quantum well collector. Indeed, in this geometry, the phase shift between the spin channels is equivalent to a precession of the spin by the angle $-2nQa$ around the DP-field direction.

We thank Isabelle Sagnes and Roland Teissier for useful discussions and Travis Wade for a critical reading of the manuscript.

[1] W. H. Butler, X.-G. Zhang, T. C. Schulthess, and J. M. MacLaren, Phys. Rev. B **63**, 054416 (2001); **63**, 092402 (2001).
[2] M. D'yakonov and V. I. Perel', Zh. Eksp. Teor. Fiz. **60**, 1954 (1971) [Sov. Phys. JETP. **33**, 1053 (1971)]; M. D'yakonov and V. I. Perel', Fiz. Tverd. Tela (Leningrad) **13**, 3581 (1971) [Sov. Phys. Solid State **13**, 3023 (1972)].
[3] T. L. Hoai Nguyen, H.-J. Drouhin, J.-E. Wegrowe, and G. Fishman, Phys. Rev. B **79**, 165204 (2009).
[4] V. I. Perel, S. A. Tarasenko, I. N. Yassievich, S. D. Ganichev, V. V. Bel'kov, and W. Prettl, Phys. Rev. B **67**, 201304(R) (2003).
[5] J.-M. Jancu, R. Scholz, E. A. de Andrada e Silva, and G. C. La Rocca, Phys. Rev. B **72**, 193201 (2005).

Conclusion

Au cours de cette thèse, l'incidence du spin sur la nature des états évanescents a été étudiée dans le cas d'un semi-conducteur modèle, de type GaAs, pour lequel un calcul analytique des fonctions d'ondes est possible. Alors que la prise en compte du spin dans la structure de bandes réelle apparaît comme un rafinement qui conduit à la levée de dégénérescence des états selon certaines directions crystallographiques, suivant lesquelles le champ de D'yakonov-Perel' est non nul, les conséquences sur la structure des états évanescents sont plus profondes. Suivant les directions où le champ D'yakonov-Perel est non nul, les états évanescents ne peuvent plus être associés à des vecteurs d'onde purement imaginaires. Les vecteurs d'ondes évanescents incorporent alors une partie réelle, propagative, donnant naissance à des bandes complexes, dont la nature générale avait été étudiée par Kohn [KOH], Heine [HEI] et Jones [JON]. Sur cet exemple, si l'on considère spécifiquent les états évanescents dans la bande interdite, on observe une topologie originale. La notion de bandes dédoublées de spin, si familière dans les bandes réelles, trouve un analogue direct mais assez original le long de directions de type $K[\tan\theta, 0, i]$, la bande dédoublée se trouvant remplacée par une boucle reliant deux sous-bandes de spin, qui ne correspondent toutefois pas à des spins exactement opposés en centre de zone. Une telle boucle peut être vue comme un chemin sur la sphère unité sur laquelle est représentée le vecteur spin, joignant deux localités situées à des positions symmétriques dans l'hémisphère nord et dans l'hémisphère sud - les deux sous bandes du modèle D'yakonov-Perel. Cette structure en boucle apparaît finalement comme "naturelle", puique Jones a montré qu'une bande ne peut jamais s'arrêter. Selon des directions de type [110] où le champ D'yakonov-Perel' est maximum dans la bande de conduction réelle, la situation n'a pas d'analogue simple : à une énergie fixée, il y a exactement quatre états correspondants aux vecteurs d'onde complexes $(Q \pm iK)\left(1/\sqrt{2}\right)[110] \quad \uparrow$ et $(-Q \pm iK)\left(1/\sqrt{2}\right)[110] \quad \downarrow$. La structure de bandes complexes ne peut être bien décrite que via des vecteurs d'ondes qui appartiennent à un espace vecto-

riel de dimension 6 sur $\mathbb{R}$ de sorte qu'une représentation graphique simple n'est pas possible en général. Ces états évanescents sont impliqués dans les processus tunnels mettant en jeu une barrière semi-conductrice. Lorsque les boucles évanescentes sont pertinentes, ce qui est le cas lors de la transmission tunnel au travers d'une barrière orientée selon la direction [100] sous incidence oblique, on retrouve, cela devenant intuitif, un processus habituel, l'électron n'ayant pas le même coefficient de transmission selon son spin, puisqu'à énergie fixée, le vecteur d'onde associé est différent. Si l'on y regarde de plus près, le fait que les sous bandes en centre de zone n'aient pas un spin opposé empêche *stricto sensu* de séparer les canaux up et down de spin : les équations du problème, qui traduisent la continuité de la fonction d'onde et de la dérivée aux deux interface, doivent alors être projetées sur les deux canaux de spin, conduisant à un système linéaire de 8 équations couplées à 8 inconnues. Pour une barrière orientée selon la direction $[1, 1, 0]$, les réflexes habituels ne fonctionnent plus : la notion de courant de probabilité elle même, qui joue un rôle physique essentiel, doit être réexaminée pour cet Hamiltonien effectif non-quadratique et les conditions de raccord sont à réexaminer. Au final, on trouve que la dérivée de la fonction d'onde subit une discontinuité aux interfaces - même si la masse effective est la même de part et d'autre de l'interface. Une conclusion simple est que les deux canaux de spin peuvent ici être séparés et que l'onde transmise subit un déphasage opposé dans chaque canal de spin, la direction de quantification étant prise selon la direction (réelle) du champ D'yakonov-Perel. Dans le cas d'une sucession de barrières, ces déphasages se cumulent. Ici encore, le résultat est (presque) intuitif : un spin incident orienté dans le plan perpendiculaire au champ D'yakonov-Perel' précesse autour du champ durant la traversée de la barrière... il ne faut tout de même pas perdre de vue que, si la direction du champ D'yakonov-Perel' est réelle, le champ, lui, est complexe... Autre résultat important : on sait bien résoudre le problème de transport tunnel au travers d'une hétérostructure, en l'absence d'interaction spin-orbite, la méthode standard s'appuyant sur la construction de l'Hamiltonien effectif de BenDaniel et Duke. Partant de cette solution, nous avons donné un procédé simple pour déduire les états lorsque l'on "branche" l'interaction spin-orbite. Un point-clé est que la valeur du courant de probabilité n'est pas modifiée par cette opération. Cette étude a ainsi été l'occasion d'illustrer sur des exemples concrets un certain nombre de propriétés de spin des états évanescents et d'en tirer les conséquences sur les phénomènes de transport. La physique du spin des états évanescents est très différente de celle mise en jeu habituellement dans

les bandes réelles. Resterait maintenant à valider les prédictions de cette étude sur des dispositifs expérimentaux. Si la croissance de structures III-V selon la direction [110] est délicate, elle n'est pas impossible. Le choix de GaAs comme matériau de base n'est pas le meilleur et nous proposons d'utiliser des structures à base de GaSb, dans lesquelles le coefficient γ définissant l'intensité du champ D'yakonov-Perel' est plus grand. D'autres développement semblent intéressants (et nous les avons pour partie déjà entrepris). Il s'agit d'abord de réexaminer les techniques de construction des Hamiltoniens effectifs, de type BenDaniel-Duke, en partant de considérations générales. Ce type d'Hamiltonien permet de traiter la question du saut de masse effective entre deux matériaux. Le problème d'un saut de champ interne est beaucoup plus ardu. Par exemple, la situation - *a priori* élémentaire - d'un électron libre franchissant par effet tunnel une barrière de semi-conducteur type GaAs ne rentre pas (strictement) dans le formalisme que nous avons développé. Une autre question est liée au calcul du coefficient γ. il s'agit en l'occurence de tester des jeux de paramètres pertinents de la théorie $\mathbf{k}\cdot\mathbf{p}$. Le détail n'est guère important quand il s'agit seulement de visualiser les bandes d'énergie utiles, comme cela a été le cas dans ce manuscrit, mais il en va autrement si on essaie d'avoir une description précise et cohérente pour retrouver les résultats expérimentaux relatifs aux énergies (le cas le plus simple étant la masse effective qui donne une dispersion parabolique), au facteur de Landé et au splitting de spin de la bande de conduction. La difficulté vient du fait que, pour le calcul du facteur de Landé, les termes provenant de la perturbation au troisième ordre sont nettement supérieurs, par un coefficient de l'ordre de cinq, à ceux venant du second ordre, et qu'il en est de même pour le splitting "en k^3", les termes du quatrième ordre étant eux aussi supérieurs aux termes du troisième ordre. Cela introduit un certain nombre de paramètres supplémentaires mal connus et, dans tous les cas, modifie considérablement - d'un à deux ordres de grandeur - la valeur admise de certains paramètres depuis un trentaine d'années. C'est dans GaAs, où les données expérimentales sont les plus fiables, que le problème se pose particulièrement [SFD]. Une des suites de cette thèse sera de déterminer, via les méthodes propres à la théorie $\mathbf{k}\cdot\mathbf{p}$, quels sont les paramètres pertinents qui redonneront l'ensemble, et non plus seulement quelques uns, des paramètres expérimentaux.

Annexes

.

Annexe A

Pauli operator in the valence-conduction subset

Let us fist recall the properties of the Pauli operator which acts on the *up* and *down* spin states :

$$\sigma_x \ \uparrow \ = \downarrow \qquad \sigma_y \uparrow = i \downarrow \qquad \sigma_z \uparrow = \uparrow \tag{A.1}$$

$$\sigma_x \ \downarrow \ = \uparrow \qquad \sigma_y \downarrow = -i \uparrow \qquad \sigma_z \downarrow = - \downarrow \tag{A.2}$$

We have to calculate the matrices elements which represent the three components of the Pauli operator in the basis given in chapter 1. Note that the Pauli operator only acts on the spin but not on the orbital part, and that these orbital functions are orthogonal. The scalar product between two states in the different subspaces Γ_{5C}, Γ_6, and Γ_5 are equal to 0, so that only the Pauli-operator matrix elements calculated inside the subspaces $\{\Gamma_{7C},\ \Gamma_{8C}\}$, $\{\Gamma_6\}$, and $\{\Gamma_7,\ \Gamma_8\}$ are non-zero. We can write these $\boldsymbol{\sigma}$ matrices in block-diagonal form

$$\boldsymbol{\sigma} = \begin{pmatrix} \boldsymbol{\sigma}^A & 0 & 0 \\ 0 & \boldsymbol{\sigma}^C & 0 \\ 0 & 0 & \boldsymbol{\sigma}^B \end{pmatrix} \tag{A.3}$$

where $\boldsymbol{\sigma}^A$ operates in the subspace $\{\Gamma_{7C}, \Gamma_{8C}\}$, $\boldsymbol{\sigma}^C$ in the $\{\Gamma_6\}$ subspace, and $\boldsymbol{\sigma}^B$ in the $\{\Gamma_7, \Gamma_8\}$ subspace. Besides, the set of basis functions $\{|cM\rangle, |c \pm 7/2\rangle\}$ of $\{\Gamma_{7C}, \Gamma_{8C}\}$ and $\{|M\rangle, |\pm 7/2\rangle\}$ of $\{\Gamma_7, \Gamma_8\}$ have a very similar form (with X_C, Y_C, and Z_C being substituted with X, Y, and Z), therefore $\boldsymbol{\sigma}^A = \boldsymbol{\sigma}^B$.

Let us first consider the $\boldsymbol{\sigma}^C$ matrix in the $\{|S\uparrow\rangle, |S\downarrow\rangle\}$ basis of Γ_6. We have

$$\begin{aligned} &\langle S \ \uparrow \ |\sigma_x^C|S\uparrow\rangle = \langle S\uparrow|S\downarrow\rangle = 0\,; \quad \langle S\downarrow|\sigma_x^C|S\downarrow\rangle = \langle S\downarrow|S\uparrow\rangle = 0 \\ &\langle S \ \uparrow \ |\sigma_x^C|S\downarrow\rangle = \langle S\downarrow|\sigma_x^C|S\uparrow\rangle^* = \langle S\uparrow|S\uparrow\rangle = 1\,; \end{aligned} \tag{A.4}$$

$$\langle S \uparrow | \sigma_y^C | S \uparrow \rangle = i\langle S \uparrow | S \downarrow \rangle = 0\,; \quad \langle S \downarrow | \sigma_y^C | S \downarrow \rangle = -i\langle S \downarrow | S \uparrow \rangle = 0.$$
$$\langle S \uparrow | \sigma_y^C | S \downarrow \rangle = \langle S \downarrow | \sigma_y^C | S \uparrow \rangle^* = -i\langle S \uparrow | S \uparrow \rangle = -i\,; \tag{A.5}$$

$$\langle S \uparrow | \sigma_z^C | S \uparrow \rangle = \langle S \uparrow | S \uparrow \rangle = 1\,; \quad \langle S \downarrow | \sigma_z^C | S \downarrow \rangle = -\langle S \downarrow | S \downarrow \rangle = -1$$
$$\langle S \uparrow | \sigma_z^C | S \downarrow \rangle = \langle S \downarrow | \sigma_z^C | S \uparrow \rangle^* = \langle S \downarrow | S \downarrow \rangle^* = 0\,; \tag{A.6}$$

We see that $\boldsymbol{\sigma}^C$ is equal to the Pauli matrix $\boldsymbol{\sigma}$ expressed in the $\{\uparrow, \downarrow\}$ pure spin space.

Now we calculate the of 6×6 matrices $\boldsymbol{\sigma}^A = \boldsymbol{\sigma}^B$. Let us consider $\boldsymbol{\sigma}^B$ in the basis $\{|3/2\rangle, |1/2\rangle, |-1/2\rangle, |-3/2\rangle, |7/2\rangle, |-7/2\rangle\}$. Note that every ket has orthogonal orbital components associated to opposite spin states. Moreover, the operator $\sigma_{x,y}$ change spin up to spin down (and *vice versa*), so that the matrix elements on the diagonal of $\sigma_{x,y}^B$ are equal to 0. The elements below the diagonal are the complex conjugates of the matrix elements above the diagonal that are calculated as follows

1i)

$$\langle 3/2|\sigma_x|1/2\rangle = \left\{\tfrac{i}{\sqrt{2}}\langle X \uparrow| + \tfrac{1}{\sqrt{2}}\langle Y \uparrow|\right\}\left\{i\left[\sqrt{\tfrac{2}{3}}|Z \downarrow\rangle - \tfrac{1}{\sqrt{6}}|X \uparrow\rangle - \tfrac{i}{\sqrt{6}}|Y \uparrow\rangle\right]\right\}$$
$$= \quad 1/2\sqrt{3} + 1/2\sqrt{3} = 1/\sqrt{3}.$$

$$\langle 3/2|\sigma_x|-1/2\rangle = \left\{\tfrac{i}{\sqrt{2}}\langle X \uparrow| + \tfrac{1}{\sqrt{2}}\langle Y \uparrow|\right\}\left\{i\sqrt{\tfrac{2}{3}}|Z \uparrow\rangle + \tfrac{i}{\sqrt{6}}|X \downarrow\rangle + \tfrac{1}{\sqrt{6}}|Y \downarrow\rangle\right\}$$
$$= 0.$$

$$\langle 3/2|\sigma_x|-3/2\rangle \quad = \quad \left\{\tfrac{i}{\sqrt{2}}\langle X \uparrow| + \tfrac{1}{\sqrt{2}}\langle Y \uparrow|\right\}\left\{\tfrac{i}{\sqrt{2}}|X \uparrow\rangle + \tfrac{1}{\sqrt{2}}|Y \uparrow\rangle\right\}$$
$$= 0.$$

$$\langle 3/2|\sigma_x|7/2\rangle = \left\{\tfrac{i}{\sqrt{2}}\langle X \uparrow| + \tfrac{1}{\sqrt{2}}\langle Y \uparrow|\right\}\left\{\tfrac{i}{\sqrt{3}}|Z \downarrow\rangle + \tfrac{i}{\sqrt{3}}|X \uparrow\rangle - \tfrac{1}{\sqrt{3}}|Y \uparrow\rangle\right\}$$
$$= -1/\sqrt{6} - 1/\sqrt{6} = -\sqrt{2/3}.$$

$$\langle 3/2|\sigma_x|-7/2\rangle = \left\{\tfrac{i}{\sqrt{2}}\langle X \uparrow| + \tfrac{1}{\sqrt{2}}\langle Y \uparrow|\right\}\left\{-\tfrac{i}{\sqrt{3}}|Z \uparrow\rangle + \tfrac{i}{\sqrt{3}}|X \downarrow\rangle + \tfrac{1}{\sqrt{3}}|Y \downarrow\rangle\right\}$$
$$= 0.$$

1ii)

$$\langle 1/2|\sigma_x|-1/2\rangle = \left\{-i\sqrt{\tfrac{2}{3}}|Z \uparrow\rangle + \tfrac{i}{\sqrt{6}}|X \downarrow\rangle + \tfrac{1}{\sqrt{6}}|Y \downarrow\rangle\right\}$$

$$\times \left\{ i\sqrt{\tfrac{2}{3}}|Z\uparrow\rangle + \tfrac{i}{\sqrt{6}}|X\downarrow\rangle + \tfrac{1}{\sqrt{6}}|Y\downarrow\rangle \right\}$$
$$= 2/3 - 1/6 + 1/6 = 2/3.$$

$$\langle 1/2|\sigma_x|-3/2\rangle = \left\{ -i\sqrt{\tfrac{2}{3}}|Z\uparrow\rangle + \tfrac{i}{\sqrt{6}}|X\downarrow\rangle + \tfrac{1}{\sqrt{6}}|Y\downarrow\rangle \right\}$$
$$\times \left\{ \tfrac{i}{\sqrt{2}}|X\uparrow\rangle + \tfrac{1}{\sqrt{2}}|Y\uparrow\rangle \right\}$$
$$= 0.$$

$$\langle 1/2|\sigma_x|7/2\rangle = \left\{ -i\sqrt{\tfrac{2}{3}}|Z\uparrow\rangle + \tfrac{i}{\sqrt{6}}|X\downarrow\rangle + \tfrac{1}{\sqrt{6}}|Y\downarrow\rangle \right\}$$
$$\times \left\{ \tfrac{i}{\sqrt{3}}|Z\downarrow\rangle + \tfrac{i}{\sqrt{3}}|X\uparrow\rangle - \tfrac{1}{\sqrt{3}}|Y\uparrow\rangle \right\}$$
$$= 0.$$

$$\langle 1/2|\sigma_x|-7/2\rangle = \left\{ -i\sqrt{\tfrac{2}{3}}|Z\uparrow\rangle + \tfrac{i}{\sqrt{6}}|X\downarrow\rangle + \tfrac{1}{\sqrt{6}}|Y\downarrow\rangle \right\}$$
$$\times \left\{ -\tfrac{i}{\sqrt{3}}|Z\uparrow\rangle + \tfrac{i}{\sqrt{3}}|X\downarrow\rangle + \tfrac{1}{\sqrt{3}}|Y\downarrow\rangle \right\}$$
$$= -\sqrt{2}/3 - 1/3\sqrt{2} + 1/3\sqrt{2} = -\sqrt{2}/3.$$

1iii)

$$\langle -1/2|\sigma_x|-3/2\rangle = \left\{ -i\sqrt{\tfrac{2}{3}}|Z\downarrow\rangle - \tfrac{i}{\sqrt{6}}|X\uparrow\rangle + \tfrac{1}{\sqrt{6}}|Y\uparrow\rangle \right\} \left\{ \tfrac{i}{\sqrt{2}}|X\uparrow\rangle + \tfrac{1}{\sqrt{2}}|Y\uparrow\rangle \right\}$$
$$= 1/2\sqrt{3} + 1/2\sqrt{3} = 1/\sqrt{3}.$$

$$\langle -1/2|\sigma_x|7/2\rangle = \left\{ -i\sqrt{\tfrac{2}{3}}|Z\downarrow\rangle - \tfrac{i}{\sqrt{6}}|X\uparrow\rangle + \tfrac{1}{\sqrt{6}}|Y\uparrow\rangle \right\}$$
$$\times \left\{ \tfrac{i}{\sqrt{3}}|Z\downarrow\rangle + \tfrac{i}{\sqrt{3}}|X\uparrow\rangle - \tfrac{1}{\sqrt{3}}|Y\uparrow\rangle \right\}$$
$$= \sqrt{2}/3 + 1/2\sqrt{3} - 1/2\sqrt{3} = \sqrt{2}/3.$$

$$\langle -1/2|\sigma_x|-7/2\rangle = \left\{ -i\sqrt{\tfrac{2}{3}}|Z\downarrow\rangle - \tfrac{i}{\sqrt{6}}|X\uparrow\rangle + \tfrac{1}{\sqrt{6}}|Y\uparrow\rangle \right\}$$
$$\times \left\{ -\tfrac{i}{\sqrt{3}}|Z\uparrow\rangle + \tfrac{i}{\sqrt{3}}|X\downarrow\rangle + \tfrac{1}{\sqrt{3}}|Y\downarrow\rangle \right\}$$
$$= 0.$$

1iv)

$$\langle -3/2|\sigma_x|7/2\rangle = \left\{ -\tfrac{i}{\sqrt{2}}\langle X\downarrow| + \tfrac{1}{\sqrt{2}}\langle Y\downarrow| \right\} \left\{ \tfrac{i}{\sqrt{3}}|Z\downarrow\rangle + \tfrac{i}{\sqrt{3}}|X\uparrow\rangle - \tfrac{1}{\sqrt{3}}|Y\uparrow\rangle \right\}$$
$$= 0.$$

$$\langle -3/2|\sigma_x|-7/2\rangle = \left\{ -\tfrac{i}{\sqrt{2}}\langle X\downarrow| + \tfrac{1}{\sqrt{2}}\langle Y\downarrow| \right\}$$
$$\times \left\{ -\tfrac{i}{\sqrt{3}}|Z\uparrow\rangle + \tfrac{i}{\sqrt{3}}|X\downarrow\rangle + \tfrac{1}{\sqrt{3}}|Y\downarrow\rangle \right\}$$

$$= 1/\sqrt{6} + 1/\sqrt{6} = \sqrt{2/3}.$$

1v)

$$\langle 7/2|\sigma_x|-7/2\rangle = \left\{-\tfrac{i}{\sqrt{3}}|Z\uparrow\rangle - \tfrac{i}{\sqrt{3}}|X\downarrow\rangle - \tfrac{1}{\sqrt{3}}|Y\downarrow\rangle\right\} \times \left\{-\tfrac{i}{\sqrt{3}}|Z\uparrow\rangle + \tfrac{i}{\sqrt{3}}|X\downarrow\rangle + \tfrac{1}{\sqrt{3}}|Y\downarrow\rangle\right\} = -1/3 + 1/3 - 1/3 = -1/3.$$

Similarly for σ_y^B, the matrix elements above the diagonal are

2i)

$$\langle 3/2|\sigma_y|1/2\rangle = \left\{\tfrac{i}{\sqrt{2}}\langle X\uparrow| + \tfrac{1}{\sqrt{2}}\langle Y\uparrow|\right\} \times \left\{-\sqrt{\tfrac{2}{3}}|Z\downarrow\rangle - \tfrac{1}{\sqrt{6}}|X\uparrow\rangle - \tfrac{i}{\sqrt{6}}|Y\uparrow\rangle\right\} = -i\left(1/2\sqrt{3} + 1/2\sqrt{3}\right) = -i/\sqrt{3}.$$

$$\langle 3/2|\sigma_y|-1/2\rangle = \left\{\tfrac{i}{\sqrt{2}}\langle X\uparrow| + \tfrac{1}{\sqrt{2}}\langle Y\uparrow|\right\} \times \left\{\sqrt{\tfrac{2}{3}}|Z\uparrow\rangle - \tfrac{1}{\sqrt{6}}|X\downarrow\rangle + \tfrac{i}{\sqrt{6}}|Y\downarrow\rangle\right\} = 0.$$

$$\langle 3/2|\sigma_y|-3/2\rangle = \left\{\tfrac{i}{\sqrt{2}}\langle X\uparrow| + \tfrac{1}{\sqrt{2}}\langle Y\uparrow|\right\}\left\{\tfrac{1}{\sqrt{2}}|X\uparrow\rangle - \tfrac{i}{\sqrt{2}}|Y\uparrow\rangle\right\} = i\,(1/2 - 1/2) = 0.$$

$$\langle 3/2|\sigma_y|7/2\rangle = \left\{\tfrac{i}{\sqrt{2}}\langle X\uparrow| + \tfrac{1}{\sqrt{2}}\langle Y\uparrow|\right\} \times \left\{-\tfrac{1}{\sqrt{3}}|Z\downarrow\rangle + \tfrac{1}{\sqrt{3}}|X\uparrow\rangle + \tfrac{i}{\sqrt{3}}|Y\uparrow\rangle\right\} = -i\left(-1/\sqrt{6} - 1/\sqrt{6}\right) = i\sqrt{2/3}.$$

$$\langle 3/2|\sigma_y|-7/2\rangle = \left\{\tfrac{i}{\sqrt{2}}\langle X\uparrow| + \tfrac{1}{\sqrt{2}}\langle Y\uparrow|\right\} \times \left\{-\tfrac{1}{\sqrt{3}}|Z\uparrow\rangle - \tfrac{1}{\sqrt{3}}|X\downarrow\rangle + \tfrac{i}{\sqrt{3}}|Y\downarrow\rangle\right\} = 0.$$

2ii)

$$\langle 1/2|\sigma_y|-1/2\rangle = \left\{-i\sqrt{\tfrac{2}{3}}|Z\uparrow\rangle + \tfrac{1}{\sqrt{6}}|X\downarrow\rangle + \tfrac{1}{\sqrt{6}}|Y\downarrow\rangle\right\} \times \left\{\sqrt{\tfrac{2}{3}}|Z\uparrow\rangle - \tfrac{1}{\sqrt{6}}|X\downarrow\rangle + \tfrac{i}{\sqrt{6}}|Y\downarrow\rangle\right\} = i\left(-2/3 - 1/6 + 1/6\right) = -2i/3.$$

$$\langle 1/2|\sigma_y|-3/2\rangle = \left\{-i\sqrt{\tfrac{2}{3}}|Z\uparrow\rangle + \tfrac{1}{\sqrt{6}}|X\downarrow\rangle + \tfrac{1}{\sqrt{6}}|Y\downarrow\rangle\right\}\left\{\tfrac{1}{\sqrt{2}}|X\uparrow\rangle - \tfrac{i}{\sqrt{2}}|Y\uparrow\rangle\right\} = 0.$$

$$\langle 1/2|\sigma_x|7/2\rangle = \left\{-i\sqrt{\tfrac{2}{3}}|Z\uparrow\rangle + \tfrac{1}{\sqrt{6}}|X\downarrow\rangle + \tfrac{1}{\sqrt{6}}|Y\downarrow\rangle\right\} \times \left\{-\tfrac{1}{\sqrt{3}}|Z\downarrow\rangle + \tfrac{1}{\sqrt{3}}|X\uparrow\rangle + \tfrac{i}{\sqrt{3}}|Y\uparrow\rangle\right\} = 0.$$

$$\langle 1/2|\sigma_y|-7/2\rangle = \left\{-i\sqrt{\tfrac{2}{3}}|Z\uparrow\rangle + \tfrac{1}{\sqrt{6}}|X\downarrow\rangle + \tfrac{1}{\sqrt{6}}|Y\downarrow\rangle\right\} \times \left\{-\tfrac{1}{\sqrt{3}}|Z\uparrow\rangle - \tfrac{1}{\sqrt{3}}|X\downarrow\rangle + \tfrac{i}{\sqrt{3}}|Y\downarrow\rangle\right\} = i\left(\sqrt{2}/3 - 1/3\sqrt{2} + 1/3\sqrt{2}\right) = i\sqrt{2}/3.$$

2iii)

$$\langle -1/2|\sigma_y|-3/2\rangle = \left\{-i\sqrt{\tfrac{2}{3}}|Z\downarrow\rangle - \tfrac{i}{\sqrt{6}}|X\uparrow\rangle + \tfrac{1}{\sqrt{6}}|Y\uparrow\rangle\right\}\left\{\tfrac{1}{\sqrt{2}}|X\uparrow\rangle - \tfrac{i}{\sqrt{2}}|Y\uparrow\rangle\right\} = -i\left(1/2\sqrt{3} + 1/2\sqrt{3}\right) = -i/\sqrt{3}.$$

$$\langle -1/2|\sigma_y|7/2\rangle = \left\{-i\sqrt{\tfrac{2}{3}}|Z\downarrow\rangle - \tfrac{i}{\sqrt{6}}|X\uparrow\rangle + \tfrac{1}{\sqrt{6}}|Y\uparrow\rangle\right\} \times \left\{-\tfrac{1}{\sqrt{3}}|Z\downarrow\rangle + \tfrac{1}{\sqrt{3}}|X\uparrow\rangle + \tfrac{i}{\sqrt{3}}|Y\uparrow\rangle\right\} = i\left(\sqrt{2}/3 - 1/2\sqrt{3} + 1/2\sqrt{3}\right) = i\sqrt{2}/3.$$

$$\langle -1/2|\sigma_y|-7/2\rangle = \left\{-i\sqrt{\tfrac{2}{3}}|Z\downarrow\rangle - \tfrac{i}{\sqrt{6}}|X\uparrow\rangle + \tfrac{1}{\sqrt{6}}|Y\uparrow\rangle\right\} \times \left\{-\tfrac{1}{\sqrt{3}}|Z\uparrow\rangle - \tfrac{1}{\sqrt{3}}|X\downarrow\rangle + \tfrac{i}{\sqrt{3}}|Y\downarrow\rangle\right\} = 0.$$

2iv)

$$\langle -3/2|\sigma_y|7/2\rangle = \left\{-\tfrac{i}{\sqrt{2}}\langle X\downarrow| + \tfrac{1}{\sqrt{2}}\langle Y\downarrow|\right\}\left\{-\tfrac{1}{\sqrt{3}}|Z\downarrow\rangle + \tfrac{1}{\sqrt{3}}|X\uparrow\rangle + \tfrac{i}{\sqrt{3}}|Y\uparrow\rangle\right\} = 0.$$

$$\langle -3/2|\sigma_y|-7/2\rangle = \left\{-\tfrac{i}{\sqrt{2}}\langle X\downarrow| + \tfrac{1}{\sqrt{2}}\langle Y\downarrow|\right\} \times \left\{-\tfrac{1}{\sqrt{3}}|Z\uparrow\rangle - \tfrac{1}{\sqrt{3}}|X\downarrow\rangle + \tfrac{i}{\sqrt{3}}|Y\downarrow\rangle\right\}$$

$$= i\left(1/\sqrt{6} + 1/\sqrt{6}\right) = i\sqrt{2/3}.$$

2v)

$$\begin{aligned}\langle 7/2|\sigma_y|-7/2\rangle &= \left\{-\tfrac{i}{\sqrt{3}}|Z\uparrow\rangle - \tfrac{i}{\sqrt{3}}|X\downarrow\rangle - \tfrac{1}{\sqrt{3}}|Y\downarrow\rangle\right\} \\ &\qquad \times \left\{-\tfrac{1}{\sqrt{3}}|Z\uparrow\rangle - \tfrac{1}{\sqrt{3}}|X\downarrow\rangle + \tfrac{i}{\sqrt{3}}|Y\downarrow\rangle\right\} \\ &= i\left(-1/3 + 1/3 - 1/3\right) = -i/3.\end{aligned}$$

3i)

Now, we determine the σ_z^B matrix. Note that the σ_z operator does not change the spin direction, so that the elements $\langle U_{n_\sigma}|\sigma_z|U_{n\sigma'}\rangle$, with $|U_{n\sigma}\rangle = f(Z)\uparrow + g(X,Y)\downarrow$ and $|U_{m\sigma'}\rangle = f'(Z)\downarrow + g'(X,Y)\uparrow$, f, g, f', g' being arbitrary functions, are equal to zero. For example, the matrix elements between $|3/2\rangle$ and $\{|1/2\rangle, |-3/2\rangle, |7/2\rangle\}$, or between $|1/2\rangle$ and $\{|-1/2\rangle, |-7/2\rangle\}$, or between $|-1/2\rangle$ and $\{|-3/2\rangle, |7/2\rangle\}$, or between $|-3/2\rangle$ and $|-7/2\rangle$, or between $|7/2\rangle$ and $|-7/2\rangle$ are zero. The remaining terms above the diagonal are :

$$\begin{aligned}\langle 3/2|\sigma_y|-1/2\rangle &= \left\{\tfrac{i}{\sqrt{2}}\langle X\uparrow| + \tfrac{1}{\sqrt{2}}\langle Y\uparrow|\right\} \\ &\qquad \times \left\{-i\sqrt{\tfrac{2}{3}}|Z\downarrow\rangle + \tfrac{i}{\sqrt{6}}|X\uparrow\rangle + \tfrac{1}{\sqrt{6}}|Y\uparrow\rangle\right\} \\ &= \left(-1/2\sqrt{3} + 1/2\sqrt{3}\right) = 0.\end{aligned}$$

$$\begin{aligned}\langle 3/2|\sigma_z|-7/2\rangle &= \left\{\tfrac{i}{\sqrt{2}}\langle X\uparrow| + \tfrac{1}{\sqrt{2}}\langle Y\uparrow|\right\}\left\{\tfrac{i}{\sqrt{3}}|Z\downarrow\rangle + \tfrac{i}{\sqrt{3}}|X\uparrow\rangle + \tfrac{1}{\sqrt{3}}|Y\uparrow\rangle\right\} \\ &= \left(-1/\sqrt{6} + 1/\sqrt{6}\right) = 0.\end{aligned}$$

$$\begin{aligned}\langle 1/2|\sigma_z|-3/2\rangle &= \left\{-i\sqrt{\tfrac{2}{3}}|Z\uparrow\rangle + \tfrac{i}{\sqrt{6}}|X\downarrow\rangle - \tfrac{1}{\sqrt{6}}|Y\downarrow\rangle\right\}\left\{-\tfrac{i}{\sqrt{2}}|X\downarrow\rangle + \tfrac{1}{\sqrt{2}}|Y\downarrow\rangle\right\} \\ &= \left(1/2\sqrt{3} - 1/2\sqrt{3}\right) = 0.\end{aligned}$$

$$\begin{aligned}\langle 1/2|\sigma_z|7/2\rangle &= \left\{-i\sqrt{\tfrac{2}{3}}|Z\uparrow\rangle + \tfrac{i}{\sqrt{6}}|X\downarrow\rangle + \tfrac{1}{\sqrt{6}}|Y\downarrow\rangle\right\} \\ &\qquad \times \left\{\tfrac{i}{\sqrt{3}}|Z\uparrow\rangle - \tfrac{i}{\sqrt{3}}|X\downarrow\rangle + \tfrac{1}{\sqrt{3}}|Y\downarrow\rangle\right\} \\ &= \left(\sqrt{2}/3 + 1/3\sqrt{2} + 1/3\sqrt{2}\right) = 2\sqrt{2}/3.\end{aligned}$$

$$\begin{aligned}\langle -1/2|\sigma_z|-7/2\rangle &= \left\{-i\sqrt{\tfrac{2}{3}}|Z\downarrow\rangle - \tfrac{i}{\sqrt{6}}|X\uparrow\rangle + \tfrac{1}{\sqrt{6}}|Y\uparrow\rangle\right\} \\ &\qquad \times \left\{\tfrac{i}{\sqrt{3}}|Z\downarrow\rangle + \tfrac{i}{\sqrt{3}}|X\uparrow\rangle + \tfrac{1}{\sqrt{3}}|Y\uparrow\rangle\right\} \\ &= \left(\sqrt{2}/3 + 1/3\sqrt{2} + 1/3\sqrt{2}\right) = 2\sqrt{2}/3.\end{aligned}$$

3ii)

The elements in the diagonal are

$$\begin{aligned}\langle 3/2|\sigma_z|3/2\rangle &= \left\{\tfrac{i}{\sqrt{2}}\langle X\uparrow| + \tfrac{1}{\sqrt{2}}\langle Y\uparrow|\right\}\left\{-\tfrac{i}{\sqrt{2}}\langle X\uparrow| + \tfrac{1}{\sqrt{2}}\langle Y\uparrow|\right\}\\ &= (1/2+1/2) = 1.\end{aligned}$$

$$\begin{aligned}\langle 1/2|\sigma_z|1/2\rangle &= \left\{-i\sqrt{\tfrac{2}{3}}|Z\uparrow\rangle + \tfrac{i}{\sqrt{6}}|X\downarrow\rangle - \tfrac{1}{\sqrt{6}}|Y\downarrow\rangle\right\}\\ &\qquad\times\left\{i\sqrt{\tfrac{2}{3}}|Z\uparrow\rangle + \tfrac{i}{\sqrt{6}}|X\downarrow\rangle - \tfrac{1}{\sqrt{6}}|Y\downarrow\rangle\right\}\\ &= (2/3-1/6+1/6) = 1/3.\end{aligned}$$

$$\begin{aligned}\langle -1/2|\sigma_z|-1/2\rangle &= \left\{-i\sqrt{\tfrac{2}{3}}|Z\downarrow\rangle - \tfrac{i}{\sqrt{6}}|X\uparrow\rangle + \tfrac{1}{\sqrt{6}}|Y\uparrow\rangle\right\}\\ &\qquad\times\left\{-i\sqrt{\tfrac{2}{3}}|Z\downarrow\rangle + \tfrac{i}{\sqrt{6}}|X\uparrow\rangle + \tfrac{1}{\sqrt{6}}|Y\uparrow\rangle\right\}\\ &= (-2/3+1/6+1/6) = -1/3.\end{aligned}$$

$$\begin{aligned}\langle -3/2|\sigma_z|-3/2\rangle &= \left\{-\tfrac{i}{\sqrt{2}}\langle X\downarrow| + \tfrac{1}{\sqrt{2}}\langle Y\downarrow|\right\}\left\{-\tfrac{i}{\sqrt{2}}\langle X\downarrow| - \tfrac{1}{\sqrt{2}}\langle Y\downarrow|\right\}\\ &= (-1/2-1/2) = -1.\end{aligned}$$

$$\begin{aligned}\langle 7/2|\sigma_z|7/2\rangle &= \left\{-\tfrac{i}{\sqrt{3}}|Z\uparrow\rangle - \tfrac{i}{\sqrt{3}}|X\downarrow\rangle - \tfrac{1}{\sqrt{3}}|Y\downarrow\rangle\right\}\\ &\qquad\times\left\{\tfrac{i}{\sqrt{3}}|Z\uparrow\rangle - \tfrac{i}{\sqrt{3}}|X\downarrow\rangle + \tfrac{1}{\sqrt{3}}|Y\downarrow\rangle\right\}\\ &= (1/3-1/3-1/3) = -1/3.\end{aligned}$$

$$\begin{aligned}\langle -7/2|\sigma_z|-7/2\rangle &= \left\{\tfrac{i}{\sqrt{3}}|Z\downarrow\rangle - \tfrac{i}{\sqrt{3}}|X\uparrow\rangle - \tfrac{1}{\sqrt{3}}|Y\uparrow\rangle\right\}\\ &\qquad\times\left\{\tfrac{i}{\sqrt{3}}|Z\downarrow\rangle + \tfrac{i}{\sqrt{3}}|X\uparrow\rangle + \tfrac{1}{\sqrt{3}}|Y\uparrow\rangle\right\}\\ &= (1/3+1/3-1/3) = 1/3.\end{aligned}$$

We obtain the $\boldsymbol{\sigma}$ matrix used in the article [Phys. Rev. B **80**, 075207 (2009)] of chapter 2.

Annexe B

Numerical calculation program of the spin vector

%This program is written using the MATLAB code.
%Define the three 14×14 Pauli matrices in the space $\{\Gamma_{7C}, \Gamma_{8C}, \Gamma_6, \Gamma_7, \Gamma_8\}$

%σ_x

```
sig_x=zeros(14,14) ;
sig_x(1,2)=1/sqrt(3) ;
sig_x(1,5)=-sqrt(2/3) ;
sig_x(2,1)=1/sqrt(3) ; sig_x(2,3)=2/3 ; sig_x(2,6)=-sqrt(2)/3 ;
sig_x(3,2)=2/3 ; sig_x(3,4)=1/sqrt(3) ; sig_x(3,5)=sqrt(2)/3 ;
sig_x(4,3)=1/sqrt(3) ; sig_x(4,6)=sqrt(2/3) ;
sig_x(5,1)=-sqrt(2/3) ; sig_x(5,3)=sqrt(2)/3 ; sig_x(5,6)=-1/3 ;
sig_x(6,2)=-sqrt(2)/3 ; sig_x(6,4)=sqrt(2/3) ; sig_x(6,5)=-1/3 ;
sig_x(7,8)=1 ;
sig_x(8,7)=1 ;
sig_x(9,10)=1/sqrt(3) ; sig_x(9,13)=-sqrt(2/3) ;
sig_x(10,9)=1/sqrt(3) ; sig_x(10,11)=2/3 ; sig_x(10,14)=-sqrt(2)/3 ;
sig_x(11,10)=2/3 ; sig_x(11,12)=1/sqrt(3) ; sig_x(11,13)=sqrt(2)/3 ;
sig_x(12,11)=1/sqrt(3) ; sig_x(12,14)=sqrt(2/3) ;
sig_x(13,9)=-sqrt(2/3) ; sig_x(13,11)=sqrt(2)/3 ; sig_x(13,14)=-1/3 ;
sig_x(14,10)=-sqrt(2)/3 ;sig_x(14,12)=sqrt(2/3) ;sig_x(14,13)=-1/3 ;
```

```
%σ_y

sig_y=zeros(14,14);
sig_y(1,2)=-i*1/sqrt(3); sig_y(1,5)=i*sqrt(2/3);
sig_y(2,1)=i*1/sqrt(3); sig_y(2,3)=-i*2/3; sig_y(2,6)=i*sqrt(2)/3;
sig_y(3,2)=i*2/3; sig_y(3,4)=-i*1/sqrt(3); sig_y(3,5)=i*sqrt(2)/3;
sig_y(4,3)=i*1/sqrt(3); sig_y(4,6)=i*sqrt(2/3);
sig_y(5,1)=-i*sqrt(2/3); sig_y(5,3)=-i*sqrt(2)/3; sig_y(5,6)=i*1/3;
sig_y(6,2)=-i*sqrt(2)/3; sig_y(6,4)=-i*sqrt(2/3); sig_y(6,5)=-i*1/3;
sig_y(7,8)=-i;
sig_y(8,7)=i;
sig_y(9,10)=-i*1/sqrt(3); sig_y(9,13)=i*sqrt(2/3);
sig_y(10,9)=i*1/sqrt(3); sig_y(10,11)=-i*2/3; sig_y(10,14)=i*sqrt(2)/3;
sig_y(11,10)=i*2/3; sig_y(11,12)=-i*1/sqrt(3); sig_y(11,13)=i*sqrt(2)/3;
sig_y(12,11)=i*1/sqrt(3); sig_y(12,14)=i*sqrt(2/3);
sig_y(13,9)=-i*sqrt(2/3); sig_y(13,11)=-i*sqrt(2)/3; sig_y(13,14)=i*1/3;
sig_y(14,10)=-i*sqrt(2)/3; sig_y(14,12)=-i*sqrt(2/3);sig_y(14,13)=-i*1/3;

%σ_z

sig_z=zeros(14,14);
sig_z(1,1)=1;
sig_z(2,2)=1/3; sig_z(2,5)=2*sqrt(2)/3;
sig_z(3,3)=-1/3; sig_z(3,6)=2*sqrt(2)/3;
sig_z(4,4)=-1;
sig_z(5,2)=2*sqrt(2)/3; sig_z(5,5)=-1/3;
sig_z(6,3)=2*sqrt(2)/3; sig_z(6,6)=1/3;
sig_z(7,7)=1;
sig_z(8,8)=-1;
sig_z(9,9)=1;
sig_z(10,10)=1/3; sig_z(10,13)=2*sqrt(2)/3;
sig_z(11,11)=-1/3; sig_z(11,14)=2*sqrt(2)/3;
sig_z(12,12)=-1;
sig_z(13,10)=2*sqrt(2)/3; sig_z(13,13)=-1/3;
sig_z(14,11)=2*sqrt(2)/3; sig_z(14,14)=1/3;
```

%Function to calculate the spin value at N points located in the wave-vector interval [kplotInf, kplotSUp] of the loop corresponding to $\tan\theta$ =ta.

```
function spin03_07_08(N,kplotInf, kplotSup, ta)
sg_x ; sg_y ; sg_z ;
% k · p parameters
P=9.88 ; %eVA (P)
Pp=0.41 ; %eVA (P')
Px=8.68 ; %eVA (P_X)
delta=10^(-10) ;
delt=0.341 ; %eV, spin-splitting between Γ8 and Γ7 (Δ)
Eg=1.519 ; %eV, bandgap energy ; (E_G)
Edel=2.969 ; %eV, energy between Γ7C and Γ6 (E^Δ)
delC=0.171 ; %, energy between Γ7C and Γ8C (Δ^C)
delp=-0.170 ; %eV (Δ')
% Luttinger's Parameters
gc=-0.896 ;
g1=-1.656 ;
g2=0.023 ;
g3=-0.0645 ;
h=6.6260693*10^(-34) ;
hbar=h/(2*pi) ;
mo=9.1*10^(-31) ;
e=1.6*10^(-19) ;
t=hbar^2/(2*mo*e)*10^(20) ;%(eV.A^(-2))
gc=gc*t ;
g1=g1*t ;
g2=g2*t ;
g3=g3*t ;
```

For the sake of simplicity, we assume that the Luttinger's parameters for $\{\Gamma_{7C}, \Gamma_{8C}\}$ are equal to 0. We consider these bands to be flat bands. This means that we are not interested in the detail of these bands, but only in their influence on the Γ_6 conduction band and on the Γ_7 and Γ_8 valence bands.

```
E6=0 ; E8=E6-Eg ; E7=E8-delt ;
E7C=E6+Edel ; E8C=E7C+delC ;
a=5.6533 ;%A
```

```
b=2*pi/a; %A^(-1)
kplotMax=kplotSup;%*b;
kplotMin=kplotInf;%*b;
%N=5000;
dkplot=(kplotMax-kplotMin)/N;
kplot=kplotMin;
kx=0;ky=0;kz=0;
%Kz=Kmin;
H=zeros(14,14);
fid=fopen('spin','w');
for n=1:N
Kz=sqrt(kplot*kplot/(1+ta*ta))
kz=i*Kz
kx=ta*Kz;
%kplot=sqrt(Kz^2+ky^2);
kxq=kx^2;
kyq=ky^2;
kzq=kz^2;
ksq=kxq+kyq+kzq;
kus=2*kzq-kxq-kyq;
kp=kx+i*ky;
km=kx-i*ky;
U=g2*kus;
Bp=2*sqrt(3)*g3*kz*km;
Bpe=2*sqrt(3)*g3*kz*kp;
Cp=sqrt(3)*(g2*(kxq-kyq)-2*i*g3*kx*ky);
Cpe=sqrt(3)*(g2*(kxq-kyq)+2*i*g3*kx*ky);

%Elements of the 14 × 14 k · p matrix

H(1,1)=E8C; H(1,7)=-1/sqrt(2)*Pp*km;H(1,9)=(1/3)*delp;
H(1,10)=1/sqrt(3)*Px*kp; H(1,11)=1/sqrt(3)*Px*kz;
H(1,13)=1/sqrt(6)*Px*kp; H(1,14)=sqrt(2/3)*Px*kz;
H(2,2)=E8C; H(2,7)=sqrt(2/3)*Pp*kz; H(2,8)=-1/sqrt(6)*Pp*km;
H(2,9)=-1/sqrt(3)*Px*km; H(2,10)=(1/3)*delp;
H(2,12)=1/sqrt(3)*Px*kz; H(2,14)=-1/sqrt(2)*Px*kp;
```

H(3,3)=E8C ; H(3,7)=1/sqrt(6)*Pp*kp ; H(3,8)=sqrt(2/3)*Pp*kz ;
H(3,9)=-1/sqrt(3)*Px*kz ; H(3,11)=(1/3)*delp ;
H(3,12)=-1/sqrt(3)*Px*kp ; H(3,13)=1/sqrt(2)*Px*km ;
H(4,4)=E8C ; H(4,8)=1/sqrt(2)*Pp*kp ; H(4,10)=-1/sqrt(3)*Px*kz ;
H(4,11)=1/sqrt(3)*Px*km ; H(4,12)=(1/3)*delp ;
H(4,13)=sqrt(2/3)*Px*kz ; H(4,14)=-1/sqrt(6)*Px*km
H(5,5)=E7C ; H(5,7)=1/sqrt(3)*Pp*kz ; H(5,8)=1/sqrt(3)*Pp*km ;
H(5,9)=-1/sqrt(6)*Px*km ; H(5,11)=-1/sqrt(2)*Px*kp ;
H(5,12)=-sqrt(2/3)*Px*kz ; H(5,13)=-(2/3)*delp ;
H(6,6)=E7C ; H(6,7)=1/sqrt(3)*Pp*kp ; H(6,8)=-1/sqrt(3)*Pp*kz ;
H(6,9)=-sqrt(2/3)*Px*kz ; H(6,10)=1/sqrt(2)*Px*km ;
H(6,12)=1/sqrt(6)*Px*kp ; H(6,14)=-(2/3)*delp ;
H(7,1)=-1/sqrt(2)*Pp*kp ; H(7,2)=sqrt(2/3)*Pp*kz ;
H(7,3)=1/sqrt(6)*Pp*km ; H(7,5)=1/sqrt(3)*Pp*kz ;
H(7,6)=1/sqrt(3)*Pp*km ; H(7,7)=E6+gc*ksq ;
H(7,9)=-1/sqrt(2)*P*kp ; H(7,10)=sqrt(2/3)*P*kz ;
H(7,11)=1/sqrt(6)*P*km ; H(7,13)=1/sqrt(3)*P*kz ;
H(7,14)=1/sqrt(3)*P*km ; H(8,2)=-1/sqrt(6)*Pp*kp ;
H(8,3)=sqrt(2/3)*Pp*kz ; H(8,4)=1/sqrt(2)*Pp*km ;
H(8,5)=1/sqrt(3)*Pp*kp ; H(8,6)=-sqrt(1/3)*Pp*kz ;
H(8,8)=H(7,7) ; H(8,10)=-1/sqrt(6)*P*kp ;
H(8,11)=sqrt(2/3)*P*kz ; H(8,12)=1/sqrt(2)*P*km ;
H(8,13)=1/sqrt(3)*P*kp ; H(8,14)=-sqrt(1/3)*P*kz ;
H(9,1)=(1/3)*delp ; H(9,2)=-1/sqrt(3)*Px*kp ;
H(9,3)=-1/sqrt(3)*Px*kz ; H(9,5)=-1/sqrt(6)*Px*kp ;
H(9,6)=-sqrt(2/3)*Px*kz ; H(9,7)=-1/sqrt(2)*P*km ;
H(9,9)=E8-g1*ksq+U ; H(9,10)=Bp ;
H(9,11)=Cp ; H(9,13)=1/sqrt(2)*Bp ;
H(9,14)=sqrt(2)*Cp ; H(10,1)=1/sqrt(3)*Px*km ;
H(10,2)=(1/3)*delp ; H(10,4)=-1/sqrt(3)*Px*kz ;
H(10,6)=1/sqrt(2)*Px*kp ; H(10,7)=sqrt(2/3)*P*kz ;
H(10,8)=-1/sqrt(6)*P*km ; H(10,9)=Bpe ;
H(10,10)=E8-g1*ksq-U ; H(10,12)=Cp ;
H(10,13)=-sqrt(2)*U ; H(10,14)=-sqrt(3/2)*Bp ;
H(11,1)=1/sqrt(3)*Px*kz ; H(11,3)=(1/3)*delp ;
H(11,4)=1/sqrt(3)*Px*kp ; H(11,5)=-1/sqrt(2)*Px*km ;

```
H(11,7)=1/sqrt(6)*P*kp; H(11,8)=sqrt(2/3)*P*kz;
H(11,9)=Cpe; H(11,11)=H(10,10);
H(11,12)=-Bp;
H(11,13)=-sqrt(3/2)*Bpe; H(11,14)=sqrt(2)*U;
H(12,2)=1/sqrt(3)*Px*kz; H(12,3)=-1/sqrt(3)*Px*km;
H(12,4)=(1/3)*delp; H(12,5)=-sqrt(2/3)*Px*kz;
H(12,6)=1/sqrt(6)*Px*km; H(12,8)=1/sqrt(2)*P*kp;
H(12,10)=Cpe; H(12,11)=-Bpe;
H(12,12)=H(9,9); H(12,13)=-sqrt(2)*Cpe;
H(12,14)=1/sqrt(2)*Bpe; H(13,1)=1/sqrt(6)*Px*km;
H(13,3)=1/sqrt(2)*Px*kp; H(13,4)=sqrt(2/3)*Px*kz;
H(13,5)=-(2/3)*delp; H(13,7)=1/sqrt(3)*P*kz;
H(13,8)=1/sqrt(3)*P*km; H(13,9)=sqrt(1/2)*Bpe;
H(13,10)=-sqrt(2)*U; H(13,11)=-sqrt(3/2)*Bp;
H(13,12)=-sqrt(2)*Cp; H(13,13)=E7-g1*ksq;
H(14,1)=sqrt(2/3)*Px*kz; H(14,2)=-1/sqrt(2)*Px*km;
H(14,4)=-1/sqrt(6)*Px*kp; H(14,6)=-(2/3)*delp;
H(14,7)=1/sqrt(3)*P*kp; H(14,8)=-1/sqrt(3)*P*kz;
H(14,9)=sqrt(2)*Cpe; H(14,10)=-sqrt(3/2)*Bpe;
H(14,11)=sqrt(2)*U; H(14,12)=1/sqrt(2)*Bp;
H(14,14)=H(13,13);

%Diagonalize the Hamiltonian.

[Vtemp,D]=eig(H);
m=max(size(Vtemp));
% Energy and eigenvectors.
for p=1 :m
Dtemp(p)=D(p,p);
end
vec=conj(Vtemp');
seteig=[Dtemp' vec]
%Sort the energies in order of decreasing real part.
[d1,d2]=size(seteig);
for t=1 :d1-1
[Y,q]=max(real(seteig(t :d1,1)));
```

```
C=seteig(t, :) ;
seteig(t, :)=seteig(t+q-1, :) ;
seteig(t+q-1, :)=C ;
end
%Delete the imaginary energies and their corresponding wave vectors
new=10*ones(d1,d2) ;
for p=1 :d1
a1=abs(imag(seteig(p,1))) ;
b1=abs(real(seteig(p,1))) ;
err=a/b ;
if (a1<delta)|(err<delta)
new(p,1)=real(seteig(p,1)) ;
new(p,2 :d2)=seteig(p,2 :d2) ;
end
end
d=0 ;
for k1=1 :d1
if new(k1,1)==10
d=d+1 ;
temp(d)=k1 ;
end
end
for k1=1 :d
temp(k1)=temp(k1)-(k1-1) ;
end
for k1=1 :d
new(temp(k1), :)=[] ;
end
%Choose energies in the bandgap.
[m0,n0]=size(new) ;
d0=0 ;
for k0=1 :m0
if ((new(k0,1))>0.5)|(new(k0,1)<-1.4)
d0=d0+1 ;
temp0(d0)=k0 ;
end
```

```
end
for j0=1 :d0
temp0(j0)=temp0(j0)-(j0-1);
end
for j1=1 :d0
new(temp0(j1), :)=[];
end
%E=new( :,1);
%if length(E)<1
% break
%end
[m1,n1]=size(new);

% Calculation of the mean spin value.

for q=1 :m1
fprintf(fid,'%g ',kplot);
fprintf(fid,'%g ',kx);
fprintf(fid,'%g ',new(q,1));
vtemp_e=conj(new(q,2 :n1));
SGX= vtemp_e*sig_x*vtemp_e';
SGY=vtemp_e*sig_y*vtemp_e';
SGZ=vtemp_e*sig_z*vtemp_e';
VSG=sqrt(SGX*SGX+SGY*SGY+SGZ*SGZ)
plot(kplot,new(q,1))
fprintf(fid,'%g ',real(SGX));
fprintf(fid,'%g ',real(SGY));
fprintf(fid,'%g\n',real(SGX)/real(VSG));
hold on
end
kplot=kplot+dkplot;
end
fclose(fid);
hold off
```

Annexe C

Mathematical structure of the free-electron-current conserving waves

We look for the largest vectorial space $\mathfrak{E}$ consisting of free-electron-current conserving evanescent waves at energy E. For clarity, we will construct it step-by-step. Then, we will search for vectorial subspaces and for plausible solutions inside these subspaces. Let us recall that $\Uparrow = e^{iQz} \uparrow$, $\Downarrow = e^{-iQz} \downarrow$.

At a given energy, the general form of the wave in the barrier is

$$\Psi_{II} = \left[A_2 e^{-Kz} + B_2 e^{Kz}\right] \Uparrow + \left[\widetilde{A}_2 e^{-Kz} + \widetilde{B}_2 e^{Kz}\right] \Downarrow \tag{C.1}$$

We have seen in the equation 2.18 of the article in the chapter 3 that we must have $|A_2| = \left|\widetilde{A}_2\right|$ and $|B_2| = \left|\widetilde{B}_2\right|$ which lead to $A_2 = \mathcal{A}e^{i\theta_A}$, $\widetilde{A}_2 = \mathcal{A}e^{-i\theta_A}$, $B_2 = \mathcal{B}e^{i\theta_B}$, $\widetilde{B}_2 = \mathcal{B}e^{-i\theta_B}$. It follows that the current-conserving-wave subset is *not* stable under addition. Indeed, let us consider

$$\Psi'_{II} = \left[A'_2 e^{-Kz} + B'_2 e^{Kz}\right] \Uparrow + \left[\widetilde{A}'_2 e^{-Kz} + \widetilde{B}'_2 e^{Kz}\right] \Downarrow \tag{C.2}$$

with $|A'_2| = \left|\widetilde{A}'_2\right|$ and $|B'_2| = \left|\widetilde{B}'_2\right|$

$$\begin{aligned}\Psi_{II} + \Psi'_{II} = \left[(A_2 + A'_2)e^{-Kz} + (B_2 + B'_2)e^{Kz}\right] \Uparrow \\ + \left[(\widetilde{A}_2 + \widetilde{A}'_2)e^{-Kz} + (\widetilde{B}_2 + \widetilde{B}'_2)e^{Kz}\right] \Downarrow\end{aligned} \tag{C.3}$$

We must have :

$$|A_2 + A'_2| = \left|\widetilde{A}_2 + \widetilde{A}'_2\right| = \left|A_2 e^{i\theta_A} + A'_2 e^{i\theta'_A}\right| = \left|A_2 + A'_2 e^{i(\theta'_A - \theta_A)}\right| \tag{C.4a}$$

$$|B_2 + B'_2| = \left|B_2 e^{i\theta_B} + B'_2 e^{i\theta'_B}\right| = \left|B_2 + B'_2 e^{i(\theta'_B - \theta_B)}\right| \tag{C.4b}$$

These equalities are not verified except in special cases, i.e. $\theta'_A - \theta_A = n\pi$, $\theta'_B - \theta_B = m\pi$.

The general form of constant probability waves, given in Eq. 2.19 of the chapter 3 can be rewritten as

$$\Psi_{II}(z) = \mathcal{A}e^{-Kz}\left[\cos\theta_A\ S_1(z) - i\sin\theta_A\ \widehat{S}_1(z)\right] + \mathcal{B}e^{Kz}\left[\cos\theta_B\ S_1(z) - i\sin\theta_B\ \widehat{S}_1(z)\right] \tag{C.5}$$

Let us define

$$\Phi_{\mathcal{A},\mathcal{B}} = \Phi_{\mathcal{A},\mathcal{B}}(z) = \mathcal{A}e^{-Kz} + \mathcal{B}e^{Kz} \tag{C.6}$$

We have

$$\mathcal{A}e^{-Kz} = \frac{1}{2}\left(\Phi_{\mathcal{A},\mathcal{B}} - \frac{1}{K}\Phi'_{\mathcal{A},\mathcal{B}}\right) \tag{C.7a}$$

$$\mathcal{B}e^{Kz} = \frac{1}{2}\left(\Phi_{\mathcal{A},\mathcal{B}} + \frac{1}{K}\Phi'_{\mathcal{A},\mathcal{B}}\right) \tag{C.7b}$$

$\Psi_{II}(z)$ writes

$$\begin{aligned}\Psi_{II}(z) = {} & \frac{1}{2}\left[\cos\theta_A + \cos\theta_B\right]\Phi_{\mathcal{A},\mathcal{B}}\, S_1 - \frac{i}{2}\left[\sin\theta_A + \sin\theta_B\right]\Phi_{\mathcal{A},\mathcal{B}}\,\widehat{S}_1 \\ & - \frac{1}{2}\left[\cos\theta_A - \cos\theta_B\right]\frac{1}{K}\,\Phi'_{\mathcal{A},\mathcal{B}}\, S_1 + \frac{i}{2}\left[\sin\theta_A - \sin\theta_B\right]\frac{1}{K}\,\Phi'_{\mathcal{A},\mathcal{B}}\,\widehat{S}_1\end{aligned}$$

It is useful to take the following notations :

$$\theta_+ = \frac{\theta_A + \theta_B}{2} \text{ and } \theta_- = \frac{\theta_A - \theta_B}{2} \tag{C.8}$$

so that

$$\begin{aligned}\Psi_{II}(z) &= \cos\theta_+\ \cos\theta_-\ \Phi_{\mathcal{A},\mathcal{B}}\, S_1 - i\sin\theta_+\ \cos\theta_-\ \Phi_{\mathcal{A},\mathcal{B}}\,\widehat{S}_1 \\ &\qquad + \sin\theta_+\ \sin\theta_-\ \frac{1}{K}\Phi'_{\mathcal{A},\mathcal{B}}\, S_1 + i\sin\theta_-\ \cos\theta_+\ \frac{1}{K}\Phi'_{\mathcal{A},\mathcal{B}}\,\widehat{S}_1 \\ &= \cos\theta_-\ \left[\cos\theta_+\ S_1 - i\sin\theta_+\ \widehat{S}_1\right]\Phi_{\mathcal{A},\mathcal{B}} \\ &\qquad + \sin\theta_-\ \left[\sin\theta_+\ S_1 + i\cos\theta_+\ \widehat{S}_1\right]\frac{1}{K}\,\Phi'_{\mathcal{A},\mathcal{B}} \\ &= \cos\theta_-\ \Phi_{\mathcal{A},\mathcal{B}}\, S_{\exp i\theta_+} + i\ \sin\theta_-\ \frac{1}{K}\,\Phi'_{\mathcal{A},\mathcal{B}}\,\widehat{S}_{\exp i\theta_+}\end{aligned} \tag{C.9}$$

Now, with $\lambda \in \mathbb{C}$ and $\theta_\Phi \in \mathbb{R}$, let us more generally define $(\Phi_{\mathcal{A},\mathcal{B}}\, S)_{\lambda,\,\theta_\Phi}$ as

$$(\Phi_{\mathcal{A},\mathcal{B}}\, S)_{\lambda,\,\theta_\Phi} = \cos\theta_\Phi\, \Phi_{\mathcal{A},\mathcal{B}}\, S_\lambda + \sin\theta_\Phi\, \frac{1}{K}\, \Phi'_{\mathcal{A},\mathcal{B}} \left(i\widehat{S}_\lambda\right) \tag{C.10}$$

One can also write

$$\begin{aligned}(\Phi_{\mathcal{A},\mathcal{B}}\, S)_{\lambda,\,\theta_\Phi} &= \lambda \left[e^{i\theta_\Phi}\mathcal{A}e^{-Kz} + e^{-i\theta_\Phi}\mathcal{B}e^{Kz}\right] \Uparrow + \lambda^* \left[e^{-i\theta_\Phi}\mathcal{A}e^{-Kz} + e^{i\theta_\Phi}\mathcal{B}e^{-Kz}\right] \Downarrow \\ &= \mathcal{A}e^{-Kz} S_{\lambda \exp i\theta_\Phi} + \mathcal{B}e^{Kz} S_{\lambda \exp -i\theta_\Phi} \\ &= |\lambda| \left[\mathcal{A}e^{-Kz} S_{\exp i(\theta_\lambda + \theta_\Phi)} + \mathcal{B}e^{Kz} S_{\exp i(\theta_\lambda - \theta_\Phi)}\right]\end{aligned} \tag{C.11}$$

Thus θ_λ tunes the dephasing between the up- and the down-spin channels, whereas θ_Φ tunes the dephasing between the $\mathcal{A}$ and $\mathcal{B}$ components. The sum of two functions of the subset $(\Phi_{\mathcal{A},\mathcal{B}} S)_{\lambda,\,\theta_\Phi}$ is

$$\begin{aligned}(\Phi_{\mathcal{A},\mathcal{B}} S)_{\lambda,\,\theta_\Phi} + (\Phi_{\mathcal{A},\mathcal{B}} S)_{\lambda',\,\theta'_\Phi} &= \left[\left(\lambda e^{i\theta_\Phi} + \lambda' e^{i\theta'_\Phi}\right)\mathcal{A}e^{-Kz} + \left(\lambda e^{-i\theta_\Phi} + \lambda' e^{-i\theta'_\Phi}\right)\mathcal{B}e^{Kz}\right] \Uparrow \\ &+ \left[\left(\lambda^* e^{-i\theta_\Phi} + \lambda'^* e^{-i\theta'_\Phi}\right)\mathcal{A}e^{-Kz} + \left(\lambda^* e^{i\theta_\Phi} + \lambda'^* e^{i\theta'_\Phi}\right)\mathcal{B}e^{-Kz}\right] \Downarrow\end{aligned} \tag{C.12}$$

This sum is a probability-current conserving wave as

$$\begin{aligned}\left|\lambda e^{i\theta_\Phi} + \lambda' e^{i\theta'_\Phi}\right| &= \left|\lambda^* e^{-i\theta_\Phi} + \lambda'^* e^{-i\theta'_\Phi}\right| \text{ for } \mathcal{A} \\ \left|\lambda e^{-i\theta_\Phi} + \lambda' e^{-i\theta'_\Phi}\right| &= \left|\lambda^* e^{i\theta_\Phi} + \lambda'^* e^{i\theta'_\Phi}\right| \text{ for } \mathcal{B}\end{aligned} \tag{C.13}$$

Similarly, considering linear combinations with coefficients r and r', we have

$$\left|r\lambda e^{i\theta_\Phi} + r'\lambda' e^{i\theta'_\Phi}\right| = \left|r\lambda^* e^{-i\theta_\Phi} + r'\lambda'^* e^{-i\theta'_\Phi}\right| \text{ for } \mathcal{A}, \text{ idem for } \mathcal{B}, \text{ if } r,\, r' \in \mathbb{R} \tag{C.14}$$

Probability-current conservation holds provided that r and r' are real.

The subset is stable under addition if we can write

$$\begin{aligned}\lambda e^{i\theta_\Phi} + \lambda' e^{i\theta'_\Phi} &= \lambda'' e^{i\theta''_\Phi} \text{ for } \mathcal{A} \\ \lambda e^{-i\theta_\Phi} + \lambda' e^{-i\theta'_\Phi} &= \lambda'' e^{-i\theta''_\Phi} \text{ for } \mathcal{B}\end{aligned} \tag{C.15}$$

This implies that

$$\lambda e^{i\theta_\Phi} + \lambda' e^{i\theta'_\Phi} = \left[\lambda e^{-i\theta_\Phi} + \lambda' e^{-i\theta'_\Phi}\right]\, e^{2i\theta''_\Phi} \tag{C.16}$$

This equation does not necessarily have a solution. Indeed, we have to ensure $\left|e^{2i\theta''_\Phi}\right| = 1$:

$$\begin{aligned}\left|\lambda e^{i\theta_\Phi} + \lambda' e^{i\theta'_\Phi}\right|^2 &= |\lambda|^2 + |\lambda'|^2 + \lambda\lambda'^* e^{i(\theta_\Phi - \theta'_\Phi)} + \lambda^*\lambda' e^{-i(\theta_\Phi - \theta'_\Phi)} \\ \left|\lambda e^{-i\theta_\Phi} + \lambda' e^{-i\theta'_\Phi}\right|^2 &= |\lambda|^2 + |\lambda'|^2 + \lambda\lambda'^* e^{-i(\theta_\Phi - \theta'_\Phi)} + \lambda^*\lambda' e^{i(\theta_\Phi - \theta'_\Phi)}\end{aligned} \tag{C.17}$$

Generally, these two quantities are unequal so that the whole set $\left\{(\Phi_{\mathcal{A},\mathcal{B}}S)_{\lambda,\theta_\Phi}\right\}$ is not a vectorial space.

Let us extend this set to recover a vectorial space by considering

$$\Psi_{\alpha,\beta} = \left(\alpha\mathcal{A}e^{-Kz} + \beta\mathcal{B}e^{Kz}\right) \Uparrow + \left(\alpha^*\mathcal{A}e^{-Kz} + \beta^*\mathcal{B}e^{Kz}\right) \Downarrow \tag{C.18}$$

With $\alpha = |\alpha|\, e^{i\theta_\alpha}$, $\beta = |\beta|\, e^{i\theta_\beta}$

$$\Psi_{\alpha,\beta} = \mathcal{A}e^{-Kz}S_\alpha + \mathcal{B}e^{Kz}S_\beta = |\alpha|\,\mathcal{A}e^{-Kz}S_{\exp i\theta_\alpha} + |\beta|\,\mathcal{B}e^{Kz}S_{\exp i\theta_\beta} \tag{C.19}$$

$$\begin{aligned}\Psi_{\alpha,\beta} \;=\; & \cos\frac{\theta_\alpha-\theta_\beta}{2}\,\Phi_{|\alpha|\mathcal{A},\,|\beta|\mathcal{B}}\,S_{\exp\left[i\left(\theta_\alpha+\theta_\beta\right)/2\right]} \\ & +i\sin\frac{\theta_\alpha-\theta_\beta}{2}\,\frac{1}{K}\,\Phi'_{|\alpha|\mathcal{A},\,|\beta|\mathcal{B}}\,\widehat{S}_{\exp\left[i\left(\theta_\alpha+\theta_\beta\right)/2\right]}\end{aligned} \tag{C.20}$$

Now the relative amplitudes of the two up- (down-) spin components are tunable. From Eq. C.18 it is straightforward to show that $\mathfrak{E} = \{\Psi_{\alpha,\beta}\}$ is stable under linear combinations with real coefficients : $r\,\Psi_{\alpha,\beta} + r'\,\Psi_{\alpha',\beta'} = \Psi_{\alpha'',\beta''}$ with $\alpha'' = r\alpha + r'\alpha'$ because $(r\alpha + r'\alpha')^* = r\alpha^* + r'\alpha'^*$ while $(c\alpha + c'\alpha)^* \neq c\alpha^* + c'\alpha'^*$ if $c,\, c' \notin \mathbb{R}$. The same conclusion holds for β and β'. $\mathfrak{E}$ is a vectorial space over $\mathbb{R}$ and not over $\mathbb{C}$.

$\mathfrak{E}$ is the largest vectorial space allowing current conservation. Indeed, let us try to extend it by adding some other element. Any additional vector is to be of the form ($\mu,\, \mu' \in \mathbb{R}$)

$$\Psi^{\mu,\mu'}_{\alpha,\beta} = \left[e^{i\mu}\alpha\mathcal{A}e^{-Kz} + e^{i\mu'}\beta\mathcal{B}e^{Kz}\right] \Uparrow + \left(\alpha^*\mathcal{A}e^{-Kz} + \beta^*\mathcal{B}e^{Kz}\right) \Downarrow \tag{C.21}$$

since $|A_2| = \left|\widetilde{A}_2\right|$, $|B_2| = \left|\widetilde{B}_2\right|$ to comply with current conservation. Then

$$\Psi^{\mu,\mu'}_{\alpha,\beta} = \mathcal{A}e^{-Kz}\left[e^{i\mu}\alpha \Uparrow + \alpha^* \Downarrow\right] + \mathcal{B}e^{Kz}\left[e^{i\mu'}\beta \Uparrow + \beta^* \Downarrow\right] \tag{C.22}$$

which is not of the right form indicated in Eq.2.20 of the chapter 3 unless $\mu = \mu' = 0\ [2\pi]$.

Looking for vectorial subspaces in $\mathfrak{E}$, we eventually distinguish two cases :

1) $\left\{(\Phi_{\mathcal{A},\mathcal{B}}S)_{\lambda,0}\right\} = \{\Phi_{\mathcal{A},\mathcal{B}}\} \otimes \{S_\lambda\}$ is stable under addition and external multiplication by real numbers. It is an eigen subspace of energy and a vectorial subspace over $\mathbb{R}$. $\lambda = \exp i\theta_\lambda$ allows one to study any spin direction in the $\mathbf{\Pi}_{\boldsymbol{\chi}}$ plane. In this subspace $\mathbf{J}\left[\Phi_{\mathcal{A},\mathcal{B}}S_\lambda\right] = 2\,|\lambda|^2\,\mathbf{J}\left[\Phi_{\mathcal{A},\mathcal{B}}\right]$.

2) $\left\{(\Phi_{\mathcal{A},\mathcal{B}}S)_{\lambda,\theta_\Phi}\right\}_{\theta_\lambda}$ is a vectorial subspace at fixed θ_λ.

In short, as the Schrödinger equation is linear, any linear combination, with complex coefficients, of solutions is a solution. But only some of them are physical - e.g. match the "boundary condition" : *No-absorption in the barrier*, providing a constant probability current.

We now take into account physical constraints. Let us consider in $\mathfrak{E}$ the general wave $\Psi_{\alpha,\beta}$. The current of probability carried by $\Psi_{\alpha,\beta}$ is

$$\begin{aligned}\mathbf{J}\left[\Psi_{\alpha,\beta}\right] &= \left[\langle S_\alpha|S_\beta\rangle - i\frac{Q}{K}\left\langle S_\alpha|\widehat{S}_\beta\right\rangle\right]\mathbf{J}\left[\Phi_{\mathcal{A},\mathcal{B}}\right] \\ &= 2\left|\alpha\right|\left|\beta\right|\left[\cos\left(\theta_\beta-\theta_\alpha\right)-\frac{Q}{K}\sin\left(\theta_\beta-\theta_\alpha\right)\right]\mathbf{J}\left[\Phi_{\mathcal{A},\mathcal{B}}\right] \qquad \text{(C.23)}\end{aligned}$$

where $\mathbf{J}\left[\Phi_{\mathcal{A},\mathcal{B}}\right]=\frac{\hbar K}{m}i\left(\mathcal{A}\mathcal{B}^*-\mathcal{A}^*\mathcal{B}\right)$ is the current carried by $\Phi_{\mathcal{A},\mathcal{B}}$. The linear combination with real coefficients of two solutions with a current of probability of the sign of $\mathbf{J}\left[\Phi_{\mathcal{A},\mathcal{B}}\right]$ (resp. of the opposite sign) also has to be a solution associated to a current of probability of the same sign, whatever Q. It can be seen in Eq. C.23 that this implies that the sign of the cosine term is positive (resp. negative).

Assume that we have two solutions

$$\begin{aligned}\Psi_{\alpha,\beta} &= \mathcal{A}e^{-Kz}S_\alpha+\mathcal{B}e^{Kz}S_\beta \\ \Psi_{\alpha,\beta'} &= \mathcal{A}e^{-Kz}S_\alpha+\mathcal{B}e^{Kz}S_{\beta'} \qquad \text{(C.24)}\end{aligned}$$

which carry a current of probability of the same sign. We combine these two waves with real coefficients :

$$r\Psi_{\alpha,\beta}+r'\Psi_{\alpha,\beta'}=\Psi_{\mu,\nu}=\mathcal{A}e^{-Kz}S_\mu+\mathcal{B}e^{Kz}S_\nu \qquad \text{(C.25)}$$

where r and $r'\in\mathbb{R}$. To simplify, we can take $\alpha=\exp i\theta_\alpha$, $\beta=\exp i\theta_\beta$, and $\beta'=\exp i\theta'_\beta$

$$r_\mu e^{i\theta_\mu}=\left(r+r'\right)e^{i\theta_\alpha} \qquad \text{(C.26)}$$

$$r_\nu e^{i\theta_\nu}=re^{i\theta_\beta}+r'e^{i\theta'_\beta} \qquad \text{(C.27)}$$

where r_μ and $r_\nu\in\mathbb{R}$. If the vectors associated to $e^{i\theta_\beta}$ and $e^{i\theta'_\beta}$ were independent, by linear combination with real coefficients, we could generate any value θ_ν. Then, the sign of the current of probability could be inverted. We conclude that either $\theta'_\beta=\theta_\beta$ or $\theta'_\beta=\theta_\beta+\pi$. The last condition yields a current which is opposite to $\mathbf{J}\left[\Phi_{\mathcal{A}\mathcal{B}}\right]$ and has to be rejected. Consequently, we must have $\theta'_\beta=\theta_\beta$ and we can assert that θ_β is a unique function of θ_α, $\theta_\beta=g\left(\theta_\alpha\right)$.

Furthermore, for the same reason, g has to verify the following stability property :

$$\forall\, r,\, r' \in \mathbb{R}\ :\ r\Psi_{\exp i\theta_\alpha,\, \exp ig(\theta_\alpha)} + r'\Psi_{\exp i\theta'_\alpha,\, \exp ig(\theta'_\alpha)} = \Psi_{r_{\theta_\mu} \exp i\theta_\mu,\, r_{g(\theta_\mu)} \exp ig(\theta_\mu)} \tag{C.28}$$

Therefore

$$\begin{aligned} r_{\theta_\mu}\, e^{i\theta_\mu} &= r\, e^{i\theta_\alpha} + r'\, e^{i\theta'_\alpha} \\ r_{g(\theta_\mu)}\, e^{ig(\theta_\mu)} &= r\, e^{ig(\theta_\alpha)} + r'\, e^{ig(\theta'_\alpha)} \end{aligned} \tag{C.29}$$

where r_μ and $r_\nu \in \mathbb{R}$. As no angle is playing any particular role, this leads to : $\forall\ \vartheta,\, \vartheta^{'},\, r,\, r' \in \mathbb{R}$,

$$g\left(\operatorname{arctri}\frac{r\operatorname{tri}\vartheta + r'\operatorname{tri}\vartheta'}{\sqrt{r^2 + r'^2 - 2rr'\cos\left[\vartheta - \vartheta'\right]}}\right) = \operatorname{arctri}\left(\frac{r\operatorname{tri} g\left(\vartheta\right) + r'\operatorname{tri} g\left(\vartheta'\right)}{\sqrt{r^2 + r'^2 - 2rr'\cos\left[g\left(\vartheta\right) - g\left(\vartheta'\right)\right]}}\right) \tag{C.30}$$

where either $\operatorname{tri}\vartheta = \cos\vartheta$ or $\operatorname{tri}\vartheta = \sin\vartheta$.

The identity $g\left(\vartheta\right) = \vartheta$ obviously meets all these criteria.

Annexe D

Spin filters and spin rotators

Let us first consider the simple case of two media separated by a tunnel barrier, the spin being quantized with respect to an arbitrary axis. The tunnel process arises at a given energy and we assume that at least in one of the materials, the spin degeneracy is lifted so that the wave vectors are different for the two spin states. The transmission can be described as follows

$$|+\rangle \longrightarrow |\chi_+\rangle = t_{++}(\mathbf{q},\mathbf{k})\,|+\rangle + t_{+-}(\mathbf{q},\mathbf{k})\,|-\rangle \quad = t_{++}\,|+\rangle + t_{+-}\,|-\rangle \tag{D.1}$$

$$|-\rangle \longrightarrow |\chi_-\rangle = t_{-+}(\mathbf{q}',\mathbf{k}')\,|+\rangle + t_{--}(\mathbf{q}',\mathbf{k}')\,|-\rangle = t'_{-+}\,|+\rangle + t'_{--}\,|-\rangle \tag{D.2}$$

or

$$\begin{bmatrix} |\chi_+\rangle \\ |\chi_-\rangle \end{bmatrix} = \begin{bmatrix} t_{++} & t_{+-} \\ t'_{-+} & t'_{--} \end{bmatrix} \begin{bmatrix} |+\rangle \\ |-\rangle \end{bmatrix} = T \begin{bmatrix} |+\rangle \\ |-\rangle \end{bmatrix} \tag{D.3}$$

where $[t_{ij}]$ is the transmission matrix. The transmission asymmetry is

$$\mathcal{T} = \frac{||\chi_+||^2 - ||\chi_-||^2}{||\chi_+||^2 + ||\chi_-||^2} = \frac{|t_{++}|^2 + |t_{+-}|^2 - |t'_{--}|^2 - |t'_{-+}|^2}{|t_{++}|^2 + |t_{+-}|^2 + |t'_{--}|^2 + |t'_{-+}|^2} \tag{D.4}$$

Let us assume that we can diagonalize T so that

$$T\ |\pm\rangle_T = t_\pm\,|\pm\rangle_T \tag{D.5}$$

If, furthermore $|+\rangle_T$ and $|-\rangle_T$ are orthogonal, by chosing an appropriate phase factor $\widehat{K}\,|+\rangle_T = |-\rangle_T$. Then

$$\begin{aligned} |+\rangle &= a\,|+\rangle_T + b\,|-\rangle_T \\ \widehat{K}\,|+\rangle &= |-\rangle = a^*\,|-\rangle_T - b^*\,|+\rangle_T \end{aligned} \tag{D.6}$$

$$|+\rangle = a\,|+\rangle_T + b\,|-\rangle_T \longrightarrow \left|\chi_+^T\right\rangle = at_+\,|+\rangle_T + bt_-\,|-\rangle_T \quad \text{(D.7)}$$

$$\widehat{K}\,|+\rangle = |-\rangle = a^*\,|-\rangle_T - b^*\,|+\rangle_T \rightarrow \left|\chi_-^T\right\rangle = a^*t_-\,|-\rangle_T - b^*t_+\,|+\rangle_T \quad \text{(D.8)}$$

Then the transmission asymmetry is

$$\begin{aligned}
\mathcal{T} &= \frac{\left|\left|\chi_+^T\right|\right|^2 - \left|\left|\chi_-^T\right|\right|^2}{\left|\left|\chi_+^T\right|\right|^2 + \left|\left|\chi_-^T\right|\right|^2} \\
&= \frac{|a|^2\,|t_+|^2 + |b|^2\,|t_-|^2 - |a|^2\,|t_-|^2 - |b|^2\,|t_+|^2}{|a|^2\,|t_+|^2 + |b|^2\,|t_-|^2 + |a|^2\,|t_-|^2 + |b|^2\,|t_+|^2} \\
&= \frac{|a|^2\left(|t_+|^2 - |t_-|^2\right) - |b|^2\left(|t_+|^2 - |t_-|^2\right)}{|a|^2\left(|t_+|^2 + |t_-|^2\right) + |b|^2\left(|t_+|^2 + |t_-|^2\right)} \\
&= \frac{|a|^2 - |b|^2}{|a|^2 + |b|^2}\,\frac{|t_+|^2 - |t_-|^2}{|t_+|^2 + |t_-|^2}
\end{aligned} \quad \text{(D.9)}$$

If $|t_+|^2 = |t_-|^2$, $\mathcal{T} = 0$ so that both spin states are equally transmitted : we have a "pure spin rotator" .

If $|t_+|^2 \neq |t_-|^2$, we have a "pure spin filter" along the direction defined by the $\{|\pm\rangle_T\}$ basis, i.e. we have differential transmission through two decoupled channels.

More generally, the transmission asymmetry $\mathcal{T}$ of the ket $|\varphi_0\rangle$ can be defined as

$$\mathcal{T} = \frac{\left|\left|T\ \left(|\varphi_0\rangle\right)\right|\right|^2 - \left|\left|T\ \left(\widehat{K}\,|\varphi_0\rangle\right)\right|\right|^2}{\left|\left|T\ \left(|\varphi_0\rangle\right)\right|\right|^2 + \left|\left|T\ \left(\widehat{K}\,|\varphi_0\rangle\right)\right|\right|^2} \quad \text{(D.10)}$$

Equivalently, these results can be rewritten in the framework of the density operator.

$$|+\rangle = a\,|+\rangle_T + b\,|-\rangle_T \quad \text{(D.11)}$$

$$|-\rangle = -ib^*\,|+\rangle_T + ia^*\,|-\rangle_T \quad \text{(D.12)}$$

$$\left|\chi_+^T\right\rangle = at_+\,|+\rangle_T + bt_-\,|-\rangle_T \quad \text{(D.13)}$$

$$\left|\chi_-^T\right\rangle = -ib^*t_+\,|+\rangle_T + ia^*t_-\,|-\rangle_T \quad \text{(D.14)}$$

$$\rho_I = A\,|+\rangle\langle+| + B\,|-\rangle\langle-| \quad \text{(D.15)}$$

$A = B$ for a completely unpolarized system.

In the region III

$$\rho_{III} = c\left|\chi_+^T\right\rangle\left\langle\chi_+^T\right| + d\left|\chi_-^T\right\rangle\left\langle\chi_-^T\right| \quad \text{(D.16)}$$

Let us take

$$\begin{aligned}
\rho_{III} &= \sum_{\sigma=\pm} \left|\chi_\sigma^T\right\rangle \left\langle\chi_\sigma^T\right| \rho_I \left|\chi_\sigma^T\right\rangle \left\langle\chi_\sigma^T\right| \\
&= \left|\chi_+^T\right\rangle \left\langle\chi_+^T\right| \{\, A\left|+\right\rangle\left\langle+\right| + B\left|-\right\rangle\left\langle-\right| \,\} \left|\chi_+^T\right\rangle \left\langle\chi_+^T\right| \\
&\quad + \left|\chi_-^T\right\rangle \left\langle\chi_-^T\right| \{\, A\left|+\right\rangle\left\langle+\right| + B\left|-\right\rangle\left\langle-\right| \,\} \left|\chi_-^T\right\rangle \left\langle\chi_-^T\right| \\
&= \left|\chi_+^T\right\rangle \left\langle\chi_+^T\right| \left\{ A\left||a|^2 t_+ + |b|^2 t_-\right|^2 + B\left|ab\left(t_+ - t_-\right)\right|^2 \right\} \\
&\quad + \left|\chi_-^T\right\rangle \left\langle\chi_-^T\right| \left\{ A\left|-ib^*a^*t_+ + ib^*a^*t_-\right|^2 + B\left||b|^2 t_+ + |a|^2 t_-\right|^2 \right\} \\
&= \left|\chi_+^T\right\rangle \left\langle\chi_+^T\right| \left\{ A\left||a|^2 t_+ + |b|^2 t_-\right|^2 + B|a|^2|b|^2|t_+ - t_-|^2 \right\} \\
&\quad + \left|\chi_-^T\right\rangle \left\langle\chi_-^T\right| \left\{ A|a|^2|b|^2|t_+ - t_-|^2 + B\left||b|^2 t_+ + |a|^2 t_-\right|^2 \right\} \qquad \text{(D.17)}
\end{aligned}$$

Finally we have :

$$c = A\left||a|^2 t_+ + |b|^2 t_-\right|^2 + B|a|^2|b|^2|t_+ - t_-|^2 \qquad \text{(D.18)}$$

$$d = A|a|^2|b|^2|t_+ - t_-|^2 + B\left||b|^2 t_+ + |a|^2 t_-\right|^2 \qquad \text{(D.19)}$$

For a completely unpolarized beam, $A = B$, and

$$c = A\left(\left||a|^2 t_+ + |b|^2 t_-\right|^2 + |a|^2|b|^2|t_+ - t_-|^2\right) \qquad \text{(D.20)}$$

$$d = A\left(|a|^2|b|^2|t_+ - t_-|^2 + \left||b|^2 t_+ + |a|^2 t_-\right|^2\right) \qquad \text{(D.21)}$$

The transmission asymmetry is

$$\mathcal{T} = \frac{c-d}{c+d} = \frac{\left(|a|^2 - |b|^2\right)\left(|t_+|^2 - |t_-|^2\right)}{\left(|a|^2 + |b|^2\right)\left(|t_+|^2 + |t_-|^2\right)} \qquad \text{(D.22)}$$

Annexe E

Polarization and first-order wave-function calculation in Perel's case

E.1 Polarization

Here, we explicitly perform the calculation of the polarization $\mathcal{P}$ of the transmitted beam in Perel's case, the final result being given in Subsec. B of chapter 3. As stated in chapter 3 (p. 65 or p. 165204-14, Eq.4.13),

$$\mathcal{P} = \frac{\left|t_0^+\right|^2 - \left|t_0^-\right|^2}{\left|t_0^+\right|^2 + \left|t_0^-\right|^2} \tag{E.1}$$

where

$$\begin{aligned} \left|t_0^+\right|^2 &\approx \left|\frac{4qKe^{-Ka}}{(K-iq)^2}\right|^2 = \frac{16\left(qK\right)^2 e^{-2Ka}}{\left(K^2+q^2\right)^2} \\ \left|t_0^-\right|^2 &\approx \left|\frac{4qK'e^{-K'a}}{(K'-iq)^2}\right|^2 = \frac{16\left(qK'\right)^2 e^{-2K'a}}{\left(K'^2+q^2\right)^2} \end{aligned} \tag{E.2}$$

So, we obtain the polarization

$$\begin{aligned}
\mathcal{P} &= \frac{|t^+|^2 - |t^-|^2}{|t^+|^2 + |t^-|^2} \\
&= \frac{K^2\left(K'^2+q^2\right)^2 e^{-2Ka} - K'^2\left(K^2+q^2\right)^2 e^{-2K'a}}{K^2\left(K'^2+q^2\right)^2 e^{-2Ka} + K'^2\left(K^2+q^2\right)^2 e^{-2K'a}} \\
&= \frac{K^2\left[\left(K'^2+q^2\right)^2 + 4q^2K'^2\right] e^{-2Ka} - K'^2\left[\left(K^2+q^2\right)^2 + 4q^2K^2\right] e^{-2K'a}}{K^2\left[\left(K'^2+q^2\right)^2 + 4q^2K'^2\right] e^{-2Ka} - K'^2\left[\left(K^2+q^2\right)^2 + 4q^2K^2\right] e^{-2K'a}} \\
&= \frac{\left(\frac{K}{K_0}\right)^2\left[\left(\frac{K'}{K_0}\right)^2 + \left(\frac{q}{K_0}\right)^2\right]^2 e^{-2Ka} - \left(\frac{K'}{K_0}\right)^2\left[\left(\frac{K}{K_0}\right)^2 + \left(\frac{q}{K_0}\right)^2\right]^2 e^{-2K'a}}{\left(\frac{K}{K_0}\right)^2\left[\left(\frac{K'}{K_0}\right)^2 + \left(\frac{q}{K_0}\right)^2\right]^2 e^{-2Ka} + \left(\frac{K'}{K_0}\right)^2\left[\left(\frac{K}{K_0}\right)^2 + \left(\frac{q}{K_0}\right)^2\right]^2 e^{-2K'a}}
\end{aligned}$$

We define $\alpha = \frac{q}{K_0}$. Observe that $\left(\frac{K}{K_0}\right)^2 = 1 - \frac{\delta K}{K_0}$ and $\left(\frac{K'}{K_0}\right)^2 = 1 + \frac{\delta K}{K_0}$, then :

$$\mathcal{P} = \frac{\left(1-\frac{\delta K}{K_0}\right)\left(1+\frac{\delta K}{K_0}+\alpha\right)^2 e^{-2Ka} - \left(1+\frac{\delta K}{K_0}\right)\left(1-\frac{\delta K}{K_0}+\alpha\right)^2 e^{-2K'a}}{\left(1-\frac{\delta K}{K_0}\right)\left(1+\frac{\delta K}{K_0}+\alpha\right)^2 e^{-2Ka} + \left(1+\frac{\delta K}{K_0}\right)\left(1-\frac{\delta K}{K_0}+\alpha\right)^2 e^{-2K'a}} \tag{E.3}$$

We can use the approximation $\left(1 \pm \frac{\delta K}{K_0} + \alpha\right)^2 \approx (1+\alpha)^2 \pm 2(1+\alpha)\frac{\delta K}{K_0}$ because $\frac{\delta K}{K_0} \ll 1$. The polarization becomes

$$\mathcal{P} = \frac{\left(1-\frac{\delta K}{K_0}\right)\left[1+\beta\frac{\delta K}{K_0}\right] e^{-2Ka} - \left(1+\frac{\delta K}{K_0}\right)\left[1-\beta\frac{\delta K}{K_0}\right] e^{-2K'a}}{\left(1-\frac{\delta K}{K_0}\right)\left[1+\beta\frac{\delta K}{K_0}\right] e^{-2Ka} + \left(1+\frac{\delta K}{K_0}\right)\left[1-\beta\frac{\delta K}{K_0}\right] e^{-2K'a}} \tag{E.4}$$

where $\beta = 2/(1+\alpha) = 2/(1+q/K_0) = 2K_0/(K_0+q)$. $q < K$ so $\alpha < 1$ and

$\gamma - 1 > 0$.

$$\begin{aligned}
\mathcal{P} &= \frac{\left[1+(\beta-1)\frac{\delta K}{K_0}\right]e^{-2Ka} - \left[1-(\beta-1)\frac{\delta K}{K_0}\right]e^{-2K'a}}{\left[1+(\beta-1)\frac{\delta K}{K_0}\right]e^{-2Ka} + \left[1-(\beta-1)\frac{\delta K}{K_0}\right]e^{-2K'a}} \\
&= \frac{e^{-2Ka} - e^{-2K'a} + (\beta-1)\frac{\delta K}{K_0}\left(e^{-2Ka} + e^{-2K'a}\right)}{e^{-2Ka} + e^{-2K'a} + (\beta-1)\frac{\delta K}{K_0}\left(e^{-2Ka} - e^{-2K'a}\right)} \\
&= \frac{e^{a\,\delta K} - e^{-a\,\delta K} + (\beta-1)\frac{\delta K}{K_0}\left(e^{a\,\delta K} + e^{-a\,\delta K}\right)}{e^{a\,\delta K} + e^{-\delta K' a} + (\beta-1)\frac{\delta K}{K_0}\left(e^{a\,\delta K} - e^{-a\,\delta K}\right)} \\
&= \frac{\tanh a\,\delta K + (\beta-1)\frac{\delta K}{K_0}}{1+(\beta-1)\frac{\delta K}{K_0}\tanh a\,\delta K} \\
&= \frac{\tanh a\,\delta K + \frac{K_0-q}{K_0+q}\frac{\delta K}{K_0}}{1+\frac{K_0-q}{K_0+q}\frac{\delta K}{K_0}\tanh a\,\delta K}
\end{aligned} \tag{E.5}$$

To the limit where $\frac{\delta K}{K_0}$ is negligible, we recover Perel's formula $\mathcal{P}_0 = \tanh a\,\delta K$.

E.2 First-order wave function

Let us first determine the $\widetilde{B}_2$ coefficient. Recall that, in chapter 3 (p. 64 or p. 165204-15, Eq. 4.22b; also see p. 70 or p. 165204-19, Eqs. C1), we have derived

$$\widetilde{B}_2 = \frac{i\xi}{2K'}\left[A_2 e^{-K_0 a}\frac{\sinh(\delta/2)}{\sinh(K'a)} + B_2 e^{-\delta/2}\frac{\sinh(K_0 a)}{\sinh(K'a)}\right] \tag{E.6}$$

Because $\sinh(K'a) = \left(e^{K'a} - e^{-K'a}\right)/2 = e^{K'a}\left(1 - e^{-2K'a}\right)/2$, neglecting the $e^{-2K_0 a}$ term, we obtain $\sinh(K'a) \simeq e^{K'a}/2$. The $\widetilde{B}_2$ coefficient becomes

$$\widetilde{B}_2 \simeq \frac{i\xi}{2K'}\left[A_2 e^{-K_0 a}\sinh\frac{a\delta K}{2} + B_2 e^{-a\delta K/2}\sinh K_0 a\right] 2e^{-(K_0+\delta K/2)a} \tag{E.7}$$

where A_2 and B_2 do not include any first-order term in ξ/K_0, i.e., these terms are equal to the a_2 and b_2 coefficients in the standard tunneling problem to the first-order in ξ/K_0 (Eq. 2.25 p. 57 or p. 165204-6), so that

$$\frac{B_2}{A_2} = \frac{-q+iK}{q+iK}e^{-2Ka} \tag{E.8}$$

or

$$B_2 e^{Ka}(iK+q) = A_2 e^{-Ka}(iK-q) \tag{E.9}$$

$$B_2 e^{K_0 a} e^{-a\delta K/2}(iK+q) = A_2 e^{-Ka} e^{a\delta K/2}(iK-q) \tag{E.10}$$

We obtain

$$\begin{aligned}
\widetilde{B}_2 &\simeq \frac{i\xi}{K_0}\left[e^{K_0 a}B_2 e^{-a\delta K}\frac{iK_0+q}{iK_0-q}\sinh\frac{a\delta K}{2}+B_2 e^{-a\delta K/2}\sinh K_0 a\right]e^{-K_0 a}e^{-a\delta K/2}\\
&\simeq \frac{i\xi}{K_0}\left[e^{K_0 a}B_2 e^{-a\delta K}\frac{iK_0+q}{iK_0-q}\sinh\frac{a\delta K}{2}+B_2 e^{-a\delta K/2}\frac{e^{K_0 a}}{2}\right]e^{-K_0 a}e^{-a\delta K/2}\\
&\simeq \frac{i\xi}{2K_0}B_2 e^{-a\delta K}\left[2\frac{iK_0+q}{iK_0-q}e^{-a\delta K/2}\sinh\frac{a\delta K}{2}+1\right] \qquad \text{(E.11)}
\end{aligned}$$

which is the expression given in Eq. 4.24 (p. 64 or p. 165204-15).

Now we are going to calculate the transmission coefficient $\tilde{A}_3$ and reflection coefficient $\widetilde{B}_1$. We start from Eq. C1g (p. 70 or p. 165204-19) :

$$\begin{aligned}
\tilde{A}_3 e^{iqa} &\simeq \frac{i\xi}{2K}A_2 e^{-Ka}-\frac{i\xi}{2K}B_2 e^{Ka}+\tilde{A}_2 e^{-K'a}+\widetilde{B}_1 e^{K'a}\\
&\simeq \frac{i\xi}{2K}A_2 e^{-Ka}-\frac{i\xi}{2K}B_2 e^{Ka}+\tilde{A}_2 e^{-K'a}+\widetilde{B}_1 e^{K'a} \qquad \text{(E.12)}
\end{aligned}$$

Note that $\xi/K \simeq \xi/K_0$. From Eq. 4.23 (p. 64 or p. 165204-15), we have $\tilde{A}_2 = -\dfrac{i\xi}{2K_0}A_2$. If we take $\widetilde{B}_2 \simeq \dfrac{i\xi}{2K_0}B_2$ (which arises from the zeroth-order approximation with respect to $a\delta K$, i.e., $a\delta K \to 0$), we have

$$\begin{aligned}
\tilde{A}_3 e^{iqa} &\simeq \frac{i\xi}{2K_0}A_2 e^{-Ka}-\frac{i\xi}{2K_0}B_2 e^{Ka}-\frac{i\xi}{2K_0}A_2 e^{-(K+\delta K)a}+\frac{i\xi}{2K_0}B_2 e^{(K+\delta K)a}\\
&\simeq \frac{i\xi}{2K}e^{-Ka}A_2\left(1-e^{-a\delta K}\right)-\frac{i\xi}{2K}e^{Ka}A_2\left(1-e^{a\delta K}\right)\\
&\simeq \frac{i\xi}{2K}e^{-Ka}e^{-a\delta K/2}\left(2\sinh\frac{a\delta K}{2}\right)A_2+\frac{i\xi}{2K}e^{Ka}e^{a\delta K/2}\left(2\sinh\frac{a\delta K}{2}\right)B_2\\
&\simeq \frac{i\xi}{K}\sinh\frac{a\delta K}{2}\left[e^{-Ka}e^{-a\delta K/2}A_2+e^{Ka}e^{a\delta K/2}B_2\right]\\
&\simeq \frac{i\xi}{K}\sinh\frac{a\delta K}{2}\left[e^{-Ka}A_2\left(-\sinh\frac{a\delta K}{2}+\cosh\frac{a\delta K}{2}\right)\right]\\
&\qquad +\frac{i\xi}{K}\sinh\frac{a\delta K}{2}\left[e^{Ka}B_2\left(\sinh\frac{a\delta K}{2}+\cosh\frac{a\delta K}{2}\right)\right]\\
&\simeq \frac{i\xi}{K}\sinh\frac{a\delta K}{2}\left[\cosh\frac{a\delta K}{2}\left(e^{-Ka}A_2+e^{Ka}B_2\right)+\sinh\frac{a\delta K}{2}\left(-e^{-Ka}A_2+e^{Ka}B_2\right)\right]
\end{aligned} \qquad \text{(E.13)}$$

Because $\left(-e^{-Ka}A_2+e^{Ka}B_2\right) = -2q^2e^{-Ka}/(q+iK)^2$ is a second-order term, we obtain

$$\begin{aligned}
\tilde{A}_3 e^{iqa} &\simeq \frac{i\xi}{2K}\sinh a\delta K\ \left(e^{-Ka}A_2+e^{Ka}B_2\right)\\
&\simeq \frac{i\xi}{2K}\sinh a\delta K\ A_3 e^{iqa} \qquad \text{(E.14)}
\end{aligned}$$

$$\tilde{A}_3 = \frac{i\xi}{2K} \sinh a\delta K \; A_3 \tag{E.15}$$

Now we calculate the correction to $\tilde{A}_3$ which comes from the difference between $\widetilde{B}_2$ and $\frac{i\xi}{2K_0} B_2$. We have

$$\begin{aligned}
\Delta\widetilde{B}_2 &= \widetilde{B}_2 - \frac{i\xi}{2K_0} B_2 \\
&\simeq \frac{i\xi}{2K_0} B_2 e^{-a\delta K} \left[2\frac{iK+q}{iK-q} e^{-a\delta K/2} \sinh\frac{a\delta K}{2} + 1 - e^{-a\delta K} \right] \\
&= \frac{i\xi}{2K_0} B_2 e^{-a\delta K} \left[2\frac{iK+q}{iK-q} e^{-a\delta K/2} \sinh\frac{a\delta K}{2} - e^{a\delta K/2} 2\sinh\frac{a\delta K}{2} \right] \\
&= \frac{i\xi}{K_0} B_2 e^{-a\delta K} \sinh\frac{a\delta K}{2} \left[\frac{iK+q}{iK-q} e^{-a\delta K/2} - e^{a\delta K/2} \right]
\end{aligned} \tag{E.16}$$

Note that

$$\frac{iK+q}{iK-q} = -1 + \frac{2iK}{iK-q} \tag{E.17}$$

so that

$$\begin{aligned}
\Delta\widetilde{B}_2 &= \frac{i\xi}{K_0} B_2 e^{-a\delta K} \sinh\frac{a\delta K}{2} \left[-2\cosh\frac{a\delta K}{2} + \frac{2iK}{iK-q} e^{-a\delta K/2} \right] \\
&= -\frac{i\xi}{K_0} B_2 e^{-a\delta K} \left[\sinh a\delta K - \frac{2iK}{iK-q} e^{-a\delta K/2} \sinh\frac{a\delta K}{2} \right]
\end{aligned} \tag{E.18}$$

or

$$\begin{aligned}
\Delta\widetilde{B}_2 &= -\frac{i\xi}{K_0} B_2 e^{-a\delta K} \left[\sinh a\delta K - 2e^{-a\delta K/2} \sinh\frac{a\delta K}{2} \right] \\
&= -\frac{i\xi}{K_0} B_2 e^{-a\delta K} \left[\sinh a\delta K + 2\left(\sinh\frac{a\delta K}{2} - \cosh\frac{a\delta K}{2} \right) \sinh\frac{a\delta K}{2} \right] \\
&= -\frac{i\xi}{K_0} B_2 e^{-a\delta K} \left[2\sinh^2\frac{a\delta K}{2} \right]
\end{aligned} \tag{E.19}$$

When $a\delta K << 1$ and $q/K << 1$, $\Delta\widetilde{B}_2$ vanishes to the first order.

When $a\delta K >> 1$ the second term is negligible and B_2 tends to zero.

Let us refer to the correction to $e^{iqa}\widetilde{A}_3$ originating from $\Delta\widetilde{B}_2$ as $e^{iqa}\Delta\widetilde{A}_3$. We have

$$\begin{aligned}
e^{iqa}\Delta\widetilde{A}_3 &= -\frac{i\xi}{K_0} B_2 e^{-a\delta K} \left[2\sinh^2\frac{a\delta K}{2} \right] e^{K'a} \\
&= -\frac{i\xi}{K_0} B_2 e^{-a\delta K} \left[2\sinh^2\frac{a\delta K}{2} \right] e^{K_0 a} e^{a\delta K} \\
&= -\frac{i\xi}{K_0} B_2 e^{K_0 a} \left[2\sinh^2\frac{a\delta K}{2} \right]
\end{aligned} \tag{E.20}$$

Because $B_2/A_3 = (1/2)\, e^{-Ka} e^{iqa} A_3 = (1/2)\, e^{-K_0 a} e^{\delta K a} e^{iqa} A_3$ (see Eqs. 2.25, p. 57 or p. 165204-6)

$$e^{iqa} \Delta \widetilde{A}_3 = -\frac{i\xi}{2K_0} e^{a\delta K/2} \left[2 \sinh^2 \frac{a\delta K}{2} \right] e^{iqa} A_3 \tag{E.21}$$

or

$$\Delta \widetilde{A}_3 = -\frac{i\xi}{2K_0} e^{a\delta K/2} \left[2 \sinh^2 \frac{a\delta K}{2} \right] A_3 \tag{E.22}$$

Finally

$$\widetilde{A}_3 = \frac{i\xi}{2K} \left(\sinh a\delta K - 2e^{a\delta K/2} \sinh^2 \frac{a\delta K}{2} \right) A_3 \tag{E.23}$$

which is Eq. 4.26 (p. 64 or p. 165204-15).

Concerning $\widetilde{B}_1$, from Eq. C1e (p. 70 or p. 165204-19), we have

$$\begin{aligned}
\widetilde{B}_1 &= \frac{i\xi}{2K} (A_2 - B_2) - \left(\widetilde{A}_2 + \widetilde{B}_2 \right) \\
&\simeq \frac{i\xi}{2K_0} (A_2 - B_2) - \left(\widetilde{A}_2 + \widetilde{B}_2 \right) \\
&= \frac{i\xi}{2K_0} (A_2 - B_2) - \left(-\frac{i\xi}{2K_0} A_2 + \frac{i\xi}{2K_0} B_2 + \Delta \widetilde{B}_2 \right) \\
&= -\Delta \widetilde{B}_2 \\
&= \frac{2i\xi}{\overline{K}} B_2 e^{-a\delta K} \sinh^2 \frac{a\delta K}{2}
\end{aligned} \tag{E.24}$$

Besides,

$$\frac{B_2}{B_1} = \frac{-2q}{(q+iK)} e^{-2Ka} = \frac{-2q}{(q+iK)} e^{-2K_0 a} e^{\delta K a} \tag{E.25}$$

so that

$$\widetilde{B}_1 = -\frac{2i\xi}{K_0} \frac{2q}{q - iK} e^{-2K_0 a} B_1 \sinh^2 \frac{a\delta K}{2} = 0 \tag{E.26}$$

to first order.

Bibliographie

[AB] A. Abragam and B. Bleaney, *Electron Paramagnetism Resonance of Transition Ions*, Clarendon Press (1970).

[BDD] B. J. BenDaniel and C. B. Duke, *Space-Charge Effects on Electron Tunneling*, Phys. Rev. **152**, 683 (1966).

[BDM] R. Balian, D. Bessis and G. A. Mezincescu, *Form of kinetic energy in effective-mass Hamiltonians for heterostructures*, Phys. Rev. B **15**, 17624 (1995) ; *Mesoscopic Description of Heterojunctions,* J. Phys. I **- 6**, 1377 (1996).

[CHA] Y. C. Chang, *Complex band structures of zinc-blende materials*, Phys. Rev. B **25**, 605 (1982).

[DP] M. I. D'yakonov and V. I. Perel', *Spin Relaxation of Conduction Electron in Noncetrosymmetric semiconductors*, Sov. Phys. Solid State **13**, 3023 (1972).

[DRE.55] G. Dresselhaus, *Spin-Orbit Coupling Effects in Zinc Blende Structures,* Phys. Rev. **100**, 580 (1955).

[GB] G. Bastard, *Wave Mechanics applied to semiconductor heterostructure* (Éditions de Physique, Les Ulis,1992).

[GF] G. Fishman, *Semi-conducteurs : les bases de la théorie* $\mathbf{k} \cdot \mathbf{p}$ (Les Editions de l'Ecole Polytechnique, Palaiseau, 2010).

[HAR] W. A. Harrison, *Tunneling from an Independent-Particle Point of View*, Phys. Rev. **123**, 85 (1961).

[HEI] V.Heine, *On the general Theory of Surface States and Scattering of Electron in Solids*, Proc. Phys. Soc. London **81**, 300 (1963).

[JON] R. O. Jones, *Surface Representations and complex band structure of a diamond-type semiconductor*, Proc. Phys. Soc. London **89**, 443 (1966).

[JSAL] J.-M. Jancu, R. Scholz, E. A. de Andrada e Silva, and G. C. LaRocca, *Atomistic spin-orbit coupling and* $\mathbf{k}\cdot\mathbf{p}$ *parameters in III-V semiconductors*, Phys. Rev. B **72**, 193201 (2005).

[KAN] E. O. Kane, *Band Structure of Idium Atimonide*, J. Phys. Chem. Solids **1**, 249 (1957).

[KIT] C. Kittel, *Quantum theory of Solids* (John Wiley & Sons, 1987).

[KOH] W.Kohn, *Analytic Properties of Bloch Waves and Wannier Functions*, Phys. Rev. **115**, 809 (1959).

[KOS] G. F. Koster, J. O. Dimmock, R. G. Wheeler, and H. Statz, *Properties of the Thirty-Two Point Groups* (M.I.T Press, Cambridge, Massachusetts, U.S.A,1963.).

[LK] J. M. Luttinger and W. Kohn, *Motion of Electrons and Holes in Perturbed Periodic Fields*, Phys. Rev. **97**, 869 (1955).

[LUT.55] J. M. Luttinger, *Quantum Theory of Cyclotron Resonance in Semiconductors : General Theory*, Phys. Rev. **102**, 1030 (1956).

[MES] A. Messiah, *Mécanique quantique*, Dunod, Paris (1995).

[PB] C. R. Pidgeon and R. N. Brown, *Interband Magneto-Absorption and Faraday Rotation in InSb,* Phys. Rev. **146**, 575 (1966).

[PER] V. I. Perel', S. A. Tarasenko, and I. N. Yassievich, *Spin-dependent tunneling through a symmetric semiconductor barrier,* Phys. Rev. B **67**, 201304(R) (2003).

[RDRF] S. Richard, H.-J. Drouhin, N. Rougemaille and G. Fishman, *Structure of spin-split evanescent states in the fundamental gap of zinc-blende-type semiconductors*, Appl. Phys. **97**, 0835706 (2005).

[RDRGS] N. Rougemaille, H.-J. Drouhin, S. Richard, G. Fishman, and A. K. Schmid, *Spin-induced forbidden evanescent states in III-V semiconductors*, Phys. Rev. Lett. **95**, 186406 (2005).

[SCH] L. I. Schiff, *Quantum Mechanics*, 3rd Edition, McGraw Hill, pages 490-534 (1968).[SEE] K. Seeger, *Semiconductor Physics*, Springer-Verlag (1999).

[SFD] M-H. Serre, G. Fishman and H-J. Drouhin, *Inconsistency of standard k.p parameters*, Proc. SPIE, Vol. 6195, 61951B (2006).

[SH] M. F. H. Schuurmans and G. W. 't Hooft, *Simple calculations of confinement states in a quantum well*, Phys. Rev. B **31**, 8041 (1985).

[SHO] W. Shockley, *On the Surface States Associated with a Periodic Potential*, Phys. Rev. **56**, 317 (1939).

[SLA] J. C. Slater, *Electrons in Perturbed Periodic Lattices*, Phys. Rev. **76**, 1592 (1949).

[VMR] I. Vurgaftman, J. R. Meyer and L. R. Ram-Mohan, *Band parameters for III–V compound semiconductors and their alloys*, J. Appl. Phys. **89**, 5815 (2001).